



The University of
Nottingham

UNITED KINGDOM • CHINA • MALAYSIA

**PHOSPHATE GLASS FIBRE REINFORCED COMPOSITE FOR
BONE REPAIR APPLICATIONS: INVESTIGATION OF
INTERFACIAL INTEGRITY IMPROVEMENTS
VIA CHEMICAL TREATMENTS**

Muhammad Sami Hasan

Thesis submitted to the University of Nottingham for the

Degree of Doctor of Philosophy

Division of Materials, Mechanics and Structures

Faculty of Engineering

August

2012

To the City of Knowledge

ABSTRACT

Bone repair devices made from degradable polymers, such as poly lactic acid (PLA) have limitation in terms of matching the mechanical property requirements for bone repair, both initially and for the duration of repair. For this reason the use of totally degradable phosphate glass fibre (PGF) reinforced PLA composite has proved attractive. A crucial part of the success of such implants is maintenance of interfacial integrity between the polymer matrix and reinforcement phases of the composite. It is well known that most fibre reinforced composites loose 50% or more of their strength due to interfacial integrity loss. In this study candidate chemical treatments for PGF reinforced PLA composite are being investigated in terms of their reactivity, biocompatibility, effect on interfacial mechanical properties and degradation behaviour of these composites.

As a crucial part of this project, phosphate based glass (PBG) formulations were devised and assessed for structural, thermal, degradation and cytocompatibility variations with varying P_2O_5 or Fe_2O_3 content. Selected formulations were drawn into fibres and tested for single fibre tensile strength. Finally, a glass formulation (P45Ca16Mg24Na11Fe4, number indicates percentage molar concentration of oxides) was selected for surface modification and composite production.

Chemical surface treatments were selected on the basis of potential to react with PBG and PLA. Mode of chemical interaction between PBG and surface treatments chemicals were analysed using surface analyses techniques (FTIR and XPS). It was found that aminopropyltriethoxy silane (APS), etidronic acid (EA) and hexamethylene diisocyanate (HDI) were linked through covalent bonds, other agents making hydrogen bonds with PBG. Chemical treatments were optimised and

investigated for their effect on interfacial shear strength (IFSS) between polymer/glass, wettability and degradation behaviour. Chemically treated PBG was also assessed for cytocompatibility of elution products, short-term direct contact with MG63 osteosarcoma and long term direct contact with primary human osteoblasts. All selected surface treatment chemicals except amino phosphonic acid (APA) improved the interfacial bond between PBG and PLA. However, the covalently linked agents (HDI, APS and EA) saw up to 4-fold improvement in IFSS. SPLA also improved the IFSS significantly, which was attributed to the presence of several -OH groups. There was no significant effect on degradation rate of PBG. All agents demonstrated acceptable cytocompatibility for their elution products and in direct contact.

Selected chemicals (APS, EA, SPLA and HDI) were investigated further in PGF reinforced PLA composite. PGF mats (UD or non-woven), treated with surface treatment chemical were sandwich-pressed between PLA sheets. Flexural mechanical properties with degradation, water-uptake, degradation rate and cytocompatibility were tested. It was found that surface chemical treatment improved the initial flexural properties (APS, SPLA) and/or delayed the mechanical integrity loss (HDI, APS), latter was attributed to the reduced water-uptake and maintenance of relatively strong interface. Human osteoblasts were found to perform normal functions when cultured on prepared composites.

ACKNOWLEDGEMENT

First and foremost, thanks be to Allah who provided me with life, health, strength and opportunity to carry out this work.

I wish to extend my utmost gratitude to my respected supervisors, Dr Colin Scotchford and Prof. Gavin Walker for their continuous support and guidance throughout the course of project or even before that. I feel particularly indebted to Dr Scotchford, who was the first academic whom I encountered at the University of Nottingham that took a chance on me to enable my entry to the MSc programme. It was through his mentoring that I successfully continued into doctoral studies in the sphere of Biomaterials; I am honoured to have worked under Dr Scotchford's guidance.

I'm thankful to the dean of engineering for supporting my PhD financially with prestigious "Dean of Engineering Research Scholarship" award.

I wish to thank and acknowledge the senior researchers of Biocomposite Group, Dr Ifty Ahmed and Dr Andy Parsons for their technical help, motivation and time for discussion who were always there when needed.

I wish to thank all the hard working and serene technical staff of Wolfson building and ITRC, Tom Buss (profilometry/ polishing/FTIR), Martin Roe (XPS/EDX/SEM), Julie Thornhill (cell culture/SEM), George Anderson (biomaterials lab), Rogers (composite production lab), Geoff (Mechanical testing lab) and last but not the least Keith Dinsdale (Thermal analysis and everything else).

I also want to extend my gratitude to all post-graduates in the biomaterials (Tim, Louise, Jon, Jin, Matt, Liana, and Jinn) and biocomposite groups (Papia, Reda, Na-Han, Sharifa, Xioling, Madhi, Zakir and Nusrat) for their time, knowledge sharing and above all for creating an ideal research environment: relaxed, friendly, yet healthily competitive!

I am also obliged to my dearest parents who dedicated their life for my upbringing and education. I'm also in debt to my siblings especially to the eldest brother (Taqi) for supporting and encouraging me both morally & financially.

I am really grateful to my sweet Aunt Mrs Ahmad and Cousin Dr Shuja Ahmad for providing me a home away from home and tolerating my annoying behaviour at times.

I am also indebted to Al-Zahra Foundation Nottingham, where I find peace of mind and a place to escape after work. My beloved Agha Mirza Abbas, Asrar bhai, Imran bhai, Zaigham, Tanweer, Nawazish, Salamn, Raza and Rizwan will never be forgotten for their love, time and care. I shall always cherish their friendship.

LIST OF ABBREVIATIONS

ISO	International Organization for Standardization
ASTM	American Society for Testing and Materials
PLA	Poly(Lactic Acid)
PLLA	Poly-L-Lactide Acid
PCL	Poly(E-Caprolactone)
PBG	Phosphate Glass
PGF	Phosphate Glass Fibre
IFSS	Interfacial Shear Strength
HA	Hydroxyapatite
SD	Standard Deviation
FDA	Food and Drug Administration (US)
PMMA	Polymethylmethacrylate
PTFE	Polytetrafluoroethylene
PVC	Polyvinyl Chloride
PDMS	Polydimethylsiloxane
PGA	Polyglycolic Acid
DBO	Doubly Bonded Oxygen
XPS	X-Ray Photoelectron Spectroscopy
NMR	Nuclear Magnetic Resonance
PBS	Phosphate Buffered Saline
HBSS	Hank's Balanced Salt Solution

HOB	Human osteoblast
MTT	(3-(4,5-Dimethylthiazol-2-yl)-2,5-diphenyltetrazolium bromide
MPC	Muscle Precursor Cell
TCP	Tissue Culture Plastic
T _g	Glass-Transition Temperature
T _c	Crystallisation temperature
T _m	Melting temperature
APS	Aminopropyltriethoxy Silane
Poly (HEMA)	Poly(2-hydroxyethyl methacrylate)
HEPES	4-(2-hydroxyethyl)-1-piperazineethanesulfonic Acid
EDTA	Ethylenediaminetetraacetic Acid
DTA	Differential thermal analysis
TNE	100mM Tris; 2M NaCl; 10mM EDTA
NRU	Neutral Red Uptake
DMEM	Dulbecco's Modified Eagle Medium
ANOVA	Analysis of Variance
EDX	Energy-dispersive X-ray spectroscopy
FTIR	Fourier Transform Infrared Spectroscopy
NBO	Non-Bridging Oxygen
BO	Bridging Oxygen
HDA	Hexamethylene Diamine
HDI	Hexamethylene Diisocyanate
SFTT	Single Fibre Tensile Test
DMF	Dimethylformamide

DDW	Doubly distilled water
EA	Etidronic Acid
PPA	Phosphonopropionic Acid
Na-PLA	Sodium-ended Poly(Lactic Acid)
SPLA	Sorbitol-ended Poly(Lactic Acid)
GP	Glycerol Phosphate

TABLE OF CONTENTS

CHAPTER 1. INTRODUCTION.....	1
1.1 Background	1
1.2 Hypothesis	5
1.3 Aims and Objectives	6
CHAPTER 2. LITERATURE REVIEW.....	8
2.1 Introduction	8
2.2 Bone.....	8
2.2.1 Bone Cells	9
2.2.2 Bone Repair.....	11
2.2.3 Mechanical Properties of Bone	11
2.3 Implant Materials	13
2.3.1 Metals.....	14
2.3.2 Ceramics.....	15
2.3.3 Polymers.....	16
2.3.4 Degradable Implants	17
2.4 Glasses and Glass Properties	18
2.4.1 Bioactive Glass.....	18
2.4.2 Phosphate Glass	19
2.4.2.1 Phosphate Glass Structure	20
2.4.2.2 Classification of Phosphate.....	21
2.4.2.2.1 Linear Polyphosphates: ([O]/[P] > 3.0)	21

2.4.2.2.2	Cyclophosphates ($[O]/[P] = 3.0$).....	22
2.4.2.2.3	Ultraposphate: ($2.5 = < [O]/[P] < 3.0$).....	23
2.4.2.3	Classification of Phosphate With Respect to Modifiers.....	23
2.4.2.3.1	Vitreous Glass ($[O]/[P] = 2.5$).....	23
2.4.2.3.2	Binary Phosphate Glasses.....	23
2.4.2.3.3	Ternary Phosphate Glasses.....	25
2.4.2.3.4	More Complex Glass Systems.....	25
2.4.2.4	Phosphate Glass Degradation.....	26
2.4.2.4.1	Effect of Modifier on PBG degradation.....	27
2.4.2.5	Cytocompatibility Studies on PBGs.....	29
2.4.3	Biodegradable Polymers.....	35
2.4.3.1	Poly (Lactic Acid).....	36
2.4.3.1.1	Synthesis of PLA.....	37
2.4.3.1.2	Physical Properties of PLA.....	38
2.4.3.1.3	Degradation and Hydrolysis of PLA.....	39
2.4.3.1.4	Mechanical Properties of PLA.....	40
2.4.3.1.5	Biocompatibility of PLA.....	40
2.4.4	Composite.....	42
2.4.4.1	Types of Composite.....	43
2.4.4.1.1	Fibre–Reinforced Composites.....	43
2.4.4.2	Biocomposite.....	44

2.4.4.2.1	Types of Biocomposites.....	45
2.4.4.3	PGF Reinforced Composite.....	45
2.4.5	Role of Interface.....	48
2.4.5.1	Potential Surface Treatment Agents	49
2.4.5.1.1	Silanes.....	51
2.4.5.1.2	Phosphonic Acids	53
2.4.5.1.2.1	Phosphonopropionic Acid.....	55
2.4.5.1.2.2	Etidronic Acid.....	55
2.4.5.1.2.3	Amino–methyl Phosphonic Acid (APA)	56
2.4.5.1.2.4	Glycerol phosphate (GP).....	57
2.4.5.1.3	PLA Oligomers	57
2.4.5.1.4	Hexamethylene Diisocyanate (HDI).....	58
2.5	Conclusions	59
CHAPTER 3. PHOSPHATE GLASSES		61
3.1	Introduction	61
3.2	Materials and Methods	63
3.2.1	Glass Production	63
3.2.2	Material Characterisation.....	64
3.2.2.1	Energy dispersive X-ray (EDX)	64
3.2.2.2	X–ray Photoelectron Spectroscopy (XPS).....	64
3.2.2.3	Fourier Transform Infrared Spectroscopy (FTIR)	64

3.2.2.4	Thermal Analysis	65
3.2.2.5	Density Measurement	65
3.2.3	Degradation and pH Study	65
3.2.4	Cytocompatibility Study	66
3.2.4.1	Cell Culture	66
3.2.4.2	Alamar Blue	67
3.2.4.3	Alkaline Phosphatase Activity	67
3.2.4.4	DNA Quantification	68
3.2.4.5	Elution Study	68
3.2.5	Glass Fibre Production	69
3.2.6	Single Fibre Tensile Test (SFTT)	70
3.2.7	Statistical Analyses	72
3.3	Results	73
3.3.1	Glass Composition	73
3.3.2	Glass Structure	73
3.3.3	Density Measurement	77
3.3.4	Thermal Properties	78
3.3.5	Degradation Study	78
3.3.6	Biocompatibility	80
3.3.6.1	Alamar Blue Assay	80
3.3.6.2	Alkaline Phosphatase Activity Assay	81

3.3.6.3	Elution Study	82
3.3.7	Glass Fibre Production	83
3.3.8	Single Fibre Tensile Test (SFTT)	84
3.4	Discussion	86
3.5	Conclusions	92
CHAPTER 4. SURFACE TREATMENTS FOR PHOSPHATE GLASS		93
4.1	Introduction	93
4.2	Materials and Methods	97
4.2.1	Glass Synthesis	97
4.2.2	Surface Modification for Phosphate Glass.....	97
4.2.3	Fourier Transform Infrared (FTIR) Spectroscopy	98
4.2.4	X-ray Photoelectron spectrometry (XPS)	99
4.2.5	Push–Out Test for IFSS Measurement.....	99
4.2.6	Degradation Study.....	102
4.2.7	Wettability Measurement	102
4.2.8	Statistical Analyses	103
4.3	Results	104
4.3.1	FTIR	104
4.3.2	XPS	107
4.3.3	Interfacial Shear Strength Measurement (Push–Out Test).....	109
4.3.4	Surface Modified Glass Degradation.....	112

4.3.5	Surface Wettability Measurement.....	113
4.4	Discussion	114
4.5	Conclusions	120
CHAPTER 5. CYTOCOMPATIBILITY ASSESSMENT FOR SURFACE-TREATED GLASSES..... 121		
5.1	Introduction	121
5.2	Materials and Methods	123
5.2.1	Glass Synthesis	123
5.2.2	Chemical Modification for Glass Surface.....	123
5.2.3	Cytotoxicity Assessment.....	123
5.2.4	Short–Term Direct Contact Test	124
5.2.4.1	Cell Culture.....	124
5.2.4.2	Alamar Blue.....	124
5.2.4.3	Alkaline Phosphatase Activity.....	124
5.2.4.4	DNA Quantification.....	125
5.2.5	Primary Hobs in Direct Contact.....	125
5.2.5.1	Cell Culture.....	125
5.2.5.2	Proliferation	126
5.2.5.3	Differentiation.....	126
5.2.5.3.1	Alkaline Phosphatase Activity.....	126
5.2.5.3.2	Collagen Quantification.....	126
5.2.5.3.3	Osteocalcin Quantification	127

5.2.5.4	Morphology Assessment.....	128
5.2.6	Statistical Analyses	128
5.3	Results	129
5.3.1	Elution Study.....	129
5.3.2	Short Term Direct Contact Test	131
5.3.2.1	Metabolic Activity	131
5.3.2.2	DNA Quantification.....	132
5.3.2.3	Differentiation.....	133
5.3.3	Primary HOB in Direct Contact.....	134
5.3.3.1	Proliferation	134
5.3.3.2	Differentiation.....	135
5.3.3.2.1	Alkaline Phosphatase Activity.....	135
5.3.3.2.2	Collagen Production	136
5.3.3.2.3	Osteocalcin Quantification	137
5.3.3.3	Morphology (SEM).....	138
5.4	Discussion	143
5.5	Conclusions	152
CHAPTER 6. PHOSPHATE GLASS FIBRE REINFORCED		
COMPOSITE 154		
6.1	Introduction	154
6.2	Materials and Methods	156
6.2.1	Glass Synthesis	156

6.2.2	Glass Fibre Production.....	156
6.2.3	Single Fibre Tensile Test (SFTT)	156
6.2.4	PGF/PLA Composite Production.....	156
6.2.4.1	Treatment of PGFs.....	156
6.2.4.2	Non–Woven Fibre Mat Production.....	156
6.2.4.3	Unidirectional Fibre Mat Production.....	157
6.2.4.4	PLA Sheet Preparation.....	158
6.2.4.5	Composite Production.....	158
6.2.5	Degradation Study for Composites	159
6.2.6	Flexural Mechanical Properties Measurement.....	159
6.2.7	Physical (SEM) Analysis	160
6.2.8	Cytocompatibility of Primary Human Osteoblast to the Composites	160
6.2.8.1	Primary Human Osteoblast Cell Culture on Composite.....	160
6.2.8.2	Proliferation	160
6.2.8.3	Differentiation.....	160
6.2.8.3.1	Alkaline Phosphatase Activity.....	161
6.2.8.3.2	Collagen Quantification.....	161
6.2.8.3.3	Osteocalcin Quantification	161
6.2.8.4	Morphology	161
6.3	Results	162
6.3.1	Initial Mechanical Properties	162

6.3.2	Physical Analysis with Degradation	164
6.3.3	Water Uptake and Degradation of Composite	168
6.3.4	Retention of Mechanical Properties with Degradation	170
6.3.5	Cytocompatibility of Composites	172
6.3.5.1	Proliferation	172
6.3.5.2	Differentiation.....	173
6.3.5.2.1	Alkaline Phosphatase Activity.....	173
6.3.5.2.2	Collagen Production	174
6.3.5.2.3	Osteocalcin Quantification	176
6.3.5.3	Cell Morphology (SEM).....	177
6.4	Discussion:	180
6.5	Conclusions	189
CHAPTER 7. GENERAL DISCUSSION, CONCLUSIONS &		
RECOMMENDATIONS		190
7.1	General Discussion.....	190
7.2	Conclusions	202
7.3	Recommendations for Future Work	204

LIST OF TABLES

Table 1-1: Mechanical properties of commonly used materials for fracture fixation in comparison with human bone. PGA: polyglycolic acid, PLA: polylactic acid, SR: Self-reinforced.....	3
Table 2-1: Mechanical properties of human cortical and cancellous bone along with their testing conditions	12
Table 2-2: Applications and required properties of commonly used polymers in biomedical implants. PMMA: Polymethylmethacrylate, pHEMA: Poly(2-hydroxyethyl methacrylate), PE: polyethylene, PEO: polyethylene oxide, PP: polypropylene, PLGA: poly(lactic-co-glycolic acid).....	16
Table 2-3: Thermal, mechanical, and degradation properties of degradable polymers used as biomaterials. Properties are representative of bulk material without any reinforcement or cross linking.	36
Table 2-4: Range of physical properties for PLA as reported in the literature [126-129]	39
Table 2-5: Mechanical properties of bulk L-PLA compared to D-PLA with an average molecular weight of 55000 Daltons. Mechanical characterization was performed on specimens maintained in anhydrous conditions [128, 131].....	40
Table 2-6: <i>In-vitro</i> or <i>in-vivo</i> biocompatibility studies of PLA-based biomaterials and their outcomes	42
Table 2-7: Examples of fibre reinforced composite used as medical implant material	44

Table 2-8: Summary of selected investigations on phosphate glass fibre reinforced composites and their mechanical properties. PCL: Poly-caprolactone, PLA: poly-lacticacid, POE: poly-orthoester, PGF: phosphate glass fibre, MAmOL: methacrylate-modified oligolactide, UD: unidirectional.	47
Table 2-9: A summary of literature reviewed for chemical agents used to mediate polymer/glass interface within composites for biomedical applications. PGF: phosphate glass fibre, PLLA: poly-L-lactic acid, HA: hydroxyapatite, PP: polypropylene, APTES: aminopropyl triethoxy silane, NR: not reported, PPA: phosphonopropionic acid.	49
Table 3-1: Glass codes and their respective oxides within phosphate glass network, values represent molar percentage	63
Table 3-2: Glass codes and their respective oxides (molar percentage) within phosphate glass network, as measured by EDX analysis. Values after \pm represent standard deviation computed from three replicates	73
Table 3-3: Major peaks and their assignments from FTIR–ATR spectral analysis of phosphate glasses	75
Table 3-4: BO/NBO ratios and chain lengths calculated using theoretical equations and XPS data. Values after \pm represent standard deviation computed from three replicates.	77
Table 3-5: Thermal properties of the PBG samples measured by DTA; \pm represents SD where n=3.....	78

Table 3-6: Rate of degradation in ($\text{g cm}^{-2} \text{h}^{-1}$) for glass compositions studies. The numbers represent mass (g) loss per unit area (mm^2) over time (t). Values after \pm represent standard deviation computed from three replicates.....79

Table 3-7: Tensile strength and modulus of glass fibres drawn from different glass compositions. A single fibre tensile test (SFTT) was used along with laser gauge to measure diameter. Number after \pm represents SD where n=30. * represent the data provided by Reda Felfel.85

Table 4-1: Peak assignment from IR analysis of PBG samples before and after surface treatments.....106

LIST OF FIGURES

Figure 2-1: Structure of bone showing both compact (cortical) and trabecular (cancellous) bones. Osteon of compact bone and trabeculae of spongy bone are also highlighted along with blood supply for the bone [34].	9
Figure 2-2: Sketch of cells concerned with the production, maintenance and modelling of the osteoid [41]. All forms of bone cells including osteoblast (bone former), osteoclast (bone eater), osteocytes (mature osteoblast) and bone lining cells are highlighted in their respective position within bone matrix.	11
Figure 2-3: Phosphate based glass tetrahedra in Q^i terminology, where “i” represents the number of bridging oxygens per tetrahedron.	20
Figure 2-4: Schematic diagram of typical phosphate bridge; adapted from [77].	21
Figure 2-5: Schematic diagram of linear phosphate showing basic building block and a general formula structure for linear phosphate where n is an integer greater than 1, adapted from [77].	22
Figure 2-6: Preparation and hydrolysis of cyclo-phosphate.	23
Figure 2-7: Schematic diagram of metal cation effect on phosphate tetrahedra; structure adapted from [73].	24
Figure 2-8: Proposed scheme for CaP glass dissolution showing initial hydration of the P–O–P chains followed by stoichiometric dissolution; adapted from Rinehart <i>et al.</i>	27
Figure 2-9: Synthesis methods for high molecular weight PLA through ring opening polymerisation [124]	37

Figure 2-10: Ring opening polymerisation of lactic acid using Tin–octoate as catalyst [124].....	38
Figure 2-11: Simplistic schematic for hydrolysis of PLA showing cleavage of ester linkages within polymer backbone.....	39
Figure 2-12: In–vivo degradation mechanism for PLA	41
Figure 2-13: Different fillers (particle, flake, fibre) and respective composite.	43
Figure 2-14: Schematic of fibre types: Unidirectional, Chopped & Woven.....	44
Figure 2-15: A 5 step (hydrolysis, condensation, intermediate hydrogen bonding, rearrangement and surface grafting) coupling mechanism of silane on glass surface [164].....	52
Figure 2-16: Generic chemical structure for phosphonic acids	53
Figure 2-17: Chemical structure for phosphonopropionic acid with two different binding sites for glass and polymer matrix.	55
Figure 2-18: Chemical structure for etidronic acid with two distinct functional groups to react with glass and polymer.....	56
Figure 2-19: Chemical structure for amino–methyl phosphonic acid with –OH group to react with glass and NH ₂ to make covalent bond with polymer.	56
Figure 2-20: Chemical structure for glycerol phosphate, -OH group was expected to react with glass and –ONa to provide reactive site for polymer.....	57
Figure 2-21: Chemical structure for PLA–oligomer prior to functional group attachment	58

Figure 2-22: Chemical structure for hexamethylene diisocyanate before grafting on glass surface	58
Figure 3-1: Glass fibre drawing tower; glass is melted in the furnace (on the top) which is drawn into fibre and collected on the rotating drum (at the bottom).....	70
Figure 3-2: FTIR–ATR spectra of PBG with increasing a) Fe ₂ O ₃ content b) P ₂ O ₅ content showing change in glass structure within Q2 to Q1 species.	74
Figure 3-3: Representative high resolution XPS O1s spectra for a phosphate glass.	76
Figure 3-4: Density measurement of PBG measured using a pycnometer; Error bars represent standard error of mean where n=10. * indicating the statistical significance.	77
Figure 3-5: Effect of increasing Fe ₂ O ₃ content on degradation behaviour of PBGs containing fixed 40% P ₂ O ₅ content; error bars represents standard error of mean where n=3.....	79
Figure 3-6: Effect of increasing P ₂ O ₅ content on degradation behaviour of PBGs containing fixed 4% Fe ₂ O ₃ content; error bars represents standard error of mean where n=3.....	80
Figure 3-7: Metabolic activity of MG63 cells, as measured by the Alamar blue assay, cultured on PBGs up to 168 hours; Error bars represent the standard error of mean where n = 6. No significant difference found (P > 0.05) between glass samples.	81
Figure 3-8: Alkaline phosphatase activity of MG63 cells cultured on PBGs for 168 hours. The data is normalised to DNA concentration of samples. Error bars represent the standard error of mean where n = 6. * indicating significant difference between PBG samples.	82

Figure 3-9: Effect of neat aliquots of PBGs elution products (eluted for 7 days at 37°C) on MG63 cells viability, as measured by the NRU assay. Here, Higher NRU implies greater number of viable cells. Error bars represent the standard error of mean where n = 6. * indicating statistical significance. P50Fe4 was significantly lower than the rest of samples excluding TCP.....83

Figure 3-10: Melt drawn P45Fe4 glass fibre bundle, shows ease of fibre drawing with higher phosphate content84

Figure 4-1: Flow chart of PBG sample modification with different chemicals. Solvents (double distilled water (DDW), Ethanol, dimethylformamide (DMF), chloroform) were selected on the basis of solubility of surface treatment agents.98

Figure 4-2: Different events during the single–fibre pull–out test are indicated: 1) crack initiation 2) frictional debonding 3–4) crack completion 5) frictional zone steady pull–out and 6) end of frictional zone (pull out). Figure adapted from [207]. 100

Figure 4-3: A schematic diagram of (a) Push–out test sample with all dimensions L = length of glass rod; d = diameter of glass rod; l = thickness of PLA disc; b = diameter of PLA disc (b) push out test setup 101

Figure 4-4: IR spectra of (A) Control PBG; (B) APS mPBG; (C) EA mPBG; (D) HDI mPBG indicating the covalent bond between PBG and surface treatment agents. 105

Figure 4-5: High resolution XPS spectra of (A) Control PBG O1s and P 2p; (B) APS mPBG O1s and Si 2p; (C) EA mPBG O1s and P2p; (D) HDI mPBG O1s and N 1s.

O1s spectra indicate covalent bond formation and Si 2p, C 1s and N 1s spectra provide supplementary evidence.....	108
Figure 4-6: Representative curve obtained from load versus extension for glass rod push-out test adapted for this study, ▲ represents; F_{max} required for crack initiation and debonding.	110
Figure 4-7: IFSS values as measured by push-out test for 3-aminopropyltriethoxy silane (APS); 3-phosphonopropionic acid (PPA); Glycerol 2-phosphate disodium salt (GP); etidronic acid (EA); hexamethylene diisocyanate (HDI); sorbitol/sodium ended PLA oligomers. * indicating at significant difference compared to control.	111
Figure 4-8: Effect of surface treatments on glass degradation profile in PBS at 37°C. Error bars represent standard error of mean where n = 3.....	112
Figure 4-9: Wettability of mPBGs as measured by distilled water contact angle, error bars represent standard deviation where n=3. * indicating at significant difference.	113
Figure 4-10: Chemical reaction schemes devised on the bases of inorganic chemistry principles and surface analyses (FTIR/XPS) data.....	117
Figure 5-1: Cell viability of MG63 osteosarcoma, as measured by the neutral red uptake assay, cultured in culture medium with the extracts from modified phosphate glasses, x-axis represents concentration of extracts containing media in basal media and a summary of neat (100% extract containing media) aliquots from all treated glasses (x-axis represent treatments). Error bar represents standard error of mean, n = 6. * indicating significantly low NRU for Na-PLA and HDI treated phosphate glass.....	130

Figure 5-2: Metabolic activity of MG63 osteosarcoma, as measured by the alamar blue assay, cultured on modified phosphate glasses, x-axis represents surface treatments. Error bar represents standard error of mean, n = 6. * indicating significant difference of treated samples compared to control (PBG)..... 131

Figure 5-3 Cell proliferation of MG63 osteosarcoma, as measured by the DNA (Hoechst 33258) assay, cultured on modified phosphate glasses, x-axis represents surface treatments. Error bar represents standard error of mean, n = 6. There was no significant found for treated samples versus control (PBG) at any time point. 132

Figure 5-4: Alkaline phosphatase (ALP) activity of MG63 osteosarcoma cells, as measured by ALP assay, cultured on modified phosphate glasses, x-axis represents surface treatments. Data was normalised with corresponding DNA concentration for each individual sample. * indicating significant difference of treated samples compared to control (PBG). 133

Figure 5-5: Proliferation of primary human osteoblasts, as measured by the DNA (Hoechst 33258) assay, cultured on modified phosphate glasses, x-axis represents surface treatments. Error bar represents standard error of mean, n = 6. There were no significant found for treated samples versus control (PBG) at any time point. 134

Figure 5-6: Alkaline phosphatase (ALP) activity of primary human osteoblasts, as measured by ALP assay, cultured on modified phosphate glasses, x-axis represents surface treatments. Data was modified with DNA values obtained for each individual sample. Error bar represents standard error of mean, n = 6. * indicating significant difference of treated samples compared to control (PBG)..... 135

Figure 5-7: Amount of collagen produced by primary human osteoblasts, as measured by Sircol assay, cultured on modified phosphate glasses. Data was

modified with DNA values obtained for each individual sample. Error bar represents standard error of mean, n = 6. There were no significant found for treated samples versus control (PBG) at any time point..... 136

Figure 5-8: Quantity of osteocalcin produced by of primary human osteoblasts, as measured by ELISA assay, cultured on modified phosphate glasses, x-axis represents surface treatments. All data is modified with DNA values obtained for each individual sample. Error bar represents standard error of mean, n = 6. * indicating significant difference of treated samples compared to control (PBG)... 137

Figure 5-9: SEM images of human osteoblast cultured on phosphate based glass (control) up to 28 days. Arrows indicating at cluster of cells, cell matrix and mineralisation..... 139

Figure 5-10: SEM images of human osteoblast cultured on APS modified PBG up to 28 days. Arrows indicating at cluster of cells, cell matrix and mineralisation. 139

Figure 5-11: SEM images of human osteoblast cultured on GP modified PBG up to 28 days. Arrows indicating at cluster of cells, cell matrix and mineralisation. 140

Figure 5-12: SEM images of human osteoblast cultured on EA modified PBG up to 28 days. Arrows indicating at cluster of cells, cell matrix and mineralisation. 140

Figure 5-13: SEM images of human osteoblast cultured on SPLA modified PBG up to 28 days. Arrows indicating at cluster of cells, cell matrix and mineralisation. ... 141

Figure 5-14: SEM images of human osteoblast cultured on HDI modified PBG up to 28 days. Arrows indicating at cluster of cells, cell matrix and mineralisation. 141

Figure 5-15: SEM images of human osteoblast cultured on tissue culture polystyrene up to 28 days. Arrows indicating at cell matrix and mineralisation..... 142

Figure 6-1: Air-lay method fixture setup and random fibre mat. Chopped fibres were fed into to end of coned shaped metal box which was connected to high vacuum from its bottom end. Fibre mat was collected from the steel mesh..... 157

Figure 6-2: Initial flexural mechanical properties obtained for the untreated and surface-treated non-woven randomly dispersed PGF reinforced PLA composites produced with approximate fibre volume fraction of 20%. Error bar represents standard error of mean where n =3. 162

Figure 6-3: Initial flexural mechanical properties obtained for the untreated surface-treated unidirectional PGF reinforced PLA composites produced with approximate fibre volume fraction of 35%. Error bar represents standard error of mean where n =3. * indicating the significant difference with respect to control..... 163

Figure 6-4: PGF showing severe corrosion with EA exposure for 15 minutes (left) and 5 minutes (right). 164

Figure 6-5: EA modified PGF reinforced composite shows severe corrosion and inferior mechanical properties 164

Figure 6-6: Snap shots of random fibre composites APS (left) versus Control (right) shows non-uniform distribution of APS mPGF compared to control PGF within PLA matrix..... 165

Figure 6-7: SEM images of HDI treated random PGF reinforced PLA composite before (left) and after (right) 28 days of degradation in PBS at 37 °C. Arrows indicating at long fibre pull-out and holes representing interfacial integrity loss while circles pointing out short fibre pull-out and strong interface between PGF and PLA matrix. 166

Figure 6-8: SEM micrographs from top to bottom: untreated (control) composite, APS treated, SPLA treated, HDI treated unidirectional PGF reinforced PLA composite, before (left) and after (right) 28 days of immersion in PBS at 37°C. Micrometer scale-bar = 50µm. Arrows indicate holes and long fibre pull-out due to interface failure and circles highlight intact interfacial integrity and short fibre lengths. Better interface i.e. shorter fibre length was observed in case of HDI treated composites compared to others after 28 days of immersion. 167

Figure 6-9: Water–uptake profiles obtained for untreated and –treated PGF reinforced PLA UD composites produced with approximate fibre volume fraction of 35%. Studies were conducted for up to 4 weeks in PBS at 37 °C. Secondary y–axis presents the profile of SPLA series only. Error bar represents standard error of mean where n =3. 169

Figure 6-10: Degradation profiles obtained for untreated and –treated PGF reinforced PLA UD composites produced with approximate fibre volume fraction of 35%. Studies were conducted for up to 4 weeks in PBS at 37°C. Secondary y–axis presents the profile of SPLA series only. Error bar represents standard error of mean where n =3. 170

Figure 6-11: Flexural strengths of control and APS, SPLA AND HDI treated UD PGF/PLA composites. All degraded Samples were tested wet after immersion in PBS at 37°C. Due to rapid loss of mechanical strength SPLA series sample was not analysed after 14 days. Error bar represents standard error of mean where n =3. ... 171

Figure 6-12: Flexural modulus of control and APS, SPLA and HDI treated UD PGF/PLA composites. All degraded samples were tested wet after immersion in PBS

at 37°C. Due to rapid loss of mechanical strength SPLA series sample was not analysed after 14 days. Error bar represents standard error of mean where n =3...172

Figure 6-13: DNA concentration of primary human osteoblast cells, as measured by the DNA (Hoechst 33258) assay, cultured on modified PGF reinforced PLA composites; x-axis represents surface treatments. Error bar represents standard error of mean, n = 6. No significant difference was found amongst the samples.....173

Figure 6-14: Cell alkaline phosphatase (ALP) activity of primary human osteoblasts cultured on UD PGF reinforced PLA composite surfaces, as measured by ALP assay, x-axis represents surface treatments. All data is modified with DNA values obtained for each individual sample. Error bar represents standard error of mean, n = 6. * indicating significantly low ALP activity with respect to control.174

Figure 6-15: Collagen production by primary human osteoblasts cultured on modified UD PGF reinforced PLA, measured by Sircol assay. All values were normalised with DNA values for corresponding sample. Error bar represents standard error of mean, n = 6. * indicating significantly low collagen concentration on HDI treated sample compared to control.175

Figure 6-16: Collagen production by primary human osteoblasts cultured on PGF reinforced PLA composites, as measured by Sircol assay. Error bar represents standard error of mean, n = 6.175

Figure 6-17: Quantity of osteocalcin produced by of primary human osteoblasts, as measured by ELISA assay, cultured on PGF reinforced PLA composite surfaces, x-axis represents surface treatments. All data is normalised with DNA values obtained for each individual sample. Error bar represents standard error of mean n = 6. *

implies that osteocalcin level on day 14 was found significantly higher than treated composites..... 176

Figure 6-18: Quantity of osteocalcin produced by of primary human osteoblasts, as measured by ELISA assay, cultured on PGF reinforced PLA composite surfaces, x-axis represents surface treatments. Error bar represents standard error of mean, n = 6. 177

Figure 6-19: SEM images of human osteoblast cultured on (from top to bottom): untreated (control) composite, APS treated, SPLA treated, HDI treated unidirectional PGF reinforced PLA composite, after 14 days (left) and 28 (right) days of culture. Micrometer scale-bar = 50 μm . Arrows indicates at complete coverage of composite surface with cell matrix and circles pointing out glass fibre..... 178

CHAPTER 1. INTRODUCTION

1.1 Background

Fracture fixation for major load-bearing bones rely significantly on the development of mechanically strong and biocompatible materials [1]. Material's biocompatibility is the ability for a biological or synthetic material to operate without obstructing the host tissue for short or prolonged periods [2]. Although the above simplistic definition still stands, due to its complexity Williams [3], has divided medical devices' biocompatibility into subgroups of long-term implantable devices, short-term implantable devices and tissue-engineering products, defining them separately. For the purpose of this project we can use the definition of long-term implantable devices which states that "The biocompatibility of a long-term implantable medical device refers to the ability of the device to perform its intended function, with the desired degree of incorporation in the host, without eliciting any undesirable local or systemic effects in that host" [3]. For a typical implant, biocompatibility considerations include acute and local as well as systemic and chronic responses.

Metallic devices that are currently used as fracture fixation implants include but are not limited to stainless steel, titanium, cobalt/chromium and alloys of these metals. The common problems encountered with metal implants include allergic reactions to the metal, foreign body reaction and disuse atrophy due to stress shielding [4]. According to Wolff's law, disuse atrophy due to stress shielding is the natural resorption of bone due to the absence or reduction of necessary stress-induced

stimulation to the tissue to maintain its structure [4]. It is also suggested by Cater and Giori that an optimal stress is necessary for the development of bone during early stages of healing and maturation of healing bone [5]. Therefore, it can be deduced that transfer of force from the implant to bone is required during the healing period as fracture healing shifts from repair to remodelling. It is well known that the high stiffness of metal implants provides good initial support by taking off most of the load from healing bone. However, due to their very high modulus of elasticity (~60-230 GPa), metal implants hinders structural maintenance in the later stages of remodelling [6, 7].

It has been a major challenge for bioengineers to develop a synthetic device which can replace the current metallic alloy-based implants for fracture fixation with a fixation device [8, 9] that could provide strong support in the early stages of the implant period and allow the gradual transfer of the load to the healing bone during the later stages [4].

Different terms (e.g. degradable, absorbable, and resorbable) are being used to specify that a particular material will in time disappear after serving its function in a living organism. The American Society for Testing of Materials (ASTM) and the International Standards Organization (ISO) define degradable plastics as those which undergo a significant change in chemical structure under specific environmental conditions. These changes result in a loss of physical and mechanical properties, as measured by standard methods. However, a material can only be classified as bioresorbable if it is absorbed through bioabsorption by the tissues and organs of organisms. To accomplish a time dependent load transfer, the material should be

biodegradable as well as resorbable at a controlled rate. The degradation products also need to be biocompatible as the body metabolises them.

Bone repair devices made from degradable polymers alone, such as poly-(lactic acid) (PLA) have limitations in terms of matching the mechanical property requirements for bone repair, both initially and for the duration of repair [10, 11]. As a minimal requirement for load-bearing application, degradable polymer should possess initial mechanical properties closer to cortical bone i.e. tensile strength in the range of 100–200 MPa, compressive strength ~150 MPa, Young’s modulus ~25 GPa and fracture toughness of around 8 MPa/m^{1/2}. Table 1–1 provides different mechanical properties comparison of commonly used materials for bone fracture fixation applications.

Table 1-1: Mechanical properties of commonly used materials for fracture fixation in comparison with human bone. PGA: polyglycolic acid, PLA: polylactic acid, SR: Self-reinforced.

Material	Bending strength (MPa)	Shear Strength (MPa)	Elastic Modulus (GPa)	Reference
PGA	218	95	7	Christel 1980 [12]
SR-PGA	330-415	260	13-18	Tormala 1992 [13]
PLLA	40-140	-	5 to 10	Tormala 1998 [10]
PDLA	200	-	9	Weiler 1996
SR-PLA	228-274	140-152	5.4-8.4	Pihlajamaki 1992, Riih� 1993 [14, 15]
Stainless steel	465–950	-	205–210	Navarro 2008[16]
Titanium	620	-	100	Navarro 2008[16]
Bone	100-200	68	7 to 40	Reilly 1974, Rho 1998 [17-19]

Therefore, over the last two decades research has been focused on the development of composite materials that may provide solutions for the issues noted above.

Self-reinforced polymers have been developed with greater strength and improved Young's modulus [10, 13, 20, 21]. For example, self-reinforced poly-DL-lactide has been found to have moderate Young's modulus (~12 GPa) and acceptable biocompatibility, which made them useful as fixation screws. However, the strength was found to be insufficient for fixation of major load-bearing bones [10]. Totally degradable composites have also been fabricated with degradable fibres embedded within polymer matrix like PLA, poly (caprolactone) (PCL) and polyorthoester (POE), yielding tensile modulus values of 29.9 GPa. Lin *et al.* tested PLLA reinforced with 55% (by volume) biodegradable calcium phosphate glass fibres [22]. The initial mechanical properties of their samples with unidirectional fibres were well characterised: tensile, compressive, flexural, and short beam shear strengths were 200, 186, 161, and 19 MPa respectively, and tensile and flexural moduli were 29.9 GPa and 27 GPa respectively. However, samples retained only 35% and 45% of their tensile strength and modulus respectively after 23 days in buffered saline, pH 7.4, at 37 °C.

Recent work has explored degradable fibre reinforced composites, although the initial strength and modulus of the composites were found sufficient for load-bearing applications, the above mentioned composite experienced rapid loss of mechanical properties when exposed to *in-vitro* aqueous conditions [7, 23, 24]. The rapid degradation of the composite would result in improper fixation of the fracture during the early stages of healing and compromise the bone repair process.

This rapid drop in mechanical properties of the totally resorbable composites can be explained by two phenomena: the first, early hydration at the polymer-reinforcement interface which creates a molecular bonding gap and a stress concentration site

which prevent the transfer of stress from the polymer to the reinforcement. Polymer swelling is the second phenomenon which generates hydrostatic forces that could crack the reinforcement phase [7, 23, 24].

Therefore, strengthening the interface and decreasing polymer swelling are vital for long lasting mechanical properties of totally resorbable composite implant. If the interfacial degradation can be controlled then incremental loading onto bone may be possible with healing time.

Interfacial strength between polymer matrix and reinforcement can be improved by mechanical interlocking, plasma treatment or by promoting adhesion through surface treatments with suitable chemicals. However, only the chemical treatment approach was investigated during the course of the current project. The interface between the polymer and reinforcement phase was chemically bridged by using surface treatments agents.

1.2 Hypothesis

It is well established that the interface breakdown in composite material is a key factor responsible for the rapid loss of mechanical properties. This statement was also supported by previous work carried out at The University of Nottingham that [23-28]. The phosphate glass fibre reinforced polylactic acid composite material considered for this study breakdown due to the hydration of the material interface and polymer swelling, thus creating stress concentration sites in this region.

For the purpose of this study, it was hypothesised that the biocompatible chemicals that have been demonstrated to be capable of reacting (either covalently or through

hydrogen bonding) with free hydroxyl ions present on the surface of similar material (silica glass/hydroxyapatite) could also be used to modify phosphate glass surface. It was hypothesised that after chemical treatment phosphate glass surface will have a functional group that could react with polyester through a strong covalent bridge. It was expected that introduction of covalent bonds at the interface will improve interfacial integrity between two distinct phases of intended composite. Chemical treatment of phosphate glass surface, in some cases, may also introduce hydrophobicity at the interface which could provide better glass/polymer adhesion and cause delay in hydration in the region and help to reduce the internal stress of the system.

A better interface will also enable further control over the retention of mechanical properties of composite by providing predictable/efficient load transfer between the two phases of the composite. It was also recognised that all the chemicals selected for this study and the degradation products of the composites after chemical treatment should be non-cytotoxic and biocompatible.

1.3 Aims and Objectives

The aim of current project was to develop a phosphate glass fibre reinforced polylactic acid composite for bone fracture fixation applications. The composite was intended to be used as a load bearing bone-plate/screw fixation system. In particular, initial mechanical properties and their retention were aimed to improve by improving phosphate glass fibre and polylactic acid interface using chemical surface treatment of phosphate glass fibre. Initial flexural properties exceeding cortical bone (strength 100-200 MPa, Modulus = 10-30 GPa) and 70% properties retention after 4 weeks of

degradation were desirable [17-19, 29]. The proposed work in this thesis will cover the following specific objectives:

1. Production of a composition of phosphate based glass (PBG) with a target degradation rate, ease of fibre drawing and cytocompatibility
2. Identification of potential chemical treatments that can provide covalent link by reacting with both PBG and the polymer matrix
3. Identification of chemical surface treatments that can increase the hydrophobicity of phosphate glass
4. Development of a method to measure interfacial shear strength (IFSS) between PBG and PLA at a micro level and investigation of the effect of chemical agents on IFSS
5. Assessment of the *in-vitro* cytocompatibility of surface treatments agents using indirect and direct contact methods with human osteoblast cells
6. Synthesis and testing of chemically surface-treated phosphate glass fibre (PGF) reinforced PLA composite for flexural mechanical properties and cytocompatibility at a macro level.

CHAPTER 2. LITERATURE REVIEW

2.1 Introduction

This chapter reviews the literature on the structure and mechanical properties of bone, implantable fixation materials/devices, phosphate glasses and their properties, poly(lactic acid) (PLA) and its characteristics, chemical surface treatments and their mechanism to improve interfacial shear strength interfacial shear strength (IFSS) and finally biodegradable composites as fracture fixation devices.

2.2 Bone

Bone is a specialised form of connective tissue that provides internal support to the body in all higher vertebrates. In addition to its supportive function, it has several metabolic functions; it protects and encompasses the brain, the spinal cord and bone marrow, and plays an essential role in maintaining blood calcium levels and supporting haematopoiesis (the formation and development of blood cells) [30, 31]. Bones develop from an organic extracellular matrix, strengthened by the deposition of mineral. Although bones are hard and mineralized they are living tissue containing blood vessels and various cell types. A typical bone consists of a hard and compact outer shell (the cortex) which surrounds a hollow cavity that is filled with bone marrow. At specific locations, bone is strengthened with a fine network of sponge-like trabecular bone (Figure 2–1). The combination of the relatively dense cortex together with the relatively lighter trabecular bone gives the bone strength with minimal weight [30, 31].

The mineral substance of bone is a calcium phosphate called hydroxyapatite (HA): $\text{Ca}_{10}(\text{PO}_4)_6(\text{OH})_2$, which includes calcium phosphate, calcium carbonate, calcium fluoride, calcium hydroxide and citrate. The HA crystals are believed to be in the spaces between the collagen fibrils but their exact shape is under discussion [32]. The mineral phase of bone acts as an ion reservoir and largely responsible for the mechanical properties of bone. The mechanical properties of bone result from the impregnation of the soft organic matrix with the very hard and brittle HA crystals [30, 31, 33].

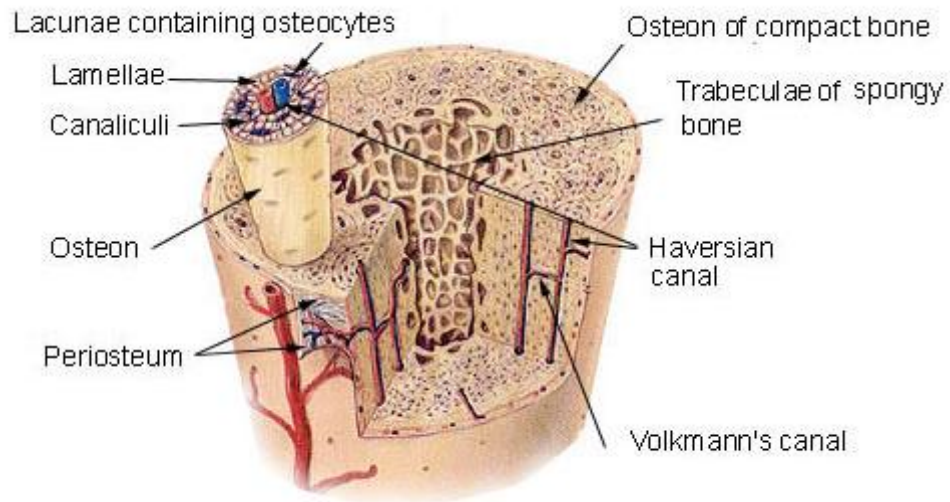


Figure 2-1: Structure of bone showing both compact (cortical) and trabecular (cancellous) bones. Osteon of compact bone and trabeculae of spongy bone are also highlighted along with blood supply for the bone [34].

2.2.1 Bone Cells

Bone is a dynamic tissue that is continuously maintained and renewed by four different kinds of bone cells: 1) osteoclasts, 2) osteoblasts, 3) osteocytes, and 4) lining cells (Figure 2-2). Osteoclasts are located at the bone surface where they are responsible for resorption of bone tissue. They are giant multinucleated cells and

resorb bone via local acidification and secretion of specific proteases. Acidification is necessary to dissolve the mineral in bone, whereas the proteases degrade the proteins of the extracellular matrix [35]. Osteoblasts are the bone forming cells; they synthesise the organic matrix of bone by secretion of a wide variety of extracellular matrix proteins. In addition to matrix production, they also participate in the mineralisation process and in the control of osteoclast function [36-38]. At the terminal differentiation stage of an osteoblast when it is entrapped in its self-produced bone matrix it is called an osteocyte. Osteocytes are the most abundant cells in bone they are sensitive to mechanical strains [39] and thus maintain bone remodelling by sensing mechanical strain and translate that strain into biochemical signals of resorption or formation related to the intensity and distribution of the strain signals [40]. They have a typical morphology with long thin cytoplasmic processes, which form a fine network of connections with other osteocytes and with the osteoblasts located at the surface of the bone (see osteocyte structures in Figure 2-2). Another bone cell that is formed by osteoblastic differentiation is the lining cell. Lining cells cover the bone surfaces and thus separate the bone surface from the bone marrow. However, the exact function of bone lining cells is still unclear [38]. Bone can be defined as a self-repairing structural material that is capable of adapting its mass, shape and properties to the changes in mechanical and physiological requirements through its cells. During bone remodelling bone mass is controlled by the balance between osteoclastic bone resorption and osteoblastic bone formation. First osteoclasts resorb bone by acidification and secretion of a wide variety of proteases and, in turn, osteoblasts replace the resorbed bone by producing new bone matrix.

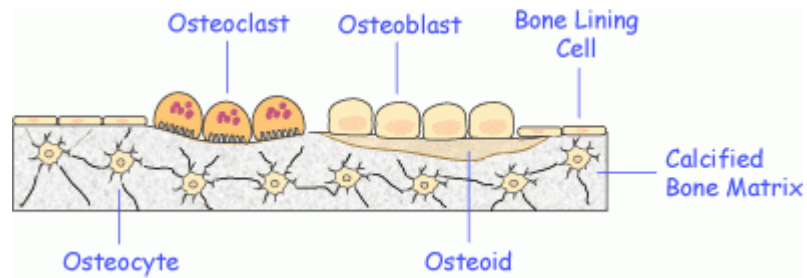


Figure 2-2: Sketch of cells concerned with the production, maintenance and modelling of the osteoid [41]. All forms of bone cells including osteoblast (bone former), osteoclast (bone eater), osteocytes (mature osteoblast) and bone lining cells are highlighted in their respective position within bone matrix.

2.2.2 Bone Repair

When fracture occurs, dense connective tissue and newly formed cartilage cover the fracture site to produce a fibro–cartilaginous callus to stabilise and bind the fractured bone. Meanwhile, osteoprogenitor cells differentiate into osteoblast cells that deposit new bone adjacent to both ends of the fracture site, invading the callus and replacing it with a bony callus. While compact bone is being formed, the bony callus is removed by the action of osteoclasts, and the gradual remodelling restores the bone to its original shape [42]. Bone repair can last from 6 to 12 weeks, but the healing process can be accelerated by the use of external materials such as plates and screws.

2.2.3 Mechanical Properties of Bone

The mechanical properties of bone can be measured by testing whole bone units or specimens prepared to isolate particular structural components. The mechanical properties of cortical bone have been reported extensively (Table 2-1). They can be measured via techniques such as: uniaxial compressive or tensile testing, or three or four–point bending for flexural properties. They have also been tested using

ultrasound techniques or micro and nano-indentation. Cortical bone exhibits a high degree of anisotropy. The values of mechanical properties are also reported to be dependent on animal species, bone location and testing conditions, age and disease. Testing conditions may also vary and affect the measured properties. For example, testing dry samples, testing wet samples at room temperature or 37 °C and embedding them or not [43]. For example, trabecular bone tested wet by three-point bending test method had an elastic modulus of 3.81 GPa [44], but an elastic modulus of 10.4 ± 3.5 GPa was reported for dry trabecular bone [19, 29]. Brear *et al.* determined the effect of variations in temperature (20–37 °C) on mechanical properties from a uniaxial compressive test. A 13 % decrease in the maximum strength at 37 °C was reported [45].

Table 2-1: Mechanical properties of human cortical and cancellous bone along with their testing conditions

Cortical Bone						
Test method	Strength (MPa ± SD)	Testing condition	Reference	Modulus (GPa)	Testing conditions	Reference
Tension	130 ± 20	Wet from various sites	[17, 46]	14.1	Rewetted	[17, 18, 47]
Compression	159 ± 4.1	Wet femur	[17, 48]	10.4	Wet	[17, 18]
Bending	164 ± 29	Wet femur	[17]	15.8	Wet	[17]
Cancellous Bone						
Tensile	-	-	-	10.4 ± 3.5 14.8 ± 1.4	Dry Wet	[19, 29]
Uniaxial Stress	0.34-7.72	Fresh frozen	[49]	-	-	-

Measuring the properties of cancellous bone is far more complex than cortical bone, due to the small dimensions of the individual trabeculae. It is speculated that

differences in moduli between cortical and cancellous bone are entirely due to the bone density. Thus, as can be seen in Table 2–1, some authors found value of elastic modulus of cancellous bone as high as those for cortical bone [17].

The Food and Drug Administration (FDA), USA has recommended the use of mechanical tests which are essential to demonstrate the effects of bone therapy [50]. However, in the scientific literature, the standardization of specific and reproducible mechanical tests evaluating properties of trabecular bone and compact bone has not been defined and there is a requirement to produce standardised test conditions and directions.

2.3 Implant Materials

Biomedical implants are used to restore, support or replace living tissue or organs that are performing below a satisfactory level. An implant's reliability heavily depends on the corrosion, wear and fatigue resistance of the materials used to make the implant. The most important characteristics of implant metals are biocompatibility, strength (yield, tensile and fatigue) and corrosion resistance [16, 51]. The material should be non-toxic, non-allergenic when placed *in vivo*, should not cause changes in plasma proteins or enzymes, should be inert and non carcinogenic and should have non mutagenic effects [16, 51]. Since the early 1900s, metal alloys have been used for these applications mainly due to their physical and chemical properties, such as strength, durability and corrosion resistance. Biomaterials include a wide variety of materials, such as metals, ceramics and polymers [52]. Further to this, two classes of materials may be combined to form a composite, which is a relatively new class of biomaterial. A self-reinforced

polymer however, has the same chemical composition of matrix and reinforcement phase, it will also be classed as composite due to different orientation of reinforcement (e.g. polymer fibres) and matrix polymer.

2.3.1 Metals

Three main classes of metals have been used in orthopaedics today: stainless steel, cobalt–chromium alloys and titanium (as alloys and as commercially pure). Orthopaedic applications of metal alloys include joint replacement surgery (arthroplasty), bone fracture fixation (osteosynthesis) and in spinal and maxillofacial devices.

For these materials to be considered as successful, they must have physical properties that allow the implant to perform the desired function, must be biocompatible or should not adversely affect the physiological environment. The corrosion resistance of metals and alloys is the key to the ease with which these materials interact with a particular environment [53].

Of the three families of metal alloys used today, stainless steel alloys 316 and 316L are probably the oldest [51]. Stainless steel is easy to machine, has a low content of impurities, and a high strength and ductility. However, poor erosion due to intergranular corrosion, pitting and fretting remained as a drawback for 316L [54]. Biocompatibility, and fatigue life of stainless steel is also considered inferior compared to other alloys. Stainless steel can corrode inside the body when in a highly stressed and oxygen depleted region, making it suitable for use only in temporary implant devices, such as fracture plates, screws and hip nails [51, 55].

Two types of cobalt chromium alloys; CoCrMo or vitallium (60% cobalt, 20% chromium, 5% molybdenum, and other substances like C, Fe, Ni, Mn and Si) and CoNiCrMo are being used. They have a higher corrosion resistance than the iron-based alloys, and are resistant to fatigue and to cracking caused by corrosion, yet have failed because of fatigue fracture. The superior fatigue and ultimate tensile strength of the wrought CoNiCrMo alloy make it suitable for long term applications [16, 51, 56, 57].

Titanium alloys is another family of orthopaedic alloys. For approval by the FDA, they are required to be comprised of at least the following elements, titanium, aluminium, and vanadium. Titanium and its alloys are very popular biomaterials due to their high strength, low weight, low modulus of elasticity (~60 GPa) and excellent corrosion resistance, however, they suffer from low fracture toughness and poor wear properties [42].

2.3.2 Ceramics

Ceramics are inorganic, non-metallic compounds with high strength and stiffness, resistance to corrosion and wear, and low density which makes them candidate material for a broad range of biomedical applications [58]. Ceramics can be used as implants in; dentistry as crowns, orthopaedics as joint and bone segment replacement and temporary bone repair devices [59]. Ceramics are also used as coatings for implants made of other materials to provide a biocompatible interface between the tissue and the implant [60]. Two most important ceramics in biomaterials are alumina and hydroxyapatite due to their high biocompatibility/bioactivity, high

compressive strength, wear resistance and high chemical stability in physiologic environment.

2.3.3 Polymers

There is a wide range of polymers used as biomaterials in number of different applications in human body with great success. The appropriate polymer should be chosen based on the body and tissue reactions, the mechanical and thermal properties and synthesis route. Examples of most commonly used polymers (Table 2-2) are; polymethylmethacrylate (PMMA), polytetrafluoroethylene (PTFE), polyurethane, polyvinylchloride (PVC), polydimethylsiloxane (PDMS) and polyesters like PLA, poly (glycolic acid) (PGA) and poly (caprolactone).

Table 2-2: Applications and required properties of commonly used polymers in biomedical implants. PMMA: Polymethylmethacrylate, pHEMA: Poly(2-hydroxyethyl methacrylate), PE: polyethylene, PEO: polyethylene oxide, PP: polypropylene, PLGA: poly(lactic-co-glycolic acid)

Application	Properties and design requirements	Polymers used
Dental	<ul style="list-style-type: none"> • stability and corrosion resistance, plasticity • strength and fatigue resistance, coating activity • good adhesion/integration with tissue • low allergenicity 	PMMA-based resins for fillings/prosthesis polyamides poly(Zn acrylates)
Ophthalmic	<ul style="list-style-type: none"> • gel or film forming ability, hydrophilicity • oxygen permeability 	polyacrylamide gels pHEMA and copolymers
Orthopedic	<ul style="list-style-type: none"> • strength and resistance to mechanical restraints and fatigue • good integration with bones and muscles 	PE, PMMA PLA, PGA, PLGA
Cardiovascular	<ul style="list-style-type: none"> • fatigue resistance, lubricity, sterilizability • lack of thrombus, emboli formation • lack of chronic inflammatory response 	silicones, Teflon, poly(urethanes), PEO
Drug Delivery	<ul style="list-style-type: none"> • appropriate drug release profile • compatibility with drug, biodegradability 	PLGA, silicones, HEMA
Sutures	<ul style="list-style-type: none"> • good tensile strength, strength retention • flexibility, knot retention, low tissue drag 	silk, catgut, PLGA, PP, nylon

2.3.4 Degradable Implants

Different terms (e.g. degradable, absorbable, and resorbable) are being used to specify that a particular material will in time chemically disintegrate into its basic units (e.g. $\text{CO}_2 + \text{H}_2\text{O}$ in case of polyesters) after serving its function in a living organism. Since degradable implant does not require to be removed they help to avoid complications associated with the presence of foreign materials in the body for a long period of time and also obviate the need of second surgery. For example, cobalt–chromium alloy has cobalt, chromium, nickel and molybdenum. There is a concern that the corrosion of cobalt–chrome in human body may release toxic ions into the body and thus possibly cause cancerous tumours [61].

Key issues that are associated with degradable materials include the biocompatibility, toxic contaminants (e.g. residual monomers and stabilizers) leaching and the potential toxicity of degradation products and metabolic residues. Degradable materials therefore have to go through tougher scrutiny than their non degradable counterparts [50, 62].

A natural tissue requires artificial support if it is weakened by disease, injury, or surgery. For example, during bone healing the degradable implant (screw, plate or nail) would provide temporary mechanical support until the broken bone healed and regained its strength. Therefore, the degradation rate of the implant needs to be customised to the healing rate of the surrounding tissue. For example, if a degradable material is used within a fracture fixation device the degradation rate of that device should not be faster than the rate of bone formation, and the rate of loss of mechanical properties for a fixation device should closely match the increase in

tissue strength to guarantee a steady stress transfer from implant to healing bone [63, 64].

Biodegradable products that have passed through tough scrutiny and have successfully been used in orthopaedic surgery include bio-resorbable sutures, pins, and bone fixation screws for non-load-bearing applications. The number and variety of biodegradable materials suitable for implantable devices is small as compared to the wide range of material properties required for implants and devices for various applications.

This gap in biodegradable material demand and limited availability of materials with suitable properties has forced researchers to develop composite biomaterials. The advantage of composite material is that they can be tailored to a particular application. A composite can be designed, within defined physical, chemical and/or mechanical properties depending on the base material properties.

2.4 Glasses and Glass Properties

Glass refers to a hard, brittle and amorphous solid, an inorganic product of fusion cooled to a rigid condition without crystallising. Common glasses contain silica as their glass former. However, some glasses do not contain silica as a major component or backbone these include fluoride glasses, phosphate glasses, germanate glasses and borate glasses [65].

2.4.1 Bioactive Glass

Due to their active interaction with bone cells and potential as reinforcement bioactive glasses are being studied as implantable material.

Bioactive-glass is a family of non-degradable bioactive material which can develop a bond with bone [66, 67]. It is a silica based glass that contains phosphate, calcium and sodium: the Ca/P molar ratio has to be at least 5 as bioactive glasses with lower ratios do not make a bond to bone [68]. After implantation, alkali ion/hydrogen ion exchange occurs producing an alkali deficient surface. Si–O–Si bonds in the glass hydrolyse to give silanols, resulting in a silica gel layer. Calcium, phosphate and carbonate ions adsorb onto the glass surface and crystallise to form hydroxyl carbonate apatite, it is this layer which bonds to bone.

Bioglass has been used extensively in non-load-bearing applications such as alveolar ridge augmentation and maxillofacial reconstruction. However, its use is limited by its brittleness, which present difficulties in shaping the implant and limits the applications [66].

2.4.2 Phosphate Glass

Phosphate glass is a special class of optical glasses that uses P_2O_5 as a network former like SiO_2 in silicate glasses. P_2O_5 is one of the four Zachariasen glass forming oxides; the other three are SiO_2 , GeO_2 and B_2O_3 . Due to the fast degradation of phosphate glass in aqueous environments, the research about its structure, properties and application was very limited. Van Wazer *et al.* suggested that with the addition of 30% molar fraction metal oxide, the degradation rate of phosphate glass can be reduced significantly [69].

2.4.2.1 Phosphate Glass Structure

The phosphate glass is formed by network linkages between the PO_4 tetrahedra. In vitreous P_2O_5 , these groups are connected to neighbouring units by three of their four vertices; one place is occupied by a terminal, doubly-bonded oxygen atom (DBO). The addition of metal oxide causes depolymerisation of the network with breaking the P–O–P links [69-73].

The tetrahedra are classified using the Q^i terminology, where “i” represents the number of bridging oxygens per tetrahedron (shown schematically in Figure 2-3). The networks of phosphate glasses can be classified by the oxygen to phosphorus ratio, which sets the number of tetrahedral linkages, through bridging oxygens, between neighbouring tetrahedra [74-76].

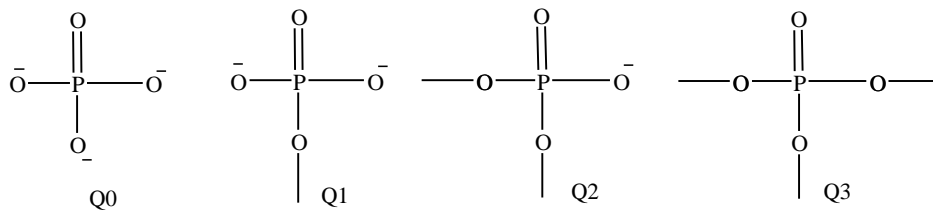


Figure 2-3: Phosphate based glass tetrahedra in Q^i terminology, where “i” represents the number of bridging oxygens per tetrahedron.

Phosphate glasses can be made with a range of structures, from a cross-linked network of Q^3 tetrahedra (vitreous P_2O_5) to polymer-like metaphosphate chains of Q^2 tetrahedra to “invert” glasses based on small pyro (Q^1) and orthophosphate (Q^0) anions, depending on the $[\text{O}]/[\text{P}]$ ratio as set by glass composition [74-76].

2.4.2.2 Classification of Phosphate

Phosphates are defined as compounds which contain P–O linkages. The P–O has a bond length of 1.62 Å, with bond angles of 130° at the O atoms and 102° at the P atoms.

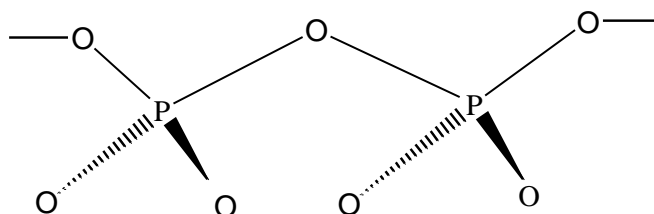


Figure 2-4: Schematic diagram of typical phosphate bridge; adapted from [77].

According to Graham [77], orthophosphates contain discrete $[\text{PO}_4]^{-3}$ ions while pyrophosphates and metaphosphates are now known as condensed phosphates, which are formed by repeated condensation (polymerisation) of tetrahedral $[\text{PO}_4]$ units, this result in chains of tetrahedra, each sharing the oxygen atom at one or two corners of the $[\text{PO}_4]$ tetrahedron.

Condensed phosphates are divided into three sub categories: linear polyphosphates, cyclophosphates (metaphosphates), and ultraphosphates. These are the most widely used families of phosphates and thus most of the research has been carried out in this field.

2.4.2.2.1 Linear Polyphosphates: ($[\text{O}]/[\text{P}] > 3.0$)

These are the salts of the linear poly–phosphoric acids. Figure 2-5 shows structure of linear polyphosphates. The basic building block of linear polyphosphate is the orthophosphate ion $[\text{PO}_4]^{-3}$. This can be denoted as the first member of chain series, with the di– and tri phosphate being the second and the third members, respectively.

Many polyphosphate are under research but alkali and alkaline earth metal salts have received most attention.

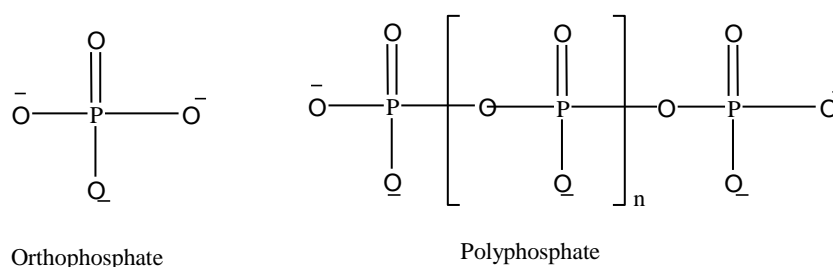


Figure 2-5: Schematic diagram of linear phosphate showing basic building block and a general formula structure for linear phosphate where n is an integer greater than 1, adapted from [77].

The long chain polyphosphates were originally called metaphosphates, and have been confused with ringed compounds. If the number of units in the polymer 'n' is very large, the formula of a chain polyphosphate $[(\text{PO}_3)^{n-1} \text{PO}_4]^{n+2}$ becomes indistinguishable from that of a true metaphosphate. The long chain compounds are sometimes termed as linear metaphosphates [77].

2.4.2.2.2 Cyclophosphates ($[\text{O}]/[\text{P}] = 3.0$)

According to IUPAC metaphosphate should be indicated with the term cyclo. It is the family of ring compounds with the composition $[\text{P}_n\text{O}_{3n}]^{-n}$, where n can have any value.

They can be prepared by heating orthophosphates and on hydrolysis produce corresponding polyphosphate and then eventually split into orthophosphates ions (Figure 2-6) [77].

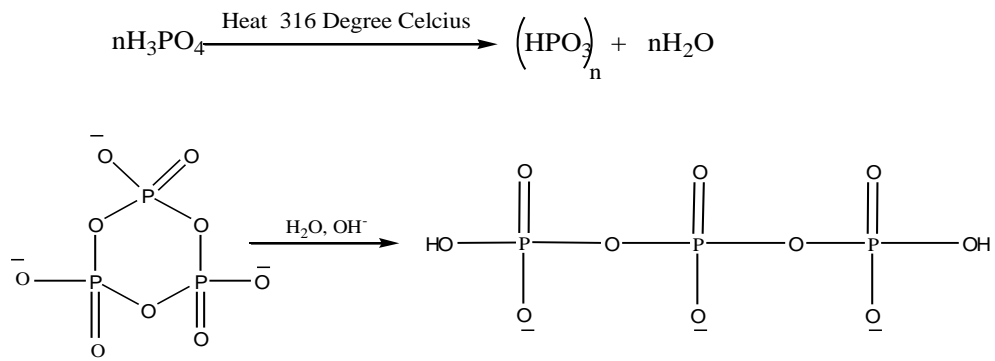


Figure 2-6: Preparation and hydrolysis of cyclo-phosphate

2.4.2.2.3 Ultraphosphate: ($2.5 < [O]/[P] < 3.0$)

The ultraphosphates are one of the simplest compositions. If the bridging oxygen (BO) of one PO_4^{-3} tetrahedral in phosphate glass is attached with neighbouring PO_4^{-3} tetrahedral, then it is called as metaphosphate or Q^2 species. On the other hand, if it consists of three BOs it is known as Q^3 units or ultraphosphate and its structure is a 3D network.

2.4.2.3 Classification of Phosphate With Respect to Modifiers

Phosphate glass can also be classified into different categories with respect to number of network modifiers included in the structure.

2.4.2.3.1 Vitreous Glass ($[O]/[P] = 2.5$)

A glass produced by P_2O_5 only, without using any additives, is called a vitreous phosphate glass. Some work has been carried out but is limited due to its poor durability in aqueous environment.

2.4.2.3.2 Binary Phosphate Glasses

By introducing network modifiers like Ca or Na, the structure and properties of the glasses can be changed significantly. Generally, when an alkali oxide is added to

phosphate glasses, the structural groups change from Q^3 to Q^2 to Q^1 to Q^0 depending on the change in the ratios of M_2O (or MO)/ P_2O_5 changes from 0 to 1 to 2 and to 3 as depicted in the Figure 2-7 [69-73].

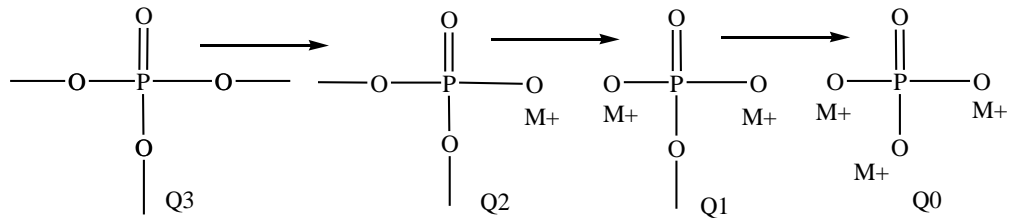


Figure 2-7: Schematic diagram of metal cation effect on phosphate tetrahedra; structure adapted from [73].

Figure 2–7 also indicates different species of condensed glasses, classified into four groups on the basis of P_2O_5 to M_2O ratio.

$P_2O_5 + 3 M_2O$ (orthophosphates)

$P_2O_5 + 1 \text{ to } 2 M_2O$ (pyrophosphates)

$P_2O_5 + 1 M_2O$ (metaphosphates)

$P_2O_5 + <1 M_2O$ (ultraphosphates)

A large amount of work has been carried out to understand the complex structure of these glasses [74-76, 78-80]. According to Van Wazer, the phosphate glass network is formed mainly by the linkages between the PO_4 tetrahedra. In case of vitreous P_2O_5 , these groups are connected to adjacent units by three of their four vertices; one place is occupied by a terminal, doubly bonded oxygen atom (DBO). Addition of metal oxide results in a depolymerisation of the network with breaking P–O–P links [69-73]. For several compositional series of glasses, this breakage is confirmed by determining the frequencies of phosphorous atoms in tetrahedral units with different numbers of links using P magic angle spinning nuclear magnetic resonance (MAS–

NMR) [76] and by O (1s) X-ray photoelectron spectroscopy (XPS) [81] obtaining the ratio of bridging to NBO (terminal) sites. However, in Hoppe's theoretical model, based on published data, and knowledge about the ultraphosphate region, in addition to the depolymerisation process there are other structural principles at work [78]. For a simple system consisting of the P_2O_5 network former to which a metal oxide is added, initially there is a large excess of terminal oxygen atoms in the pure P_2O_5 . As the metal (M) is added, it initially occupies positions with high M–O coordination numbers surrounded by terminal oxygen atoms on M–O–P bridges. However, as the M content increases, a point is reached at which all the terminal oxygen atoms occupy this M–O–P state. As the M content is now further increased, a modified random network develops.

2.4.2.3.3 Ternary Phosphate Glasses

Ternary phosphate glass is a system that contains two oxides other than phosphate. A significant amount of work has been carried out on this type glasses, particularly Na_2O – CaO – P_2O_5 system of glasses [82-87]. The addition of oxides helps to reduce the degradation rate of phosphate glass. For example, Ahmed *et al.* reported variation in degradation rate between $0.58 \times 10^{-3} \text{ mg cm}^{-2} \text{ h}^{-1}$ for P50Ca40Na10 to $1.55 \times 10^{-4} \text{ mg cm}^{-2} \text{ h}^{-1}$ for glass P45Ca40Na15 (numbers after element symbols indicate molar concentration of oxides) [85].

2.4.2.3.4 More Complex Glass Systems

Adding more modifiers may result in more complex but useful glasses and could potentially give more control over degradation rate of the glass. A significant amount of research has been carried out on quaternary and more complex glasses with

$\text{Na}_2\text{O}-\text{CaO}-\text{K}_2\text{O}-\text{MgO}-\text{Fe}_2\text{O}_3$ and more recently titanium or strontium oxides as modifier with P_2O_5 network-former [88-95]. Degradation products from the phosphate glasses containing modifiers like calcium, magnesium, strontium, silver, and/or copper could open new application for phosphate glasses. For example glasses containing calcium or strontium are reported to be favourable for osteoblastic bone regeneration [85, 86, 96] and 10% CuO doped glasses were found most effective in killing the pathogen *staphylococcus epidermidis* [93].

2.4.2.4 Phosphate Glass Degradation

The rate of PBG dissolution is sensitive to its composition and it can be varied from a few hours (e.g. binary sodium phosphate glasses) to years (e.g. lead iron-phosphate glasses) [97]. Factors affecting the rate of hydrolysis of a condensed phosphate solution are: the number of corners shared by the PO_4 tetrahedra in the structure, the temperature, pH and concentration of ions within media [98].

According to Bunker *et al.* PBGs dissolve uniformly due to acid or base catalysed hydration of the polymeric phosphate network. He also suggested that the dissolution mechanism involves hydration of entire chains rather than cleavage of P-O bonds by hydrolysis [99].

On the other hand, based on a real time dissolution study of phosphate glass and dissolution theory of silica glass, suggesting that the degradation process for silica glass is initially nonlinear due to an ion exchange process followed by a linear glass dissolution process, a two-step dissolution theory for calcium phosphate glass was devised by Rineheart *et al.* It was suggested that initial hydration of the P-O-P

chains followed by stoichiometric dissolution of both the phosphate chains of the network and the cationic modifier ions are shown in Figure 2-8 [100].

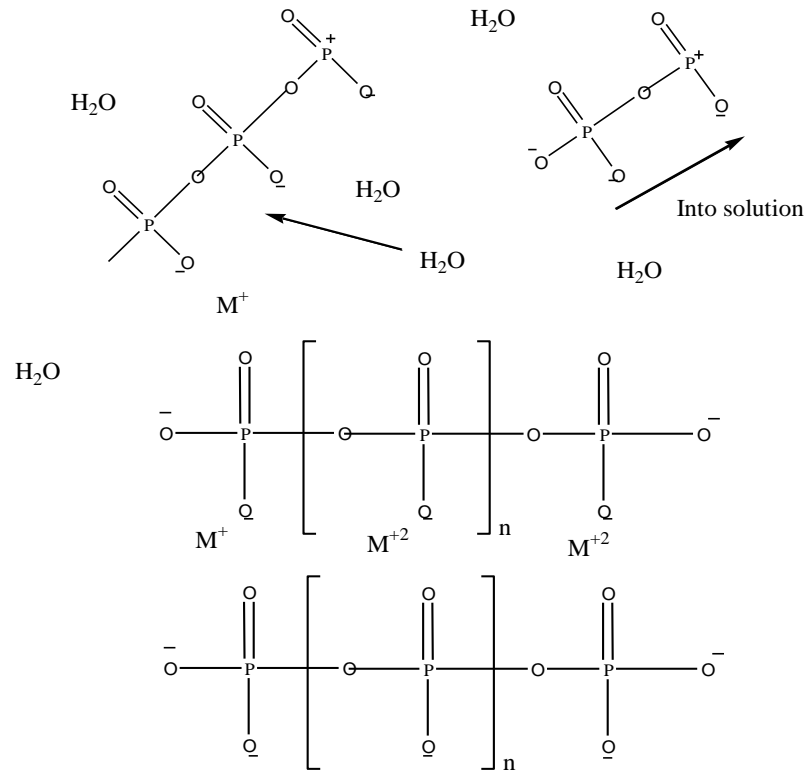


Figure 2-8: Proposed scheme for CaP glass dissolution showing initial hydration of the P–O–P chains followed by stoichiometric dissolution; adapted from Rinehart *et al.*

Although, this theory is well accepted amongst the researchers [85, 89, 92, 101, 102] no further work was carried out to provide practical evidence on glasses with simple and modified structure with cations such as Fe^{3+} or Al^{3+} .

2.4.2.4.1 Effect of Modifier on PBG degradation

From the work carried out on binary, ternary and quaternary PBGs it is clear that change in molar concentration of different modifier induces change in degradation rate of the glass.

For example, a study was carried out on ternary glass systems P_2O_5 –CaO– Na_2O by fixing the P_2O_5 content to 45, 50 and 55 mol%, and varying the CaO content at 30, 35 and 40 (molar %), it was reported that the dissolution rates reduced around an order in magnitude with an increase in CaO content [85]. The effect of CaO is well established now and is reported in many studies [83, 84, 86, 103]. However, these studies did not indicate effective minimum or maximum concentration of CaO content nor provided a comparison of CaO effect on degradation rate with other modifiers.

Increase in Fe_2O_3 content has also found to reduce the degradation rate of the glass significantly, in fact effect of Fe_2O_3 solubility of PBG was found to be greater than any other modifier and it is attributed toward its function as network former in addition to network modifier [92, 104, 105]. For example, Strohner *et al.* studied a ternary (P_2O_5 – Fe_2O_3 – Na_2O) phosphate glasses, containing from 14 to 43 mol% Fe_2O_3 and up to 13 mol% Na_2O . They reported that the glasses containing more than 25 mol% iron content demonstrated excellent chemical durability. The dissolution rate at 90°C in distilled water or in saline solution was up to 100 times lower than that of window glass. The durability of these glasses was attributed to the replacement of P–O–P bonds by stronger P–O– Fe^{2+} and P–O– Fe^{3+} bonds confirmed by Mossbauer–effect spectra [104].

MgO has been reported to have significantly reduced the degradation of phosphate glasses [89, 106]. The effect of MgO was evaluated in a quaternary glass system (P_2O_5 –CaO– Na_2O –MgO) and it was found that by replacing Ca^{2+} with smaller ionic radius Mg^{2+} the degradation rate of glass starts to decrease. However, no explanation of this unexpected behaviour was provided but, it reveals that not only valence but

the ionic radius of the network modifier affects the solubility of PBG [89]. Similar effect of MgO was reported by Ahmed *et al.* who found a decrease in degradation rate of almost two orders of magnitude between glass MgO 0 mol% and MgO 30 mol% when NaO content was replaced in quaternary glass system $40\text{P}_2\text{O}_5-25\text{CaO}-x\text{MgO}-y\text{Na}_2\text{O}$ [106]. Ahmed *et al.* supported the magnesium anomaly observed in their experiments with previous reports by Suzuya *et al.*, Hoppe *et al.*, and Walter *et al.* who postulated that with higher MgO, phosphate glass structure changes from the open structure of the metaphosphate glass to a more compact structure. However, the reason for unexpected high decrease in degradation rate was left unanswered [78, 107, 108].

It can be deduced from all the studies reported above and research work reported in the literature that by changing the glass composition, some control over degradation rate can be achieved. The literature available on PBG dissolution studies have used different degradation medium (distilled water, PBS and HBSS) and a range of temperatures from room temperature, 37°C to 90°C and even variation in medium change time from continuous flow to static environment, this makes it difficult to compare results from various studies. Therefore, it would be desirable that standard testing condition (BSI-ISO 10993) be followed in order to correlate the results from different reports.

2.4.2.5 Cytocompatibility Studies on PBGs

Over the past few years an increased interest in PBGs for use as or within degradable implant materials has been observed. However, most of the research focused on glasses containing 40–50 mol% P_2O_5 or above. A number of cytocompatibility

studies have been carried out [89, 109-116] some on ternary [88, 117] and other on quaternary [100] PBG systems. Most of these studies focused on the analysis interaction of osteoblast like cell with PBG using alkaline phosphatase and alamar blue assays. As a general opinion, with increase in CaO within phosphate glass content the cytocompatibility of the glass tends to increase which was attributed to the slower degradation rate. A few studies have also reported the effectiveness of iron containing PBGs in cell adhesion and proliferation and attributed it to slow degradation rate of iron containing phosphate glasses [85, 114, 115].

Bitar *et al* investigated the cellular response on glasses in ternary system $50\text{P}_2\text{O}_5-x\text{CaO}-(50-x)\text{Na}_2\text{O}$ with x between 30 and 48 mol%. The cytocompatibility of the glasses was assessed using human osteoblasts and fibroblasts which were seeded directly on glass discs and assessed for adhesion, proliferation, and maintenance of phenotypes. Results of this study indicated that higher calcium content supported the attachment, growth and maintenance of differentiation of both cell lines. This improvement was attributed to the fact that an increasing CaO content decreases the solubility of the glasses. However, no correlation between glass chemistry and degradation products on the results was proposed [110].

Salih *et al.* tested the cell compatibility of glasses in the system $45\text{P}_2\text{O}_5-x\text{CaO}-(55-x)\text{Na}_2\text{O}$ (where, x varies between 8 and 40 mol %) using two human osteoblast cell lines (MG63 and HOS TE85). Cells were cultured on tissue culture plastic with glass extracts in the medium, cell proliferation and gene expression was assessed. Here the results showed that extracts of highly soluble phosphate glasses inhibit the growth and antigen expression while glasses with lower solubility and high Ca^{2+} ion releases improved proliferation of cells and expression of different antigens. The authors

however speculated that the difference in pH and leaching of different ionic species would have affected the cell proliferation and protein expression but stated that the observed effect of glass extracts on cell proliferation and protein expression had no clear reason [84].

Glass elution extracts in cell–material interaction experiments can give results which probably do not represent the actual interaction of cells in direct contact with the material. To confirm this Navarro *et al.* tested the cytocompatibility of two glasses in the system $44.5\text{P}_2\text{O}_5-44.5\text{CaO}-(11-x)\text{Na}_2\text{O}-x\text{TiO}_2$ where x was 0 and 5 mol%. Human skin fibroblasts were cultured in medium containing glass extracts alongside cells directly cultured on glass plates simultaneously, cytotoxicity and proliferation were measured. Their results demonstrated that the information given by two methods cannot be considered as equivalent. They also verified that the *in vitro* behaviour (toxicity, adhesion and proliferation) of soluble phosphate glasses is adjusted by the solubility of the glass. While the glass free of titania, which demonstrated a solubility 10 times higher than the titania containing glass, demonstrated more toxic response in cell cultures, cell adhesion was enhanced. In the same study Navarro *et al.* also suggested that it is difficult to estimate the *in vivo* behaviour of the cells with the *in vitro* results of cell–material interaction. The titania–free glass was evaluated in rabbit’s dorsal subcutaneous tissue and showed a good biocompatibility and did not present any adverse reaction, even with its rapid solubility. This was supported with the argument that within an *in vivo* model, the local chemical changes are buffered by the physiological environment and continuous circulation of body fluids helped to smooth local conditions [118].

Franks *et al.* investigated the response of a human osteosarcoma cell line (MG63) to glasses of the quaternary system $45\text{P}_2\text{O}_5-(32-x)\text{CaO}-23\text{Na}_2\text{O}-x\text{MgO}$, where x was between 0 and 22 mol%, glass extracts in different dilutions were used to evaluate the cell compatibility of the glass samples; an MTT test was used to measure cell proliferation. Here, results of the cell proliferation assay suggested that the growth of MG63 cells in the presence of glass extracts of four different dilutions remained largely unaffected. After five days in culture, enhanced cell proliferation was reported for some cases, particularly for those glasses containing 7 mol% MgO or more. However, the reasons for the apparent beneficial effect of these glasses have not been addressed [89].

Skelton *et al.* [115] also studied the effect of increasing CaO on the behaviour of osteoblast and osteoblast-like cells in the ternary glass system $50\text{P}_2\text{O}_5-(50-x)\text{CaO}-x\text{Na}_2\text{O}$, where x was either 2, 4, 6, 8 or 10. It was suggested that the degradation products and other factors like pH were causing an unfavourable effect on osteogenic cell adhesion, proliferation, differentiation and cell death due to the fast dissolution rates of these glasses. Only PBG containing 48 mol% CaO was able to support some osteogenic proliferation and early differentiation [115].

Ahmed *et al.* [109] investigated phosphate glass fibres (PGF) for use as cell delivery vehicles for cell transplantation purposes. Fibres in the system $\text{P}_2\text{O}_5\text{-CaO-Na}_2\text{O-Fe}_2\text{O}_3$ containing fixed 50 mol% P_2O_5 , and varying CaO (30, 35 and 40 mol %) and Fe_2O_3 (1 to 5 mol %) balancing with Na_2O were tested with focus on their biocompatibility using a conditionally immortal muscle precursor cell (MPC) line. Cells were cultured directly onto the glass fibre surface and their ability to replicate and differentiate *in vitro* was studied. It was suggested that adding 4 to 5 mol%

Fe_2O_3 to the original $\text{P}_2\text{O}_5\text{-CaO-Na}_2\text{O}$ ternary composition reduced the glass degradation rate significantly and sufficient cell attachment and proliferation was achieved.

In another study on much more complex glass system, $\text{P}_2\text{O}_5\text{-CaO-CaF}_2\text{-MgO-ZnO}$, Lee *et al.* seeded a murine pre-osteoblast MC3T3-E1 cell line in order to determine the cytocompatibility of glasses with about 44 mol% P_2O_5 . Proliferation, differentiation and calcification were assessed. It was reported that no significant difference in cell proliferation was found on the phosphate glass and tissue culture polystyrene (TCP) controls, therefore it was concluded that the glass was non-cytotoxic. It was also reported that the cell metabolic activity was significantly enhanced and promotion of bone-like bumps formation by the calcium phosphate glass was observed at seven days or after. Apparently the phosphate glass enhanced both differentiation and calcification of MC3T3-E1 cells [116].

Uo *et al.* investigated the cytotoxicity of water soluble ternary ($\text{Na}_2\text{O-CaO-P}_2\text{O}_5$) glasses with increasing P_2O_5 and CaO contents. They found that cytotoxicity increased with greater than 50% P_2O_5 content, whilst decreasing with CaO content. This effect was attributed to a reduction in pH and higher ion concentration in the media. However, the glass studies in Motohiro Uo *et al.* study were all fast degrading and thus they reduced the pH of the distilled water from 7 to 1 [119].

Abou Neel *et al.* investigated the effect of Fe_2O_3 addition to ternary and quaternary phosphate glasses and illustrated a positive effect of increasing Fe_2O_3 content on osteoblast-like cells which was attributed toward the reduced solubility of the glass as discussed and seen above. It was suggested that an addition of 4 to 5 mol% Fe_2O_3

in the system (50 P₂O₅–30 Na₂O–(20–x) CaO) is suitable for desirable cell response [92].

Quinternary compositions (37P₂O₅–29CaO–10MgO–24Na₂O in mol %) with additions of silica and titanium were recently investigated by Brauer *et al.* [101]. They showed that addition of TiO₂ decreased the solubility of the glass in water and in simulated body fluid. It was hypothesised that dissolution rates of the glasses affect the proliferation of osteoblast-like cells (MC3T3–E1.4 murine preosteoblast). Cells were cultured over 24 and 72 h, the results demonstrated increasing cell proliferation with decreased solubility of the glass. It is recommended that resorbable bio-materials need the adjustment of degradation rate so as to facilitate cell adhesion and proliferation.

Soluble phosphate glasses have the potential to be used as degradable hard/soft tissue fixation materials. The results published in the literature can be important for some applications in the field of biomaterials for bone repair or also in the field of tissue engineering for the development of substrates with controlled dissolution rates. The control over PBG degradation rates is the key advantage which seems to play important role for implant materials and tissue engineering. However, most of the studies failed to provide correlation between the observed results with glass chemistry, pH and degradation products and only emphasised solubility of the glass. It is desirable that the effect of different ionic species leached from the glass on the cell functions should also be studied and discussed separately.

2.4.3 Biodegradable Polymers

Biodegradable polymers can be classified as natural (e.g. fibrin, collagen, chitosan, and gelatine) and synthetic polymers (e.g. PLA, PGA, PCL, and POE). Biodegradable polymers in general have a number of advantages over other materials in medical applications. Synthetic polymers offer key advantages like ability to tailor mechanical properties and degradation rate to suit a variety of applications. They are easy to process and can be moulded into various shapes with required features. Furthermore, polymer chemistry allows us to incorporate various functional groups and bioactive agents which can assist tissue in-growth.

Among the families of synthetic polymers, the polyesters family has been the most attractive choice for medical applications because of, ease of degradation by hydrolysis of ester linkage, degradation products being resorbed through the metabolic pathways in some polymers and choice to tailor the structure and to adjust degradation rates. Biodegradable polyesters like PLA, PGA and PCL have also been reported as potential materials for tissue engineering applications [120]. PGA, PLA, PCL and their copolymers have been used in a number of clinical applications such as; resorbable sutures; drug delivery systems and orthopaedic fixation devices (pins, rods and screws) [121, 122].

A comprehensive summary of the properties of biodegradable polymers was presented by Pathiraja A.Gunatillake and Raju Adhikari in their review of biodegradable polymers and which is summarised in Table 2-3 [123].

Table 2-3: Thermal, mechanical, and degradation properties of degradable polymers used as biomaterials. Properties are representative of bulk material without any reinforcement or cross linking.

Polymer	T _m (°C)	T _g (°C)	Strength or elastic modulus	Degradation time (Months)	Degradation Products
PGA	225 to 230	35 to 40	7 GPa (Modulus)	6 to 12	GA
PLLA	173 to 178	60 to 65	2.7 GPa (Modulus)	>24	LLA
PDLLA	amorphous	55 to 60	1.9 GPa (Modulus)	12 to 16	D,LLA
PDLA/PGA (85/15)	amorphous	50 to 55	2 GPa (Modulus)	5 to 6	D,LLA+GA
PCL	58 to 63	-60 to -65	0.4 GPa (Modulus)	>24	Caproic acid
PPF	-	-	2-30 MPa (compressive)	composition dependent	FA/PPG/PAFA
PCH	-	-	1.3 GPa (Modulus)	12	Dicaboxalic acid
PC	-	-		Very slow	Tyrosine/CO ₂
PU/LDI+PCL	-	-	8-40 MPa tensile strength	1 to 2	Lysine, caproic acid

2.4.3.1 Poly (Lactic Acid)

PLA belongs to the family of aliphatic polyesters commonly made from alpha-hydroxy acids. PLA is a thermoplastic of high-strength and modulus that can be synthesised from renewable resources to be used in industry as packaging material or the biocompatible, bioabsorbable medical device market. PLA is easy to process using standard plastics processing equipment to yield film, fibres or moulded parts [124].

PLA is a rigid thermoplastic polymer that can be semi-crystalline or totally amorphous, depending on the stereo-purity of the polymer backbone. L(-)-lactic

acid is the natural and most common form of the acid, however, D(+)-lactic acid can also be produced synthetically. It is one of the few polymers in which the stereochemical structure can easily be modified by polymerising a controlled mixture of the L- or D-isomers to yield high molecular-weight amorphous or crystalline polymers that can be used in food industry and are generally recognized as safe (GRAS) [125]. PLA degrades by simple hydrolysis of the ester bond and does not require the presence of enzymes to catalyse this hydrolysis. The rate of degradation is dependent on the size and shape of the article, isomer ratio and temperature.

2.4.3.1.1 Synthesis of PLA

PLA can be synthesised by both direct condensation of lactic acid and most commonly by the ring-opening polymerization of the cyclic lactide dimer, as shown in Figure 2-9.

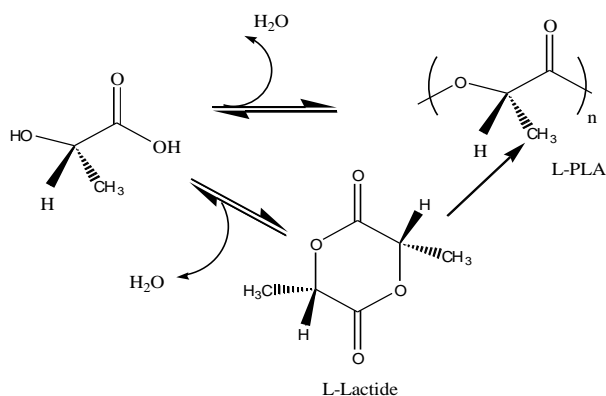


Figure 2-9: Synthesis methods for high molecular weight PLA through ring opening polymerisation [124]

Lactic acid (2-hydroxypropionic acid), the basic building block for PLA, is a highly water-soluble, three-carbon chiral acid that is naturally occurring and is most commonly found in the L(-) form. Tin compounds, especially tin(II) bis-2-ethylhexanoic acid (tin-octoate), are preferred for the bulk polymerisation of lactide

due to their solubility in molten lactide, high catalytic activity, and low rate of racemisation of the polymer.

The polymerisation of lactide monomer using tin octoate is generally explained via a coordination–insertion mechanism with ring opening of the lactide to add two lactyl units (a single lactide unit) to the growing end of the polymer chain shown in Figure 2-10 schematically.

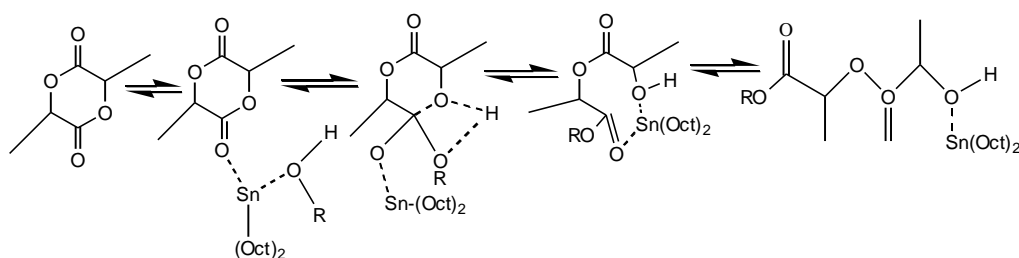


Figure 2-10: Ring opening polymerisation of lactic acid using Tin–octoate as catalyst [124]

Typical conditions for polymerisation are 180°-210°C, tin octoate concentrations of 100-1000ppm, and 2-5h to reach 95% conversion.

2.4.3.1.2 Physical Properties of PLA

Several reviews have been published indicating the physical properties of PLA (Table 2-4) [124, 126, 127]. To summarise these reviews, the physical properties of high molecular weight PLA are dependent on its transition temperatures for common qualities such as density, heat capacity, and mechanical and rheological properties. Depending on the stereochemistry and thermal history, in the solid state, PLA can be either amorphous or semi–crystalline. For semi–crystalline PLAs, T_g (~58°C) and T_m (130–230°C) are strongly affected by overall optical composition, primary structure, thermal history, and molecular weight. Above T_g , amorphous PLA undergoes

transition from glassy to rubbery and will behave as a viscous fluid upon further heating. Below T_g , PLA behaves as a glass with the ability to creep until cooled to its β -transition temperature of approximately $-45\text{ }^\circ\text{C}$. Below this temperature PLA will only behave as a brittle polymer [127].

Table 2-4: Range of physical properties for PLA as reported in the literature [126-129]

Properties	Values	Testing conditions or standard
Molecular weight (Daltons)	100,000 to 300,000	-
Glass transition temperature $^\circ\text{C}$	66–70	ASTM D3417
Melting temperature $^\circ\text{C}$	130–216	ASTM D3418
Crystallinity	10–40%	Anhydrous
Surface energy (dynes)	38	-
Specific gravity	1.25	ASTM D792
Melt-index range (g/10min)	2–20	ASTM D1238

2.4.3.1.3 Degradation and Hydrolysis of PLA

Degradation of the aliphatic polyesters occurs by bulk erosion. Degradation starts primarily with hydrolysis of the ester linkages, which occurs more or less randomly along the backbone of the polymer. It requires the presence of water according to the reaction schematically presented in Figure 2-11.

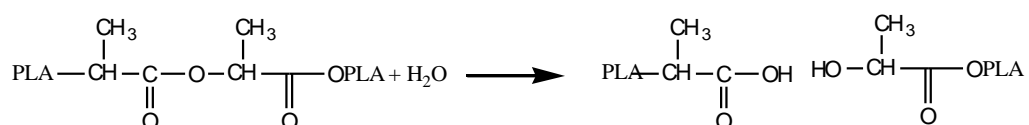


Figure 2-11: Simplistic schematic for hydrolysis of PLA showing cleavage of ester linkages within polymer backbone.

In vivo studies have shown that monomeric acids can be eliminated from the body through the Krebs cycle (citric acid cycle), primarily as carbon dioxide and water in urine. The rate of hydrolysis of the polymer chain is dependent on large changes in temperature and pH or presence of catalyst. Therefore, very little difference is reported in rate of degradation at different body sites [130].

2.4.3.1.4 Mechanical Properties of PLA

Investigative work has been carried out to measure the mechanical properties of different PLAs. A summary of the research is given in the Table 2-5 [126-128, 131].

Table 2-5: Mechanical properties of bulk L-PLA compared to D-PLA with an average molecular weight of 55000 Daltons. Mechanical characterization was performed on specimens maintained in anhydrous conditions [128, 131]

Mechanical properties	L-PLA	D,L-PLA	Standard used
Yield Strength (MPa)	70	53	ASTM D882
Tensile Strength (MPa)	66	44	ASTM D882
Elongation at Break (%)	7	5.4	ASTM D882
Flexural Strength (MPa)	106	88	ASTM D790
Notched Izod Impact ($J m^{-1}$)	26	18	ASTM D256
Vicat Penetration ($^{\circ}C$)	59	52	ASTM D1525

2.4.3.1.5 Biocompatibility of PLA

PLA is known to degrade in the body as lactic acid which is normally present in the body. Lactic acid then enters Krebs cycle and is excreted as water and carbon dioxide (Figure 2-12). No significant amounts of accumulation of degradation products of PLA have been reported in any of the vital organs [63, 125, 132-134].

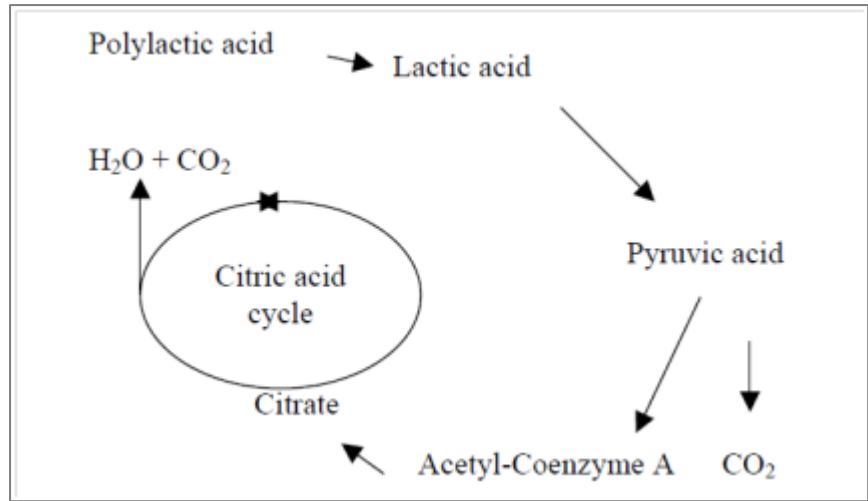


Figure 2-12: In-vivo degradation mechanism for PLA

Both *in-vitro* and *in-vivo* studies have been carried out to establish the biocompatibility of PLA. Many studies suggest that these polymers are sufficiently biocompatible [133-135] although certain studies like Daniels *et al* and Verheyen *et al* suggest otherwise [136, 137].

Concerns about the biocompatibility of PLA have also been raised by Tayler *et al.* when toxic solutions were produced probably as a result of acidic degradation [138]. Another concern is the trigger of inflammatory response due to the release of small particles during degradation. It has been reported that as the material degrades, small particles break off which are phagocytised by macrophages and multinucleated giant cells.

A summary of literature reviewed for biocompatibility is presented in the Table 2-6. It implies that conflicting reports for biocompatibility of PLA has been produced. Nevertheless, PLA is one of the biodegradable polymers (PLA, PCL, PGA, PDS used routinely) approved as an implant material by FDA/MHRA and has been used as pins, screws and sutures in surgical processes.

Table 2-6: *In-vitro* or *in-vivo* biocompatibility studies of PLA-based biomaterials and their outcomes

Application	Material	Results	Reference
Sutures in pigs and rats	Poly(lactic acid)	Non-toxic and non-tissue reactive	[135]
In-vitro toxicity	Poly(lactic acid) Poly(glycolic acid)	Can produce toxic solutions	[136]
In-vitro cell response	Poly(lactic acid)	Slightly toxic	[137]
In-vitro pneumocytes culture	3-D pore structure of PDLLA	No toxic on pneumocytes also supported cell growth.	[139]
In-vitro osteoblast culture	PLA based composite	Non-toxic and cytocompatible	[140]

Concerns with biocompatibility seemed to accompany decomposition of the implants, it was accepted that the low molecular mass degradation products of the polymers were responsible for this, which could be due to sterilisation process [63]. According to Daniels *et al.* local decrease in pH during degradation is one of the main reasons for an inflammatory response. In general, it can be concluded from the results reported for *in vitro* studies that PLA demonstrate satisfactory biocompatibility in the test systems. High concentrations of degradation products, however, had a toxic influence on the cell culture systems. This could explain the detrimental effects sometimes observed in bone tissue.

2.4.4 Composite

A Composite is a material with at least two distinct phases; a continuous phase (e.g. polymer) and a dispersed phase (e.g. glass fibres or particles). The continuous phase or matrix is responsible for making up the volume and transfer loads to the dispersed phase. The dispersed phase or the reinforcement is usually used for enhancing one or more properties of the composite [141, 142].

2.4.4.1 Types of Composite

Composite can be divided into three major categories on the basis of matrix material: MMC's Metal Matrix Composites; CMC's Ceramic Matrix Composites; PMC's Polymer Matrix Composites. Composites can also be categorized into five different categories on the basis of reinforcement: fibre; particle; flake; laminar or layered; filled composites (Figure 2-13).

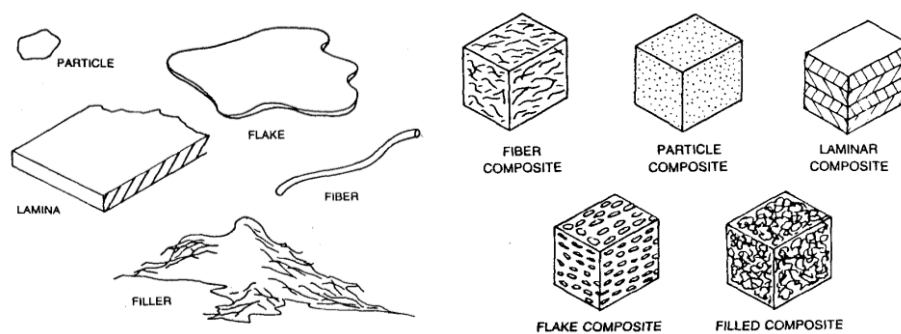


Figure 2-13: Different fillers (particle, flake, fibre) and respective composite.

2.4.4.1.1 Fibre-Reinforced Composites

Fibre-reinforced composites (FRCs) often aim to improve the strength to weight and stiffness to weight ratios (i.e. light-weight structures that possess strong mechanical properties). Glass or metal fibres are generally used as reinforcement within polymeric matrices.

Fibres are available in three basic forms: continuous fibres (long, straight and generally lay-up parallel to each other); chopped fibres (short and generally randomly distributed); woven fibres (come in cloth form and provide multidirectional strength). Therefore fibre reinforced composite can then further be divided into: non-woven fibre reinforced composite; woven fibre reinforced composite; unidirectional fibre reinforced composite (Figure 2-14).



Figure 2-14: Schematic of fibre types: Unidirectional, Chopped & Woven

Examples of fibre reinforced composites as implant material are summarised in Table 2-7.

Table 2-7: Examples of fibre reinforced composite used as medical implant material

Fibre Type	Matrix	Reference
Carbon fibre	Epoxy resin	Bradley 1980 [143]
	PMMA	Ekstrand <i>et al</i> 1987 [144]
	polysulfone	Latour and Black 1992 [145]
	polycarbonate	Latour and Black 1992[145]
	poly-ether-ether-ketone	Wenz <i>et al.</i> 1990[146]
	Poly lactide	Wan <i>et al</i> 2000[147], Zimmerman <i>et al.</i> 1987 [148]
Aramid (Kevlar)	PMMA	Pourdeyhimi <i>et al</i> , 1986, 1989 [149, 150]
	Polysulfone	Latour and Black 1992, [145]
	Polycarbonate	Latour and Black 1992 [145]
Polyethylene fibre	PMMA	Pourdeyhimi <i>et al</i> 1989 [150]
	poly(DL-lactic acid)	Reddy <i>et al</i> 2008 [151]
Bioactive glass fibre	polysulfone	Marcolongo <i>et al.</i> 1997, 1998 [152, 153]
	Polycaprolactone	Jiang 2005[154]
Phosphate glass fibre	PLA or PCL	Table 2-8

2.4.4.2 Biocomposite

From structural point of view, like most living tissues (e.g. bone, skin, cartilage), composites are anisotropic and that is why an attractive choice for medical

application. Biocomposites were developed to obtain a wide range of mechanical and biological properties and hence optimising the structure and function of biomedical devices and their interaction with surrounding tissues.

Different types of composites are already in use or currently under study to be used in the application of cardiovascular grafts, dental restorative and prosthesis materials, bone repair, tissue engineering, bone grafts, fracture fixation devices, joint prosthesis and even artificial cartilage, ligament and tendons [142, 155]

2.4.4.2.1 Types of Biocomposites

Other than the general classification of the composites, biocomposites can further be divided into three more categories based on their biodegradability: fully resorbable; partially resorbable; non-resorbable.

Resorbable biocomposite are made from the fibres (PLA/PGA, phosphate glass fibre) and matrix (degradable polymers such as PLA, PCL, and POE) which are fully absorbable in the body. These are currently under intensive investigation for internal fracture fixation (osteosynthesis) applications [23, 24, 27, 140, 156-160]. They give at least two major advantages of avoiding removal operation and stress shielding, over metal fixation counterparts.

2.4.4.3 PGF Reinforced Composite

For a completely degradable composite, both the continuous phase and the reinforcement fibres should be degradable. poly(α -hydroxy esters), especially PCL and PLA are the few synthetic polymers that have been approved for human clinical uses. However, low stiffness of these polymers (e.g. the elastic modulus of PLA

screws is about 3 GPa) in comparison to metal devices could allow excessive bone motion which is detrimental for satisfactory healing [155, 157].

Reinforcement of such polymers with totally resorbable reinforcement is therefore necessary for the development of a fully degradable compliant and strong fracture fixation device. Therefore, the use of degradable phosphate glass fibres is of special interest.

A number of studies have shown the potential of PBG particulates or fibre reinforced PLA composite to be used for fracture fixation devices (Table 2-8) [23, 24, 27, 140, 156-160]. Navarro *et al.* after the surface characterisation and cell response have concluded that the PGF reinforced PLA composite materials were biocompatible and showed flexural mechanical properties comparable to cortical bone which make them potential candidate for the production of degradable bone fixation devices [157].

Ahmed *et al.* [158] and Brauer *et al.* [140] investigated similar type of PGF reinforced composite's degradation profile and mechanical properties. They found that the flexural strength obtained for the composites matched the strength of cortical bone; however, the flexural modulus values were found lower than those for cortical bone (see table 2-8).

Table 2-8: Summary of selected investigations on phosphate glass fibre reinforced composites and their mechanical properties. PCL: Poly-caprolactone, PLA: poly-lacticacid, POE: poly-orthoester, PGF: phosphate glass fibre, MAmOL: methacrylate-modified oligolactide, UD: unidirectional.

Matrix	Reinforcement V_f (%)	Flexural Strength (MPa)	Flexural Modulus (GPa)	Reference
PCL	10mm random binary PGF (6-18%)	30	2.5	Ahmed et al 2008
PCL	Continuous UD quinary PGF (10% wt)	72	2.74	Khan 2010
PCL (<i>in situ</i> polymerisation)	Continuous UD quaternary PGF 25%	105±12	5.9±6	Khan 2009
PCL (compression moulding)	Continuous UD quaternary PGF 25%	55±8	2.1±0.3	Khan 2009
POE	Short random ternary PGF (0-50%)	65-103	1.5-9.4	Andriano & Daniels 1992
MAmOL	50 cm long quinary PGF	115±11.9	16±2.4	Brauer et al 2007
PLA	10mm random quaternary PGF 14%	90	5	Ahmed et al 2008
PLA	Continuous UD and short random PGF (40-55%)	120-350	10 to 30	Parsons et al 2009
PLA	Continuous UD and 10mm random Quinary PGF (15-20%)	106-115	6.8-9	Felfel et al 2010
MAmOL	30 cm quaternary PGF	110-190	15-20	Kobayashi et al 2010

Table 2–8 gives a summary of literature reviewed for the phosphate based glass fibre reinforced composite. Here flexural strength ranges from 30 MPa to 350 MPa and flexural modulus was reported to vary between 2.5 GPa and 30 GPa. This large variation in flexural mechanical properties is due to variation in polymer matrix (PLA, POE or PCL), strength of glass fibre, glass fibre fraction in polymer matrix,

fibre orientation and manufacturing process. It can be deduced from the literature reported in Table 2–8 that with high fibre volume fraction, unidirectional fibre orientation and *in-situ* polymerisation of strong polymer around phosphate glass fibres a high strength composite can be prepared. The resultant composite could potentially be used as load-bearing fracture fixation implantable device.

2.4.5 Role of Interface

Making a composite out of glass reinforced polymer can provide enhanced mechanical properties. However, polymers do not usually make strong mechanical or chemical bond with the glass. Combining glass and polymer to create composite materials is possible if an intermediary chemical agent is used. Surface treatment of filler (e.g. glass fibres) with chemicals can provide a covalent bridge between the two phases and/or suitable surface wettability (hydrophobicity) for polymer to adhere.

Chemical substances capable of reacting with both the reinforcement and the polymer matrix of a composite with the help to two distinct functional groups present in their structure are known as coupling agents. They may also bond inorganic fillers or fibres to organic resins to form or promote a stronger bond at the interface. Chemical treatment of filler can also acts as compatibiliser between polymer matrix resin and glass fibre. Aminopropyltriethoxy silane (APS) is the most common silane used to treat common silicate glasses [161, 162].

2.4.5.1 Potential Surface Treatment Agents

It is difficult to find suitable chemicals for biological uses as very limited range of is considered biocompatible and at the same time reactive to both polymer and glass. Especially, for glass or ceramic like materials there are very few chemicals available to functionalise glass/ceramic surface to mediate adhesion between the two phases of composite (filler and polymer) by altering wettability of filler and/or providing covalent coupling between two phases of composite. So far, reported suitable biocompatible surface treatment agents include, but are not limited to, conventional silane, various phosphonic acids, poly-(2-hydroxyethyl methacrylate), zirconate, and titanate.

After reviewing the work previously carried out on glass/ceramic (fibre or particle) reinforced polymer composite to improve their interface, a summary is presented in the Table 2-9.

Table 2-9: A summary of literature reviewed for chemical agents used to mediate polymer/glass interface within composites for biomedical applications. PGF: phosphate glass fibre, PLLA: poly-L-lactic acid, HA: hydroxyapatite, PP: polypropylene, APTES: aminopropyl triethoxy silane, NR: not reported, PPA: phosphonopropionic acid.

Surface treatment	Matrix	Reinforcement	Evaluation method	Outcomes	Reference
Silanes	PLLA	PGF	Dissolution Strength Retention	Increase mechanical properties Non toxic	Andriano <i>et al</i> 1991-1992
Silanes	PP	Mica	Morphology mechanical properties	Adhesion Enhanced viscoelastic properties	Yazdani <i>et al</i> 2006
Silanes	degradable polymers	HA	XPS	Stable coverage of mineral filler thin silane coating presumed transparent for ions	Dupraz <i>et al</i> 1996
Metoxy silanes	PLLA	HA	Cell adhesion and contact	Acute toxicity of silane dose-dependent toxicity of leachable	Dupraz <i>et al</i> 1996

				silanol	
3-APTES	HA	–	Cell study/SEM	Improved cell adhesion to collagen grafted HA	Jung <i>et al</i> 2007
HEMA	PMMA/Titania Hybrid	–	DSC/TGA, Morphological studies	successful synthesis of hybrid material with greater thermal stability & smoothness	Yeh <i>et al</i> 2004
HEMA	methacrylate–modified oligolactide	PGF	Mechanical properties Cytocompatibility	Bone equivalent moduli & strength No cytotoxicity, suitable for pre-osteoblasts	Brauer <i>et al</i> 2006
Titanate	PP	Mica	Mechanical tests fracture behaviour (SEM)	Enhanced yield stress and flexural strength	Bajaj <i>et al</i> 1989
Zirconate, silanes Titanates	EVOH	HA	Tensile tests, SEM	30% increase in modulus with acidic zirconate	Vaz <i>et al</i> 2002
Allyl PA	NR	CAP	FTIR/XPS	Successful grafting of APA with CAP via C=C	Phillips <i>et al</i> 2005
PPA	Poly-EVA	HA	XRD/FTIRTEM/cytotoxicity	successful grafting of PPA onto HA resulted in uniform dispersion of HA	Pramanik <i>et al</i> 2008
PPA	Chitosan phosphate	HA	FTIR/XRD/IFSS	Homogeneous dispersion of HA resulted in improved mechanical properties	Pramanik <i>et al</i> 2008
PLA Oligomers	PLA	PGF	GPC/DSC/NMR/MALDI-TOF MS		Barker <i>et al</i> 2009
Various PLA Oligomers	PLA	PGF	GPC/IFSS/XPS	Oligomers with greater number of –OH ions in their FG showed improvement in IFSS	Haque <i>et al</i> 2010
APS/PA/GP/ALD PLA oligomers	PLA	PGF	XPS/MALDI/IFSS	Improvement in IFSS with ALD/GP/PLA Oligomers	Haque <i>et al</i> 2010
HDI	CHP	PLA	Biodegradability cytocompatibility	Degradable, nontoxic CHP	Dong <i>et al</i> 2001
HDI	PEG/PBT	HA	Mechanical properties	successful binding between polymer and HA resulted in improved mechanical properties	Liu <i>et al</i> 1997
HDI	PLA	Bioactive glass particles	Cell studies mechanical tests	Greater tensile strength Improved biocompatibility	Liu <i>et al</i> 2008

Based on the literature reviewed and preceding work conducted within the University of Nottingham, a list of potential surface treatments (including coupling and grafting agents) was selected with the aim to investigate the effects of chemical

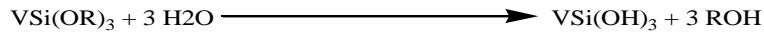
treatments on mechanical and biological properties of the composites produced. The proceeding section will provide basic chemical structure, reaction mechanism, reported effect on IFSS and cytocompatibility where available.

2.4.5.1.1 Silanes

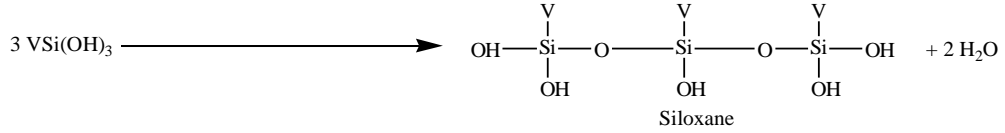
Silanes coupling agents well known to self-assemble into mono-molecular and multi-molecular layers on surfaces such as glass or silicon dioxide. One end of the silane molecule typically has di or tri methoxy or ethoxy functionality whilst the other end normally has amine or ethoxy functionality. The ethoxy functionality is believed to condense with the hydroxyl functionality on the surface of the glass whilst the amine functionality can react with the polymer [161, 162]. To select a silane for a particular application, the organo reactive group must match the chemical structure and reactivity of intended polymer. For example, Vinyl silanes are used for the crosslinking of non-polar and non-reactive polymers such as polyethylene and ethylene copolymers requiring free radical mechanism. Generally, vinyl silanes are associated with an organic peroxide to initiate grafting reaction. On the other hand, amino silane can react with most thermoplastics and thermosets [163]. Silane hydrolysable group is an intermediate in the formation of silanol groups, for chemical bonding to the surface of the filler and the other end has organic-functional group that can also entangle with polymer molecular chains by physical type of interactions [164].

Yazdani *et al.* incorporated a silane treated mica glass particles with poly-propylene and suggested a five step modification process of mica surface (Figure 2-15).

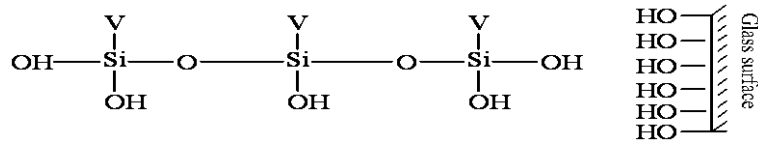
Hydrolysis:



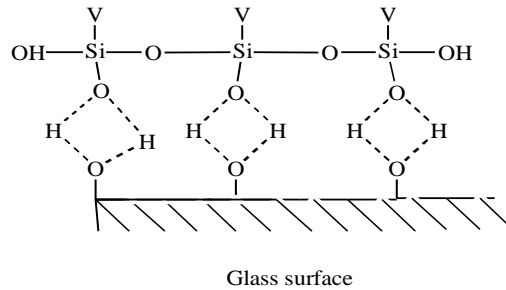
Condensation:



Hydrogen-bonding:



Rearrangement:



Surface grafting:

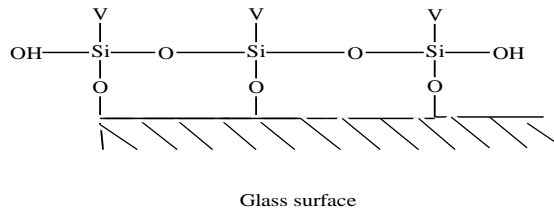


Figure 2-15: A 5 step (hydrolysis, condensation, intermediate hydrogen bonding, rearrangement and surface grafting) coupling mechanism of silane on glass surface [164].

Various researchers have reported effectiveness of silanes on IFSS between silica based glasses and polymer matrix [164-166]. For example, Park and Jin reported an increase in interlaminar shear strength (ILSS) between E-glass fibre and unsaturated polyester matrix when a combination of two silanes methacryloxypropyltrimethoxy silane (90 wt%, MPS) and aminopropyltriethoxy silane (10 wt%, APS) in methanol/distilled water (95/5 volume %) was applied to the surface treatment of

glass fibres with different concentrations. It was reported at 0.2 molar concentration, ILSS was improved from ~16 MPa (control) to ~26 MPa [166]. However, the IFSS values (8.9 ± 2.9) for the silane treated phosphate glass fibres/PLA, obtained were similar to that of the control (untreated glass fibre) [25, 167]. Similar results were also obtained by Cozien–Cazuc [168] for both unsized and silane sized P40Na20Ca16Mg24 PGFs within a PCL matrix. The difference reported for the effectiveness of silanes on silica and phosphate based glasses could be due to the fact that the concentration used for PGFs (0.043 M) was much lower than that for silica based glasses (0.1–0.5 M).

2.4.5.1.2 Phosphonic Acids

Phosphonates or phosphonic acids are organic compounds containing C–PO(OH)₂ or C–PO(OR)₂ groups (where R=alkyl, aryl) (Figure 2-16). Phosphonates are effective chelating agents that bind tightly to divalent and trivalent metal ions, preventing them from forming insoluble precipitates (scale) and suppressing their catalytic properties. They are stable under harsh conditions. They are very soluble in water and in alcohol.

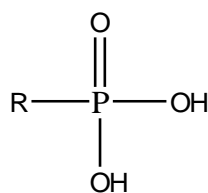


Figure 2-16: Generic chemical structure for phosphonic acids

In a study, specifically tailored organo–phosphonic acid has been synthesised to be used as a with hydroxyapatite [169]. Prepared (2–Carboxyethyl phosphonic acid) or (1–propene–3–dihydroxy phosphonic acid) had a phosphonic acid group to react with glass and organic group for polymer. This tailored organo–phosphonic acid was

applied in a novel co-precipitation reaction to form a calcium phosphate/organo-phosphonic acid co-precipitate. FTIR, FT Raman and solid state NMR spectroscopy was carried out which established that the phosphonic functional groups (P(O)(OH)₂) of the organo-phosphonic acid appear to replace a proportion of the phosphate groups in the calcium phosphate. X-ray photoelectron spectroscopy confirmed the presence of reactive groups (C=C), from the organo-phosphonic acid, on the surface of the co-precipitate. However, no experimental evidence of prepared phosphonic acid on IFSS was reported.

In the preparation of biocomposites, phosphate-based surface treatments (coupling agents) are being extensively used by various researchers in order to improve the compatibility between reinforcement and polymer matrix [169-172]. Greish and Brown have developed a biocompatible hydroxyapatite (HA)-Ca poly(vinyl phosphonate) composite for clinical applications[170, 171]. Tanaka *et al.* have reported the synthesis of surface-modified calcium hydroxyapatite with pyrophosphoric acid for use as bioceramics, particularly for orthopaedic applications [172]. All these studies suggested that phosphoric acid-based agents can be employed to enhance the interfacial bonding between reinforcement (HA-particles) and the polymer matrix. Therefore, these chemicals can improve the mechanical properties of the resulting composites. However, none of the studies directly measured the IFSS before and after chemical treatment.

Considering the potential of phosphonic acids to react with ceramics, such as hydroxyapatite, a literature survey was carried out and three different phosphonic acids were selected to be investigated for their role.

2.4.5.1.2.1 *Phosphonopropionic Acid*

Phosphonopropionic acid (PPA), also known as carboxyethyl phosphonic acid, has been used successfully to mediate interface between calcium phosphate nanoparticles and polymer matrix [173] and with PBG within the University of Nottingham, however, not much success in terms IFSS improvement was achieved in the latter [25]. It was assumed that the molar concentration and other reaction conditions need to be optimised to get the maximum coupling effect from PPA to improve IFSS between PBG and PLA.

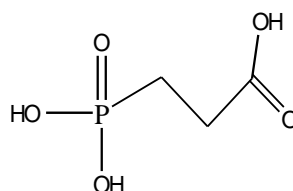


Figure 2-17: Chemical structure for phosphonopropionic acid with two different binding sites for glass and polymer matrix.

In a study, Andres *et al* showed that up to 24 weight% of 2-carboxyethyl phosphonic acid (PPA) could be applied onto anisotropic calcium phosphate nanoparticles that are used for bone implants [173].

2.4.5.1.2.2 *Etidronic Acid*

Etidronic acid is a bisphosphonate (BP), a class of bone-seeking compounds due to the strong affinity of the spatially-optimized anionic phosphonates to bone mineral. BPs originated from the inorganic pyrophosphate, which binds to bone mineral surface and prevents its dissolution. By replacing the P-O-P linkage in pyrophosphates with the P-C-P linkage (Figure 2-18), BPs become resistant to hydrolysis, and exhibits a prolonged persistence in situ. Due to its potential to react

with ceramics like HA, as shown by Nancollas [174], it was a rational choice as surface treatment.

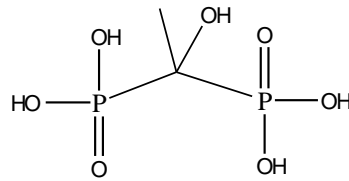


Figure 2-18: Chemical structure for etidronic acid with two distinct functional groups to react with glass and polymer.

Amongst the most common BPs, alendronate (ALD) has been used to improve IFSS between phosphate glass and polymer. The IFSS was reported to improve from ~9.5 MPa to 12.9 MPa. However, no data on osteoblast interaction with ALD-modified glass was provided [25].

Alendronate in calcium phosphate (CaP) bone cement has been used as surface treatment and reported to have provoke worsening of the mechanical properties. MG63 osteoblasts cell line grown on the cements showed a normal morphology and biological tests demonstrated normal cell proliferation and viability. In particular, Alendronate promote osteoblast proliferation and differentiation, whereas they inhibit osteoclast function [175].

Due to similarity of structure (Figure 2-18) and evidence of its strong affinity toward HA etidronic acid was selected for this study.

2.4.5.1.2.3 Amino-methyl Phosphonic Acid (APA)

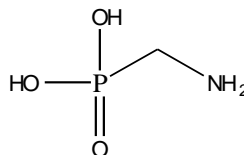


Figure 2-19: Chemical structure for amino-methyl phosphonic acid with -OH group to react with glass and NH₂ to make covalent bond with polymer.

APA was purely selected on the basis of its structure (Figure 2-19); two possible -OH sites that could react with PBG surface and NH₂ functionality that has the potential to react with polymer in the same way as the amine functionality in APS.

2.4.5.1.2.4 Glycerol phosphate (GP)

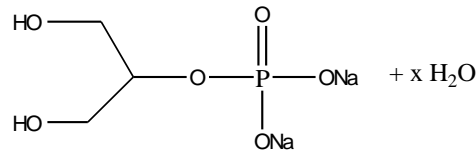


Figure 2-20: Chemical structure for glycerol phosphate, -OH group was expected to react with glass and -ONa to provide reactive site for polymer.

Reaction mechanism of glycerol 2-phosphate disodium salt and its effect on mechanical properties of composite were investigated within the University of Nottingham [25]. It is reported that GP reacted with the PBG by making P-O-Na bond and thus improved the IFSS from ~9 MPa (Control) to ~16 MPa (GP treated). [25] Therefore, in this study GP will be investigated further for IFSS as well as cytocompatibility assessment.

2.4.5.1.3 PLA Oligomers

At the University of Nottingham, research is being carried out to produce novel sizing agents with PLA oligomers (Figure 2-21) with different functional groups like Na, COOH, sorbitol, glycerol, and ethylene glycol ended PLA. From the results reported; Na and sorbitol ended PLA oligomers improved the IFSS significantly from 9±3 MPa (control) to ~17 MPa and 15 ± 2 MPa (Control) to 23 ± 3 MPa for sodium and sorbitol ended PLA treated samples respectively. [26]

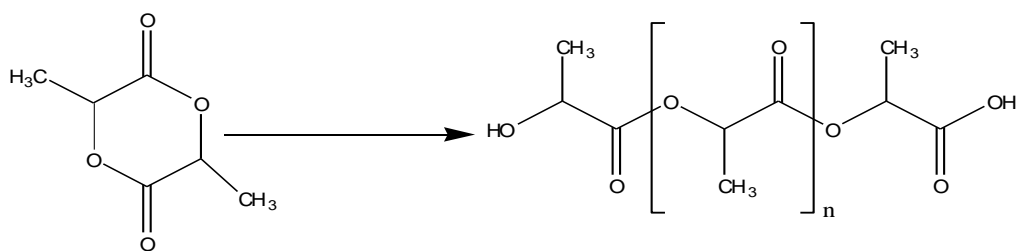


Figure 2-21: Chemical structure for PLA–oligomer prior to functional group attachment

It was reasoned that due to similarity in chemical structure to the matrix (PLA) PLA-oligomer showed a better quality of interfacial bonding between PGF and the PLA matrix. The functional end groups with a greater number of hydroxyl groups showed better compatibility (or attachment) toward PBG which was attributed to hydrogen bonding between 's end functionality and PBG surface.

To further investigate and establish the results sorbitol and sodium ended PLA oligomers will be investigated in this study with different IFSS test approach and cytocompatibility assessments.

2.4.5.1.4 Hexamethylene Diisocyanate (HDI)

HDI is a colourless or slightly yellow liquid with a melting point of $-67\text{ }^{\circ}\text{C}$. With a density of 1.05 g/cm^3 (at $25\text{ }^{\circ}\text{C}$) HDI has a density just greater than water. The substance forms oily droplets in water and hydrolyses rapidly.

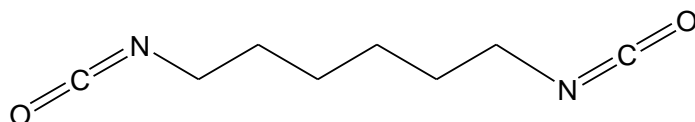


Figure 2-22: Chemical structure for hexamethylene diisocyanate before grafting on glass surface

Diisocyanate groups of HDI react with water to form the diamine [monomer for PU], and CO_2 , it can also react with the amine already formed by hydrolysis, resulting in oligo- and then poly urea. Hexamethylenediamine (HDA) is toxic and like other basic amines can cause serious burns and severe irritation.

HDI is reported to be acutely cytotoxic and irritant to skin and eyes. Despite of reported toxicology issues there is evidence of HDI uses and effectiveness as: a cross-linker in protein production [176], modifier in drug delivery systems [177] and surface-modifier/coupler in biocomposites [178]. Conversely, there are number of reports on the effectiveness of HDI as surface modifier of CaHP ceramic [177-180].

Therefore, due to limited number of surface treatment chemicals available with the potential to increase the phase compatibility in polymer resin composites and the ability of isocyanate to react with hydroxyl groups of hydroxyapatite and PLA to form isocyanate-ended PLA, it was a rational choice as surface treatment for glass reinforcement.

2.5 Conclusions

From the literature surveyed for the purpose of this project, it can be concluded that totally resorbable composite for bone repair applications is required to avoid complications of rigid metal implant and removal surgery. However, materials available for such composite are very limited, especially totally resorbable reinforcement is limited to bast fibres/plant-originated fibres (e.g. flax, hemp, jute, ramie, kenaf, abaca), alginate fibres, polymer fibres (e.g. poly (lactic acid) and poly (hydroxyalkanoate) and phosphate glass (particles, fibres). Within phosphate glass compositions issues such as degradation rates, cytocompatibility of bulk glass and

degradation products and fibre drawing capability needs further research. Another problem of bioresorbable fibre reinforced composite which needs to be counter is the loss of mechanical integrity with degradation. This rapid loss of mechanical integrity has mainly been linked with loss of interfacial integrity between reinforcement and polymer matrix and polymer swelling. Functionalisation of reinforcement surface with chemical treatment is a likely solution to counter interfacial integrity loss. However, chemical agents capable of reacting with both polymer and glass are very limited. Additionally and more importantly biocompatibility of such surface treatments needs to be proven prior to their use in a biocomposite.

CHAPTER 3. PHOSPHATE GLASSES

3.1 Introduction

From the work conducted on binary, ternary and quaternary phosphate based glasses (PBGs), it is clear that a change in molar concentration of different modifiers induces a change in the solubility of the glass [82, 83, 85, 88, 92, 94-96, 99, 101, 102, 109, 112, 114, 181, 182]. For example, in a study carried out on a ternary phosphate glass system based on $50\text{P}_2\text{O}_5-x\text{CaO}-(45-x)\text{Na}_2\text{O}$, it was shown that dissolution rates decreased an order in magnitude ($2.7 \times 10^{-6} \text{ g cm}^{-2} \text{ h}^{-1}$ to $5.1 \times 10^{-7} \text{ g cm}^{-2} \text{ h}^{-1}$) with an increase in CaO content from 30 to 40 molar percentage [85]. Similarly, an increase in Fe_2O_3 content also reported to decrease the solubility of phosphate glasses by two order of magnitude from to 1.62×10^{-4} to $2.7 \times 10^{-6} \text{ g cm}^{-2} \text{ h}^{-1}$ [92]. Similar effect of iron doping on solubility of phosphate glass has also been reported elsewhere [104, 109, 114, 183]. Additionally, the effect of MgO was evaluated in a quaternary glass system and it was found that by replacing Ca with Mg the solubility of the glasses decreased [89, 181]. Degradation rate of $0.0122 \text{ g cm}^{-2} \text{ h}^{-1}$ was reported for ternary glass system $45\text{P}_2\text{O}_523\text{Na}_2\text{O}32\text{CaO}$ (numbers before oxides represent molar percentage of oxide). After inclusion of MgO as a replacement of CaO the solubility rate was reported to reduce to $0.008 \text{ g cm}^{-2} \text{ h}^{-1}$ for $45\text{P}_2\text{O}_523\text{Na}_2\text{O}10\text{CaO}22\text{MgO}$.

With regards to the results reported in these studies and the limitations of appropriate elements for incorporation into these glasses due to concerns about cytocompatibility, a range of glass formulations that are suitable for reinforcement application in fibre reinforced composites have been devised. The aim was to produce a glass for totally degradable fibre reinforced composite with a targeted degradation rate (in the range

10^{-6} and 10^{-7} g cm⁻² h⁻¹), low T_g (<500 °C), potential to be drawn into fibres and cytocompatibility.

This chapter describes the fabrication and characterisation of novel quinary phosphate glasses in the systems of $40P_2O_5-24MgO-16CaO-(20-x)Na_2O-xFe_2O_3$ and $(50-y)P_2O_5-24MgO-16CaO-yNa_2O-4Fe_2O_3$ where, $x = 0, 2, 4$ and $y = 10, 5, 2.5, 0$. The characterisations include investigation of glass structure, thermal, degradation and *in vitro* cytocompatibility properties, considering the effect of varying Fe_2O_3 and P_2O_5 content. For the cytocompatibility studies MG63 osteosarcoma cell line was used and correlations of cytocompatibility results with the glass degradation rate and chemical structure were explored. Finally glass formulations selected on the basis of targeted properties were drawn into fibres and tested for tensile strength using single fibre fragmentation test.

The information collected for the properties of bulk phosphate glasses and glass fibres will be used to decide on glass formulations suitable as reinforcement for the intended composite.

3.2 Materials and Methods

3.2.1 Glass Production

Six glass compositions were prepared using the following precursors: NaH_2PO_4 , CaHPO_4 , $\text{MgHPO}_4 \cdot 3\text{H}_2\text{O}$, P_2O_5 and $\text{FePO}_4 \cdot 2\text{H}_2\text{O}$ (Sigma Aldrich, UK). The precursors were weighed out and mixed into a Pt/5%-Au crucible type BC18 (Birmingham Metal Company, UK), which was then dried in a furnace at 350 °C for 30 minutes, before being transferred to another furnace at 1100 °C for 90 minutes. The molten glass was poured onto a steel plate and left to cool to room temperature. Having obtained the T_g of the glasses, they were re-melted and poured into a graphite mould at 5 °C above the T_g value and left to anneal for 60 minutes. The furnace was then switched off and allowed to cool slowly to room temperature. The glass rods obtained from the mould were cut into 2 mm thick discs of 9 mm diameter using a low speed diamond wheel saw (Model 650, South Bay Technology Inc.). The codes allotted to the compositions investigated in this study can be seen in Table 3-1.

Table 3-1: Glass codes and their respective oxides within phosphate glass network, values represent molar percentage

Glass code	P_2O_5	CaO	MgO	Na_2O	Fe_2O_3
	(Mol %)				
P40 Fe0	40	16	24	20	0
P40 Fe2	40	16	24	18	2
P40 Fe4	40	16	24	16	4
P42.5 Fe4	42.5	16	24	13.5	4
P45 Fe4	45	16	24	11	4
P50 Fe4	50	16	24	6	4

3.2.2 Material Characterisation

3.2.2.1 Energy dispersive X-ray (EDX)

Glass discs from each composition were polished using SiC paper and diamond cloths, with industrial methylated spirit (IMS) as eluent. These samples were then dried and cleaned with a dry air spray and mounted onto a sample holder before being carbon coated. Energy dispersive X-ray (EDX) analysis was conducted on an EDAX model DX 4 using ZAF quantitative analysis. The accelerating voltage was 20 kV and the system's resolution was 60 eV, with an analysis time of 120 seconds. Standards used for analysis were jadeite (for Na), gallium phosphide (for P), wollastonite (for Ca), MgO (for Mg) and pyrite (for Fe).

3.2.2.2 X-ray Photoelectron Spectroscopy (XPS)

X-ray photoelectron spectroscopy was used to investigate the effect of changing composition on the structure (chain length) of PBGs. A Kratos AXIS ULTRA with a mono-chromated Al K α X-ray source (1486.6 eV) was operated at 15 mA and 10 kV anode potential. For the XPS measurement, polished glass specimens were mounted onto a sample holder and readings were taken from 3 different areas. Drift in the electron binding energy of the peaks due to surface charging effects were corrected for by referencing to the adventitious C 1s peak at 285 eV.

3.2.2.3 Fourier Transform Infrared Spectroscopy (FTIR)

Infrared spectroscopy was performed on a Brüker Tensor 27 spectrometer, fitted with a mercury cadmium telluride (MCT) detector. Spectra were recorded in the region of 600 to 2000 wavenumbers using a standard MKII Golden Gate™ single

reflection attenuated total reflectance (ATR) system with heated plate (Specac Ltd.). Samples were crushed and ground into a fine powder using a mineral mortar and pestle.

3.2.2.4 Thermal Analysis

Samples were ground to a fine powder using a pestle and mortar. Three main thermal parameters were measured: the glass transition temperature (T_g); the crystallisation temperature (T_c) and the melting temperature (T_m). The analysis was conducted on a Setaram differential thermal analyser (DTA) SDT-Q600 (TA instrument), using an inert nitrogen atmosphere and a heating rate of $20\text{ }^\circ\text{C min}^{-1}$ up to a maximum temperature of $1000\text{ }^\circ\text{C}$. The data was baseline corrected by carrying out a blank run and subtracting this from the plot obtained. Analysis was conducted using Texas Instrument's TA Universal Analysis software.

3.2.2.5 Density Measurement

Density measurements were obtained using a Micromeritics AccuPyc II 1340 two-cell gas pycnometer. This employs Archimedes' principle of fluid displacement to determine the volume of solid objects, which can be converted to a density when the mass of the sample is known. Densities were measured using glass discs that were 9 mm diameter and 5 mm thick which were weighed using a 4 decimal places sensitive balance (Ohaus Analytical standard AS 200).

3.2.3 Degradation and pH Study

Glass discs (9 mm diameter, 4 mm thick) were placed into vials containing 30 ml of phosphate buffered saline (PBS), in accordance with the degradation standard test

conditions: ISO 10993–13:2010. These were then placed into an incubator at 37 °C. The starting pH was measured to be 7.50 ± 0.1 , using a bench top pH meter (pH 212 Hanna instruments). At various time points, the discs were taken out of their respective containers and excess moisture was removed by blotting the samples dry with tissue paper. The solution was also changed at every time point. The sample weight was recorded at each time point using a 5 decimal point sensitive balance (Sartorius CP 225D). The data plotted as a percentage weight loss over time. The sample measurements were conducted in triplicate. The slope of the graphs gave a degradation rate in terms of percentage mass loss per hour, which was determined by fitting a straight line through the data and including the origin as a data point. Analysis of the pH of the supernatant was also conducted in addition to the weight loss measurement.

3.2.4 Cytocompatibility Study

3.2.4.1 Cell Culture

MG–63 cells (human osteosarcoma), obtained from European Collection of Cell Cultures (ECACC), were cultured in Complete Dulbecco's Modified Eagle Media (CDMEM) consisting of Dulbecco's Modified Eagle Media supplemented with 10% foetal calf serum (FCS), 2% hepes buffer, 2% antibacterial/antimicrobial agents, 1% glutamine, 1% non–essential amino acids (Gibco *Invitrogen*, UK) and 0.85 mM of ascorbic acid (Sigma Aldrich, UK). Cells were cultured in 75 cm³ flasks (Falcon, Becton, Dickinson and Company; UK) at 37 °C in a humidified atmosphere with 5% CO₂. Once confluent the cells were dissociated from the flask using 0.05 mg cm⁻³ trypsin–EDTA in 10mM HEPES buffer and centrifuged at 1200 rpm for 4 minutes to

produce a pellet, which was re-suspended in fresh media. Cell concentrations were determined using a haemocytometer; viable cells were identified using trypan blue exclusion.

Phosphate glass discs, of the formulations investigated, were sterilised using an autoclave and washed three times with PBS prior to cell culture. Tissue culture plastic (TCP) was used as a positive control for cell growth. Cells were seeded onto the disc sample surfaces at a concentration of 40,000 cells/cm² and incubated at 37 °C in a humidified atmosphere with 5% CO₂ for 2, 48, 96 and 168 hours.

3.2.4.2 Alamar Blue

At the designated time points, culture medium was removed from the wells and the samples were washed three times with warm PBS. One millilitre of alamar blue solution (1:9 alamar blue: warm Hanks Balanced Salt Solution (HBSS)) was added to each well and incubated for 90 minutes. From each well 100 µl aliquots were transferred to 96-well plate in triplicate and fluorescence was measured at 530 nm excitation and 590 nm emission using FLx800 microplate reader (BioTek Instruments Inc).

3.2.4.3 Alkaline Phosphatase Activity

At the designated time points, cell culture medium was removed and the samples were washed three times with warm PBS prior to the addition of 1 ml deionised water to each well. Cells were lysed using a freeze/thaw technique three times. A 50 µl aliquot of cell lysate was added to a 96-well plate along with 50 µl of the alkaline phosphatase substrate (p-nitrophenyl phosphate in diethanolamine HCl

buffer, pH 9.8). The micro plate was shaken gently and incubated for ~15 minutes before the absorbance was measured at wavelength of 405 nm with 620 nm reference using ELx800 microplate colorimeter (BioTek Instruments Inc).

3.2.4.4 DNA Quantification

Samples were washed and cells lysed using the freeze/thaw technique as described for the alkaline phosphatase method above. One hundred micro litre aliquots of cell lysate were transferred to a 96-well plate. DNA standards were prepared using calf thymus DNA (Sigma, UK) and TNE buffer (10 mM Tris, 2 M NaCl, and 1 mM EDTA in deionised water, adjusted to pH 7.4) as a diluent. One hundred micro litre of Hoechst stain 33258 was added to each well (1 mg of bis-benzimide 33258 in deionised water, further diluted to 1:50 in TNE buffer) and the plate agitated. Fluorescence was measured at 360 nm excitation and 460 nm emission using FLx800 microplate fluorimeter (BioTek Instruments Inc). DNA concentrations were derived from a standard curve generated by the software (KCjunior).

3.2.4.5 Elution Study

A cytotoxicity test for elution products (degradation products from PBG) was performed with neutral red uptake (NRU) by viable cells as the end point according to the ISO standard for biological evaluation of medical devices (10993–5 2009). The test involved following steps: PBG samples (9 mm diameter, 4 mm thick) were eluted in treatment media (DMEM + 10% HEPES) for seven days at 37 °C with standard 1 mg/ml mass to volume ratio. MG63 cells were seeded at a density of (1×10^4 cells/well) into 96-well plate to form a sub-confluent monolayer. After 24 hours of incubation culture medium was removed and cells were exposed for 24

hours to the treatment medium over a range of four concentrations (100, 75, 50 and 25%). Cells were then evaluated microscopically for morphological alterations and washed once with PBS. One hundred micro litre neutral red dye medium was added to the cells and the plates were incubated for 3 hours. The NR dye medium was then discarded and cells were washed once with PBS before adding 150 μ l NR desorbing fixative to the cells. Subsequently plates were shaken for 10 minutes and NR absorption was measured at an optical density (OD) of 540 ± 10 nm using an ELx800 Microplate Colorimeter (BioTek Instruments Inc).

3.2.5 Glass Fibre Production

Phosphate glass fibres (PGF) with an average diameter of 20 μ m were produced by melt–draw spinning using a dedicated in–house facility (see Figure 3-1). Fibres were collected on an aluminium drum covered with PTFE sheet. Fibre drawing temperature and drum speed were adjusted to 1200–1300 °C and 1200–2000 rpm. The fibres were annealed by using the following steps prior to use: ramp up the temperature to 250 °C at 20 °C/minute; ramp up again from 250°C to (T_g-5 °C) at 1 °C/minute; hold for 90 minutes; ramp down to 350 °C at 0.25 °C/min; cool down to 25°C at 1°C/minute and finally hold the fibres at room temperature (in desiccators) for 24 hours before use.

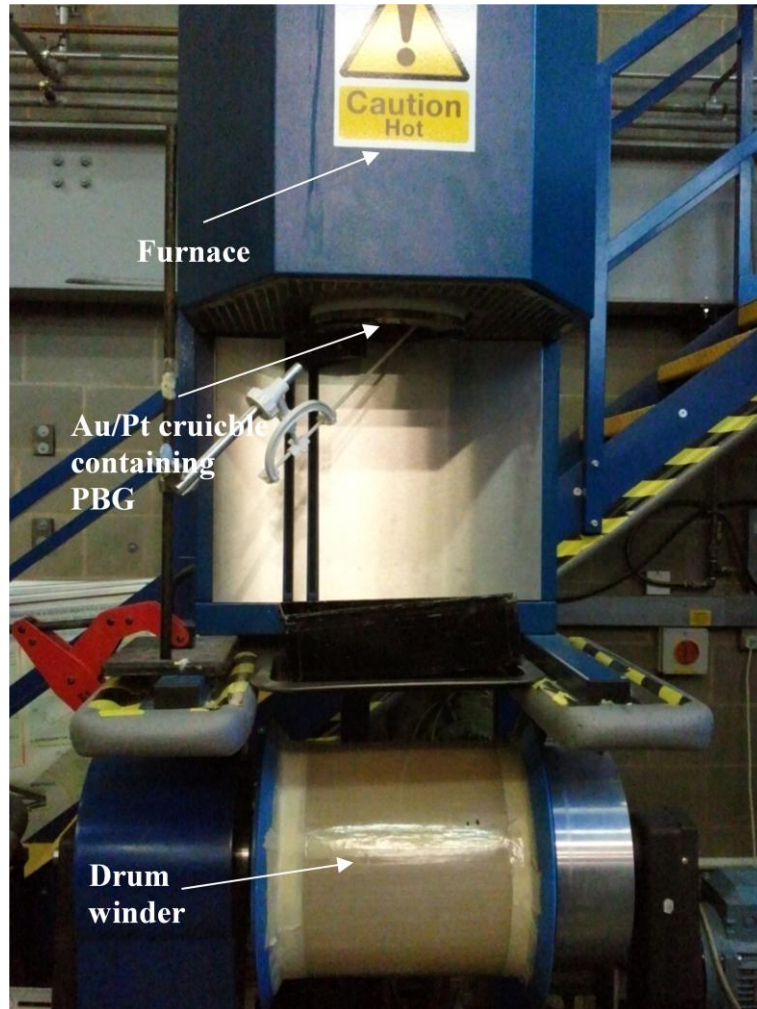


Figure 3-1: Glass fibre drawing tower; glass is melted in the furnace (on the top) which is drawn into fibre and collected on the rotating drum (at the bottom).

3.2.6 Single Fibre Tensile Test (SFTT)

PGF's diameter and tensile properties were measured by using Mitutoyo Series 544 LSM-500S laser diameter gauge and LEX810 tensile tester respectively. Samples were prepared by gluing a single fibre onto the tabs provided with UV curing glue. After measuring the diameter, samples were loaded onto tensile tester and the test was run in UVWin software. Where, tensile strength (δ_f) and modulus (E) was calculated using the following formulae:

$$\delta_f = \frac{F_f}{A_f} \quad \text{Equation 1}$$

Where:

F_f is the maximum tensile force, in Newton;

A_f is the cross-sectional area, in square millimetres, of the filament

$$E_f = \frac{\left(\frac{\Delta F}{A_f}\right)\left(\frac{L}{\Delta L}\right)}{1 - K\left(\frac{\Delta F}{\Delta L}\right)} \times 10^{-3} \quad \text{Equation 2}$$

Where:

ΔF is the difference in force, in Newtons, corresponding to the strain limits selected, depending on the nominal strain at break of the fibre,

A_f is the cross-sectional area, in square millimetres, of the filament,

L is the gauge length, in millimetres, of the specimen,

ΔL is the difference in length, in millimetres, corresponding to the strain limits selected, depending on the nominal strain at break (ϵ) of the fibre, as specified below.

K is the system compliance, in millimetres per Newton.

According to the carbon fibre testing standard ISO 11566 the following strain limits were used:

$1.2 \leq \epsilon$	0.1 – 0.6 strain
$0.6 \leq \epsilon < 1.2$	0.1 – 0.3 strain
$0.3 \leq \epsilon < 0.6$	0.05 – 0.15 strain

3.2.7 Statistical Analyses

Mean values and standard errors were computed for at least three replicate samples from two iterations of experiments. Statistical analysis was performed using the prism software package (version 3.02, GraphPad software). Two-way analysis of variance (ANOVA) was carried out with the bonferroni post-test to compare the significance of change in one factor over time. The error bars on all the data represents standard error of mean unless mentioned otherwise.

3.3 Results

3.3.1 Glass Composition

EDX analyses confirmed the final glass compositions for the samples investigated (Table 3-2). All the formulations investigated were close in composition to the expected values, and were found within a 1–2% of the nominal composition.

Table 3-2: Glass codes and their respective oxides (molar percentage) within phosphate glass network, as measured by EDX analysis. Values after \pm represent standard deviation computed from three replicates

Glass code	P ₂ O ₅	CaO	MgO	Na ₂ O	Fe ₂ O ₃
	(mol% \pm standard deviation)				
P40 Fe0	41 \pm 1.6	16 \pm 1.1	24 \pm 1.9	19 \pm 1.6	0 \pm 0.0
P40 Fe2	42 \pm 0.1	17 \pm 0.4	22 \pm 0.3	17 \pm 0.4	2 \pm 0.1
P40 Fe4	41 \pm 0.1	16 \pm 0.4	23 \pm 0.5	16 \pm 0.1	4 \pm 0.1
P42.5 Fe4	43 \pm 0.2	16 \pm 0.2	23 \pm 0.3	14 \pm 0.2	4 \pm 0.1
P45 Fe4	46 \pm 0.2	17 \pm 0.5	22 \pm 0.4	11 \pm 0.7	4 \pm 0.2
P50 Fe4	50 \pm 0.3	16 \pm 0.4	23 \pm 0.3	6 \pm 0.1	4 \pm 0.1

3.3.2 Glass Structure

For all the glass samples, there were five major IR bands present (Figure 3-2). These bands were positioned at approximately 1250 (asymmetric stretch NBO of O–P–O), 1100 (symmetric stretch of non-bridging oxygen (NBO of O–P–O), 1050 (PO₃ end groups), 900 (asymmetric stretch of P–O–P) and 700 (symmetric stretch of P–O–P) cm⁻¹. It can be seen that the peaks at 700 and 1100 cm⁻¹ were very broad. This can be explained by the fact that they consist of two overlapping peaks due to the

presence of more than 50% network modifiers like Na, Ca, Mg and Fe. It has been reported that sodium phosphate glasses containing smaller amounts of Ca or Mg produce four peaks at ~ 1250 , 1100 , ~ 900 and 750 cm^{-1} in IR spectra and with an increase in the amount of Ca or Mg the peaks at 1250 and 1100 cm^{-1} , come closer to produce a single broad peak. As the levels of Ca or Mg increase, the peak positioned at the higher wavenumber decreases in favour of the growing peak at the lower wavenumber [184].

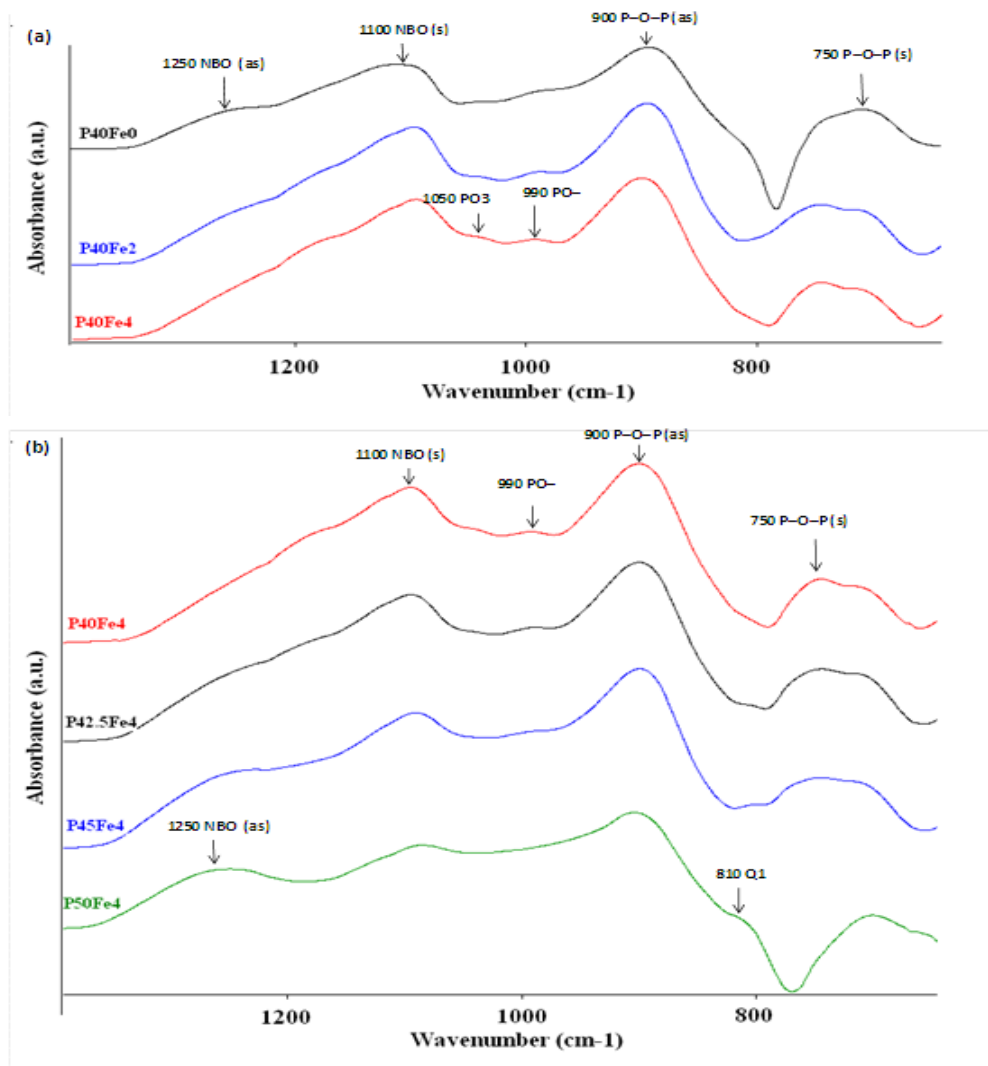


Figure 3-2: FTIR-ATR spectra of PBG with increasing a) Fe₂O₃ content b) P₂O₅ content showing change in glass structure within Q₂ to Q₁ species.

The peaks present are all generally believed to be due to vibrations within the phosphate tetrahedron which are summarised in Table 3-3.

Table 3-3: Major peaks and their assignments from FTIR–ATR spectral analysis of phosphate glasses

Band position and assignments for PBG	
Position (cm ⁻¹)	Assignment
1250	Asymmetric stretch NBO of O–P–O
1100	Symmetric stretch of NBO of O–P–O
1050	PO ₃ end groups
990	PO– chain terminator
900	Asymmetric stretch of P–O–P
750	Symmetric stretch of P–O–P

XPS helped probe the structure of the glass further by giving the signature binding energy peaks for different elements and their oxidation states. Two main O 1s peaks were detected at approximately 531.5 eV and 532.6 eV which were assigned to non-bridging oxygen (NBO) and bridging oxygen (BO), respectively (see Figure 3-3).

Given that all the compositions here lie outside the ultra-phosphate range, the number of BO and NBO for a given phosphate chain length can be predicted using the following equations:

$$\text{BO} = x - 1$$

$$\text{NBO} = 2x + 2$$

Where, x is the phosphate chain length. These two equations can be combined to give the ratio of BO to NBO for a particular phosphate chain length:

$$y = \frac{x - 1}{2x + 2}$$

Where, y is the ratio of BO/NBO.

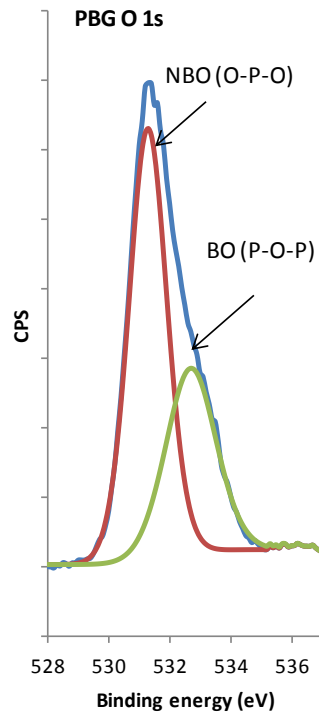


Figure 3-3: Representative high resolution XPS O1s spectra for a phosphate glass.

According to Bunker *et al* [99] theoretical chain length (n) for a phosphate glass containing 50 mol% or less P₂O₅, can be calculated using the following equation:

$$n = \frac{2}{\left[\frac{(M1 + 2M2 + 3M3)}{P} - 1 \right]}$$

Where,

M1 = Mole fraction of monovalent cation, Na

M2 = Mole fraction of divalent cations, (Ca + Mg)

M3 = Mole fraction of trivalent cation, Fe

P = Mole fraction of phosphorus, P

n = Number of phosphates in a chain

The results of theoretical chain length calculation are presented in Table 3-4 alongside chain lengths measured by XPS.

Table 3-4: BO/NBO ratios and chain lengths calculated using theoretical equations and XPS data. Values after \pm represent standard deviation computed from three replicates.

PBG Code	BO/NBO (calculated)	BO/NBO (measured)	Chain length (theoretical)	Chain length (measured)
P40 Fe0	0.30	0.34 \pm 0.03	4.00	5.25 \pm 0.57
P40 Fe2	0.26	0.31 \pm 0.03	3.33	4.26 \pm 0.41
P40 Fe4	0.24	0.27 \pm 0.03	2.85	3.34 \pm 0.31
P42.5 Fe4	0.28	0.34 \pm 0.05	3.69	5.25 \pm 0.57
P45 Fe4	0.33	0.36 \pm 0.03	5.00	6.14 \pm 0.58
P50 Fe4	0.42	0.47 \pm 0.03	∞	32.33 \pm 0.33

3.3.3 Density Measurement

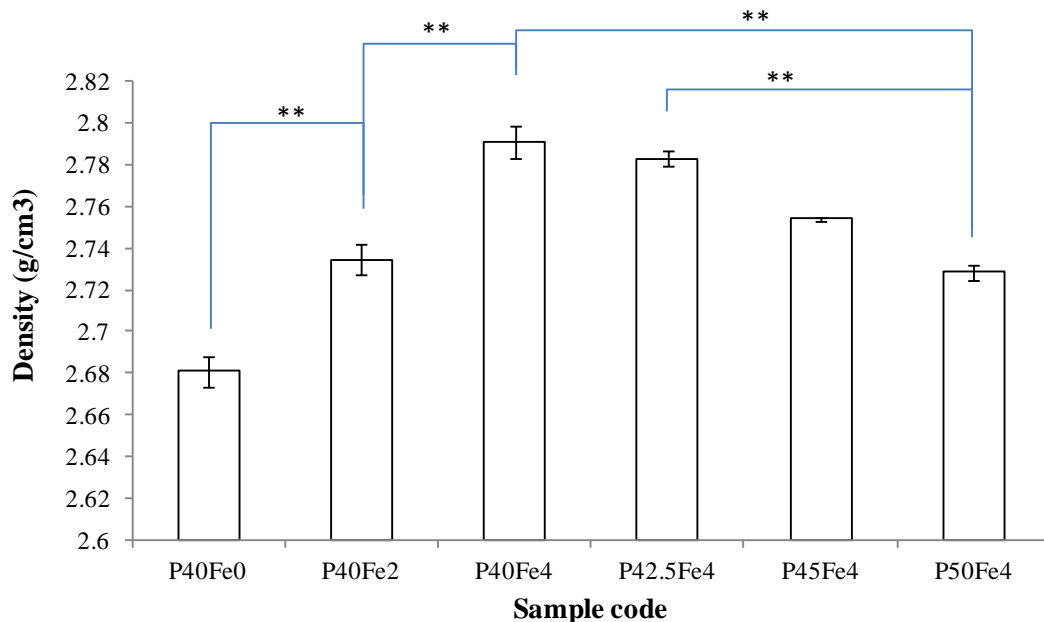


Figure 3-4: Density measurement of PBG measured using a pycnometer; Error bars represent standard error of mean where n=10. * indicating the statistical significance.

Figure 3-4 shows a ~51% increase in density with increased Fe₂O₃ in P40FeX compositions (where X= 0, 2 and 4) content and a ~48% decrease in density with increased P₂O₅ content with fixed (4%) Fe₂O₃ in all PYFe4 compositions (where Y= 40, 42.5, 45 and 50).

3.3.4 Thermal Properties

The three major thermal features (glass transition (T_g), crystallisation (T_c) and melting (T_m) temperatures) were measured by DTA, Table 3-5. A significant increase in these thermal property values was seen with increasing Fe₂O₃ mol% as expected. However, with an increase in P₂O₅ content in glass containing 4% Fe₂O₃ stability in T_g values was observed for glass containing 40 to 45 mol% P₂O₅. However, a significant increase in T_g and T_c thermal values was observed with 50 mol% P₂O₅ content. Melting temperature on the other hand remained within 30 °C (820–850 °C) between all iron doped glass compositions.

Table 3-5: Thermal properties of the PBG samples measured by DTA; ± represents SD where n=3.

	P40Fe0	P40 Fe2	P40 Fe4	P42.5 Fe4	P45 Fe4	P50 Fe4
T _g (°C)	432 ± 1	460 ± 2	480 ± 1	480 ± 3	480 ± 1	495 ± 1
T _c (°C)	610 ± 1	615 ± 2	614 ± 3	671 ± 2	708 ± 4	745 ± 4
T _m (°C)	770 ± 2	737 ± 1	848 ± 2	822 ± 2	837 ± 3	832 ± 2

3.3.5 Degradation Study

Figures 3-5 and 3-6 represent graphs of percentage weight loss against time. As can be seen, glass compositions in Figure 3-5 show decreased solubility (~85%) with an increase in Fe₂O₃ content as seen from prior investigations [92, 185]. Figure 3-6

shows the plots obtained for glasses with fixed Fe_2O_3 at 4 mol%. This graph shows a gradual decrease in percentage mass loss over time (~40%) with increasing P_2O_5 mol%. Table 3-6 gives the degradation rate in $\text{g cm}^{-2} \text{h}^{-1}$ for all glass compositions investigated in current study indicating approximately two order in magnitude difference between phosphate glass composition investigated.

Table 3-6: Rate of degradation in ($\text{g cm}^{-2} \text{h}^{-1}$) for glass compositions studies. The numbers represent mass (g) loss per unit area (mm^2) over time (t). Values after \pm represent standard deviation computed from three replicates

P50Fe4	P45Fe4	P42.5Fe4	P40Fe4	P40Fe2	P40Fe0
7.86E-07 $\pm 1\text{E}-07$	7.47E-07 $\pm 6\text{E}-07$	1.5E-06 $\pm 1\text{E}-$ 06	2.72E-06 $\pm 6\text{E}-07$	6.26E-06 $\pm 6\text{E}-$ 07	1.27E-05 $\pm 6\text{E}-07$

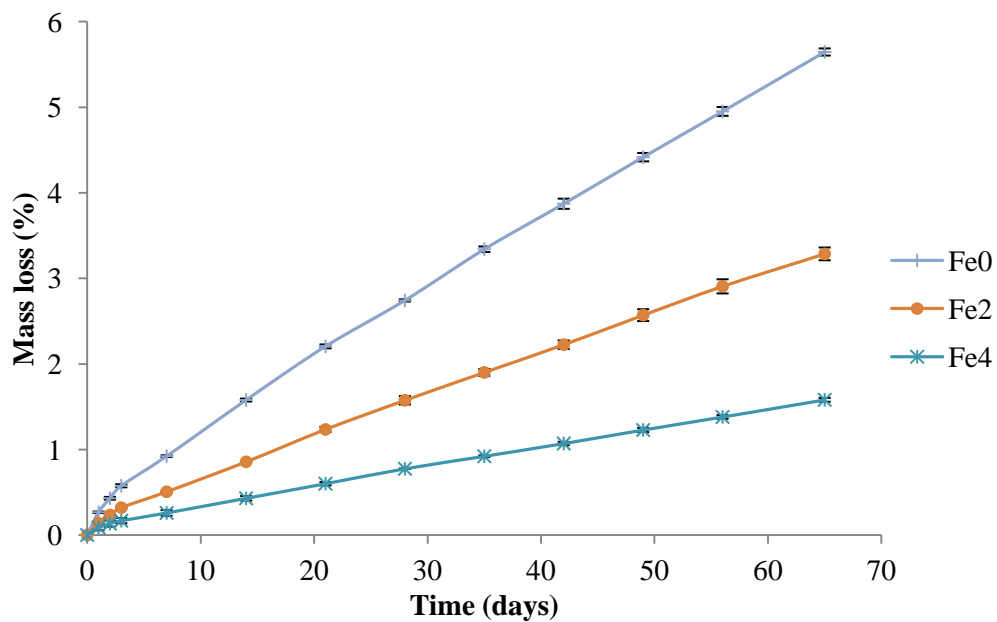


Figure 3-5: Effect of increasing Fe_2O_3 content on degradation behaviour of PBGs containing fixed 40% P_2O_5 content; error bars represents standard error of mean where $n=3$.

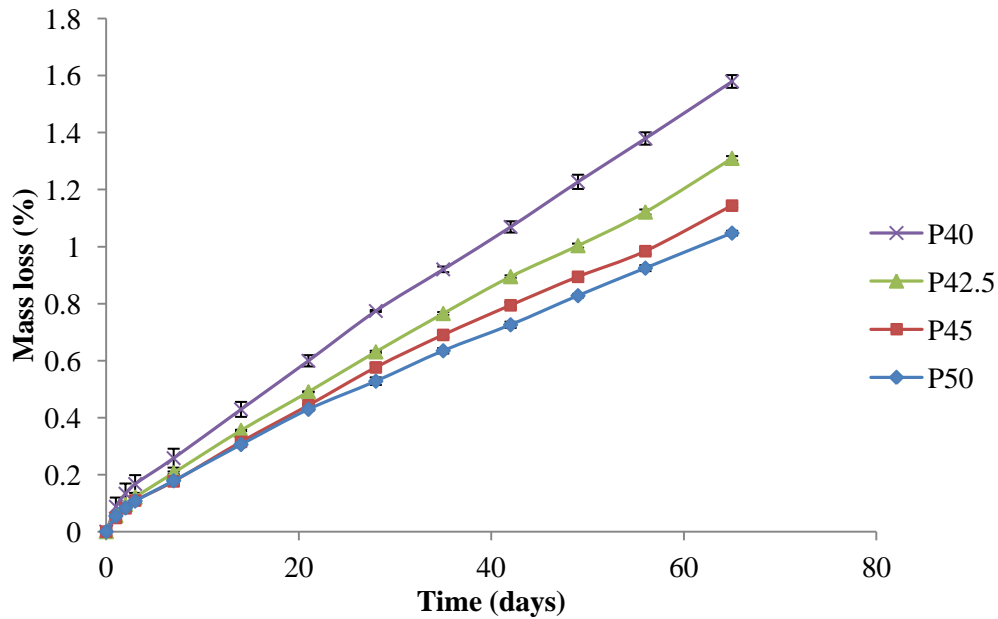


Figure 3-6: Effect of increasing P₂O₅ content on degradation behaviour of PBGs containing fixed 4% Fe₂O₃ content; error bars represents standard error of mean where n=3.

3.3.6 Biocompatibility

3.3.6.1 Alamar Blue Assay

The alamar blue assay (Figure 3-7) demonstrated the metabolic activity of MG63 cells for up to 168 hours (7 days) on the phosphate glass formulations investigated. Tissue culture polystyrene (TCP) was used as internal control. An increase in metabolic activity was seen up to 96 hours, with little further increase by 168 hours. Statistical analyses revealed no significant difference between all the glass compositions studied.

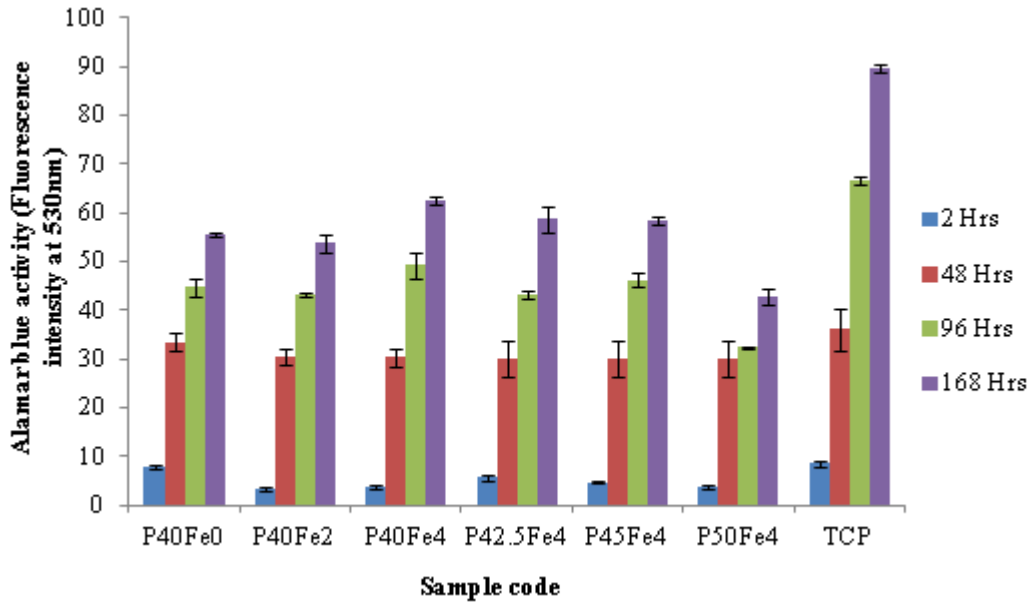


Figure 3-7: Metabolic activity of MG63 cells, as measured by the Alamar blue assay, cultured on PBGs up to 168 hours; Error bars represent the standard error of mean where n = 6. No significant difference found ($P > 0.05$) between glass samples.

3.3.6.2 Alkaline Phosphatase Activity Assay

The alkaline phosphatase (ALP) activity was normalized to the DNA content of the samples investigated. No detectable ALP activity was measured up to 48 hours and an increase in activity was found from 96 hours to 168 hours, Figure 3-8. Statistical comparison of ALP activity on all glass samples (excluding TCP) demonstrated no significant difference except for the most durable P50Fe4, which showed significantly lower activity compared to other samples.

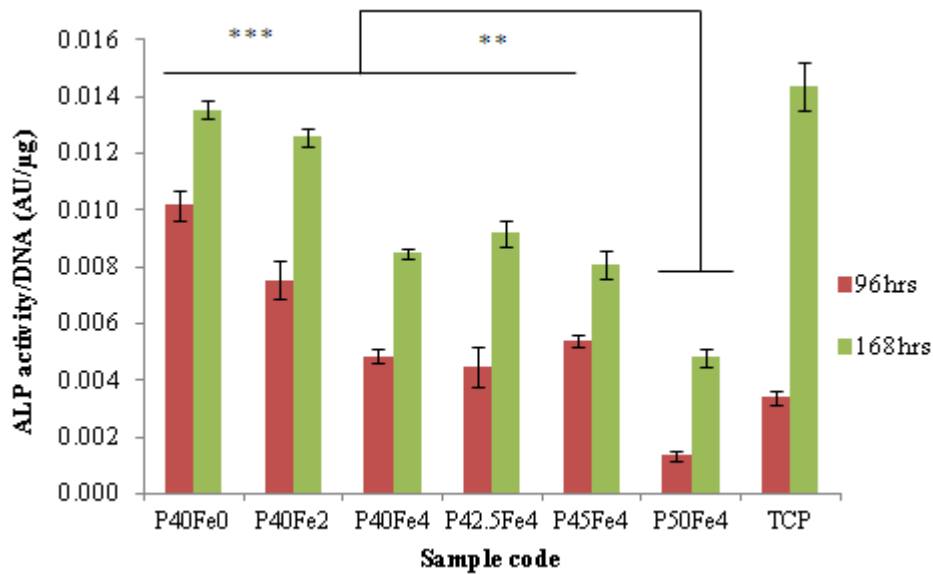


Figure 3-8: Alkaline phosphatase activity of MG63 cells cultured on PBGs for 168 hours. The data is normalised to DNA concentration of samples. Error bars represent the standard error of mean where n = 6. * indicating significant difference between PBG samples.

3.3.6.3 Elution Study

From the neutral red uptake (NRU) assay results (Figure 3-9) it was found that the relative cell viability for the highest concentration of sample extract (100% extract) was found >70 % of the control group (no aliquots) which, according to the definition given in ISO 10993-5, implies that the glass elution products were non-toxic. A gradual low neutral red uptake was observed for all glasses containing >40% P₂O₅ implies lower cell numbers on these surfaces. However, these values were still greater than control group and could be due to the slower release of Ca⁺ ions in to the medium or higher concentration of inorganic phosphate released from these glasses. Only neat aliquot results are reported here as there were similar trends for the lower concentration studies, i.e. 25, 50 and 75% dilutions.

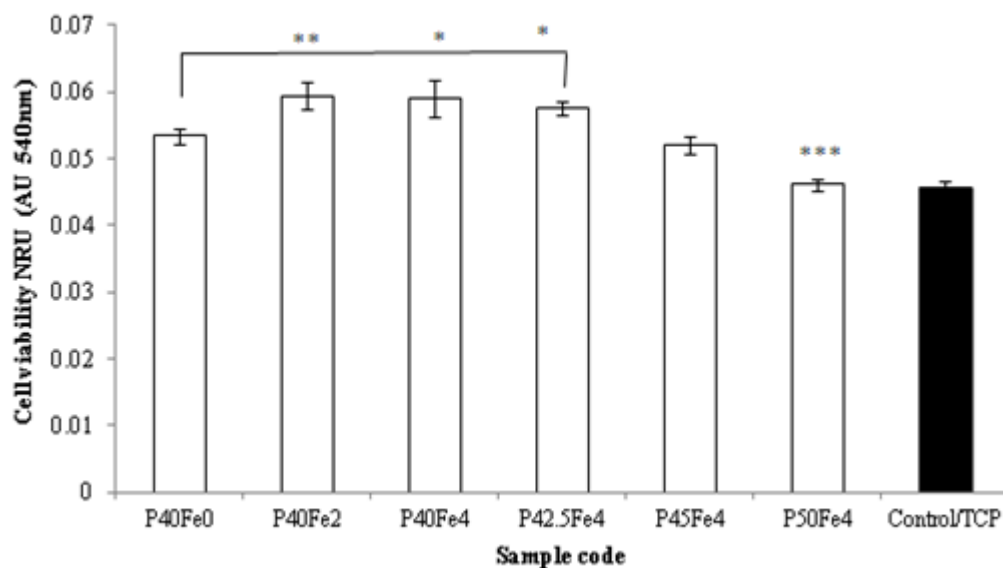


Figure 3-9: Effect of neat aliquots of PBGs elution products (eluted for 7 days at 37°C) on MG63 cells viability, as measured by the NRU assay. Here, Higher NRU implies greater number of viable cells. Error bars represent the standard error of mean where n = 6. * indicating statistical significance. P50Fe4 was significantly lower than the rest of samples excluding TCP.

3.3.7 Glass Fibre Production

Fibres were drawn from three compositions; P40Fe4, P45Fe4 and P50Fe4. These compositions were selected because they were the most durable glasses and had the longest chain length. The latter indicates these glasses should be easier to draw into fibres. It was found that with increased phosphate content fibre drawing became easier. With P50Fe4 and P45Fe4 fibre drawing was almost continuous and gave ~70–80% conversion of glass into fibre. While P40Fe4 broke several times during fibre drawing and conversion rate was around 30–40%.



Figure 3-10: Melt drawn P45Fe4 glass fibre bundle, shows ease of fibre drawing with higher phosphate content

3.3.8 Single Fibre Tensile Test (SFTT)

Fibre diameter, tensile strength and modulus were measured and are summarised in Table 3-7. Fibre diameter was found to increase with phosphate content from 19 to 25 μ m. There was no significant difference found between tensile modulus of the different compositions which was between 61-75 GPa for all samples with a maximum of 75 GPa found for P45Fe4. However, an increase in tensile strength, from 370 to 450 MPa, was seen with increasing phosphate content of the glass from 40 to 50 mol%.

Table 3-7: Tensile strength and modulus of glass fibres drawn from different glass compositions. A single fibre tensile test (SFTT) was used along with laser gauge to measure diameter. Number after \pm represents SD where n=30. * represent the data provided by Reda Fefel.

Glass code	Average diameter (μm)	Tensile Strength (MPa)	Tensile Modulus (GPa)
P40Fe4*	17 \pm 2	370 \pm 8	61 \pm 4
P45Fe4	21 \pm 3	418 \pm 75	75 \pm 14
P50Fe4	20 \pm 5	456 \pm 144	51 \pm 12

3.4 Discussion

From research conducted on similar PBGs, in terms of modifiers and degradation rates, it is reported that they show favourable response for cytocompatibility, which has generally been correlated with their reduced solubility. In addition, ions released from the glass during degradation (mainly calcium and phosphates) may also be beneficial for bone healing [96, 186]. However, glass compositions previously studied have been linked to concerns of poor chemical durability, pH effects, and unsuitable release kinetics of degradation products [119]. Therefore, application specific optimised degradation rate of PBG formulations are required; with emphasis firmly fixed on their biocompatibility properties.

PBGs were produced investigating the hypothesis that with increased iron oxide content the degradation rate will decrease and that the chain length is increased with an increase in phosphate content. Six phosphate-based glass formulations (in the system P_2O_5 -CaO-MgO- Na_2O - Fe_2O_3) were produced with fixed magnesium and calcium content at 24 and 16 mol%, respectively.

Chemical compositions of the glasses were confirmed by using EDX analyses which was expectedly found within acceptable error margin of 2% (Table 3-2).

The density of bulk glass is known to be influenced by the cross-link density and the packing structure of atoms in the glass. Therefore, it gives an indication of the degree of the change in the glass structure with change in the glass composition associated with addition of modifying metal oxides. An increase in density with increased Fe_2O_3 content and a decrease in density with increased P_2O_5 content were observed

(Figure 3-4). This trend can be explained by the structural changes in the glass due to formation of Fe–O–P bonds. Fe³⁺ can act as a network former within the P–O–P back bone due to its dual nature of tetrahedral and octahedral coordination. As the ratio of Fe³⁺ to P³⁺ decreases; less Fe–O–P bonds forms which lead to less denser glass.

Thermal analysis showed a gradual increase in all thermal property values (T_g , T_c and T_m) with increased iron content. The T_g were found unchanged with the increased phosphate content from 40 to 45% and increased for 50% (Table 3-5). This was expected as increases in T_g with increasing iron have been reported previously [103]. Parsons *et al.* reported a gradual increase, from 295 °C to 384 °C, in T_g with increasing iron content from 0 to 20 mol% in a ternary glass system [103]. The increase in T_g was proposed to be due to an increase in the cross-link density of the glass network which also improves the chemical durability. The increase in T_g with 50% phosphate content could be due to the change in structure of the glass from ortho to metaphosphate [184].

The structures of glass samples were investigated with IR and XPS analysis techniques. The identification of the peaks observed in the IR wavenumber range of 1400–600 cm⁻¹ has been well documented [187-189]. The four peaks present (Figure 3-2) are all generally believed to be due to vibrations within the phosphate tetrahedron. The peaks at approximately 1260 cm⁻¹ and 1100 cm⁻¹, and the range 1050–850 cm⁻¹, are due to non-bridging phosphorus–oxygen bonds. It has been reported by Burling, that sodium phosphate glasses containing smaller amounts of Ca or Mg produce four peaks at ~1250, 1100, ~900 and 750 cm⁻¹ in IR spectra and with an increase in the amount of Ca or Mg the peaks at 1250 cm⁻¹ and 1100 cm⁻¹,

shift in position to form what appears to be a single broad peak. As the levels of Ca or Mg increase, the peak positioned at the higher wavenumber decreases in favour of the growing peak at the lower wavenumber [184]. Therefore the broad peaks (Figure 3-2) are actually the combination of asymmetric and symmetric stretch of P–O–P at 700 cm^{-1} and O–P–O at 1100 cm^{-1} respectively. The peak at approximately 750 cm^{-1} , which was assigned to P–O–P stretching, can be seen to decrease in intensity as the Fe_2O_3 concentration is increased. The structural changes are evident from the changing amplitude of the absorption peak at $\sim 1250\text{ cm}^{-1}$ (PO_2 asymmetrical stretch), which demonstrates depolymerisation of the phosphate network with decreasing P_2O_5 content [190]. The fraction of non-bridging oxygen decreases and cross linking increases due to the formation of P–O–Fe bonds in the glass network as Fe_2O_3 replaces Na_2O [85, 109]. This agrees with the XPS data (Table 3-4) stating that the chain length and hence the concentration of P–O–P bonds decreases with increasing iron levels that indicated depolymerisation of PO_4 tetrahedra with increasing Fe_2O_3 and longer chain lengths with increasing P_2O_5 contents. Although, the chain lengths measured by XPS are slightly longer than calculated, the trend was correlated well with the theoretical model with the exception to P50Fe4 where the measured chain length was significantly higher than calculated. This difference in chain lengths could be associated with the dual nature of Fe, which is assumed as Fe^{3+} only in the calculation while it serves as network modifier (Fe^{2+}) and network former (Fe^{3+}) in the glass system.

The degradation rates of the glasses investigated decreased with increasing Fe_2O_3 content (see Table 3-6 and Figure 3-5). As multivalent (Fe) was added in place of monovalent (Na^+) cat-ion a decrease in degradation rate was expected [103].

Strohner *et al.* proposed that this was due to formation of Fe-O-P bonds that are more resistant to hydration than the P-O-P bonds [104]. Decrease in solubility with increasing P₂O₅ mol% was also observed (see Table 3-6 and Figure 3-6) as reported in quinary/complex glasses elsewhere [85]. The proposed mechanism for this decrease is that the phosphate chains are longer and require more time to hydrate before they can dissociate from the glass and dissolve [85]. The pH values, of the degradation media for all the glasses investigated in our study, remained unchanged throughout the degradation period due to the buffer effect of the degradation medium and therefore appeared to have had no effect on the degradation rate of the glasses.

Three glass formulations [(40+x)P₂O₅-16CaO-24MgO-(16-x)Na₂O-4Fe₂O₃] where x= 0, 5 and 10 were drawn into fibres using in house facility. It was found that increasing the phosphate content made the fibre drawing easier which can be correlated with the increased chain length as found from XPS analysis. The fibres were also tested for tensile properties and found similar in terms of modulus (Table 3-7). However, an increase in tensile strength was observed with increased phosphate content which is most likely due to greater orientation of phosphate chains with increasing phosphate content [191]. These properties closely match with quaternary PBGFs tensile properties reported by Ahmed *et al.* [86, 109] and Cozien-Cazuc [168].

Elution study with NRU (Figure 3-9) revealed that glass elution products had no toxic effect on cell viability, in fact all elution products from faster degrading glasses with lower phosphate content had an encouraging effect on cell viability. Direct contact cytocompatibility studies for all the formulations investigated showed cellular response, in terms of cell viability, metabolic activity (Figure 3-7),

proliferation and differentiation (Figure 3-8), comparable to TCP up to 168 hours of cell culturing. However, P50Fe4 glass composition showed relatively lower cell ALP activity. It was hypothesised that this could be due to cytotoxicity of the products released from this glass; the cytotoxicity is believed to be increased with increasing phosphate content in the glass [119]. Uo *et al.* investigated the cytotoxicity of water soluble ternary ($\text{Na}_2\text{O}-\text{CaO}-\text{P}_2\text{O}_5$) glasses with increasing P_2O_5 and CaO contents using elution products from the glass and alamar blue assay as cell viability marker. They found that cytotoxicity increased with greater than 50% P_2O_5 content, whilst decreasing with CaO content. This effect was attributed to a reduction in pH and higher ion concentration in the media. However, the glass studies in Uo *et al.* study were all fast degrading and thus they reduced the pH of the distilled water from 7 to 1 [119]. In current study, to establish the role of degradation products on cytocompatibility; NRU assay was conducted on PGs' elution products which revealed that degradation products appeared to have a positive response on cell viability as long as they are not over concentrating the media with degradation products.

Abou Neel *et al.* investigated the effect of Fe_2O_3 addition to ternary and quaternary phosphate glasses, and showed a positive effect of increasing Fe_2O_3 content on osteoblast-like cells and attributed this towards two fold decrease in degradation rate of the glass as discussed and seen above. It was suggested that an addition of 4 to 5 mol% Fe_2O_3 in the system ($50\text{P}_2\text{O}_5-30\text{Na}_2\text{O}-(20-x)\text{CaO}$) was suitable for a desirable cell response [92].

Quintenary compositions ($37\text{P}_2\text{O}_5-29\text{CaO}-10\text{MgO}-24\text{Na}_2\text{O}$ in mol %) with additions of silica and titanium were recently investigated [101]. It was reported that

the addition of TiO₂ decreased the solubility of the glass in water and in simulated body fluid. It was hypothesised that dissolution rates of the glasses affect the proliferation of osteoblast-like cells (MC3T3–E1.4 murine preosteoblast). They cultured cells for 24 and 72 h, with an increase in cell proliferation seen with decreasing solubility of the glass. It was suggested that resorbable implant materials require the adjustment of dissolution rates to facilitate cell adhesion and proliferation [101].

The cytocompatibility of PBGs has almost always been attributed to the reduced solubility of the glass. However, current study found that, although increasing Fe₂O₃ content decreased the solubility of the glass this had very minimal effect on ALP and cell metabolic activity, which remained unaffected. Therefore, an application-specific degradation rate is necessary to define a degradable glass ‘appropriate’ for that particular application. For example phosphate glass for optical use is considered to have suitable degradation rate around 10⁻⁵ g cm⁻² h⁻¹ or less [192]. However, this would be insufficient for use as a degradable material for bone repair. It is suggested by Parsons *et al.*, that a degradation rate of around 2×10⁻⁷ g cm⁻² h⁻¹ or better is required for phosphate glass fibres used as reinforcement in totally resorbable composite for bone repair application that could take up to 8–12 weeks [103]. The most durable glass found in this study (P50Fe4 which had a degradation rate of 7.8×10⁻⁷ g cm⁻² h⁻¹ (see Table 3-6) is still faster than the suggested optimum rate. It was calculated from the empirical model generated for the formulations investigated in this study that 4 to 5 mol% Fe₂O₃ affected degradation rate the most without affecting structural properties significantly; further increase of Fe₂O₃ would significantly change the structure of the glass.

In summary, PBG formulations (in the system P_2O_5 –CaO–MgO–Na₂O–Fe₂O₃) were found cytocompatible with slow degradation profiles and the possibility to be drawn into fibres thus establishing them as potential fibre reinforcement materials in totally biodegradable composites.

3.5 Conclusions

The structural changes investigated with IR and XPS analysis indicated depolymerisation of PO₄ tetrahedra with increasing Fe₂O₃ and longer chain lengths with increasing P₂O₅ contents. Degradation rates of the glasses investigated decreased with increasing Fe₂O₃ and P₂O₅ contents. Cytocompatibility studies showed favourable cellular response (up to 168 hours) and all formulations with the exception of P50 Fe4 showed no statistically significant difference amongst different glass formulations at any time point. It is also suggested that after certain durability is achieved, further reduction in the degradation rate has no effect on biocompatibility. The elution study proved that the glass degradation products can affect cellular responses. It appears that PBG degradation products may help cell viability as long as their surface is stable enough to maintain cell attachment and proliferation.

On the basis of the results it was decided that although P50Fe4 composition was the most durable and easy to draw into fibres it affected the ALP activity of the MG63 osteosarcoma cells negatively. Therefore, P45Fe4 was selected as reinforcement for polymer matrix composite.

CHAPTER 4. SURFACE TREATMENTS FOR PHOSPHATE GLASS

4.1 Introduction

Totally degradable PGF reinforced PLA composites have shown real potential for replacing existing metallic bone fracture fixation devices, in terms of their initial mechanical properties and degradation profile [23, 27, 157, 159, 193-195]. However, these composites fail to provide a suitable mechanical strength profile over the required healing period of bone (8–12 weeks). Typically it has been seen that some of these composites can lose 50% or more of their strength within the first week of degradation [23, 27, 157, 159, 193-195]. This rapid decrease in mechanical properties can be explained by two phenomena; early hydration and loss of the polymer/reinforcement interfacial properties [23, 140, 158] and polymer swelling during degradation generating hydrostatic forces that crack the reinforcement phase [6, 23].

Introducing covalent bonds and/or hydrophobicity at the interface can potentially delay hydration at the interface region and decrease polymer swelling, which can help to reduce the internal stress of the system [7]. Two potential approaches used to achieve improvement in interfacial shear strength (IFSS) are surface modification of the reinforcement phase with plasma (physical and chemical modification) or surface functionalisation with chemicals such as coupling agents/compatibiliser/cross-linkers.

Coupling agents are chemical substances capable of reacting with both the reinforcement phase and the polymer matrix within a composite, promoting a stronger bond at the interface. This enables effective stress transfer across the

fibre/matrix interface, improving overall mechanical properties [165]. Surface treatment of glass can also promote glass/polymer adhesion in the non-covalent immobilization by hydrophobic and pi stacking interactions.

A number of studies have investigated a variety of chemical treatments to improve the fibre/matrix interface, characterised by IFSS measurements [25, 26, 159, 169, 178, 196-198]. A common example is 3-aminopropyltriethoxysilane (APS), which has been used both for silica based glass [197] as well as PBG fibres [25, 196, 198]. It was reported that APS improved the IFSS significantly for silica-based glass, however, very little or no improvement was seen for PBGs. Alternative treatments that have been considered for a variety of reinforcements like hydroxyapatite (HA), Bioglass[®] and phosphate based glasses include: phosphonic acids [169]; 2-hydroxyethyl methacrylate [159]; bisphosphonates [25, 199]; hexamethylene diisocyanate (HDI) [178] and more recently PLA oligomers [26]. In general, silanes, phosphonic acids, PLA oligomers and HDI were reported as promising routes to improve the IFSS. However, the mechanisms of improvement and extent of this improvement varies for different chemical treatments, for example silanes and phosphonic acids has been reported to make a covalent bridge between polymer and reinforcement while, PLA oligomers has been reported to improve IFSS by making hydrogen bond with reinforcement.

Due to lack of a standard test, several different techniques have been employed to measure IFSS values, including: micro-bond fibre pull out test with a polymer droplet or block [200-202], shear test [203], quasi-disc type fibre pull out test [204] and single fibre fragmentation test [25, 26, 205]. In a comparative study of different techniques for IFSS measurement, Piggott *et al.* stated that it was very difficult to

compare results from these different techniques as each method had its own limitations which caused inconsistency between results [203]. To evaluate the efficacy of different micromechanical tests (single-fibre pull-out test, the microdebond test, the fragmentation test and the micro-indentation test) for the fibre/matrix IFSS in composite materials a round-robin programme was undertaken. Twelve laboratories were invited to participate in this programme. Each laboratory was supplied with untreated Caurtaulds XA fibre, a standard surface treatment, quantity of epoxy resin, hardener and catalyst and curing route were also followed. It was concluded that there is great potential for achieving standard procedures, readers are encouraged to refer for more details [206]. Major differences were found in the data processing by some laboratories. A degree of scatter was observed which was inevitable due to the nature of the fibres, the application of the surface treatments and the small sample sizes. It was concluded that, compatibility between laboratories can be improved by adhering to a common test technique and data reduction scheme. A reasonable scatter within each laboratory indicates that the fundamental procedures used in each laboratory are sound. It also indicates that there is great potential for achieving standard procedures and reducing the inter-laboratory scatter.

In this chapter, potential surface treatment agents for PGF reinforced PLA composites were investigated for their capability to react with phosphate glass. An investigation of the effect of surface treatments on shear bond strength, surface wettability and degradation rate was also carried out. Selection was made on the basis of previously reported biocompatibility and likelihood of reaction with the phosphate glass and PLA. A few of these chemicals such as hexamethylene diisocyanate (HDI) and amino phosphonic acid (APA) were investigated for other biomedical applications and have never been utilised for totally degradable fibre

reinforced polymer composites. The effectiveness of the surface treatments was assessed through use of a modified shear test to determine IFSS values and by their ability to retard degradation of the glass. A shear test method was selected since the main aim of the study was to ascertain chemical surface treatments that could improve IFSS significantly. The shear test should directly test the adhesion qualities, with minimal contribution from the matrix and glass fibre reinforcement, details of the shear test will be discussed in materials and methods section. An investigation of the surface treatment agents' reaction with PBG was carried out to optimise the reaction conditions using two surface analysis techniques; Fourier transform infrared spectroscopy (FTIR) and X-ray photoelectron spectroscopy (XPS). Effect of surface treatments on the surface wettability was measured using sessile drop contact angle measurement and effect of this change in surface wettability on glass degradation rate is also reported.

4.2 Materials and Methods

4.2.1 Glass Synthesis

Phosphate based glass (45P₂O₅ 16CaO 24MgO 11Na₂O 4Fe₂O₃ in molar %) was prepared following the protocol reported in chapter 3 section 3.2.1, using the following precursors: NaH₂PO₄, CaHPO₄, MgHPO₄.3H₂O, P₂O₅ and FePO₄.2H₂O (Sigma Aldrich, UK).

Having obtained the T_g of the glass via DSC, it was re-melted and poured into graphite moulds (9 mm or 4 mm diameter) at 5 °C above the T_g and left to anneal for 60 minutes. After this the furnace was switched off and allowed to cool slowly to room temperature. The glass rods obtained from the mould were cut into 9 mm diameter, 2 mm thick discs for chemical analysis, 4 mm thick discs for degradation studies and surface energy measurements or 4 mm diameter and 10 mm length rods for IFSS tests using a low speed diamond wheel saw (Model 650, South Bay Technology Inc.).

4.2.2 Surface Modification for Phosphate Glass

Eight different surface treatments were selected: Glycerol 2-phosphate disodium salt (GP); 3-phosphonopropionic acid (PPA); 3-aminopropyltriethoxy silane (APS); etidronic acid (EA); hexamethylene diisocyanate (HDI); sorbitol/sodium ended PLA oligomers (S/Na-PLA) and Amino phosphonic acid (APA). All the chemicals except the PLA oligomers were bought from Sigma Aldrich (U.K) and used without further modification. The PLA oligomers were synthesised following the protocol reported elsewhere [26]. The surface treatment solutions were prepared in a range of

concentrations (0.05-0.25 Molar) in suitable solvents: all phosphonic acids (PPA, EA, APA) and APS in 90:10 ethanol/water; GP in distilled water; HDI in dimethylformamide and PLA oligomers in chloroform. Glass (discs or rods) were dipped coated with prepared solutions, washed with respective solvents and cured at ~200 °C. The procedures are shown in the flow chart in Figure 4-1.

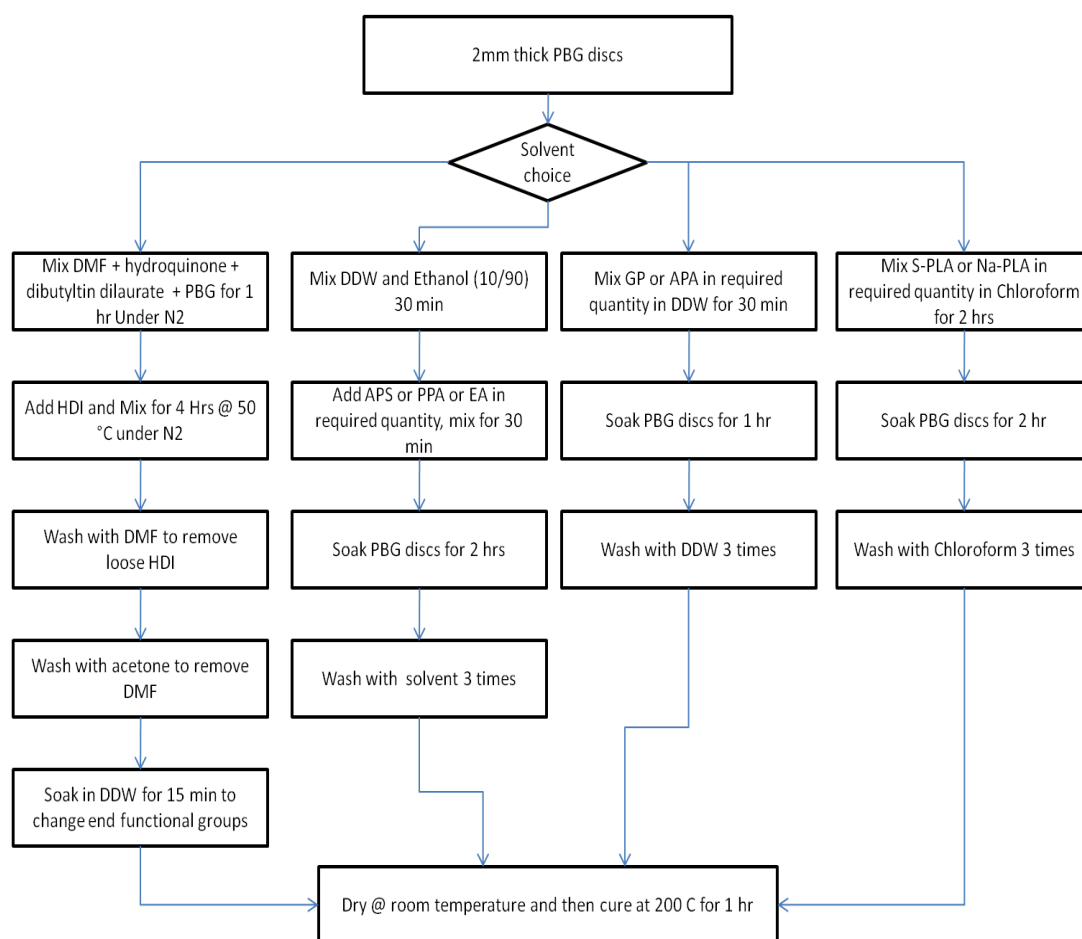


Figure 4-1: Flow chart of PBG sample modification with different chemicals. Solvents (double distilled water (DDW), Ethanol, dimethylformamide (DMF), chloroform) were selected on the basis of solubility of surface treatment agents.

4.2.3 Fourier Transform Infrared (FTIR) Spectroscopy

Infrared spectroscopy was performed on a Brüker Tensor 27 spectrometer, operated in absorbance mode. Spectra were recorded in the region of 600 cm^{-1} to 2000 cm^{-1}

wavenumbers using a standard MKII Golden Gate™ Single Reflection ATR system with heated plate (Specac Ltd.). Samples were 9mm diameter, 2mm thick discs.

4.2.4 X-ray Photoelectron spectrometry (XPS)

XPS analysis was used to investigate the surface chemistry of the modified PBG (mPBGs). A Kratos AXIS ULTRA with a mono-chromated Al K α X-ray source (1486.6 eV) was operated at 15 mA emission current and 10 kV anode potential. For XPS measurement, glass specimens were mounted on a sample holder and readings were taken from three different areas. Drift of the electron binding energy of the peaks due to the surface charging effect was calibrated by utilising the C1s peak of the contamination (285 eV).

4.2.5 Push-Out Test for IFSS Measurement

A push-out test was adopted to measure the maximum force required to push out PBG rods encircled with a PLA disc. This value was then used to calculate the IFSS. The test was derived from a single fibre pull out test [207] and it was expected that the push out test would follow the same trend of embedded length versus load curve as reported by DiFrancia *et al.* for the single fibre pull out test (Figure 4-2). Polacek and Jancar also used a modified form of single fibre pull out test to calculate the IFSS between their fibre reinforced composite axially joined with particulate reinforced composite [208].

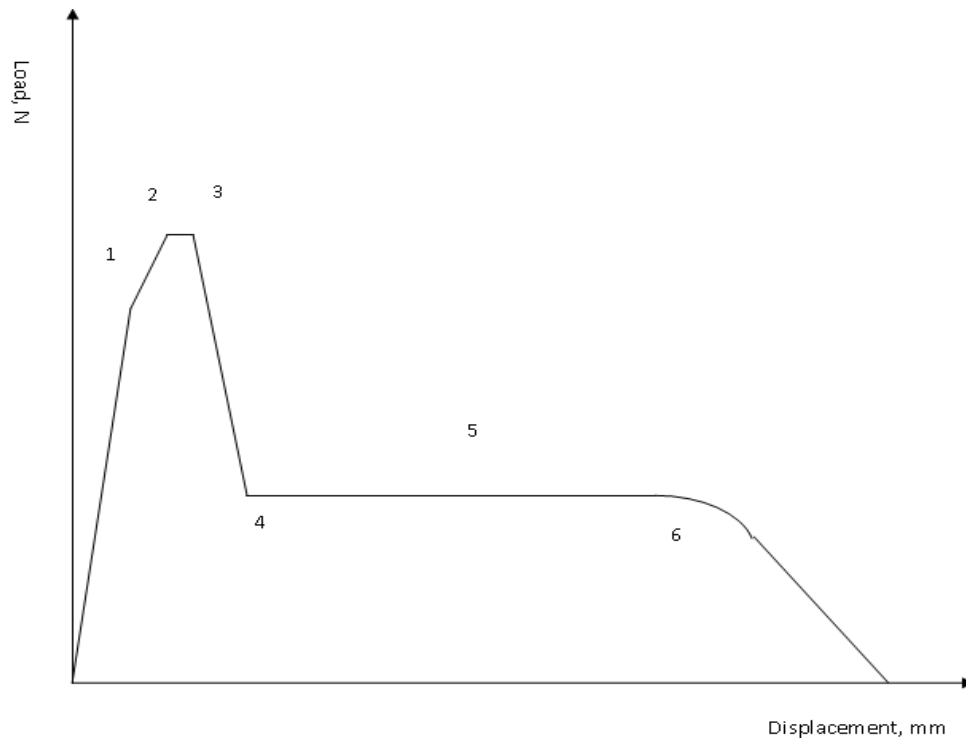


Figure 4-2: Different events during the single-fibre pull-out test are indicated: 1) crack initiation 2) frictional debonding 3-4) crack completion 5) frictional zone steady pull-out and 6) end of frictional zone (pull out). Figure adapted from [207].

The interpretation of the load versus extension trace obtained from the single-fibre pull-out test varies from researcher to researcher. However, consensus of these reports is that with debond initiation, the interfacial crack initially propagates with a significant amount of friction. As the applied load increases, the effects of friction begin to diminish. After some fibre length, the debonding becomes a steady-state event and thus the force required for crack propagation becomes constant. This steady-state debonding continues until the end of the fibre, at which time sliding commences.

Samples were fabricated by melting 1.6 g of PLA (3051D Natureworks Plc) around the 4mm glass rods in a PTFE mould with a symmetrical cylindrical cavity at 210°C for 45 minutes (Figure 4-3a). The glass rods were aligned with the axis of symmetry

to the cylindrical cavity and any extra flash on the sides of the glass rods was removed. The design of the mould ensured a constant thickness (2 ± 0.25 mm) of the PLA disc around the glass rod.

A universal tensile testing machine (Instron 5900 Systems) was used to perform the push-out measurements at room temperature. A custom made metal fixture was used to mount the specimens (Figure 4-3b). A cross-head speed of 1 mm/min was used in all measurements and the test was stopped when a plateau on the force axis was reached. Maximum stress, stress at failure and deformation at failure were recorded using the data processing software supplied by the tensile tester manufacturer.

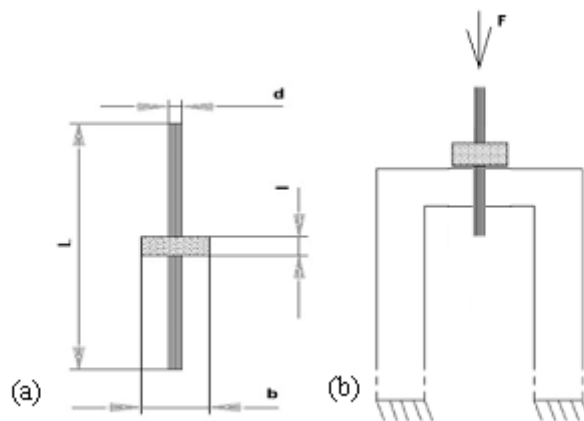


Figure 4-3: A schematic diagram of (a) Push-out test sample with all dimensions L = length of glass rod; d = diameter of glass rod; l = thickness of PLA disc; b = diameter of PLA disc (b) push out test setup

To calculate the interfacial shear strength (IFSS), τ_a , from experimental data, the following equation was used:

$$\tau_a = \frac{F_{max}}{\pi \times d \times l}$$

Where, τ_a is the average IFSS, F_{max} is the measured load at failure, ' d ' is the diameter of the glass rod specimen and ' l ' is the adhesive joint length.

4.2.6 Degradation Study

After surface modification with functionalization agents, the glass samples (9 mm diameter, 4 mm thick) were placed into vials containing 30 ml of phosphate buffered saline (PBS) in accordance with the degradation standard test conditions: ISO 10993–13:2010. These were placed into an incubator at 37 °C. The starting pH was measured to be 7.5 ± 0.05 , using a bench top pH meter (pH 212 Hanna instruments). At predetermined time points, the discs were taken out of their respective containers and excess moisture was removed by blotting the samples dry with tissue. The solution was also changed at each time point. Their new weight was recorded at each of these time points and the data plotted as percentage weight loss over time. The measurements were conducted in triplicate. The slope of the graphs gave a degradation rate in terms of percentage mass loss per hour, which was determined by fitting a straight line through the data and including the origin as a data point. The pH analyses were also conducted alongside the weight loss studies.

4.2.7 Wettability Measurement

Surface wettability can be assessed by measuring the contact angle of a water droplet [209]. In this study, surface hydrophobicity/hydrophilicity was estimated by measuring the contact angle of a 5 μ l water droplet on the glass samples' surfaces. The distance between the micro pipette and the sample was kept constant at 10 mm and the time before image capture was fixed at 10 seconds. The captured image was then analysed for contact angle using “ImageJ” image processing software.

4.2.8 Statistical Analyses

Mean values and standard deviation were computed six (IFSS) replicate samples from at least two iterations of the experiments. Statistical analysis was performed using the Prism software package (version 3.02, GraphPad Software, San Diego California USA, www.graphpad.com). Two-way analysis of variance (ANOVA) was calculated with the bonferroni post-test to compare the significance of change in one factor with time. The error bars presented represent standard error of mean.

4.3 Results

4.3.1 FTIR

IR analysis was performed on mPBG samples in order to investigate the chemical interaction of the surface functionalisation agent with the glass surface. The IR traces (Figure 4-4) were carefully analysed to confirm the presence of a layer on the PBG surface and evidence of any chemical bonding between the two.

IR peaks due to covalent bonding between the glass and surface treatment chemicals were difficult to distinguish from glass peaks, since most of the chemicals investigated in this study reacted with phosphate glass through a P–O–X bond (where X = Si, C or P). These P–O–X have signature peaks in the region of 1000-1250 cm^{-1} wavenumbers, i.e. the region of the PBG signature peaks. However, a significant drop in PBG peak intensities was seen after chemical treatment of surface and in a few cases (APS, HDI and EA mPBGs) new peaks were found which indicated the presence of an alternate layer on the surface of the PBGs. All the peaks and their assignments are summarised in Table 4-1:

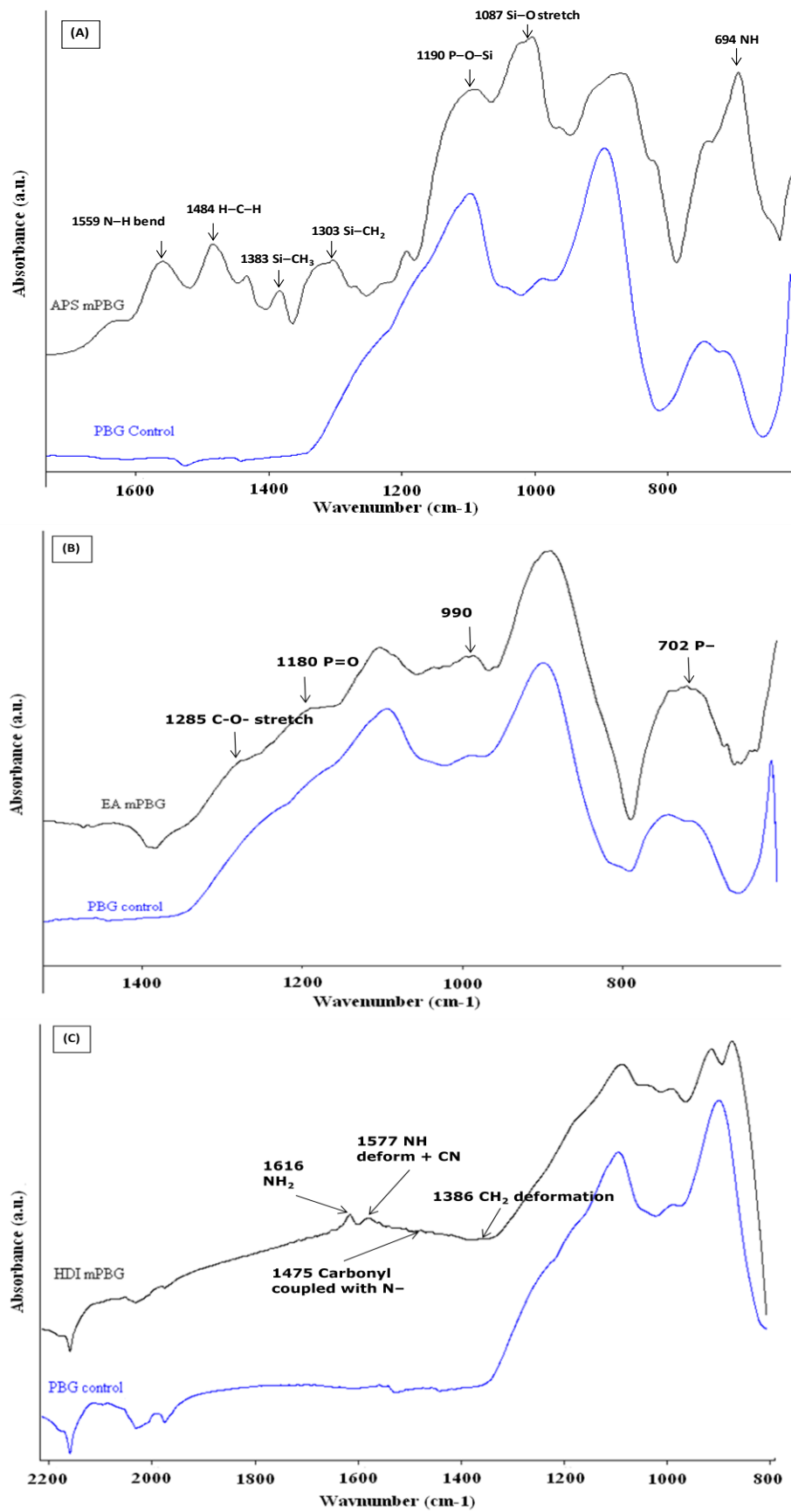


Figure 4-4: IR spectra of (A) Control PBG; (B) APS mPBG; (C) EA mPBG; (D) HDI mPBG indicating the covalent bond between PBG and surface treatment agents.

Table 4-1: Peak assignment from IR analysis of PBG samples before and after surface treatments

Sample Code	IR band (cm ⁻¹)	Assignment
PBG Control	1250	Asymmetric stretch NBO of O–P–O
	1100	Symmetric stretch of NBO of O–P–O
	1050	PO ₃ end groups
	990	PO– chain terminator
	900	Asymmetric stretch of P–O–P
	750	Symmetric stretch of P–O–P
APS	694	NH Amine
	1087	Si–O stretch
	1190	P–O–Si
	1303	Si–CH ₂
	1383	Si–CH ₃
	1484	H–C–H bend
	1559	N–H bend
	2364	Si–H silane
EA	702	P–O–P
	1180	P=O (shoulder)
	1385	Free (–OH) bending
HDI	1260	Urethane C–N, C–O stretch
	1386	CH ₂ deformation
	1475	Carbonyl coupled with N–H and N–C–N (secondary urea)
	1577	NH deform + CN stretch
	1616	NH ₂ vibration
	3317	NH ₂ vibration

For APS modified glass samples two bands at 1087 cm⁻¹ and 1190 cm⁻¹ were assigned to Si–O and P–O–Si stretching modes. The presence of the shoulder around 2980 cm⁻¹ was assigned to the asymmetric methyl stretch (–OEt) due to silane. These data indicated that the film consists of oligomeric siloxane networks.

Similarly, on HDI treated PBG samples there were several extra peaks, however, the intensity of the extra peaks was very weak. It is clear from IR spectra that no absorption band of isocyanate group (O=C=N–R) at 2270 cm⁻¹ on the spectrum of HDI mPBG sample was observed. It can be deduced that all the isocyanate groups

were grafted on PBG. It is noteworthy that a clear peak asymmetric stretching vibration of P–O–C group could not be observed at the position around 1100-1050 cm^{-1} , which could be lost in PBG absorbance peaks. However, the presence of urethane peaks at 1577, 1475, and 1260 cm^{-1} points out to the grafting of HDI onto the surface of PBG through urethane link.

A shift of around 50 cm^{-1} in symmetric stretch of P–O–P was observed when PBG surface was modified with EA which could also be detected at 700 cm^{-1} in etidronic acid powder. A clearer shoulder at 1180 cm^{-1} and symmetric stretch of P–O of PO_3^{-2} at 990 cm^{-1} also indicate the presence of new phosphate specie on the surface of PBG.

In addition to P–O–X peaks presence of other bands for example, NH in case of APS and NH_2 in case of HDI and provided with the evidence of chemical reaction and new chemical species on glass surface.

4.3.2 XPS

XPS was conducted analysing the O 1s, Si 2p, N 1s, P 2p and Na 1s binding energies. Elimination of P 2p and/or Na 1s peaks were used as an indication of total surface coverage of PBG with surface treatment chemicals. The deconvoluted binding energies and their assignments for all the samples are shown in Figure 4-5.

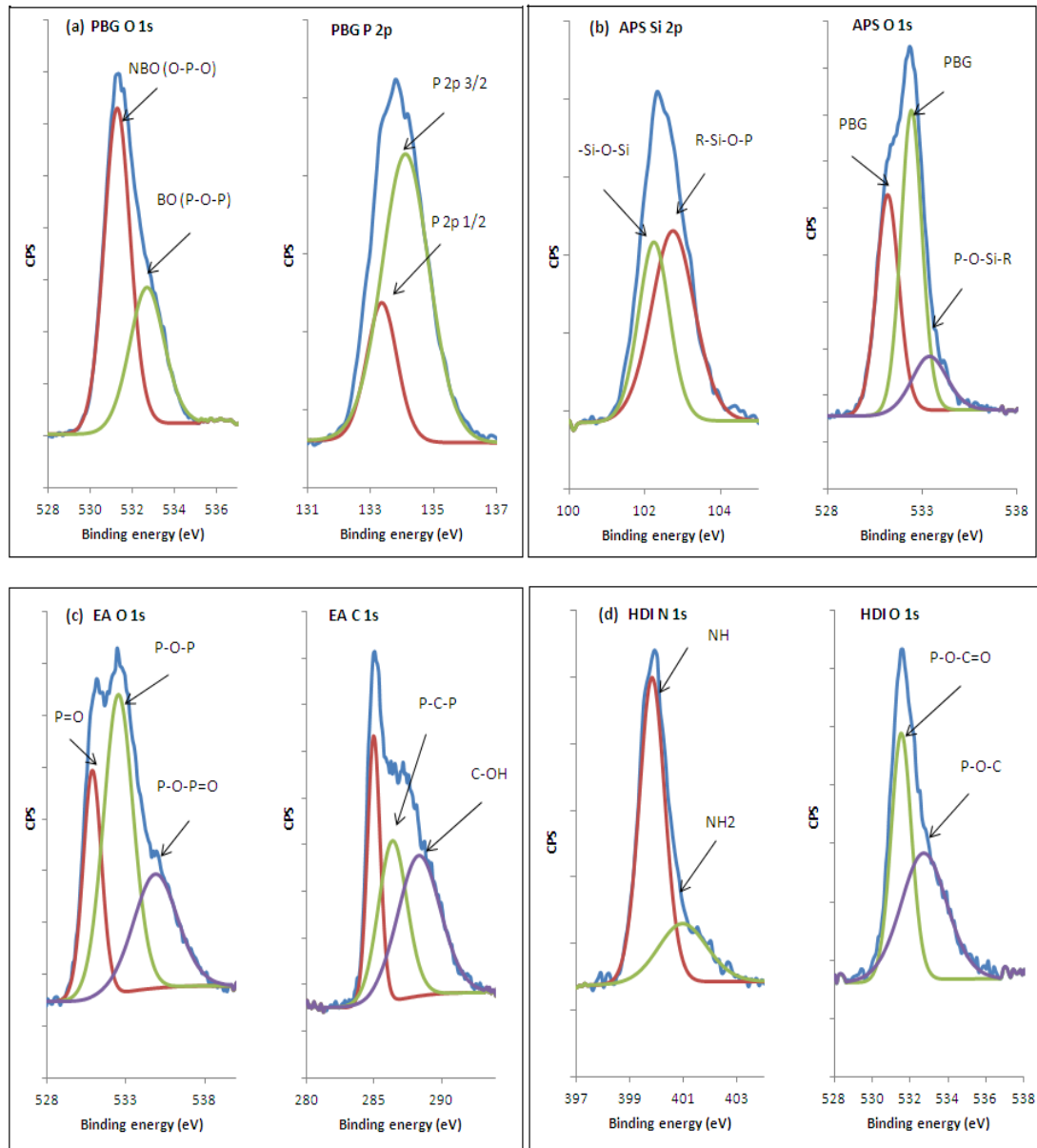


Figure 4-5: High resolution XPS spectra of (A) Control PBG O 1s and P 2p; (B) APS mPBG O 1s and Si 2p; (C) EA mPBG O 1s and P 2p; (D) HDI mPBG O 1s and N 1s. O 1s spectra indicate covalent bond formation and Si 2p, C 1s and N 1s spectra provide supplementary evidence.

An XPS spectrum was used to identify the surface of the PBG sample for different elements. Survey spectrum showed no peaks in the binding energy region of Si(2p) for the untreated PBG samples. On the other hand, APS-modified PBG, the presence of silicon signals Si (2p) in XPS narrow spectra of Si (2p) provides evidence that Si element does exist in APS mPBG. High resolution Si (2p) peak was deconvoluted

into two peaks; Si–O–Si– and R–Si–O–P. High resolution O (1s) peak was also found and deconvoluted into three peaks. The deconvoluted peak at around 533 eV and corresponded to P–O–Si–R.

Survey spectrum of PBG samples also missing N (1s) which was detected in PBG modified with HDI. High resolution spectrum of N (1s) from HDI mPBG was deconvoluted with two peaks at 399 eV (NH) and 499 eV (NH₂). High resolution O (1s) spectrum was fitted with three peaks at around 531 eV (P–O–C=O) and 533 eV (P–O–C), indicating the formation of a urethane link on PBG surface modified with HDI.

High resolution O (1s) spectrum from EA mPBG sample was fitted with three peaks around 531 eV (P=O), 533 eV (P–O–P) and 536 eV (P–O–P=O) which were different than oxygen peaks detected from untreated PBG indicating presence of etidronic acid layer covalently linked to phosphate glass. High resolution C (1s) peaks at 286.5 eV (P–C–P) and 289 eV (C–OH) also provided the evidence of etidronic acid layer on PBG.

4.3.3 Interfacial Shear Strength Measurement (Push–Out Test)

Figure 4-6 is representative of the curves obtained from load versus extension for the devised push–out test. It was clear that the push out test followed the expected events discussed in Section 4.2.5 (Figure 4-2) for single fibre pull out test with no discrepancies. In addition to this, the repeatability of the modified push out test was confirmed by the results of three different control (annealed) batches (n=6); IFSS was found to be ~6 MPa with a standard deviation between batches of ~1.5 MPa.

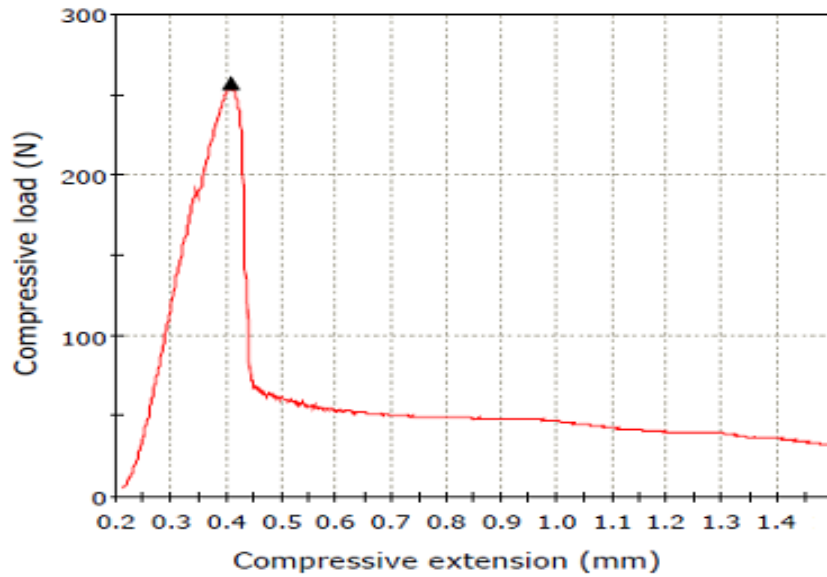


Figure 4-6: Representative curve obtained from load versus extension for glass rod push-out test adapted for this study, ▲ represents; F_{\max} required for crack initiation and debonding.

The push out test was performed on samples (4mm glass rod) surface-treated with different chemicals over a range of concentrations until a plateau or a drop in IFSS is reached. Data was analysed for IFSS and presented alongside control (annealed and chemically untreated) in Figure 4-7.

The results revealed that the surface treatments investigated in this study improved the IFSS; however, the degree of improvement and the effective concentration was not the same over the range. For APS, GP, EA and HDI modified glasses an improvement with higher concentrations (~2 M) was seen. However, after a certain concentration a decrease or plateau for IFSS values was observed.

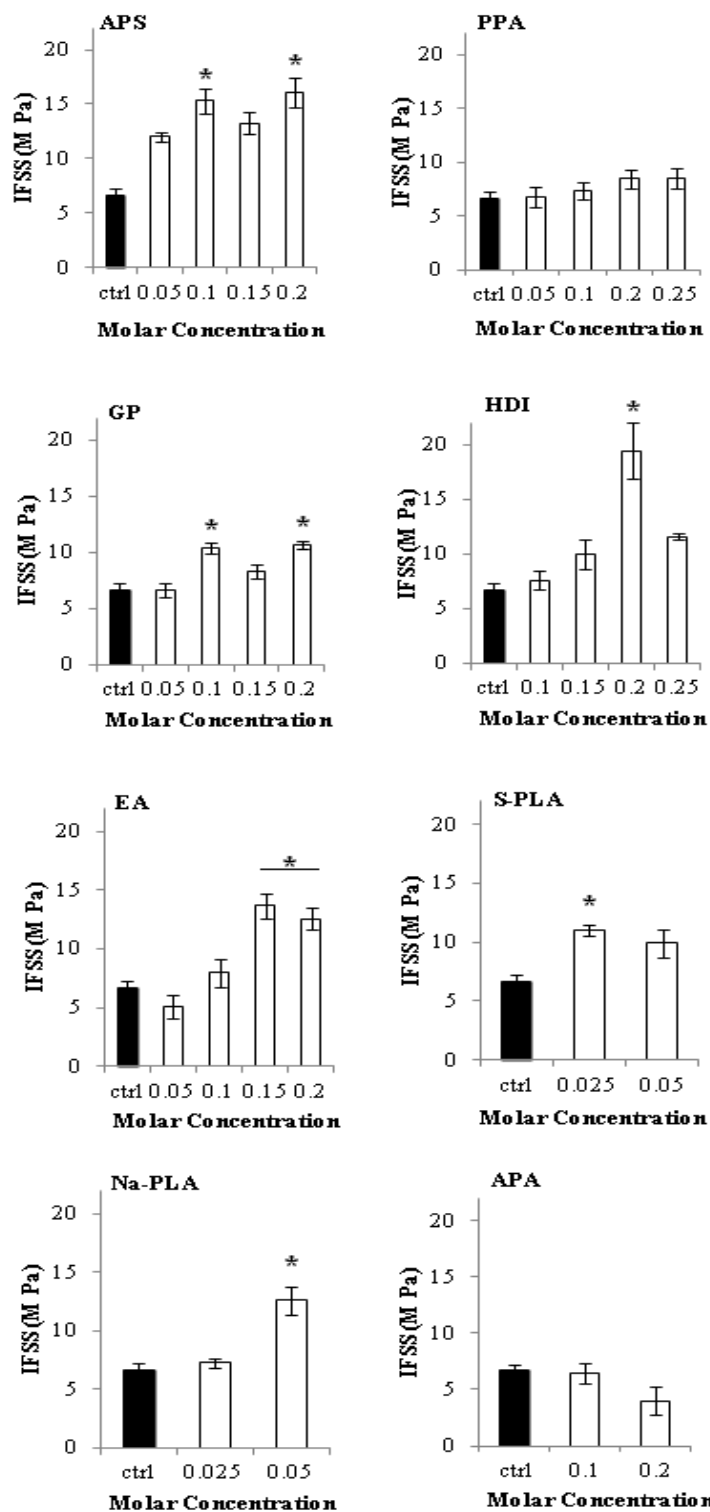


Figure 4-7: IFSS values as measured by push-out test for 3-aminopropyltriethoxy silane (APS); 3-phosphonopropionic acid (PPA); Glycerol 2-phosphate disodium salt (GP); etidronic acid (EA); hexamethylene diisocyanate (HDI); sorbitol/sodium ended PLA oligomers. * indicating at significant difference compared to control.

A consistent 6 ± 1.5 MPa IFSS value was calculated of repeated experiments for control (untreated) samples. IFSS was improved gradually with increasing concentration of APS and a 3 fold improvement was calculated with 0.1M APS treatment. However, no further improvement was observed with increasing silane concentration. Similarly, increasing EA concentration had positive effect on IFSS which was calculated to be 13 ± 1.2 MPa with 0.15–0.2 M EA solution treatment. However, most effective in terms of IFSS enhancement was HDI which improved the IFSS by 4 fold; highest IFSS value 22 ± 2.1 MPa was calculated from glass samples treated with 0.2M HDI in DMF. Other surface treatments such as PPA GP, SPLA, and Na-PLA also improved IFSS to 10 ± 1.5 MPa. A modest worsening effect of APA with increasing molar concentration was observed on IFSS.

4.3.4 Surface Modified Glass Degradation

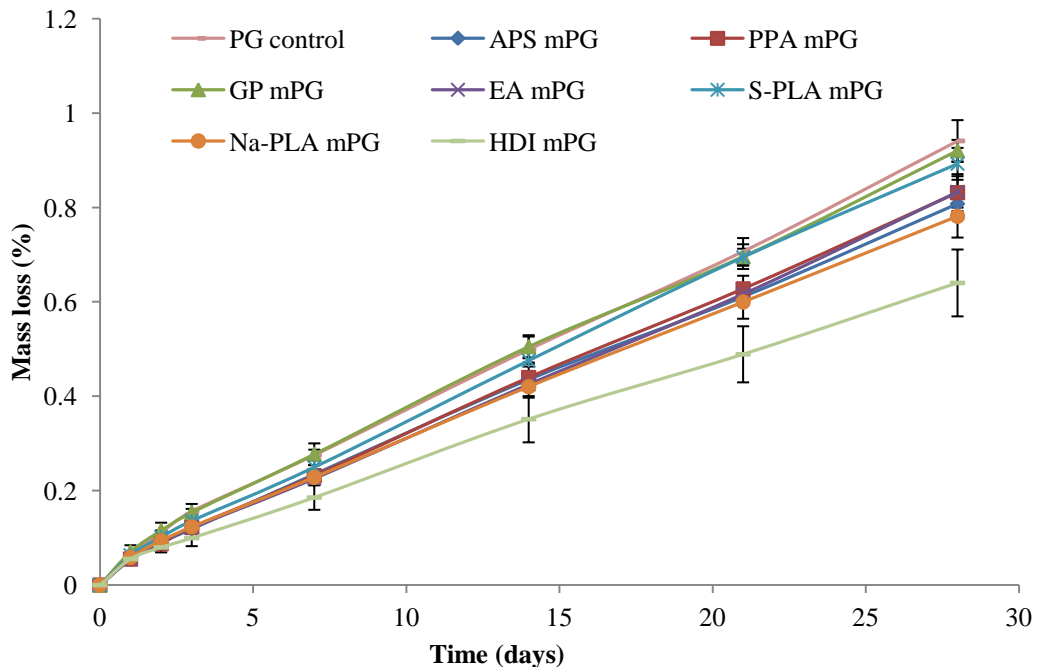


Figure 4-8: Effect of surface treatments on glass degradation profile in PBS at 37°C.

Error bars represent standard error of mean where n = 3.

The results of the mPBG (treated with optimised concentration) degradation study are presented in Figure 4-8. The results reveal a decrease in degradation rate of PBG samples treated with HDI, APS, Na-PLA, EA and PPA compared to the control (annealed and chemically untreated). However, GP and SPLA modified glasses did not show a significant difference compared to control.

4.3.5 Surface Wettability Measurement

Surface wettability of the glass samples was seen to change significantly after modification with optimised concentration of surface treatments. Alterations in the contact angle are summarised in Figure 4-9. A high contact angle for APS (~75°) and HDI (~65°) treated samples compared to control (~50°) represent a more hydrophobic surface while GP and PLA oligomers treated surfaces were found to be more hydrophilic as the contact angle was found to be significantly lower than the control specimen.

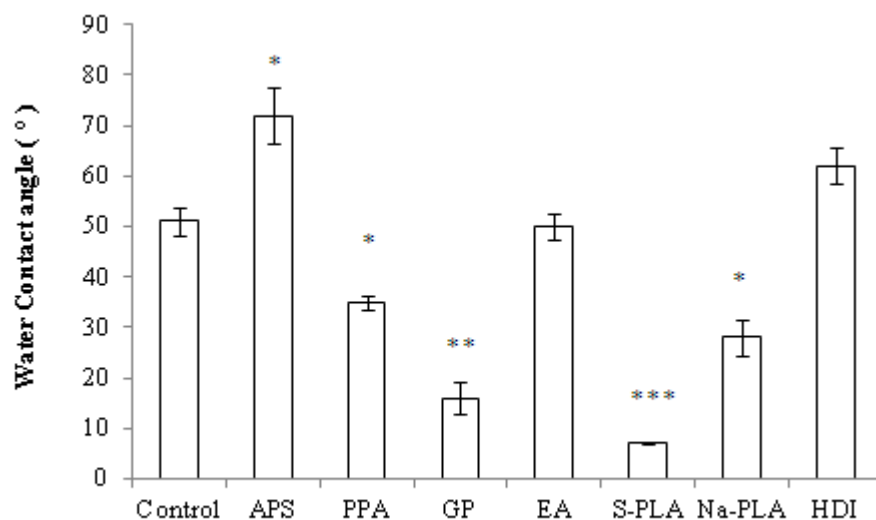


Figure 4-9: Wettability of mPBGs as measured by distilled water contact angle, error bars represent standard deviation where n=3. * indicating at significant difference.

4.4 Discussion

In the literature number of surface treatments have been investigated for their potential to improve non-degradable [197] and degradable [25-27, 159] composites reinforced with particles [169] or fibres [25-27, 159, 197, 198] for a variety of applications. In this study, eight different chemicals were investigated as potential surface treatments for degradable phosphate glass fibre reinforced composites. It was hypothesised that by varying the concentrations of the agents investigated, an improved bonding between the glass fibres to matrix could be achieved. Evidence of reaction between the agents and PBG were also investigated.

Phosphate glass (45P₂O₅ 16CaO 24MgO 11Na₂O 4Fe₂O₃ in molar %) was selected on the basis of results reported in chapter 3.

Silanes are well known to self-assemble into mono-molecular and multi-molecular layers on surfaces such as glass or silicon dioxide [164, 165, 197]. One end of the silane molecule typically has di or tri methoxy or ethoxy functionality whilst the other end in case of APS has amine functionality. The ethoxy functionality is believed to condense with the hydroxyl functionality on the surface of the glass whilst the amine functionality can react with the polymer [164, 165]. It is also reported that silanes have a hydrolysable group (ethoxy), which is an intermediate in the formation of silanol (Si-OH) groups, for chemical bonding to the surface of the filler and the other end has an organic-functional group that entangles with polymer molecular chains by reactive group [164]. Both IR and XPS examinations confirmed the covalent reaction between PBG and APS (Figure 4-4, 4-5); the absorbance band at 1190 cm⁻¹ was assigned to P-O-Si due to condensation of silane onto PBG indicating covalent bonding in agreement with previous reports, other absorbance

bands also correlated well with the results presented by Kurth and Bein [210] which showed that APS had reacted with the PBG according to the scheme presented in Figure 4-10. For APS mPBG O (1s) and Si (2p) high resolution XPS spectra were deconvoluted to fit two peaks in each (Figure 4-5). Peaks at 532.7 eV and 102.2 eV can be assigned to O (1s) and Si (2p) peaks of P–O–Si–R respectively, which indicated a P–O–Si covalent bond formation at the PBG surface. These results correlated with the results presented by Yang *et al.* in their investigative XPS study of octadecyltrichlorosilane grafted hydroxyapatite [211].

Etidronate is a bisphosphonate; a family of drugs used for osteoporosis treatment that binds with hydroxyapatite in the bone and inhibits bone resorption. While bisphosphonates are analogues of pyrophosphate structurally, they are characterised by a P–C–P bond; the linking oxygen is replaced with a carbon, which is resistant to enzymatic and chemical hydrolysis. It is known that bisphosphonates bind strongly to hydroxyapatite crystals at the sites of increased bone turnover preferentially and inhibit the formation, aggregation, and dissolution of the crystals [212]. They may also inhibit osteoclast function directly, promote osteoclast apoptosis and interfere with osteoblast–mediated osteoclast activation [175]. A study by Panzavolta *et al.* revealed the effectiveness of another bisphosphonate (alendronate) in calcium phosphate (CaP) bone cement and showed that this bisphosphonate provoked a modest reduction of the mechanical properties [199]. From IR analysis of EA mPBG (Figure 4-4), two new peaks at 702 cm^{-1} and 1260 cm^{-1} were identified and assigned to P–O–P and P=O which indicated the presence of the bisphosphonate layer on the surface of EA mPBG. Deconvoluting XPS O (1s) peak from EA mPBG (Figure 4-5) revealed three peaks that were assigned to: P=O from EA (530.8), bridging oxygen

P–O–P (532.5) and P–O–P=O (533.5) bond of bisphosphonate with PBG according to the reaction scheme (Figure 4-10).

The isocyanate group has also been reported to bind to hydroxyapatite [178]. The studies showed that isocyanate could react with hydroxyl groups of hydroxyapatite and form a covalent bond between isocyanate and hydroxyapatite. The IR spectrum of HDI–mPBG (Figure 4-4) showed several new peaks of low intensity. However, no absorption band was found that could be assigned to the isocyanate group ($\text{O}=\text{C}=\text{N}-\text{R}$). Therefore, it can be deduced that all the isocyanate groups either involved in grafting with the $-\text{OH}$ groups present on phosphate glass surface or converted into amine group after reaction with water. It was assumed that HDI grafted to the surface of PBG as follows: $\text{PBG}-\text{O}-\text{CO}-\text{NH}-(\text{CH}_2)_6-\text{N}=\text{C}=\text{O}$. It can be suggested here that only one isocyanate group of HDI took part in grafting to the phosphate glass as the length of HDI molecule prevents the other end to roll back onto the same surface again, the same mechanism was proposed elsewhere [178]. Although the peak for P–O–C was lost in the area assigned to PBG peaks, evidence of this linkage can be seen from the IR spectra of HDI mPBG with C–N, C–O bands and NH_2 deformation. High resolution XPS O (1s) and N (1s) spectrum (Figure 4-5) confirmed the presence of a P–O–C (532.9 eV) bond and a urethane linkage [178] between PBG and HDI which was converted into a primary amine group after treatment with water. These results correlated well with the study carried out on HDI modified HA [178]. A scheme of HDI grafting onto the surface of PBG is presented in Figure 4-10.

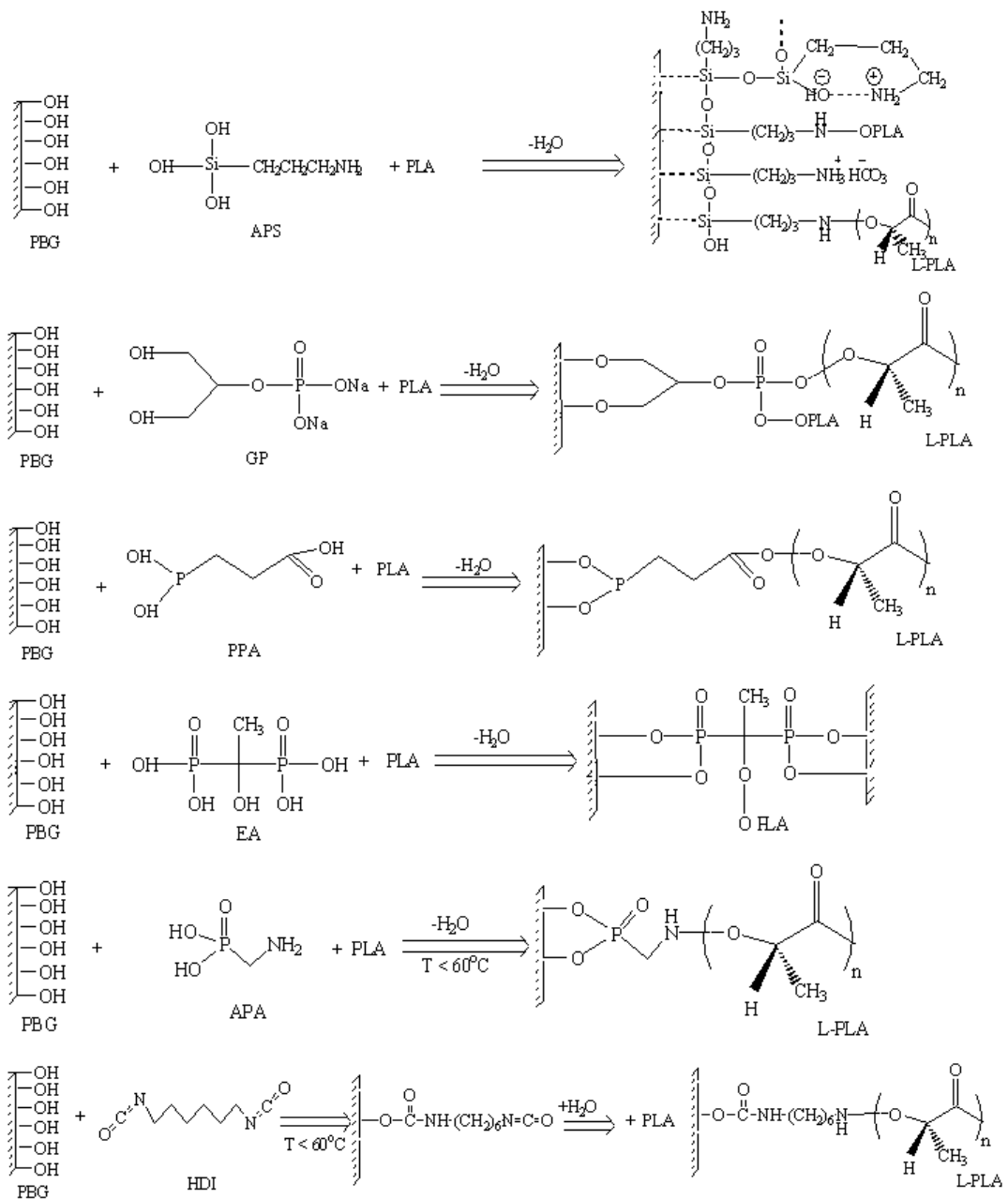


Figure 4-10: Chemical reaction schemes devised on the bases of inorganic chemistry principles and surface analyses (FTIR/XPS) data.

PLA oligomers with potentially reactive end functionalities like COOH, Na and sorbitol have been developed and investigated as potential s for PGF reinforced PLA composites [25, 26]. In a study by Haque *et al.* it was hypothesised that either the end functional group should react with the glass through esterification or the hydroxyl groups present within the end functional group would create hydrogen bonds with hydroxyl groups present on the glass surface. The prior study reported

that increasing the number of –OH groups on the end functionality improved the IFSS properties [25, 26, 167]. However, results acquired in current study did not find an ester bond between PBG and PLA oligomers which in turn suggested that PLA oligomers reacted with PBG via hydrogen bonds.

Careful analysis of IR and XPS results concluded that APS, EA, HDI reacted with the glass covalently. However, there was no evidence of covalent bonding found for the other agents investigated. Therefore, it is proposed that these agents formed hydrogen bonds or covalent P–O–P bonds, which were difficult to detect due to their similarity with the structure of PBG. However, after modification with all surface treatments the Na (1s) peak in the XPS spectra was lost which indicated the presence of a layer on the surface of the glass.

Surface wettability tests (Figure 4-9) showed that the APS and HDI coatings were more hydrophobic in comparison to the control PBG, which as stated could potentially delay the hydration of the interface. The shift in wettability also provided further evidence that the PPA, GP and PLA oligomers had successfully been applied to the surface of the PBG.

As hypothesised and observed from surface energy and degradation profiles, the hydrophobicity induced by HDI and to some extent APS treatment reduced the degradation rate of PBG (Figure 4-8), which could inhibit the interface breakdown due to hydrolysis.

Considering the rigidity of glass rod, self–alignment of test setup and relatively low IFSS values, a mode II (in–plane shear) adhesive fracture was assumed for glass push out test. The difference between shear strength of PLA used in this study (~60 MPa) [126, 127] and maximum IFSS value found for specimen (~22 MPa) also

explains fracture of interface in mode II. It was expected that the maximum shear stress concentration will always locate in the glass rod near the glass/polymer interface on the upper portion of the test specimen. No effect of concentration on fracture behaviour was observed for any investigated treatment.

Improved interfacial shear strength due to surface treatments (Figure 4-7) can be explained via chemical bonding theory. It is suggested that covalent bonds between the glass fibre and polymer matrix increase the shear bond strength markedly [6, 25, 169] as seen in the case of HDI, APS and EA modified PBG samples in this study. It has also been reported that an increase in the number of hydrogen binding sites on the surface of mPBG the greater the increment in IFSS [26], which was suggested as the most likely cause for improvements seen in PPA, SPLA, and GP modified PBG samples. However, improvement in IFSS due to hydrogen bonding is comparatively small and potentially prone to hydrolysis.

IFSS values were also used to optimise the concentrations of the surface treatments and it was found that by varying concentrations, a higher effect of coupling could be achieved (Figure 4-7). For example; 0.043 M APS was applied to PGFs by Onal *et al.* [198] with no effect on IFSS, similar results were reported by Haque *et al.* [25]. However, the results here showed a threefold improvement in IFSS for 0.2 M APS treatment. Similarly improved results were obtained by using 0.2 M HDI as compared to 0.25 M used by Dong *et al.* [178] thereby; reducing the chances of dose dependent cytotoxicity of HDI as reported by Gong *et al.* [213]. Due to their high solution viscosity, the maximum concentration of the PLA-oligomer solutions was 0.05 M. A plateau or decrease in shear bond strength was seen from the results

which could be attributed to complete surface coverage and a polymerised layer of coupling agent on the glass surface respectively.

The results showed that by applying optimal concentrations of potential surface treatments, IFSS between PBG and PLA can be improved significantly, which should improve the overall mechanical properties of composite fabricated from the same materials and may also help to retain the strength for a longer time period by retarding the interface plasticisation.

4.5 Conclusions

Evidence of covalent bonding between chemical used for surface modification and glass was found for three of the chemicals investigated: namely 3-aminopropyltriethoxy silane; etidronic acid and hexamethylene diisocyanate. These three agents also improved the interfacial shear strength and increased the hydrophobicity of the glass surface. It was found that by using optimal amount of appropriate surface treatment the interfacial shear strength between PBG and PLA matrix can be improved significantly, which could help in fibre/matrix load transfer and thus improve the overall mechanical properties of the composite. It can be concluded that by treating PBG with HDI, APS, and EA all three target parameters; IFSS, wettability and degradation rate can be improved.

CHAPTER 5. CYTOCOMPATIBILITY

ASSESSMENT FOR

SURFACE-TREATED

GLASSES

5.1 Introduction

For a material that aims to be used in medical applications a comprehensive biocompatibility assessment is required. In terms of biocompatibility, the degradable implant material must have to fulfil even more demanding requirements as they have to go through cytotoxicity assessment as well as routine cytocompatibility tests for bulk material as well as degradation products. International society of standards (ISO) has devised a set of standards for evaluating the biocompatibility of a medical device prior to a clinical study under ISO 10993 series. This set of standards provides a methodology for choosing the proper biological evaluation test programme depending on the device category: surface, external communicating and implant, and the exposure period of the material: limited (<24 hours), prolonged (24 hours to 30 days) and permanent (>30 days) [214].

Chemical agents used in this project were selected on the basis of potential or reported cytocompatibility. For example, phosphonic acid based chemicals have been employed as s by Phillips *et al.* [169], Greish and Brown [170, 171] and Tanaka *et al.* [172] where all the studies reported no cytotoxicity from the phosphonic acids used. Similarly, Sánchez–Vaquero *et al.* [215] and Jung *et al.* reported favourable cell interaction with silane containing biomaterials. However,

conflicting report of cytotoxicity or cytocompatibility have been reported for hexamethylene diisocyanate (HDI) [178-180, 216].

To ascertain cytocompatibility of surface treatments used in this project a three step assessment programme was adopted; evaluation of cytotoxicity due to degradation products [217]; short term direct contact test using MG63 osteosarcoma osteoblast-like cell line; long term direct contact study of primary human osteoblast (HOBs) cells interaction with short listed modified phosphate based glass (mPBG).

Cytotoxicity testing is rapid, standardised, sensitive, and inexpensive that represents initial phase in testing biocompatibility. It is a means to determine if a test material contains significant quantities of biologically harmful degradation products. Short term direct contact of MG63 osteosarcoma cells with chemically modified glass surfaces was used as a screening step. Finally, HOBs were employed to assess cell-material interaction including attachment, proliferation and differentiation by using cell metabolic activity, early and late differentiation marker assays for osteoblast cells. Primary HOBs' morphology was also assessed at each time point using scanning electron microscope (SEM).

5.2 Materials and Methods

5.2.1 Glass Synthesis

Phosphate glass (45P₂O₅ 16CaO 24MgO 11Na₂O 4Fe₂O₃ in molar %) was prepared following the protocol reported in chapter 3, Section 3.2.1. The glass rod (9 mm diameter) obtained from the mould was cut into 4 or 2 mm thick glass discs for different tests.

5.2.2 Chemical Modification for Glass Surface

Glass discs were treated with optimised concentrations of surface treatment agents from the conclusions made in chapter 4 following the protocol reported in chapter 4, Section 4.2.2. The fibre to solution ratio was kept constant at 1.5g: 100ml.

5.2.3 Cytotoxicity Assessment

Cytotoxicity assessment of elution products was performed according to the ISO standard for biological evaluation of medical devices (ISO 10993–5 2009) with only one discrepancy of cell-type, MG63 cells line was used instead of recommended HOS cells. Cytotoxicity of mPBG samples (9 mm diameter, 4 mm thick) was assessed by NRU following the protocol reported in chapter 3 section 3.2.4.5. The mPBG samples were eluted in treatment media (DMEM + 10% HEPES for three days with a 1mg/ml weight to volume ratio.

5.2.4 Short–Term Direct Contact Test

5.2.4.1 Cell Culture

MG63 cells (human osteosarcoma), obtained from European collection of cell cultures (ECACC), were cultured and sub-cultured in complete Dulbecco's modified eagle media (CDMEM) as reported in Chapter 3, Section 3.2.4.1.

Modified phosphate glass discs were sterilised using dry heat at 190 °C for 30 minutes and washed three times with sterilised PBS prior to cell culture. Tissue culture polystyrene (TCP) was used as a positive control for cell growth. Cells were seeded onto the disc sample surfaces at a concentration of 40,000 cells/cm² and were incubated at 37 °C in a humidified atmosphere with 5% CO₂ for 2, 48, 96 and 168 hours.

5.2.4.2 Alamar Blue

At the designated time points, culture medium was removed from the wells and the samples were washed three times with warm PBS. Protocol for alamar blue assay (Chapter 3, Section 3.2.4.2) was followed and fluorescence was measured at 530 nm excitation and 590 nm emission using FLx800 microplate reader (BioTek Instruments Inc).

5.2.4.3 Alkaline Phosphatase Activity

Alkaline phosphatase (ALP) activity was measured using the Granutest 25 alkaline phosphatase assay (Randox, UK). Cell lysate in sterilised deionised water was prepared using a 3–cycled freeze/thaw technique. The protocol for ALP assay

(Chapter 3, Section 3.2.4.3) was followed and the absorbance was measured at wavelengths of 405 and 620 nm using ELx800 microplate colorimeter (BioTek Instruments Inc).

5.2.4.4 DNA Quantification

Samples were washed and cells lysed using a freeze/thaw technique as described for the alkaline phosphatase method above. DNA concentration was quantified by following DNA quantification assay reported in Chapter 3, Section 3.2.4.4. Fluorescence was measured at 360 nm excitation and 460 nm emission using FLx800 microplate fluorimeter (BioTek Instruments Inc).

5.2.5 Primary Hobs in Direct Contact

5.2.5.1 Cell Culture

Primary human osteoblast (HOB) obtained from European collection of cell cultures (ECACC) and cultured in osteoblast growth medium (417–500) (Cell Applications, Inc.) following the same subculture protocol mentioned for MG63 cell line.

Cells were seeded onto the disc sample surfaces at a concentration 40,000 cells/cm² and incubated at 37 °C in a humidified atmosphere with 5% CO₂ up to 28 days.

At the designated time points (7, 14, 21 and 28 days) cell culture media was removed and the samples were washed three times with warm PBS prior to the addition of 1ml deionised water to each well. Cells were lysed using a freeze/thaw technique.

5.2.5.2 Proliferation

Osteoblast proliferation was assessed by quantifying DNA at each time point following standard DNA quantification assay protocol (Chapter 3, Section 3.2.4.4).

5.2.5.3 Differentiation

To cover different stages of differentiation three osteoblast specific assays were selected; alkaline phosphatase activity; collagen quantification; osteocalcin production (late osteoblast specific differentiation marker).

5.2.5.3.1 Alkaline Phosphatase Activity

Alkaline phosphatase activity was measured using the Granutest 25 alkaline phosphatase assay (Randox, UK) using the protocol described in Chapter 3, Section 3.2.4.3.

5.2.5.3.2 Collagen Quantification

Osteoblasts produce a matrix of osteoid, which is composed mainly of Type I collagen. Collagen quantification was carried out by using the soluble collagen assay (Sircol, UK). The Sircol™ collagen assay is a dye-binding method for the analysis of acid and pepsin-soluble collagens. The assay works by utilising the Sirius red dye, which is also known by the name Direct Red 80. Sirius red is an anionic dye with sulphonic side chains, it is these groups that react with the side chain groups of the basic amino acids present in collagen. The specific affinity of the dye for collagen, under assay conditions, is due to the elongated dye molecules aligning parallel with the long rigid structure of native collagens that have intact triple helix organisation [218].

The assay was performed as described in the instructions enclosed with the assay. Absorbance was measured against distilled water for the reagent blanks, standards and test samples. Collagen concentrations were calculated from the standard curve.

5.2.5.3.3 *Osteocalcin Quantification*

Osteocalcin, also known as bone Gla protein (B.G.P.) is the major non-collagenous protein of the bone matrix. It is a vitamin K dependant Ca^{2+} binding protein, which is produced exclusively by osteoblasts and odontoblasts [219]. It contains three carboxylated glutamic acid residues which bond strongly to hydroxyapatite [220].

Osteocalcin quantification was performed using a commercially available kit (KAQ1381 (96 tests) *Invitrogen*, UK). The lysate was collected and tested for the presence of osteocalcin following the kit instructions.

The *Invitrogen* human osteocalcin assay is a solid phase enzyme amplified sensitivity immune assay (EASIA). The assay uses monoclonal antibodies (Mabs) directed against distinct epitopes of human osteocalcin. Standards and samples react with the capture monoclonal antibody (Mab 1) coated on the microtiter well and with a monoclonal antibody (Mab 2) labelled with horseradish peroxidase (HRP). After incubation period (2 hours), allowing the formation of a sandwich: coated Mab 1–human osteocalcin–Mab 2–HRP, the microtiter plate was washed to remove unbound enzyme labelled antibody. Bound enzyme labelled antibody was measured through a chromogenic reaction. Chromogenic solution (TMB ready for use) was added and incubated. The reaction was stopped with the addition of stop solution and the microtiter plate was then read at the appropriate wavelength. The amount of substrate turnover was determined colorimetrically by measuring the absorbance

which is proportional to the human osteocalcin concentration. A standard curve was plotted and human osteocalcin concentration in a sample was determined by interpolation from the standard curve [221].

5.2.5.4 Morphology Assessment

Samples were washed with warm PBS at 37 °C and fixed in 3% glutaraldehyde in 0.1 M cacodylate buffer for 30 minutes, after 30 minutes fixative was replaced by a 7% sucrose solution. Fixed samples were then washed twice in 0.1 M cacodylate buffer, and post fixed in 1% osmium tetroxide in phosphate buffer saline for 45 minutes in a fume cupboard. Samples were dehydrated through a graded ethanol series (20, 30, 40, 50, 60, 70, 80, 90, 96 and 100% in water) for approximately 5 minutes each. Samples were then dried via hexamethyldisilazine (HMDS) before being sputter coated in gold and viewed with a Philips XL30 scanning electron microscope operated at 10 kV.

5.2.6 Statistical Analyses

Average values and standard deviation were computed for two iterations of the experiments. Statistical analysis was performed using the Prism software package (version 3.02, GraphPad Software, San Diego California USA, www.graphpad.com). Two-way analysis of variance (ANOVA) was calculated with the bonferroni post-test to compare the significance of change in one factor with time. The error bars presented represent standard error of mean with $n = 6$.

5.3 Results

5.3.1 Elution Study

Cytotoxicity of elution products from chemically modified phosphate glass samples surfaces was assessed by neutral red uptake (NRU), a cell viability marker, and presented in parallel with untreated PBG control sample results Figure 5-1.

Samples were degraded in a serum free treatment media and diluted to a range of concentrations (10–100%) in fresh DMEM to find out the most toxic concentration for the cells. In accordance with the definition of cytotoxicity in ISO standard (BSI–ISO 10993–5 2009) no cytotoxicity was observed since the cell viability remained over 70% of non–toxic control (no elution products) for all samples and at any concentration. However, Na–PLA, SPLA and HDI treated samples showed lower cell viability at higher concentration. For all the other samples no significant difference was observed between samples and controls and over the range of concentrations. No significant difference ($P < 0.05$) was found when data was analysed for different sample treatments for neat aliquots.

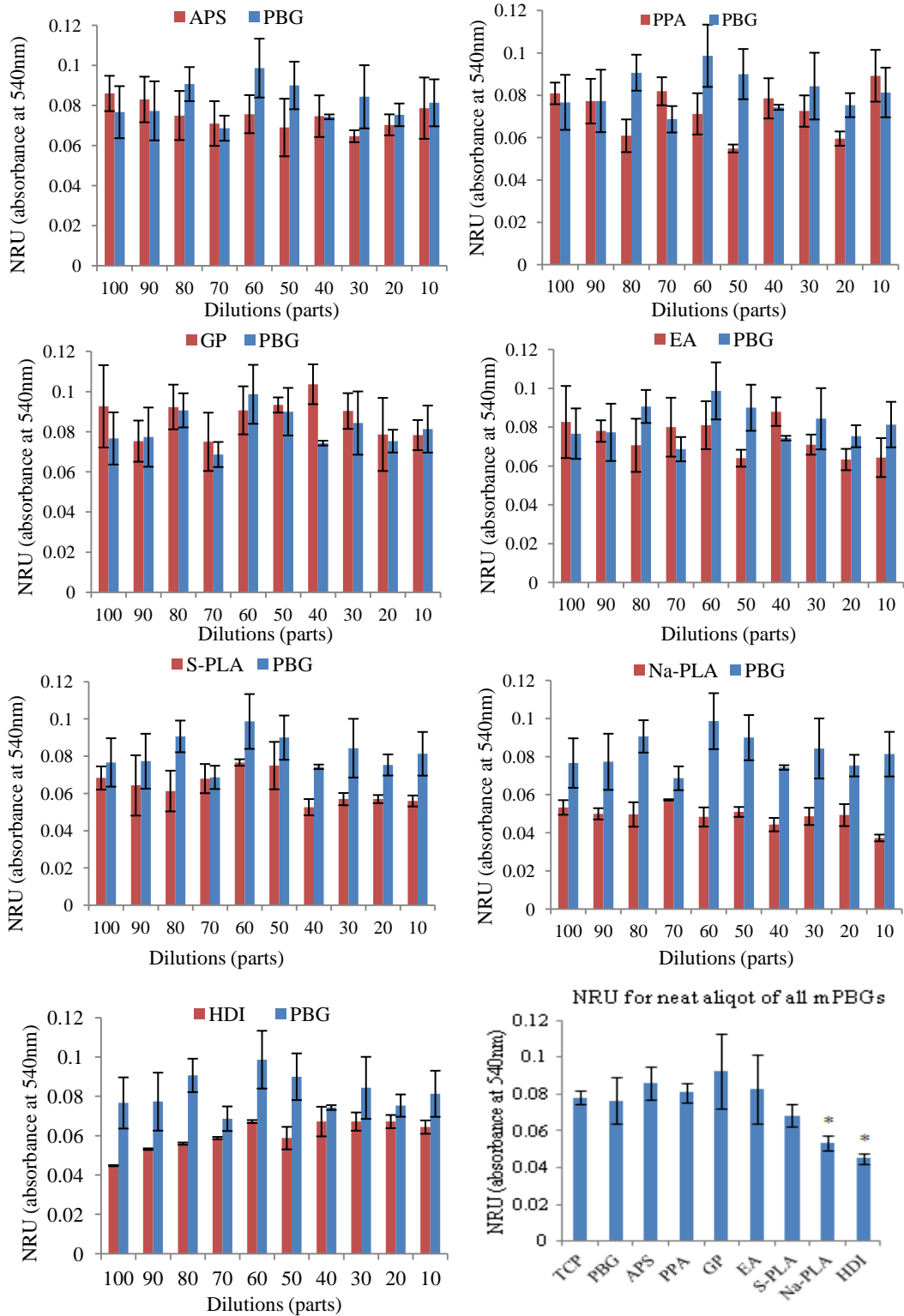


Figure 5-1: Cell viability of MG63 osteosarcoma, as measured by the neutral red uptake assay, cultured in culture medium with the extracts from modified phosphate glasses, x-axis represents concentration of extracts containing media in basal media and a summary of neat (100% extract containing media) aliquots from all treated glasses (x-axis represent treatments). Error bar represents standard error of mean, n = 6. * indicating significantly low NRU for Na-PLA and HDI treated phosphate glass.

5.3.2 Short Term Direct Contact Test

5.3.2.1 Metabolic Activity

The Alamar blue assay was used to determine the effect of surface modifications of PBG on metabolic activity of osteoblast-like cells cultured on phosphate glass modified with selected surface treatments up to seven days, Figure 5-2.

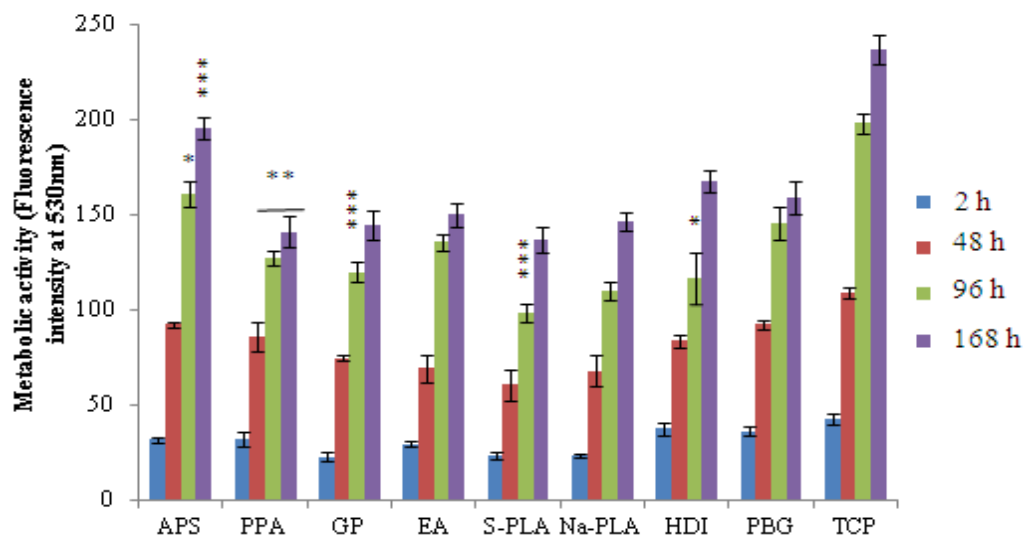


Figure 5-2: Metabolic activity of MG63 osteosarcoma, as measured by the alamar blue assay, cultured on modified phosphate glasses, x-axis represents surface treatments. Error bar represents standard error of mean, n = 6. * indicating significant difference of treated samples compared to control (PBG).

Metabolic activity was found increasing over seven day culture period, with an extremely significant difference between 2 and 168 hours for all surfaces. However, there was no significant difference in metabolic activity found for different modified glass samples at 2 hours time point ($P > 0.05$) and control PBG. However, internal control (TCP) demonstrated an elevated metabolic activity compared to other sample at later time points (96 and 168 hours) which was statistically significant ($P < 0.001$). APS modified glasses also demonstrated significantly higher ($P < 0.001$) metabolic

activity compared to control PBG. The value for metabolic activity after seven days was the greatest on TCP followed by APS and untreated PBG respectively. Repeats of this experiment have also demonstrated repeatable results.

5.3.2.2 DNA Quantification

The DNA content of cells cultured on samples was used as an indicator of cell population. DNA (Hoechst 33258) assay was used to quantify the changing concentration of DNA with time for MG63 osteosarcoma cells cultured on modified phosphate glasses, Figure 5-3. Untreated PBG was used as a positive control.

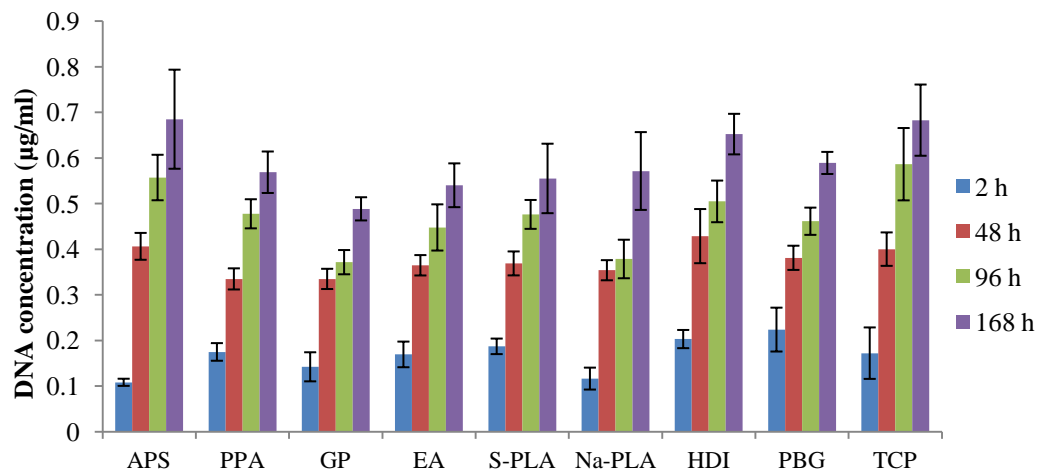


Figure 5-3 Cell proliferation of MG63 osteosarcoma, as measured by the DNA (Hoechst 33258) assay, cultured on modified phosphate glasses, x-axis represents surface treatments. Error bar represents standard error of mean, n = 6. There was no significant found for treated samples versus control (PBG) at any time point.

DNA concentration after two hours was approximately $0.2 \mu\text{g ml}^{-1}$ for all surfaces with an exception of HDI treated glass which had higher amount of DNA. Nevertheless, for all surfaces no significant difference ($P > 0.05$) was observed. For all the sample surfaces, the levels of DNA gradually increased with time up to 96 hours and then a slow increase in DNA concentration was observed from 96 to

168 hours. There was no statistically significant difference ($P > 0.05$) found between the final DNA concentrations.

5.3.2.3 Differentiation

Effect of surface modification on cell differentiation was analysed by measuring alkaline phosphatase activity of osteosarcoma cultured on surface-modified phosphate glasses, Figure 5-4. Data was normalised with the corresponding DNA concentration at each time point.

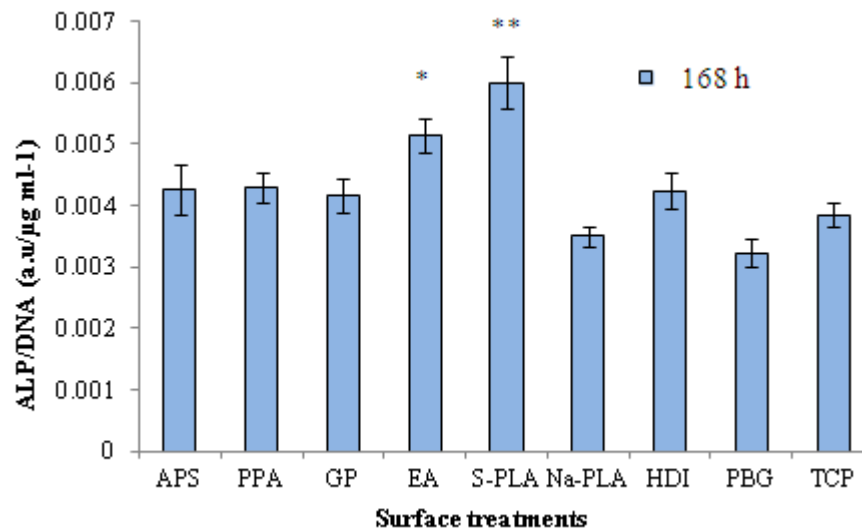


Figure 5-4: Alkaline phosphatase (ALP) activity of MG63 osteosarcoma cells, as measured by ALP assay, cultured on modified phosphate glasses, x-axis represents surface treatments. Data was normalised with corresponding DNA concentration for each individual sample. * indicating significant difference of treated samples compared to control (PBG).

For all surfaces, including the internal control (TCP), the alkaline phosphatase activity was not detectable after 2, 48 or 96 h. However, after 168 hours of culture, detectable amount of ALP activity was observed on all the surfaces with notably high values on EA and SPLA mPBGs and low value for Na-PLA mPBG sample. ALP activity of cells cultured on SPLA mPBG was significantly higher ($P < 0.05$)

than other samples excluding EA mPBG. However, there was no significant difference ($P > 0.05$) found between other samples and control PBG.

5.3.3 Primary HOB in Direct Contact

5.3.3.1 Proliferation

Effect of chemical modification of phosphate glass surfaces on the proliferation of primary human osteoblasts, was measured via DNA content of the cells cultured on mPBG surfaces over a culture period of 28 days, Figure 5-5.

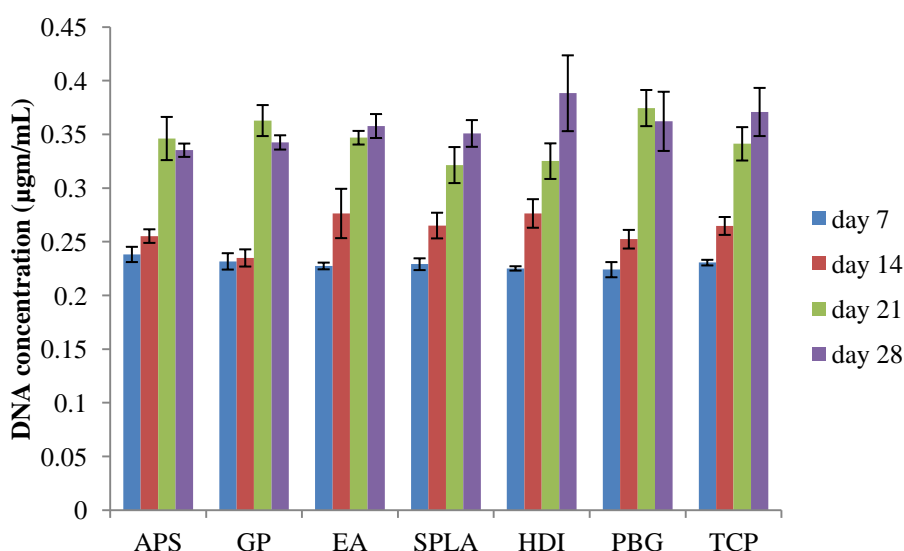


Figure 5-5: Proliferation of primary human osteoblasts, as measured by the DNA (Hoechst 33258) assay, cultured on modified phosphate glasses, x-axis represents surface treatments. Error bar represents standard error of mean, $n = 6$. There were no significant found for treated samples versus control (PBG) at any time point.

For all samples, including controls (TCP and PBG), the DNA concentrations measured were at approximately $0.24 \mu\text{g ml}^{-1}$ after 7 days in culture. A gradual increase in DNA concentration was observed from day 7 to 21. However, no significant change was observed as DNA concentration levelled out and stayed at $\sim 0.35 \mu\text{g ml}^{-1}$ after 21 days on all the surfaces. The trend was consistent for all

samples and controls. Although, DNA concentration was found comparatively higher on HDI mPBG, statistical analysis revealed no significance ($P > 0.05$) for the difference.

5.3.3.2 Differentiation

5.3.3.2.1 Alkaline Phosphatase Activity

Alkaline phosphatase activity of primary human osteoblast was used as early marker of osteoblastic differentiation. The effect of chemical modification of PBG on ALP activity of primary osteoblast cultured on glass surfaces for up to 28 days is presented in Figure 5-6.

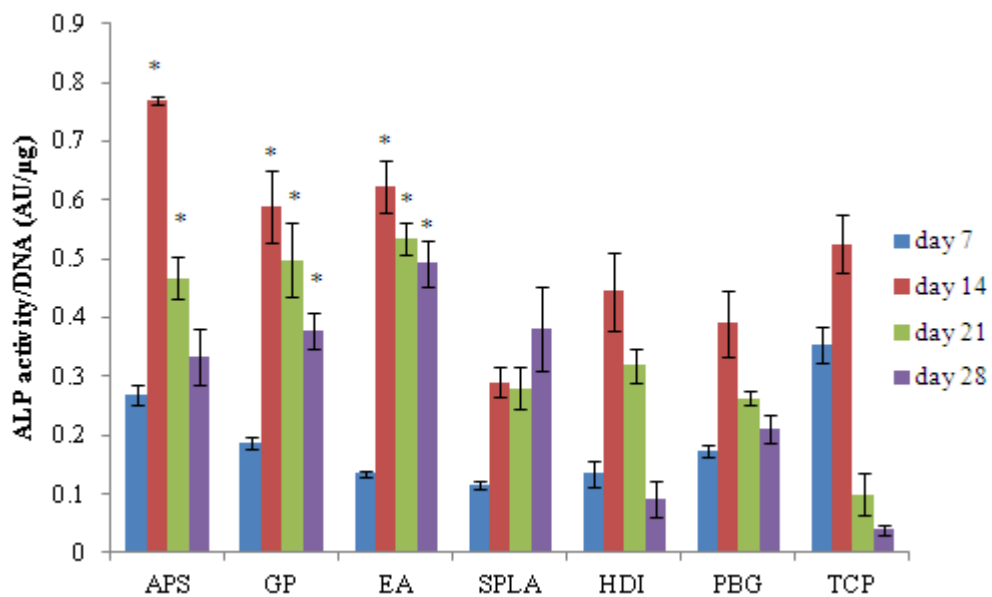


Figure 5-6: Alkaline phosphatase (ALP) activity of primary human osteoblasts, as measured by ALP assay, cultured on modified phosphate glasses, x-axis represents surface treatments. Data was modified with DNA values obtained for each individual sample. Error bar represents standard error of mean, n = 6. * indicating significant difference of treated samples compared to control (PBG).

For all mPBG surfaces and controls (PBG and TCP), an increase and then a drop in ALP activity was seen as general trend. However, SPLA mPBG surfaces demonstrated an initial increase in ALP activity which remains constant for last three time points. APS mPBG samples demonstrated the highest ALP activity which was statistically greater than control PBG ($p < 0.001$).

5.3.3.2.2 Collagen Production

Collagen production by primary human osteoblast cultured on selected surface-modified phosphate glass surfaces for up to 28 days was assessed and quantified by Sircol collagen quantification assay, Figure 5-7.

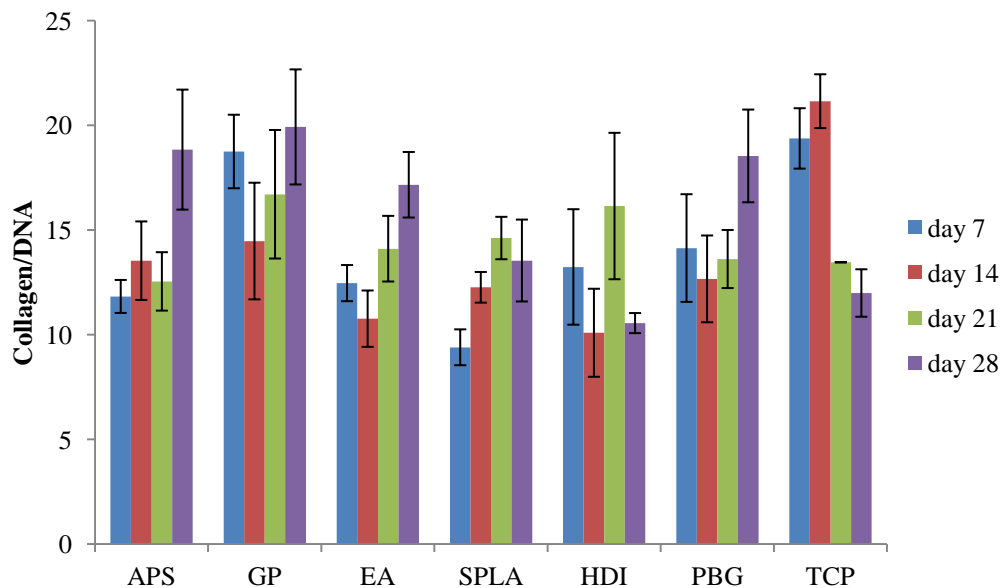


Figure 5-7: Amount of collagen produced by primary human osteoblasts, as measured by Sircol assay, cultured on modified phosphate glasses. Data was modified with DNA values obtained for each individual sample. Error bar represents standard error of mean, $n = 6$. There were no significant found for treated samples versus control (PBG) at any time point.

All samples, including the control PBG, showed no increase in collagen concentration with time. Collagen concentration was found highest on APS and GP

mPBG surface however, concentrations were similar for the remaining surfaces. Statistical analysis revealed no significant difference ($p > 0.05$) between highest values found for each surface-modified sample and control PBG. Notably, a signature down regulation of collagen production was observed for TCP.

5.3.3.2.3 Osteocalcin Quantification

Osteocalcin was detected in primary human osteoblast cultured on selected modified phosphate glass surfaces for up to 28 days was assessed and quantified by ELISA osteocalcin quantification assay kit, Figure 5-8.

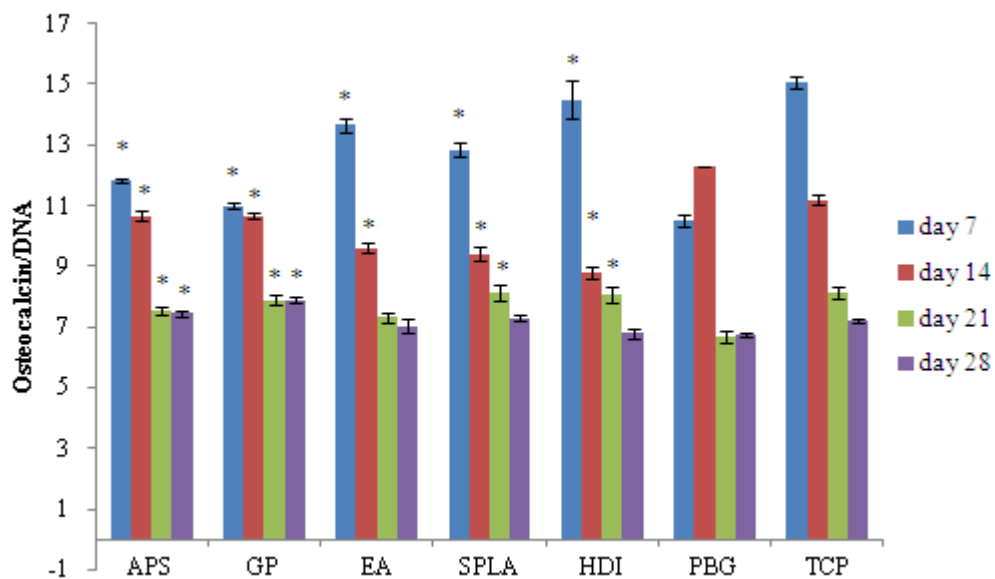


Figure 5-8: Quantity of osteocalcin produced by of primary human osteoblasts, as measured by ELISA assay, cultured on modified phosphate glasses, x-axis represents surface treatments. All data is modified with DNA values obtained for each individual sample. Error bar represents standard error of mean, n = 6. * indicating significant difference of treated samples compared to control (PBG).

Levels of osteocalcin were found not significantly different ($P > 0.05$) on all sample surfaces and between each time point. A repeat of this experiment provided with the same trend in results implies the response was consistent. However, when

osteocalcin concentration was normalised with DNA, a downward trend was observed for all samples including controls. Two-way ANOVA revealed significant difference ($P < 0.001$) between control PBG and mPBGs samples at initial time points (7 and 14 days).

5.3.3.3 Morphology (SEM)

Morphology of cells cultured on phosphate glass discs was visualized by SEM (Figure 5-9 to 5-15). Within each figure a representative image of osteoblasts cultured for 7, 14, 21 and 28 days on phosphate glass specimens is presented. In general SEM images of human osteoblasts cultured on all glass surfaces showed a confluent layer after 7 days of culture with some large osteoblast cell-cluster with lamellipodia extended to neighbouring cell resulted in the formation of a denser cell layer at the later time points. However, no mature star-shaped structure was spotted at any time point on TCP control where the cells were densely packed showing spindle-shaped cells arranged like a shoal of a fish. After 21 days much denser layer/s can be observed with mature osteoblast depositing minerals onto the sample surfaces. Collagen fibrils can also be located after 21 days of culture.

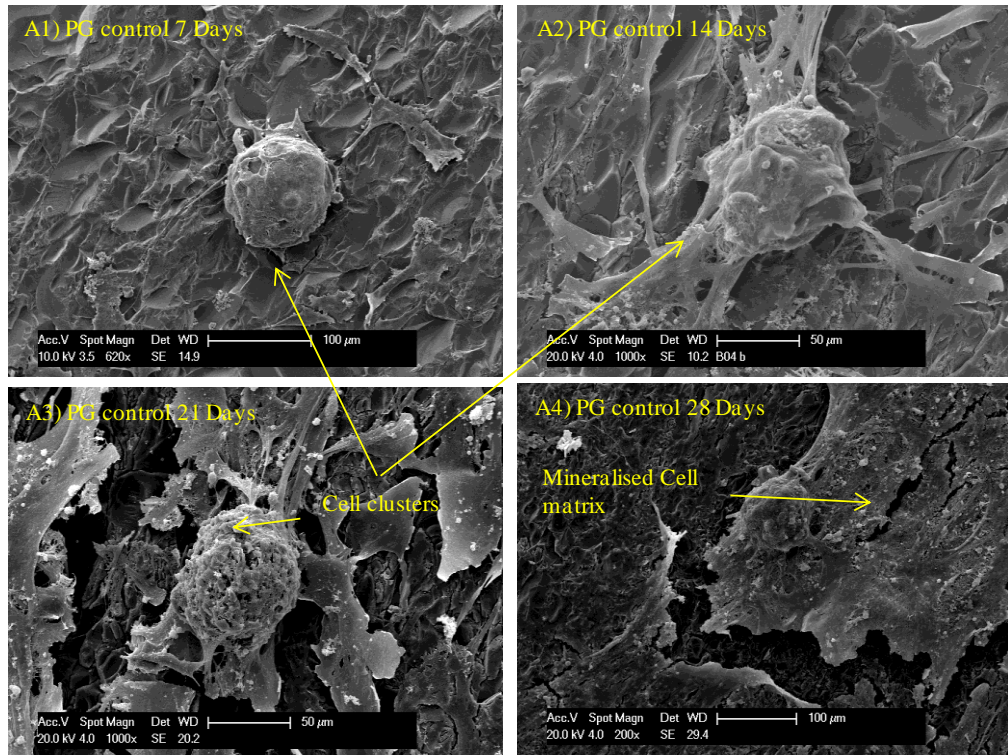


Figure 5-9: SEM images of human osteoblast cultured on phosphate based glass (control) up to 28 days. Arrows indicating at cluster of cells, cell matrix and mineralisation.

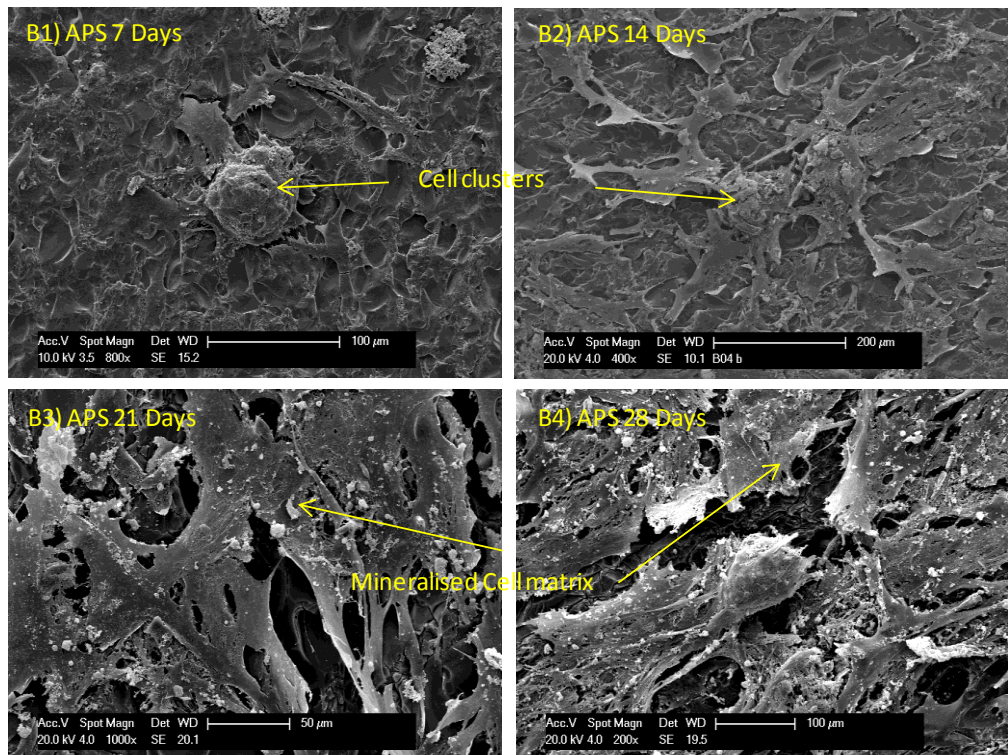


Figure 5-10: SEM images of human osteoblast cultured on APS modified PBG up to 28 days. Arrows indicating at cluster of cells, cell matrix and mineralisation.

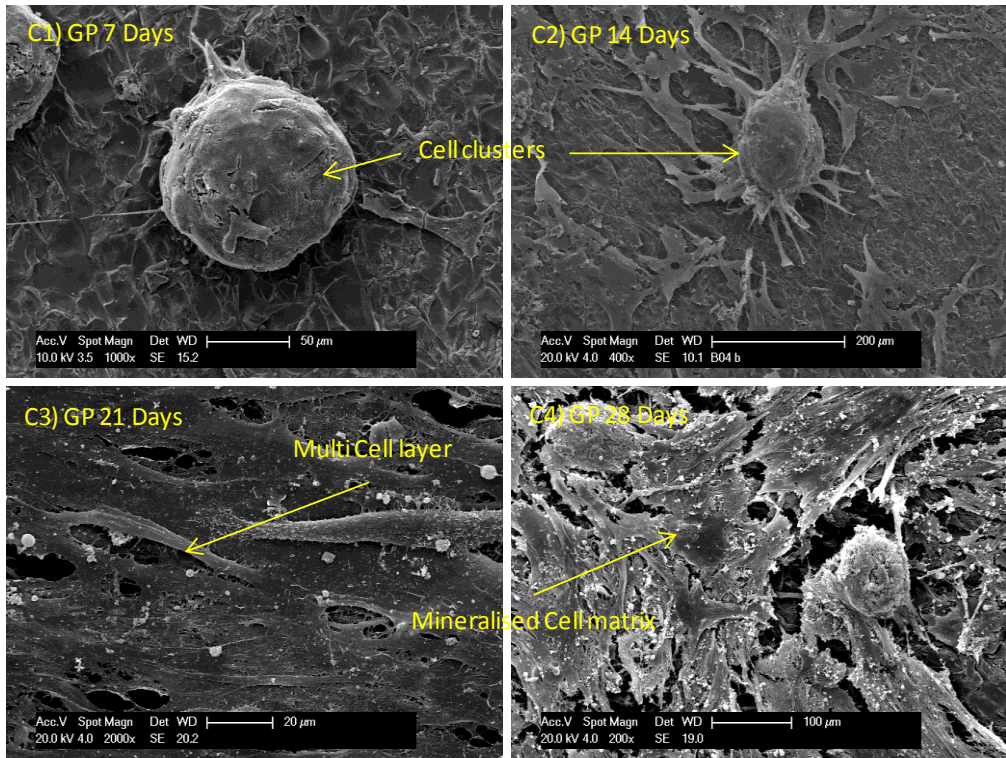


Figure 5-11: SEM images of human osteoblast cultured on GP modified PBG up to 28 days. Arrows indicating at cluster of cells, cell matrix and mineralisation.

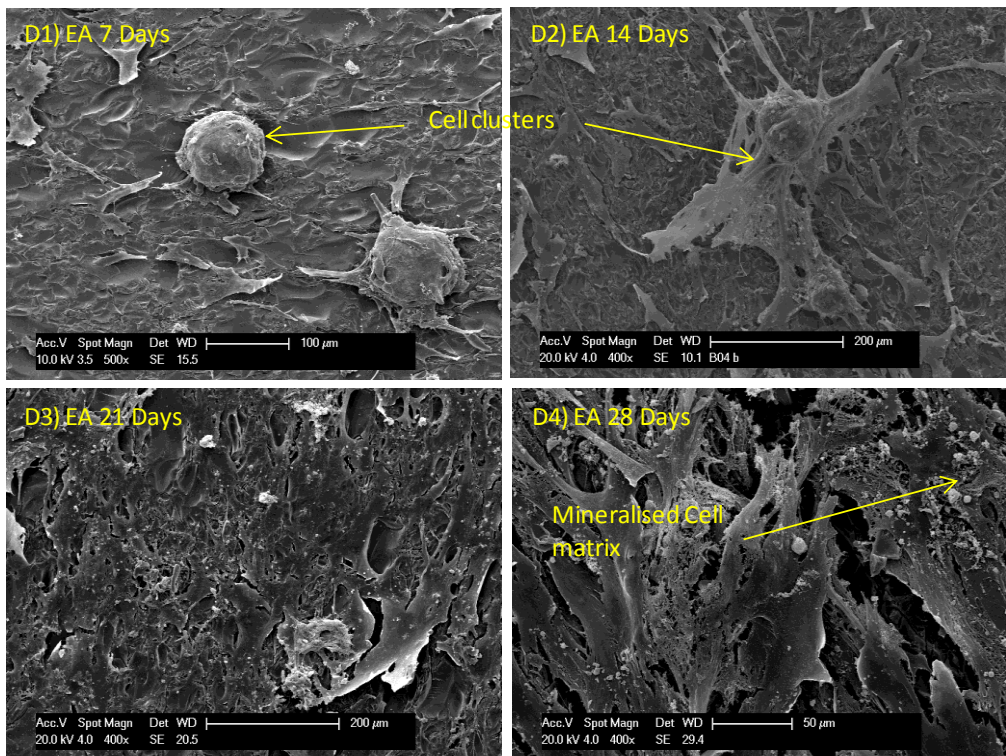


Figure 5-12: SEM images of human osteoblast cultured on EA modified PBG up to 28 days. Arrows indicating at cluster of cells, cell matrix and mineralisation.

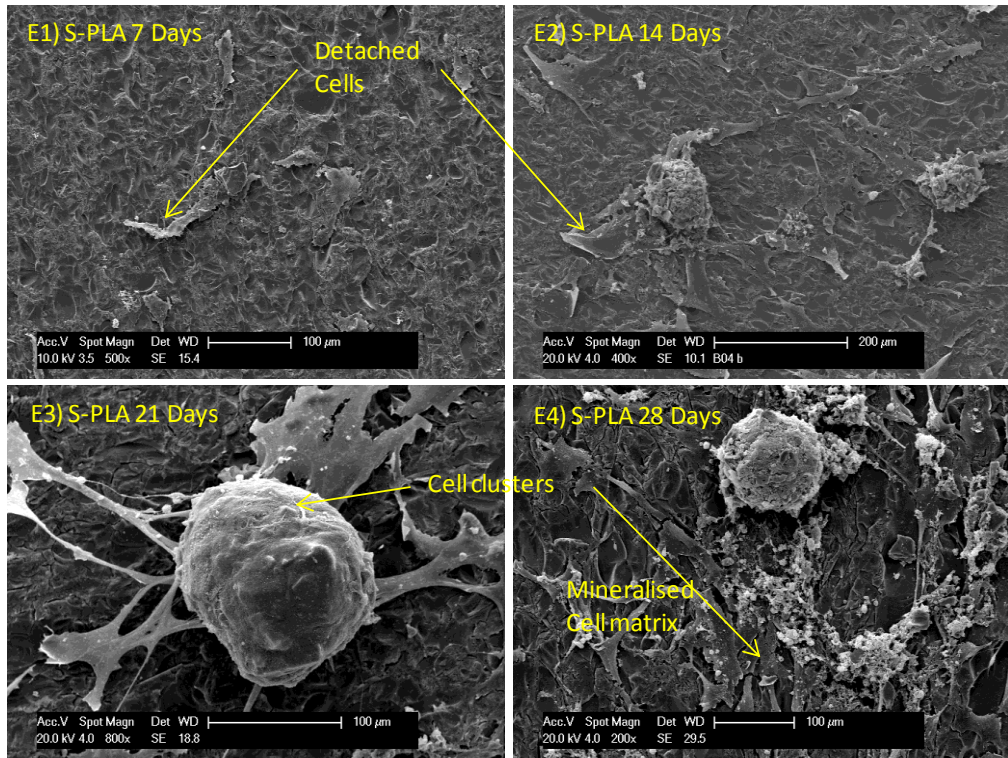


Figure 5-13: SEM images of human osteoblast cultured on SPLA modified PBG up to 28 days. Arrows indicating at cluster of cells, cell matrix and mineralisation.

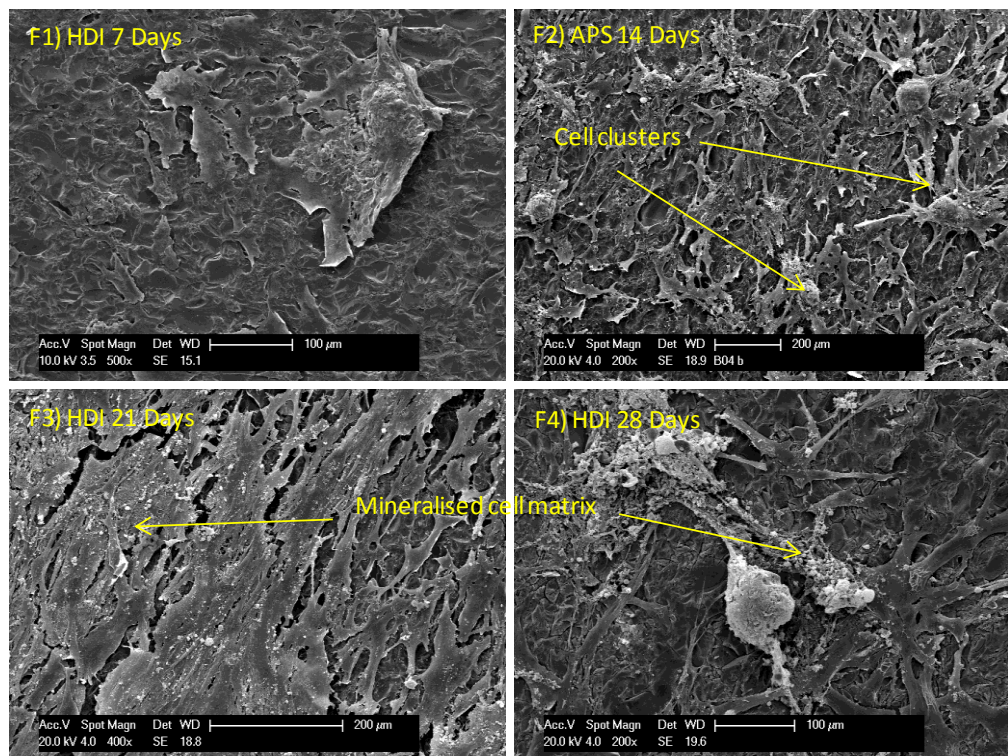


Figure 5-14: SEM images of human osteoblast cultured on HDI modified PBG up to 28 days. Arrows indicating at cluster of cells, cell matrix and mineralisation.

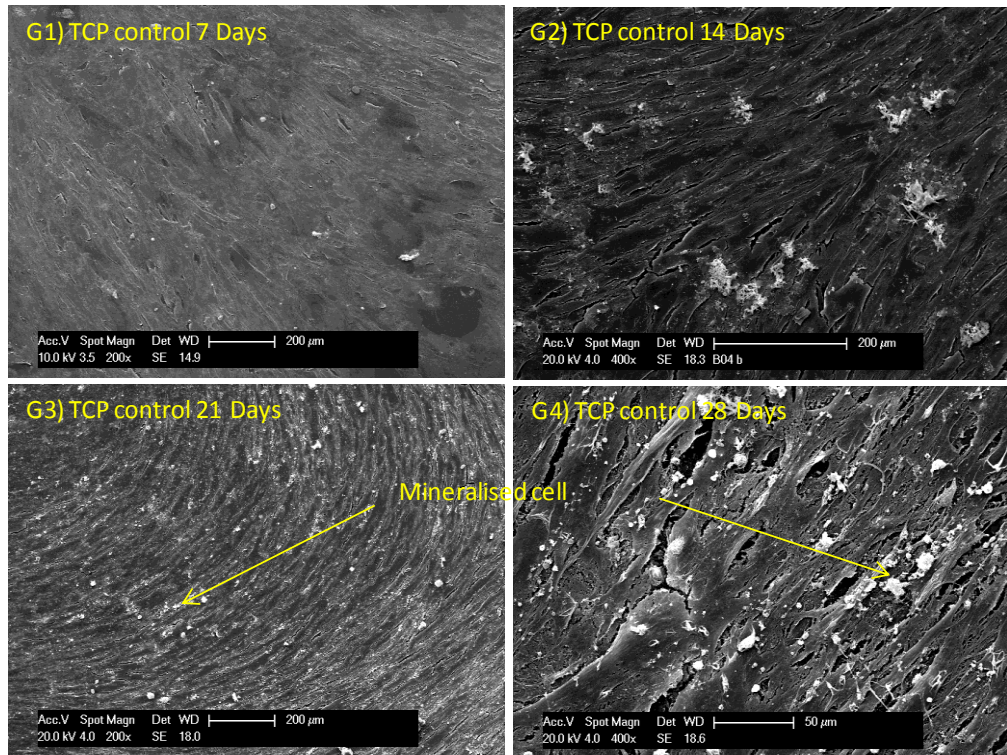


Figure 5-15: SEM images of human osteoblast cultured on tissue culture polystyrene up to 28 days. Arrows indicating at cell matrix and mineralisation.

5.4 Discussion

To ascertain the cytocompatibility of the chemical agents used in this project, as an attempt to improve interface adhesion between polymer matrix and reinforcing glass, a three step screening approach was adopted which included an indirect or elution study, short term direct contact cell viability, metabolic activity and ALP activity assessment using MG63 osteosarcoma cell line and finally long term primary human osteoblasts culture in direct contact with mPBG to evaluate cell proliferation, differentiation and morphological assessments.

To assess potential toxicity of the chemicals leaching out from the mPBG surfaces, combined degradation extracts from PBG as well as coupling agent layer were tested for cytotoxicity through neutral red uptake (NRU) (see Figure 5-1). Greater NRU was observed for GP and EA mPBG surface compared to the PBG control; suggesting that the degradation products (mainly calcium and phosphates) may be supportive in cell metabolic activity leading to greater cell number and hence a high NRU. This relatively higher cell metabolic activity was anticipated as β -glycerol phosphate is often used as a carbon source, essential for the expression of osteoblast phenotype expression. A hydrolysis product of β -glycerol phosphate (phosphates) are reported as positive effector for induction of gene expression [222]. Bisphosphonate etidronic acid is also reported to be beneficial for osteoblast growth, however, higher dosages of etidronic acid are known to impair normal skeletal mineralisation [223].

A significantly lower NRU was observed for the oligomer treated samples which was suggested to be due to acidic degradation products from the PLA oligomers, as their molecular weight was very low (20000 Da) and therefore prone to rapid hydrolysis. Ignatius and Claes reported that high concentrations of degradation products from PLA had a toxic influence on the cell culture systems they studied using MTT and BrdU cytotoxicity assays [63]. Another study revealed that increased inflammation was observed when the molecular weight of PLA/PGA copolymers decreased to between 10000 – 20000 Da [224]. Significantly ($P > 0.01$) lower NRU was also observed for HDI treated surfaces. Dong *et al.* stated that during the process of polyurethane synthesis some of the toxic hexamethylene diamine (HDA) could be released [178]. Based on information on the chemical structure of HDI grafted HA (gHA), Dong *et al.* reported three possible mechanisms for release of HDA derivatives; i) hydrolysis of the urea linkage in the extended chain; ii) hydrolysis of urethane linkage between HA and HDI and iii) ionisation of gHA. The results from this study are in agreement with Dong *et al.*[216] as the cytotoxicity was found to be dependent on the content ratios of treatment media in culture medium.

Due to the lack of evidence for cytotoxicity from any of the coupling agents investigated, all mPBGs were included in the next stage of cytocompatibility assessment, which included use of osteoblast-like MG63 cells cultured in direct contact with the mPBG surfaces and assessed for cell viability, proliferation and differentiation.

All samples including positive controls (PBG and TCP) revealed similar results for cell viability as measured via alamar blue assay, with no significant differences observed between samples and/or controls at each time point (see Figure 5-2).

However, for all surfaces investigated a linear increase in fluorescence values was seen from 2 hours to 7 days, which demonstrated that cells were metabolically active and there were no adverse effects from the surface chemistry on cell metabolic activity.

Alkaline phosphatase is an early marker of osteoblastic maturation. ALP was expectedly detected after 7 days of MG63 culture for all the samples (Figure 5-4). Significantly higher ($P < 0.05$) ALP activity was observed on EA and SPLA mPBG surfaces. EA as mentioned above helps osteoblastic metabolic activity and sorbitol which is a hydrogenated carbohydrate is reported to regulate osteoblast differentiation [225] which could be the reason of the relatively higher ALP activity shown by these two samples.

After second stage biocompatibility assessment, Na-PLA and PPA were excluded from the study mainly based on their fast degradation (not suitable for long term study) and relatively low cytocompatibility of Na-PLA. However, as HDI showed to be the most effective surface treatment in terms of improving interfacial shear strength, it was also included in this long term cytocompatibility study.

Proliferation of primary human osteoblasts in terms of DNA concentration, on glass surfaces after each time point up to 28 days, was practically equal to the controls (Figure 5-5). After seven days of culture a confluent layer can be seen from the SEM images of all sample and control surfaces. After seven days the growth rate, as expected, was slower. However, an increase in DNA content implies that; once a confluent layer is formed on the surface, proliferation is less dependent on the glass

surface as further cell growth was seen to occur on top of the present cell layer, forming multi layers as observed by SEM images (Figure 5-9 to 5-15).

Osteoblasts, when cultured on tissue culture polystyrene (TCP), are expected to be in proliferation phase up to 10 days in culture followed by matrix maturation, mineralisation and finally apoptosis [226-228]. However, the model presented by Owen *et al.* and Stein *et al.* used rat osteoblast with a cell seeding density of 5×10^5 cells/cm² and due to this high density a confluent layer after 7 days was reported. Although different cells, media and cell density was used in current experimental, it was found that a confluent layer of cells after 7 days in culture which is in agreement with the model presented by Stein *et al.* [228].

Alkaline phosphatase activity by osteoblasts *in-vitro* was expected to be up regulated as proliferation is retarded and down regulated when osteoblasts enter the mineralisation phase [227, 228]. The up and down regulation of ALP, over a 28 day period was observed on all surfaces except SPLA mPBG where an insignificant increase or a plateau was observed (Figure 5-6).

Variation in ALP activity due to surface chemistry alteration is not unusual compared to cell cultured on TCP. For example, the alkaline phosphatase activity of craniofacial osteoblast cells (CFC) cultured on phosphate glasses over 28 days was studied by Gough *et al.* It was also reported that characteristic up and down regulation of alkaline phosphatase activity was not observed. However, highest ALP activity was observed at seven days which was down regulated with time in culture [111]. This is in contradiction to Dias *et al* [229] who reported a characteristic

regulation in ALP activity with human bone marrow cells on calcium phosphate glass ceramics, and correlates well with the results observed in current study.

Glass chemistry also plays its role in cell metabolic activity. As reported by Burling and Ahmed *et al*, higher amount of magnesium release from the glass may be connected with the higher alkaline phosphatase activity seen by osteoblasts cultured on phosphate glasses containing Mg^{2+} [181, 184]. It was also reported that up to 3 times ALP activity was observed from osteoblasts cultured on phosphate glasses compared to TCP control which was not observed in this study probably because phosphate glass used in this study was two to three order in magnitude more durable and Mg^{2+} content was relatively lower [181]. Dissolved calcium and phosphate are also reported to influence cell metabolic activity as reported by Ma *et al.*, an enhanced osteoblast differentiation in the presence of additional Ca^{2+} concentration in the cell culture media and retardation of osteoblast differentiation and mineralization in the presence of additional inorganic phosphate concentration in the cell culture media [230].

For any material to be considered for orthopaedic use it is essential to support collagen formation as it is one of the most important markers of cell differentiation. Collagen formation was observed after 7 days of osteoblast cultured on all surfaces including TCP (Figure 5-7). However, no significant up and down regulation of collagen quantity was observed only TCP showed a down regulation collagen when normalised with DNA content. This trend is contradictory to the model presented by Stein *et al* where osteoblast-like cells were cultured on TCP [228]. Although the same trend of collagen quantity plateau was reported by Au *et al* [231] with MG63 cells cultured on TCP control and Consil[®] bioactive glass particles and Bosetti *et al*.

[232, 233] with rat osteoblast like cells cultured on bioactive glass powder surfaces. Bosetti *et al.* reported an up regulation from second to fourth day followed by down regulation and a plateau in collagen concentration when cells cultured on polystyrene wells. Au *et al.* also reported a constant collagen concentration when human osteoblast were culture on Consil[®] particles, the trend was consistent on TCP [231]. Another study, by Leonardi *et al.*, also reported a significant increase from day 1 to day 7 followed by constant collagen concentrations at 7 and 14 days of human bone marrow cells cultured on a resorbable phosphate based glass ceramic. Although the values were ~ 20% higher, the trend was consistent on TCP control [234]. All of the above mentioned studies did not present normalised concentration of collagen with DNA. A 50 % increase in collagen concentration from 7 to 14 days followed by an almost constant concentration up to 28 days in culture was also reported by Burling; when craniofacial osteoblast cells were cultured on ternary phosphate based glasses and TCP control [184]. The non-normalised data, quoted above, correlates well with the results obtained for current study and a rough calculation reveals similar trend for normalised data as well.

Osteocalcin, a major non-collagenous matrix protein, is a highly specific osteoblastic differentiation marker. Osteocalcin was found in detectable quantity on all the surfaces including positive controls, indicating that osteoblasts were fully differentiated to matrix maturation stage (Figure 5-8). Non normalised osteocalcin concentration was virtually the same for all samples and at each time point. However, when normalised with DNA concentration; the highest amount of osteocalcin was found after 7 days of cell culture which was the same on all surfaces including TCP. On all samples osteocalcin concentration was reduced after 7 days in culture and

finally lowest values were detected after 28 days, this trend was consistent for all the surfaces studied regardless of treatment.

Osteocalcin, as reported by Owen *et al.*[226] and Stein *et al.*[228], is a late marker of osteoblastic differentiation which is detectable after full maturation of cells that is indeed after proliferation to confluence. However results presented in this chapter differ from the model presented by Owen *et al.*[226] and Stein *et al.*[228]. The difference observed here could be due to different surface chemistry, surface morphology and origin of cells. The models mentioned above used murine osteoblast cultured on TCP and in current study human osteoblast were cultured on degradable/functionalised phosphate glass surface.

Similar trend of low osteocalcin values at early stage of cell culture with insignificant increase or a plateau and then a drop in osteocalcin expression was reported by Carpenter *et al.* [235] when osteoblasts derived from older mouse pups were culture at higher density on TCP. In another study by Varanasi *et al.*, it was reported that when osteoblast-like MC3T3-E1 supplemented by extracts from bioactive glass 45S5 and 6P53-b cell proliferation rate was enhanced by 150%, collagen synthesis was enhanced and a higher concentration of osteocalcin protein was observed. It was reported that osteocalcin was detectable after 3 days and highest values were obtained after 6 days with 45S5 glass extracts which was reduced at later time points however, no significant change in osteocalcin quantity was observed on TCP [236]. In another study by Attawia *et al.* media osteocalcin levels synthesized by osteoblasts cultured on the surface of PMA-ala:CPH (30:70) polymer matrices and TCP controls at 14 and 21 days in culture was analysed. It was reported that no significant difference found on polymer surfaces however, an up

regulation of osteocalcin observed for TCP control [237]. When human bone marrow stromal cells were cultured on a resorbable $P_2O_5-SiO_2-CaO-MgO-Na_2O-K_2O$ phosphate glass ceramic an up regulation in osteocalcin/Glyceraldehyde 3-phosphate dehydrogenase (GAPDH) gene expression was reported although this increment was statistically insignificant from day 7 to 14 [234].

Therefore, it can be deduced from the results obtained for collagen and osteocalcin quantification that degradation products from phosphate glass and some of surface treatments especially etidronic acid, glycerol phosphate and silane may have enhanced collagen production and help in up regulation of downstream markers like osteocalcin during osteoblast differentiation. However, the mechanism of chemical agents' influence on osteoblast cell activity is different for different chemical agents and is out of scope for the current project.

Most of the chemical agents used in this project have previously been investigated for their cytotoxicity or cytocompatibility and therefore expected to be biocompatible. Phosphonic acid based chemicals have been employed as s in the past. For example, Phillips *et al.* grafted a novel allyl phosphonic acid on calcium phosphate to produce a chemically bonded composite [169]. Greish and Brown developed a biocompatible HAp-Ca poly(vinyl phosphonate) composite for clinical applications [170, 171]. Tanaka *et al.* reported the synthesis of surface modified calcium hydroxyapatite with pyrophosphoric acid [172]. All these studies reported no cytotoxicity from the phosphonic acids used which correlate and support the results found in this study for PPA, GP, APA and EA.

Sánchez–Vaquero *et al.* prepared agarose hydrogels containing aminopropyl triethoxy silane and evaluated them for adhesion and proliferation of human mesenchymal stem cells (hMSCs) they found that although adhesion was lower on APS rich scaffolds, the proliferation rate on these surfaces was higher [215]. In another study, by Jung *et al.*, type I collagen was immobilised on HA surface with the help of APS it was reported that collagen–grafting on HA enhanced the fibroblast adhesion due to the excellent biocompatibility. These reports support the results found in this study for APS mPBG and explain relatively high MG63 proliferation and human osteoblasts ALP activity for APS modified PBG surface.

In the current study addition of Na or sorbitol functional groups to biocompatible PLA was hypothesised to not affect the cytocompatibility significantly. As reported in a study by Mei *et al* [225], biocompatibility of a sorbitol-containing polyester series was evaluated against a PCL control by measuring cell spreading and proliferation of a mouse fibroblast 3T3 cell line *in vitro*. It was found that sorbitol-containing polyesters and PCL had comparable biocompatibility.

A number of studies have previously employed hexamethylene diisocyanate (HDI) in a variety of applications for medical use; such as a growth factor carrier [178, 216], a coupling agent in poly(ethylene glycol)-poly(-caprolactone)-poly(ethylene glycol) copolymers[213], as a compatibiliser for bioactive glass nanoparticle reinforced poly(L-lactide) composites (g-BG/PLLA) [179] and as a coupling agent in a hydroxyapatite reinforced PEG/PBT copolymer composites [180]. Dong *et al.* reported dose dependent cytotoxicity for degradation products from HDI grafted calcium hydrogen phosphate on rat osteoblast cell metabolic activity. Conversely, biocompatibility with very low cytotoxicity was reported for PEG-PCL-PEG

copolymers cross-linked with HDI [213]. Liu *et al.* reported that *in-vitro* testing of g-BG/PLLA composites in SBF showed that apatite was deposited easily on the surface of the composite scaffolds whilst *in-vitro* biocompatibility tests showed that introduction of BG or HDI compatibilised g-BG particles into the PLA matrix, attachment and proliferation of mesenchymal stem cells was supported [179]. Therefore, due to lack of evidence on significant cytotoxicity, from results observed in current study or reported in the literature, HDI is a rationale choice for surface treatment. However, care must be taken to remove all un-reacted HDI from the system.

Eight different surface treatments were applied to a phosphate glass surface in order to make it strongly bond to the polymer. All surface treatments investigated in this study were found non-toxic to MG63 cells even at higher concentrations. Human osteosarcoma and primary human osteoblast exhibited normal cell functional (attachment, proliferation, differentiation) when cultured directly onto the surfaces of surface treated phosphate glass. Morphology of cells cultured on treated glass surfaces was also found comparable to the control (untreated phosphate glass).

5.5 Conclusions

Results obtained for the cytotoxicity/cytocompatibility of human osteosarcoma and primary human osteoblast cell lines with surface treated phosphate glass (mPBGs) revealed no cytotoxicity from extraction products on osteosarcoma cells. A comparable response of MG63 and primary human osteoblast cells with unmodified PBG and TCP in terms of cell attachment, viability, metabolic activity, proliferation and differentiation was also observed. Although some coupling agents investigated

were relatively poor (e.g. HDI, Na-PLA) others (e.g. APS, GP, EA) were excellent in terms of cytocompatibility. Variation observed in cytocompatibility could be attributed toward unreacted functional groups (e.g. O=C=N) or degradation products (e.g. acidic products from PLA oligomers). However, it can be concluded that all the coupling agents investigated and their degradation products were cytocompatible and had no adverse effect on cell functions and cell morphology.

CHAPTER 6. PHOSPHATE GLASS FIBRE REINFORCED COMPOSITE

6.1 Introduction

Internal fixation for bone fractures is a proven operative technique where rigid implant plates and screws of metals such as titanium or cobalt/chromium alloy are frequently used. Excellent reviews tracing the history of biomaterials development and describing state-of-the-art technology have been published and should be referred for more in-depth information on this subject [56, 57, 238-242]. However, problems such as disuse atrophy due to stress shielding, refractures and need for removal operation highlighted the need for an implant that can provide enough mechanical support to the healing bone, maintain its mechanical properties for a certain length of time (up to 24 weeks) and gradually degrade out of the body through normal physiological pathways.

Polymers such as PLA, PGA and PCL alone have insufficient mechanical properties to match cortical bone [4, 10, 13, 20, 122]. As discussed previously (cross reference chapter 2), different approaches such as self and particulate reinforcement have been adopted without much success. Recent studies investigating PCL reinforced with binary calcium phosphate glass fibres (PGF) revealed that these composites showed a flexural strength and modulus values of 25-30 MPa and ~2.5 GPa respectively for an approximately 18% fibre volume fraction sample which was comparable to trabecular bone [27, 159, 160]. More recently Ahmed *et al.* produced composites with randomly distributed quaternary PGFs (13.5% by volume) within a PLA

polymer matrix, the flexural strength of the composites was reported to be ~90 MPa with a flexural modulus of ~5 GPa for both non-treated and heat-treated PGF reinforced composites [158].

However, when a totally resorbable composite is exposed to an aqueous environment, it loses ~50% of mechanical properties within first few days due to water ingress, loss of interfacial integrity and polymer swelling [23, 24, 158]. Therefore, for this project it was hypothesised that a stronger and hydrophobic interface could improve the mechanical properties of composite and delays the loss of properties due to water ingress.

This chapter reports production of PGF reinforced PLA composite. An investigation for the effect of selected glass-surface treatments on the flexural mechanical properties of the composites with degradation was carried out along with primary human osteoblast interaction with these composites.

6.2 Materials and Methods

6.2.1 Glass Synthesis

Phosphate based glass (45P₂O₅ 16CaO 24MgO 11Na₂O 4Fe₂O₃ in molar %) was prepared following the protocol reported in chapter 3, Section 3.2.1.

6.2.2 Glass Fibre Production

PGFs were produced by melt drawing technique as described in chapter 3, Section 3.2.5.

6.2.3 Single Fibre Tensile Test (SFTT)

PGFs were tested for size (diameter) and tensile mechanical properties using Mitutoyo Series 544 LSM–500S laser diameter gauge and LEX810 tensile tester, respectively, as reported in chapter 3, Section 3.2.6.

6.2.4 PGF/PLA Composite Production

6.2.4.1 Treatment of PGFs

PGFs, continuous or 20 mm chopped were treated with optimised concentration of selected surface-treating chemicals (APS, EA, SPLA and HDI) following the protocol stated in chapter 4, Section 4.2.2.

6.2.4.2 Non–Woven Fibre Mat Production

Twenty millimetres chopped untreated control or chemically surface-treated glass fibres, in small bundles, were dispersed using high pressure air. These fibres were

then laid into non-woven random fibre mats (17 cm diameter round sheet) using a domestically developed “air lay” method (Figure 6-1).

The air-lay setup is shown in Figure 6-1 which is connected to a powerful vacuum pump. Desired amount of loose fibres were gradually fed into the top of the air lay table which were collected on framed mesh. The frame was removed and unbounded fibre mat was sprayed with PLA/chloroform solution in order to bind the fibres together.

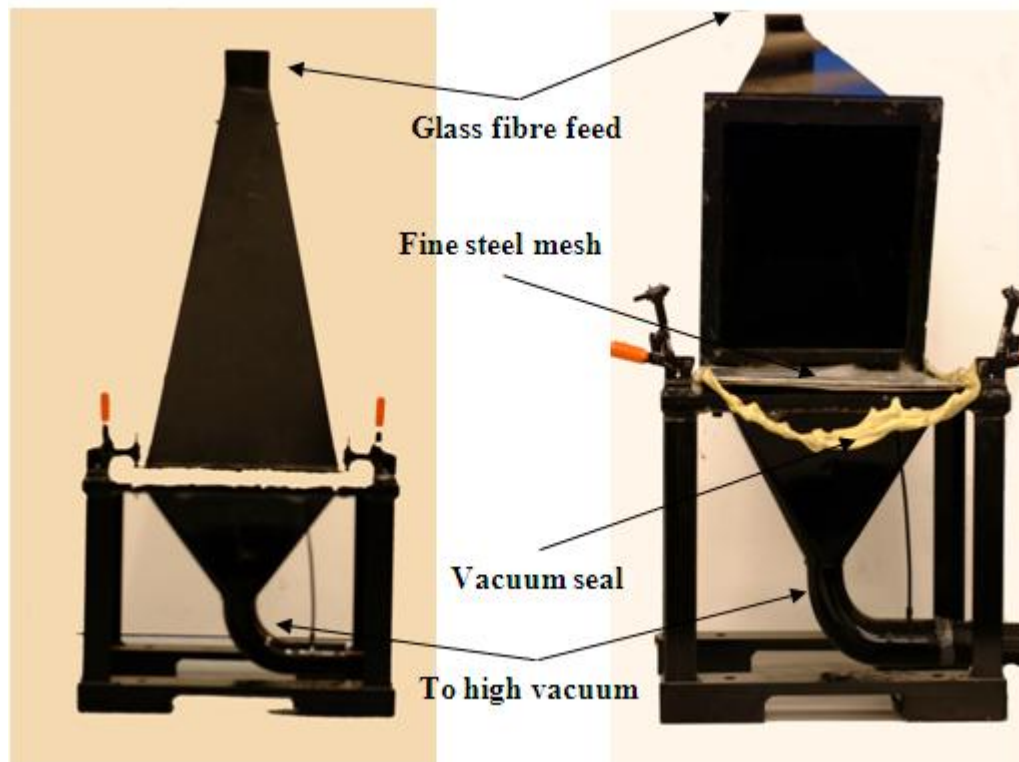


Figure 6-1: Air-lay method fixture setup and random fibre mat. Chopped fibres were fed into to end of coned shaped metal box which was connected to high vacuum from its bottom end. Fibre mat was collected from the steel mesh.

6.2.4.3 Unidirectional Fibre Mat Production

The unidirectional (UD) fibre mats were produced from continuous 180 mm fibre bundles manually aligned together on a PTFE sheet. Solution was added gently using

a spray, to treat the fibre surface. The UD mats produced were rinsed with respective solvents to remove unbounded before being dried at temperature of 50 °C for 30 minutes.

6.2.4.4 PLA Sheet Preparation

Approximately 0.2 mm thick PLA films were prepared by compression moulding 5 g of PLA pellets (3251–D NatureWorks, plc. average $M_w = 90,000-120,000$, $PDI = 1.6$, $T_m = 170.9$ °C and $T_g = 61.3$ °C). The pellets were placed between two metallic plates and heated to 210 °C in a press for 10 minutes, before being pressed at 3 bar pressure for 30 seconds. The plates were then cooled immediately by transferring to a cold (room temperature) press at the same pressure. The PLA pellets were dried in a vacuum oven at 50 °C for 48 hours prior to use.

6.2.4.5 Composite Production

Both random and unidirectional composites were prepared using a film stacking process followed by hot and cold press. For non–woven random fibre reinforced composite; 7 PLA films and 6 fibre mats were stacked alternately within a 170 mm diameter, 1.6 mm thick mould cavity between two metallic plates covered with PTFE sheet. This stack was then heated in the press for 15 minutes at 210 °C and pressed for 15 minutes at 38 bar. The plates were transferred to a second press and allowed to cool to room temperature at 38 bar for 15 minutes. The same protocol was applied for the unidirectional (UD) composite except that only 4 UD fibre mats stacked between 5 PLA sheets within the mould cavity dimensions of 170 mm×100 mm×1.6 mm (l×b×t). The resulting laminated composites were cut using a band saw into 32 mm length, 15 mm width samples for physical testing. The

fibre volume fraction of the composites was obtained using the matrix burn off method, according to the standard test method ASTM D2584–94. The target fibre volume fraction of the composites was between 20% and 35% for nonwoven and unidirectional composites respectively.

6.2.5 Degradation Study for Composites

Specimens of nonwoven random and unidirectional composites were placed individually into 30 ml glass vials. The vials were filled with PBS (pH=7.4±0.2) and maintained at a temperature of 37 °C. At predetermined time points the specimens were extracted and blot dried before weight measurements were recorded. The samples were placed back into vials with fresh PBS solution. At each time point, replicates (n = 3) of each sample were measured and the average reported. The data was plotted as percentage water uptake and dry mass change against time.

6.2.6 Flexural Mechanical Properties Measurement

The initial flexural strength and modulus were evaluated by flexural (three–point bend) test using a Hounsfield Series S testing machine. These measurements were done according to the standard BS EN ISO 14125:1998. A crosshead speed of 1 mm/min and a 1 kN load cell was used. The measurements were conducted on wet samples for following reasons: a) Drying of wet samples rapidly destroys their structure leading to a decrease of their strength in measurement conditions [20], b) Drying of wet samples cause partial restoration of ionic bonds that could lead to misleading results [7], and c) To get the mechanical properties of the composite closer to in–vitro conditions [23]. The measurements were carried out in triplicate.

6.2.7 Physical (SEM) Analysis

Composite samples cross section was exposed via freeze fracture by immersion in liquid nitrogen. The specimens were sputter-coated (SC500, Emscope) with platinum and examined using a XL 30 scanning electron microscope (Philips, UK) at an accelerating voltage of 10 kV.

6.2.8 Cytocompatibility of Primary Human Osteoblast to the Composites

6.2.8.1 Primary Human Osteoblast Cell Culture on Composite

Primary human osteoblast obtained from European collection of cell cultures (ECACC) and cultured in osteoblast growth medium (417–500) (Cell Application, Inc.). Same protocols and conditions were used as described in chapter 5, Section 5.2.5.1.

6.2.8.2 Proliferation

Osteoblast proliferation was gauged by quantifying DNA at each time point, cell lysate was used and standard DNA quantification assay protocol (chapter 5, Section 5.2.5.2) was followed.

6.2.8.3 Differentiation

To cover different stages of differentiation three osteoblast specific assays were selected; alkaline phosphatase activity (early marker); collagen quantification; and osteoblastic differentiation specific osteocalcin production.

6.2.8.3.1 Alkaline Phosphatase Activity

Alkaline phosphatase activity was measured using the Granutest 25 alkaline phosphatase assay (Randox, UK). The cell lysate was collected and the standard protocol stated in chapter 5, Section 5.2.5.3.1 was followed.

6.2.8.3.2 Collagen Quantification

Collagen quantification was done by using the soluble collagen assay (Sircol, UK). The assay was performed on cell lysate as described in chapter 5, Section 5.2.5.3.2 according to the instructions enclosed with the assay.

6.2.8.3.3 Osteocalcin Quantification

Osteocalcin quantification was performed using a commercially available kit (*Invitrogen*, UK). The lysate was collected and tested for the presence of osteocalcin following the kit instructions (chapter 5 Section 5.2.5.3.3).

6.2.8.4 Morphology

Samples were fixed in and dehydrated before being sputter coated with platinum following the protocol stated in chapter 5, Section 5.2.5.4. Prepared samples were viewed using a Philips XL30 scanning electron microscope operated at 10 to 20 kV.

6.3 Results

6.3.1 Initial Mechanical Properties

From the flexural studies conducted (three–point bend), it was observed that the initial flexural strength of non–woven randomly dispersed PGF reinforced composite was increased by approximately 20 MPa with silane treatment. However, a drop of ~5 MPa was seen for HDI treated samples in comparison with untreated control samples (Figure 6-2). The flexural modulus, however, was found to decrease from 11 ± 2 GPa (untreated non–woven composite) to 8 ± 2.5 GPa for HDI–treated, 10 ± 0.7 GPa for APS treated and 10 ± 2.6 GPa for SPLA treated PGF reinforced composites. Due to small sample numbers ($n=3$), statistical analysis revealed no significance difference ($p > 0.05$) between control and APS/SPLA treated samples.

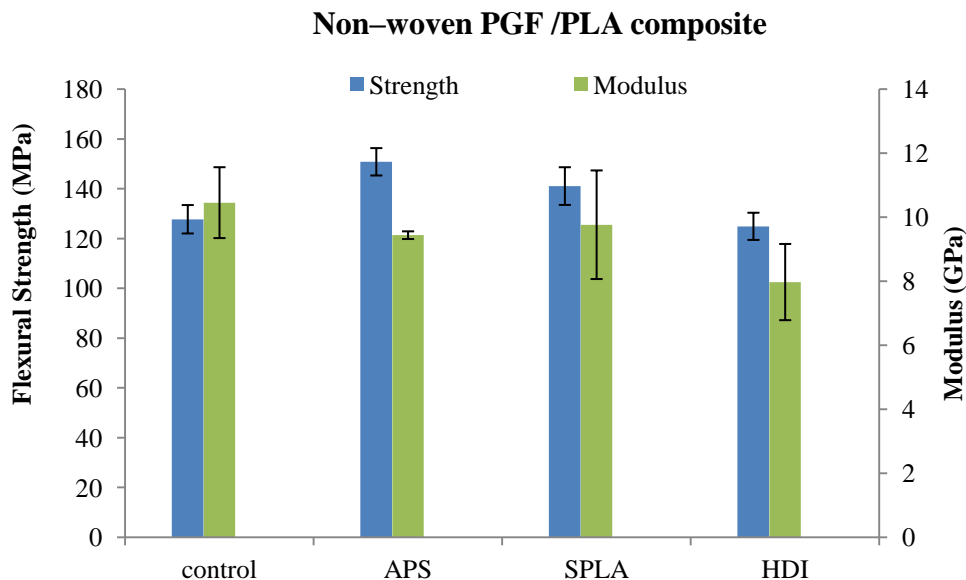


Figure 6-2: Initial flexural mechanical properties obtained for the untreated and surface-treated non–woven randomly dispersed PGF reinforced PLA composites produced with approximate fibre volume fraction of 20%. Error bar represents standard error of mean where $n = 3$.

The (three–point bend) flexural mechanical properties measurement was also performed on unidirectional PGF reinforced composites, the initial flexural strength of control PGF reinforced composite was found 215 MPa which was increased significantly ($p < 0.01$) with silane and SPLA treatments to 300 and 260 MPa, respectively (Figure 6-3). However, lower flexural strength was measured for HDI treated samples (~190 MPa) in comparison to control samples which were found statistically not significant ($P > 0.05$).

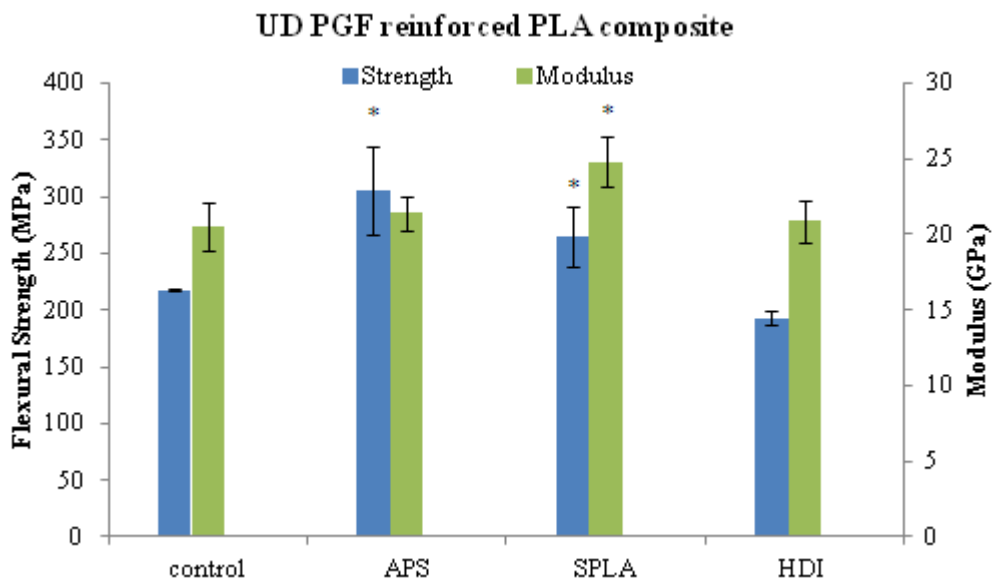


Figure 6-3: Initial flexural mechanical properties obtained for the untreated surface–treated unidirectional PGF reinforced PLA composites produced with approximate fibre volume fraction of 35%. Error bar represents standard error of mean where $n = 3$.

*** indicating the significant difference with respect to control.**

The flexural modulus (Figure 6-3), unlike random fibre composites, was found to have increased with silane and SPLA treatments from 20 GPa (for untreated UD composite) to 22 and 25 GPa with silane and SPLA treatments respectively. No change was observed for HDI treated UD PGF reinforced composite compared to control. Statistical analysis revealed that modulus value for control sample was

significantly different ($p < 0.01$) to SPLA treated sample. However, no significant difference ($P > 0.05$) was observed for APS and HDI treated samples compared to control.

6.3.2 Physical Analysis with Degradation

Figure 6–4 presents images of PGF after treatment with optimised concentration of EA for 15 minutes (left) and 5 minutes (right). It is clear that PGF severely corroded and turned white when exposed to EA for 15 minutes. Although, with 5 minutes treatment PGF did not change their colour but the resultant composite (Figure 6–5) was very brittle and thus excluded from study.



Figure 6-4: PGF showing severe corrosion with EA exposure for 15 minutes (left) and 5 minutes (right).



Figure 6-5: EA modified PGF reinforced composite shows severe corrosion and inferior mechanical properties

Non-woven random PGF reinforced composites were produced with surface-treated and control PGF. It was observed that after treatment, fibre bundles were formed which resulted in non-uniform distribution of PGFs within PLA matrix (Figure 6-6).

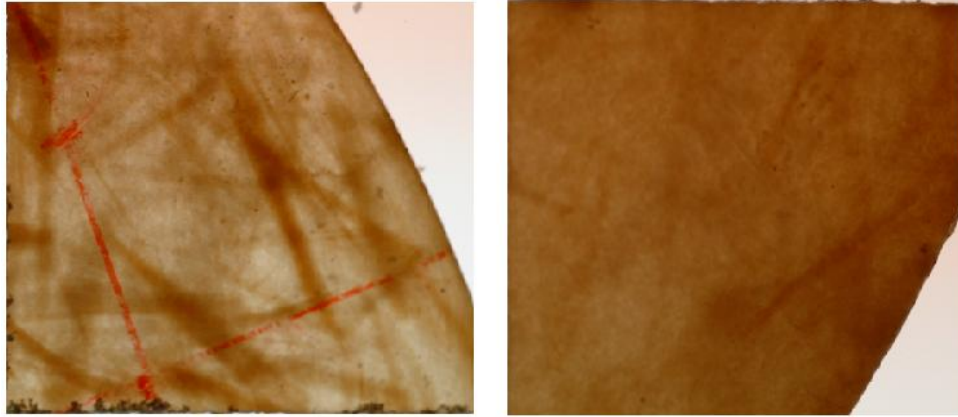


Figure 6-6: Snap shots of random fibre composites APS (left) versus Control (right) shows non-uniform distribution of APS mPGF compared to control PGF within PLA matrix.

Cross sections of composites were exposed by freeze/fracture and examined with SEM, Figure 6-7 and 6-8 shows the representative images of all the samples as made and after 28 days degradation in PBS at 37 °C. Figure 6-7 are the images taken for non-woven random PGF/PLA composites and Figure 6-8 are the representative images for unidirectional PGF/PLA composites.

It can be noticed from figures that within non degraded composites, fibres were well bonded with polymer matrix after treatment compared to untreated composite where clean fibres and holes can be spotted. However, no obvious difference between treated and non-treated composites can be noticed after 28 days of degradation, which correlates well with the results observed for flexural mechanical properties.

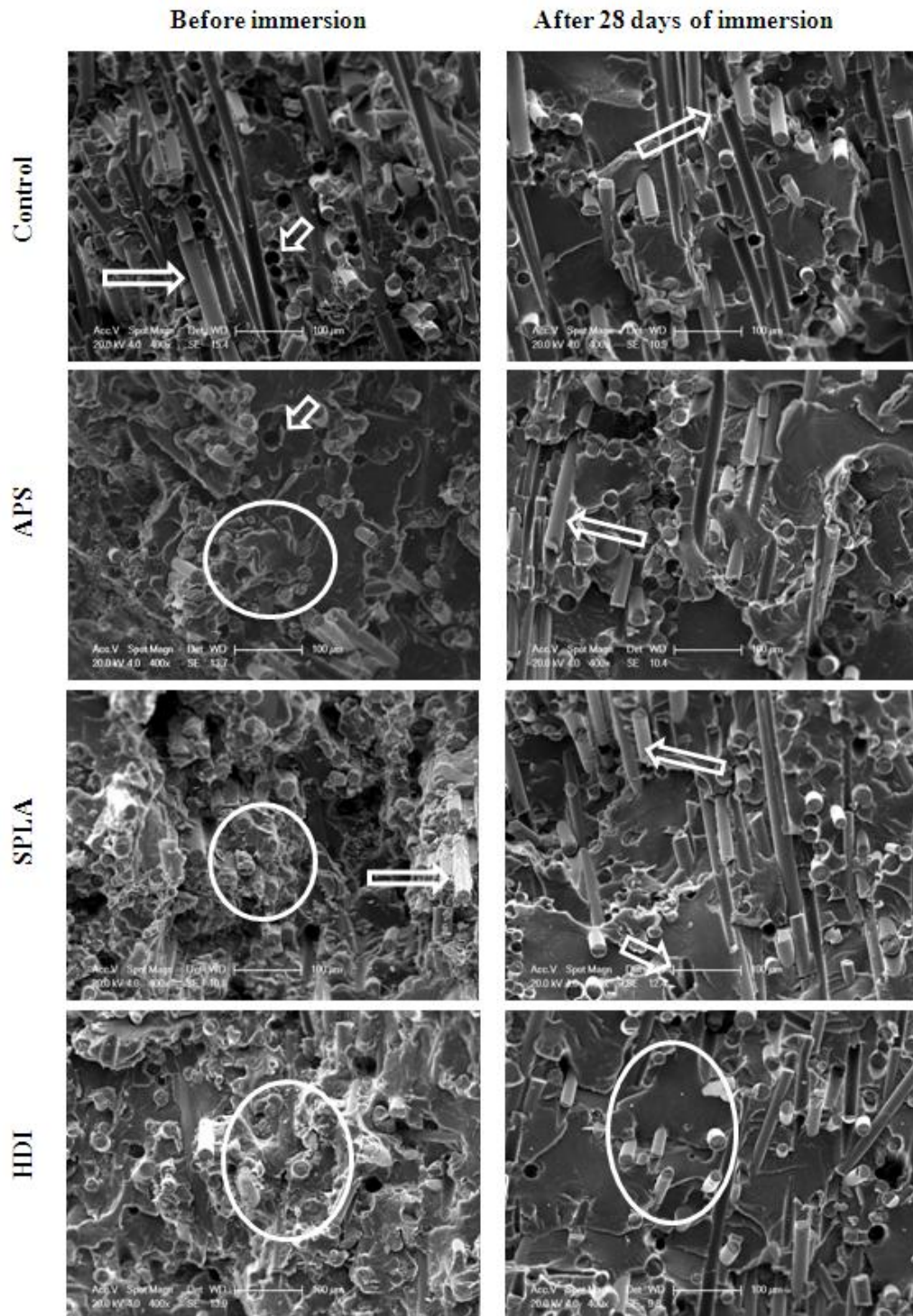


Figure 6-7: SEM images of HDI treated random PGF reinforced PLA composite before (left) and after (right) 28 days of degradation in PBS at 37 °C. Arrows indicating at long fibre pull-out and holes representing interfacial integrity loss while circles pointing out short fibre pull-out and strong interface between PGF and PLA matrix.

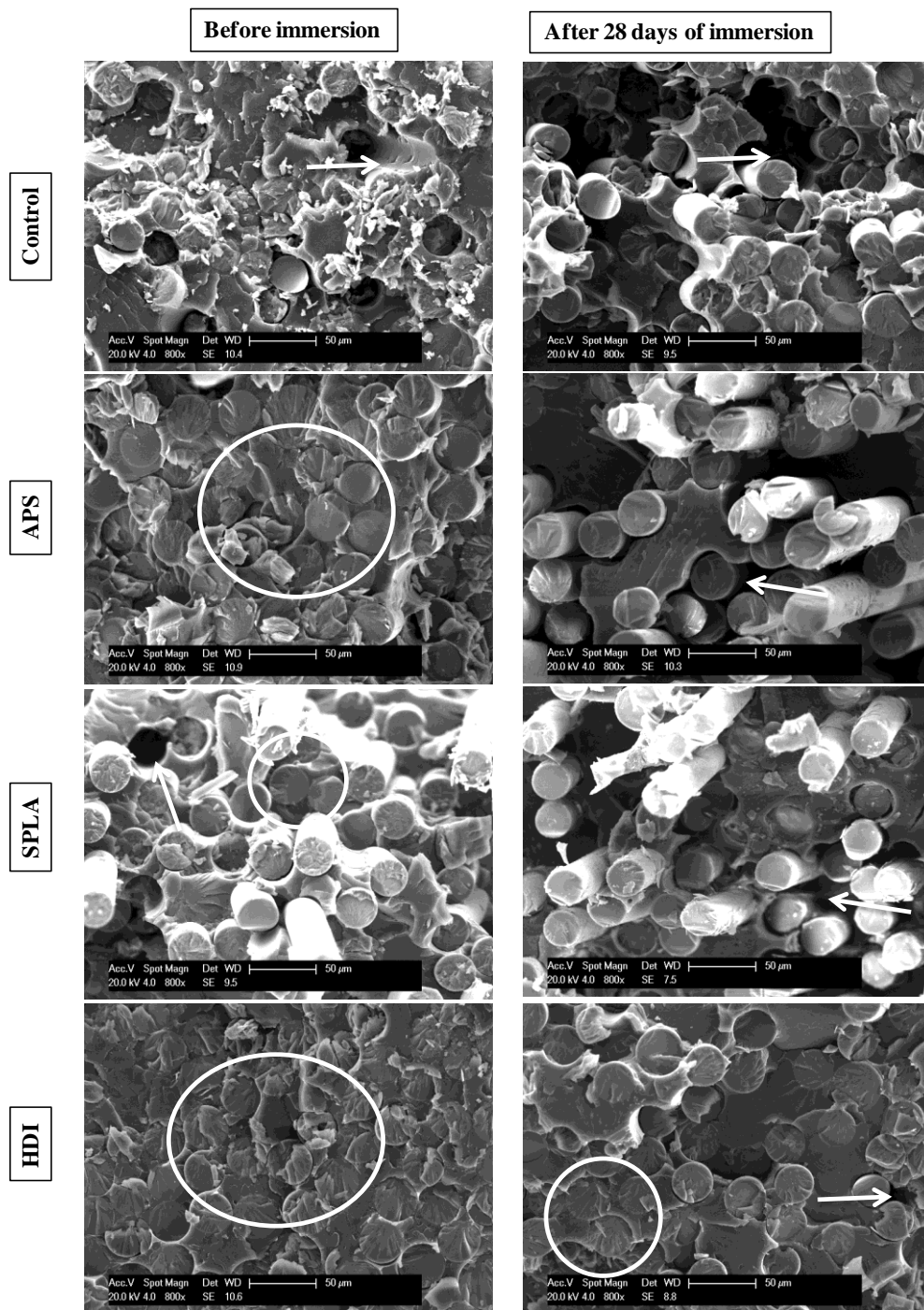


Figure 6-8: SEM micrographs from top to bottom: untreated (control) composite, APS treated, SPLA treated, HDI treated unidirectional PGF reinforced PLA composite, before (left) and after (right) 28 days of immersion in PBS at 37°C. Micrometer scale-bar = 50µm. Arrows indicate holes and long fibre pull-out due to interface failure and circles highlight intact interfacial integrity and short fibre lengths. Better interface i.e. shorter fibre length was observed in case of HDI treated composites compared to others after 28 days of immersion.

Figure 6–7 and 6–8 shows that with treatment a better interface between unidirectional PGF and PLA matrix was established as the length and number of fibre pulled out of PLA matrix was smaller than control. However, interface failure can be seen for control, APS and SPLA treated samples after degradation. HDI treated samples on the other hand were found to maintain interfacial integrity to a greater extent. It is also noticeable that short random fibres were better impregnated within the polymer matrix compared to unidirectional fibres due to relatively lower volume fraction (20% for random and 35% for UD PGF/PLA composite) and greater number of layers (6 layers for random and 4 layer for UD PGF/PLA composite) used to prepare non-woven random fibre reinforced composite.

6.3.3 Water Uptake and Degradation of Composite

Figure 6-9 represents the percentage wet mass change profile of control and treated UD PGF reinforced PLA composites plotted against time (up to 28 days). During the initial phase, the mass gradually increased for all the composites. However, a saturation point was reached for control and HDI treated composites after 2 days which was followed by a plateau (0.75%). A continuous increase in mass due to water uptake by SPLA and APS treated samples was resulted in composite swelling.

UD PG-Fibre Composites' water uptake

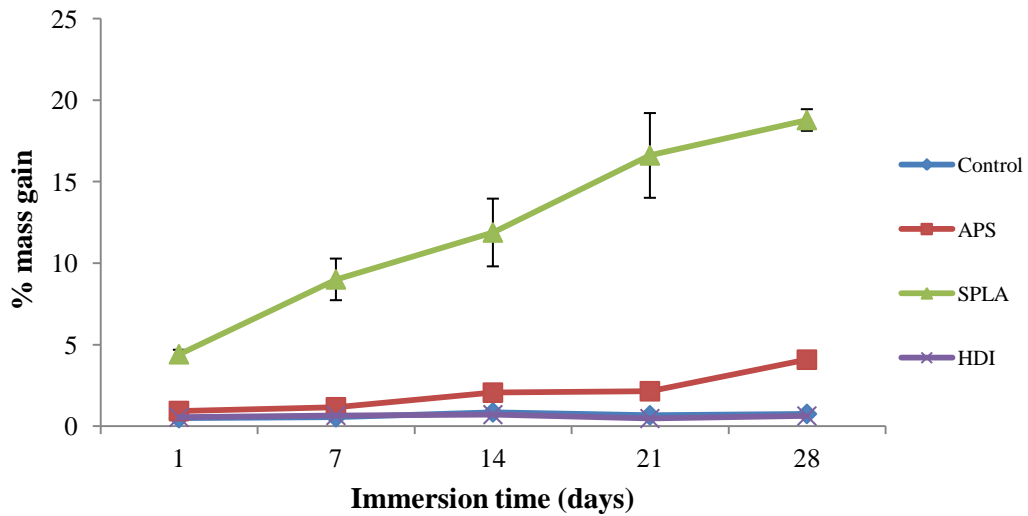


Figure 6-9: Water-uptake profiles obtained for untreated and –treated PGF reinforced PLA UD composites produced with approximate fibre volume fraction of 35%. Studies were conducted for up to 4 weeks in PBS at 37 °C. Secondary y-axis presents the profile of SPLA series only. Error bar represents standard error of mean where n =3.

Dry mass change with degradation versus time is presented in Figure 6-10. It shows that for control and HDI treated samples the mass loss was negligible. Highest mass loss of 0.2% and 0.4% was observed at time point 7 days which was then dropped to 0.1% and 0.2% for control and HDI treated samples respectively. However, relatively greater mass loss (1.4%) was observed for APS treated samples up to 21 days which was levelled out at 28 days. SPLA treated samples lost were found to lose 0.6% of their weight up to 14 days which was increased drastically to 3% at 28 days.

UD PG-Fibre Composites' Mass Loss

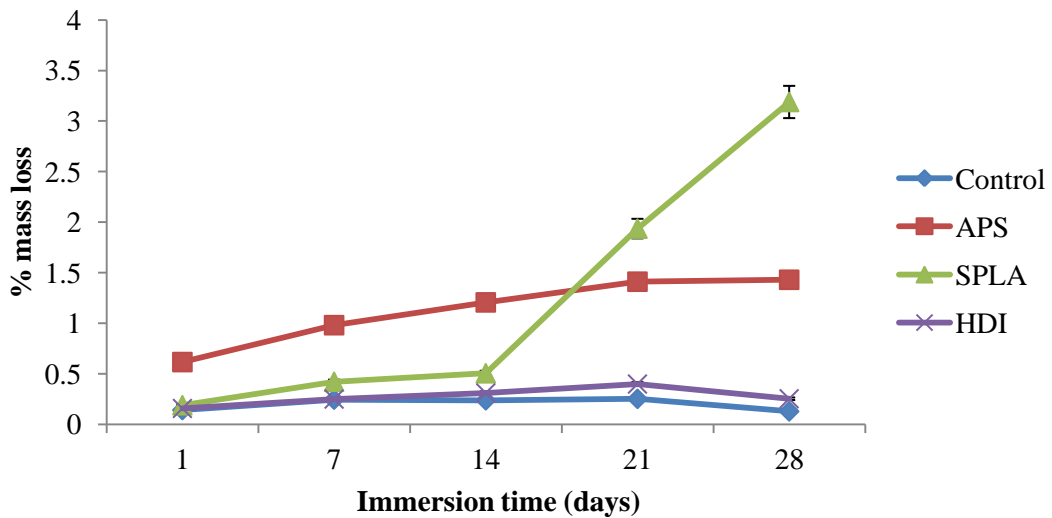


Figure 6-10: Degradation profiles obtained for untreated and –treated PGF reinforced PLA UD composites produced with approximate fibre volume fraction of 35%. Studies were conducted for up to 4 weeks in PBS at 37°C. Secondary y–axis presents the profile of SPLA series only. Error bar represents standard error of mean where n =3.

6.3.4 Retention of Mechanical Properties with Degradation

All variety of UD composites (control and treated) specimens were degraded in PBS at 37 °C up to 28 days. Three point bend flexural tests were conducted on these samples at predetermined time points to investigate mechanical integrity retention with time. For all the samples a drop in flexural strength was observed; SPLA 68%, APS 46%, control 35% and HDI 31%. However, for all the composites except SPLA rate of mechanical strength loss was approximately 1-2 MPa per day after 7 days of degradation (Figure 6-11).

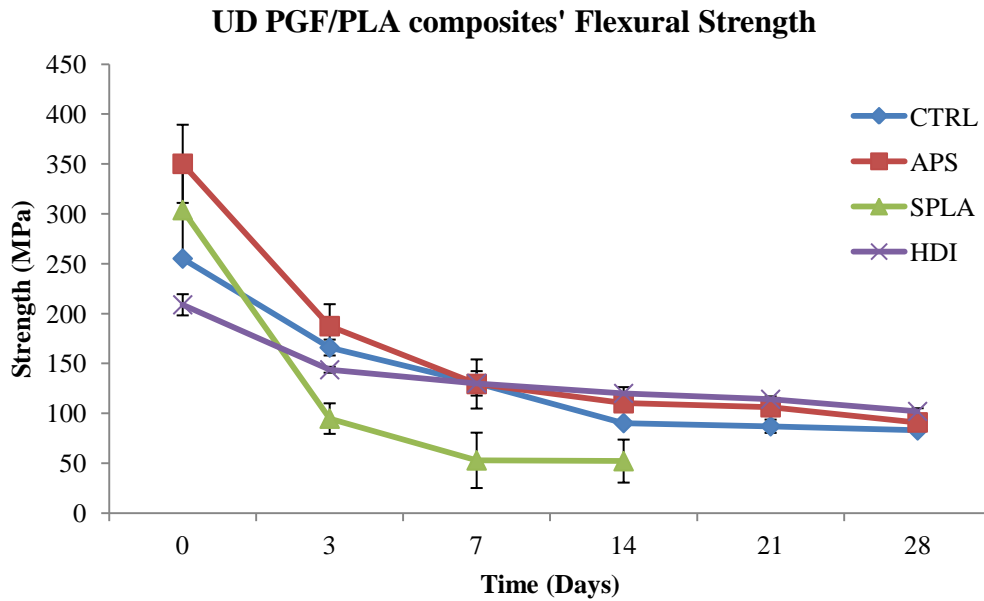


Figure 6-11: Flexural strengths of control and APS, SPLA AND HDI treated UD PGF/PLA composites. All degraded Samples were tested wet after immersion in PBS at 37°C. Due to rapid loss of mechanical strength SPLA series sample was not analysed after 14 days. Error bar represents standard error of mean where n =3.

Final flexural strength of APS (91 MPa) and HDI (101 MPa) treated composites were found to be higher than control (80 MPa) after 28 days of degradation in PBS. However, statistical analysis revealed no significance ($p > 0.05$) between control and APS and HDI treated samples.

A gradual loss in flexural modulus was also observed for all samples other than SPLA series that were dropped to ~6 GPa after 7 days. SPLA treated samples lost their mechanical integrity and excluded from study after 14 days. HDI treated samples were found to maintain the highest flexural modulus after degradation where final modulus was found at approximately 16 GPa compared to control and APS treated samples that was found at 13 GPa (Figure 6-12). However no difference of statistical significance ($p > 0.05$) was observed.

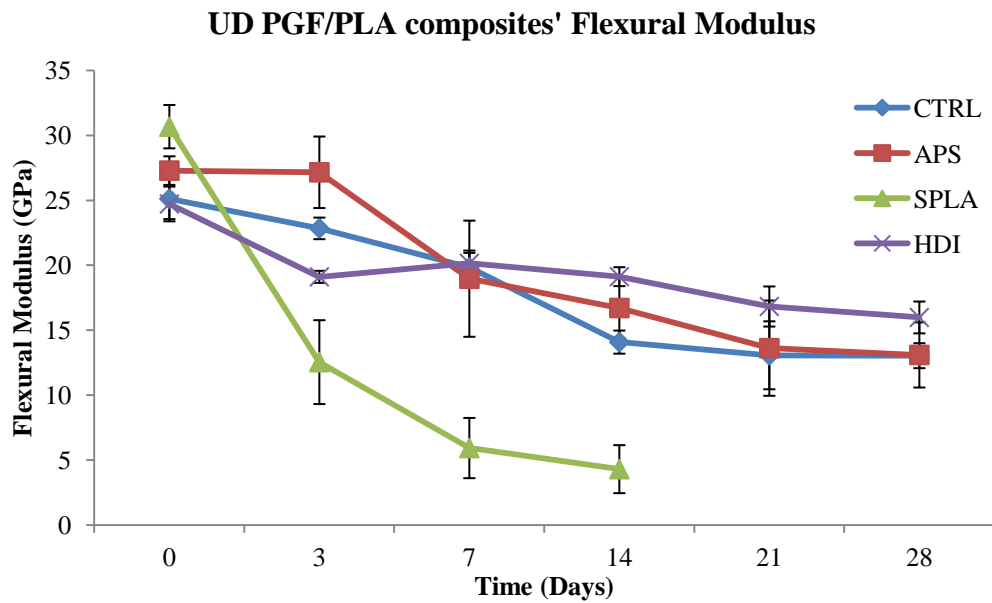


Figure 6-12: Flexural modulus of control and APS, SPLA and HDI treated UD PGF/PLA composites. All degraded samples were tested wet after immersion in PBS at 37°C. Due to rapid loss of mechanical strength SPLA series sample was not analysed after 14 days. Error bar represents standard error of mean where n =3.

6.3.5 Cytocompatibility of Composites

6.3.5.1 Proliferation

To investigate the effect of chemical modification of phosphate glass fibres with selected within the composite on the proliferation of primary human osteoblasts, DNA concentration of the cells cultured on the surfaces of different composite surfaces were measured over a period of 21 days, (Figure 6-13).

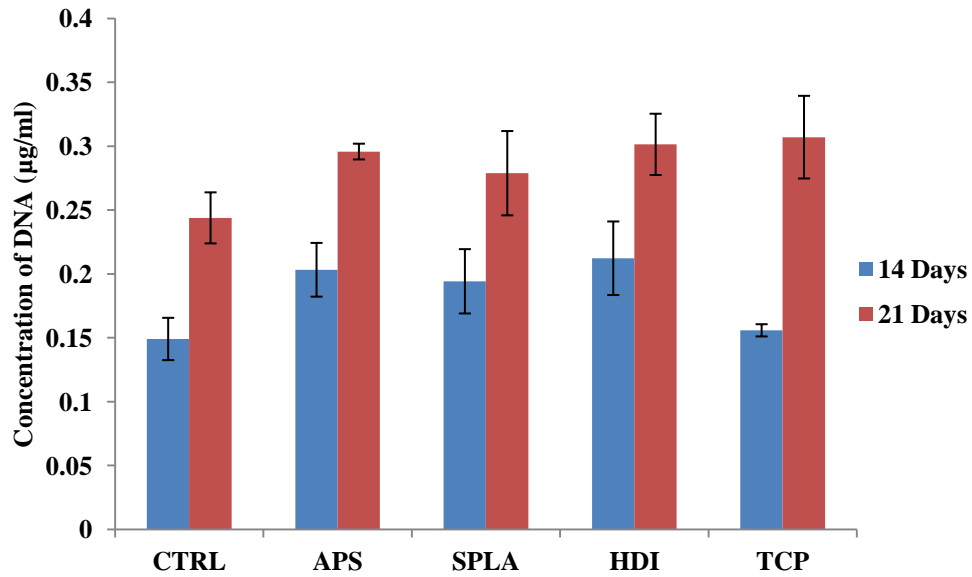


Figure 6-13: DNA concentration of primary human osteoblast cells, as measured by the DNA (Hoechst 33258) assay, cultured on modified PGF reinforced PLA composites; x-axis represents surface treatments. Error bar represents standard error of mean, n = 6. No significant difference was found amongst the samples.

For all modified samples the DNA concentration was approximately $0.2 \mu\text{g ml}^{-1}$ at 14 days in culture while for both the controls where $\sim 0.15 \mu\text{g ml}^{-1}$ DNA was measured. Enhanced osteoblast proliferation can be seen as DNA concentration increased to $\sim 0.3 \mu\text{g ml}^{-1}$ between 14 and 21 days of culture on all the surfaces. However, two-way ANOVA revealed no significant ($p > 0.05$) effect of treatments compared to control. TCP was used as internal control for experiment validation.

6.3.5.2 Differentiation

6.3.5.2.1 Alkaline Phosphatase Activity

Alkaline phosphatase activity (ALP) of primary human osteoblast cultured on composite surfaces for 14 and 21 days is presented in Figure 6-14.

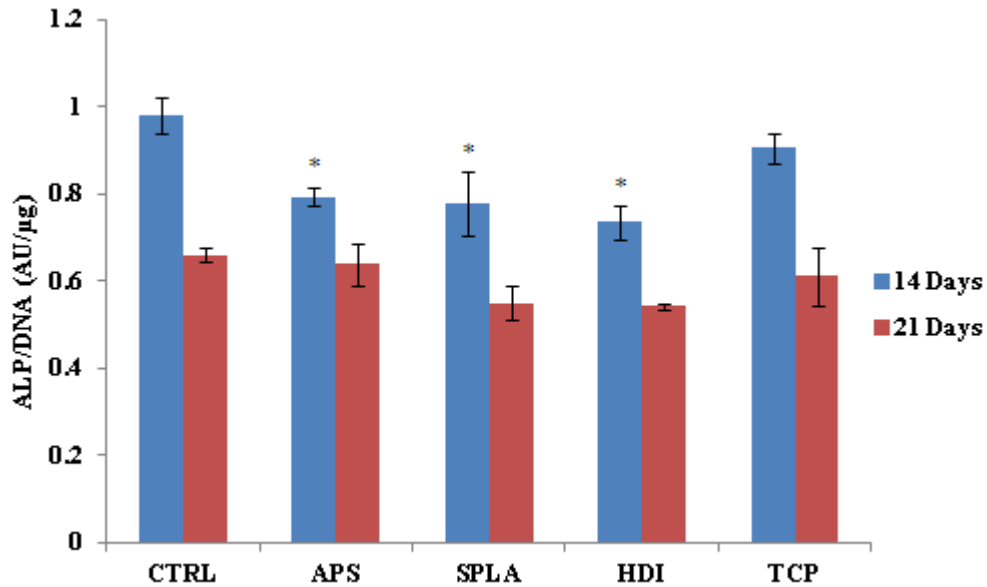


Figure 6-14: Cell alkaline phosphatase (ALP) activity of primary human osteoblasts cultured on UD PGF reinforced PLA composite surfaces, as measured by ALP assay, x-axis represents surface treatments. All data is modified with DNA values obtained for each individual sample. Error bar represents standard error of mean, n = 6. * indicating significantly low ALP activity with respect to control.

For all sample surfaces similar trend of alkaline phosphatase activity was observed where a down regulation in ALP activity was measured from day 14 to 21. Statistical analysis demonstrated no significant difference for ALP activity between treated samples at any time point. Two-way ANOVA analysis revealed significant difference ($p < 0.01$) between control and treated samples on day 14 only.

6.3.5.2.2 Collagen Production

Collagen production by primary human osteoblast cultured on selected modified phosphate glass fibre reinforced composite surfaces for up to 21 days was assessed and quantified by Sircol collagen quantification assay (Figure 6-15, 6-16).

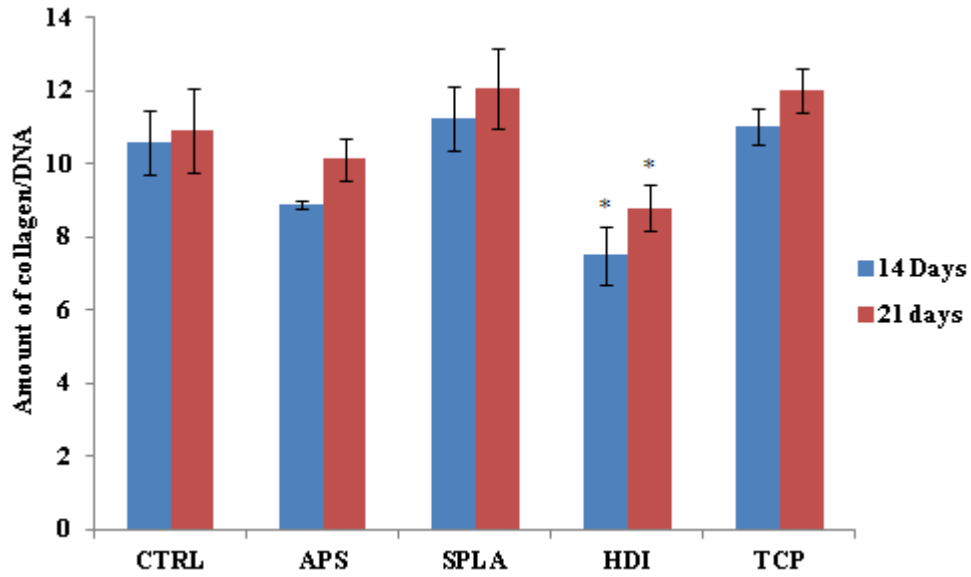


Figure 6-15: Collagen production by primary human osteoblasts cultured on modified UD PGF reinforced PLA, measured by Sircol assay. All values were normalised with DNA values for corresponding sample. Error bar represents standard error of mean, n = 6. * indicating significantly low collagen concentration on HDI treated sample compared to control.

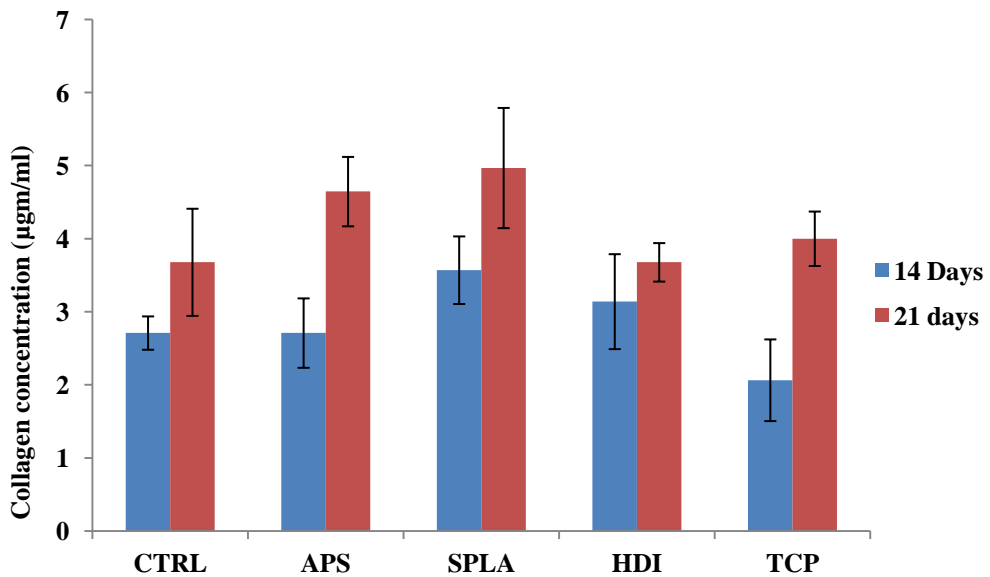


Figure 6-16: Collagen production by primary human osteoblasts cultured on PGF reinforced PLA composites, as measured by Sircol assay. Error bar represents standard error of mean, n = 6.

Although, statistically not significant ($p > 0.05$), an upward trend in collagen concentration was observed over the period of culture on all surfaces. When normalised with the DNA concentrations all samples, including the controls, showed no significant change in collagen concentration with time. Figure 6–16 shows that that amount of collagen produced on the surface of HDI treated composite was significantly lower ($p < 0.01$) than the control composite.

6.3.5.2.3 Osteocalcin Quantification

Osteocalcin concentration produced by primary human osteoblast cultured on composite surfaces for up to 21 days was assessed and quantified by ELISA osteocalcin quantification assay kit (Figure 6-17, 6–18).

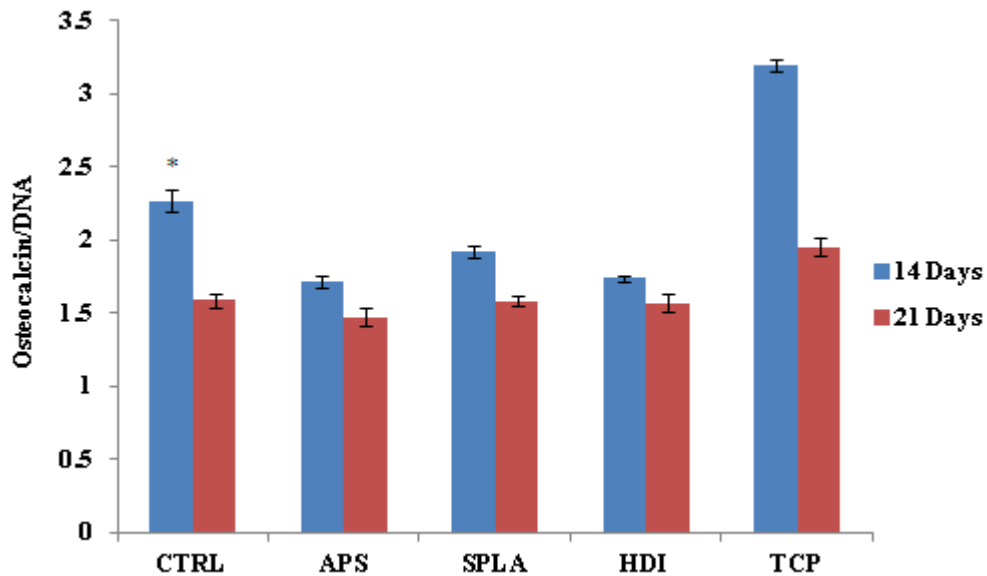


Figure 6-17: Quantity of osteocalcin produced by of primary human osteoblasts, as measured by ELISA assay, cultured on PGF reinforced PLA composite surfaces, x-axis represents surface treatments. All data is normalised with DNA values obtained for each individual sample. Error bar represents standard error of mean $n = 6$. * implies that osteocalcin level on day 14 was found significantly higher than treated composites.

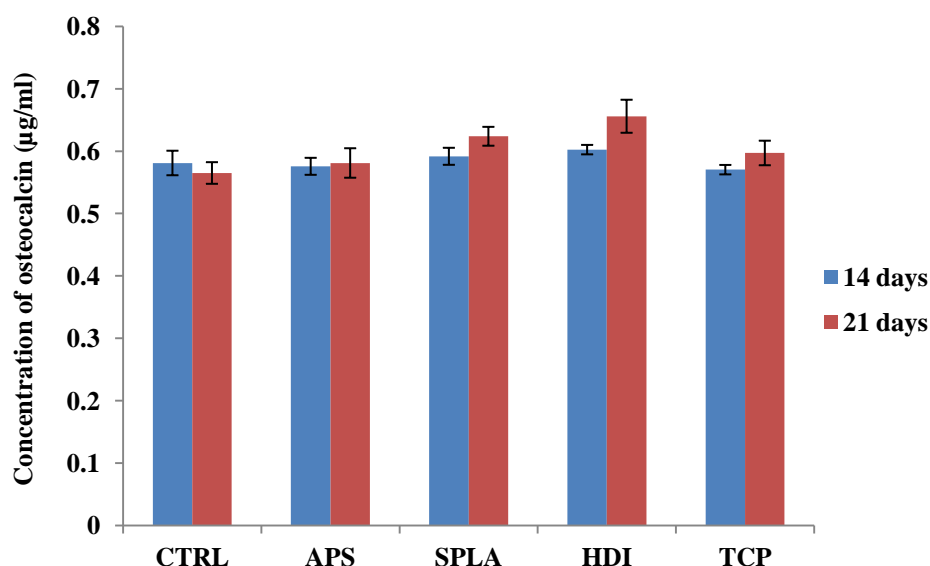


Figure 6-18: Quantity of osteocalcin produced by of primary human osteoblasts, as measured by ELISA assay, cultured on PGF reinforced PLA composite surfaces, x-axis represents surface treatments. Error bar represents standard error of mean, n = 6.

Levels of osteocalcin were found 0.6 ± 0.05 ng/ml on all sample surfaces and at each time point. A repeat of this experiment provided with the same result implies the response was consistent. However, when normalised with DNA concentrations, downward trend in osteocalcin concentration was observed (Figure 6-17). Statistical analysis of normalised data revealed significant ($p < 0.001$) difference between control and treated samples on day 14 only.

6.3.5.3 Cell Morphology (SEM)

Morphology of cells cultured on phosphate glass fibre reinforced PLA composite discs was visualized by SEM (Figure 6-19). Within the figure, are the representative images of 14 and 21 days in cell culture; showing adherence of cells to the surface of all surfaces. Cells were found to cover the surfaces homogeneously.

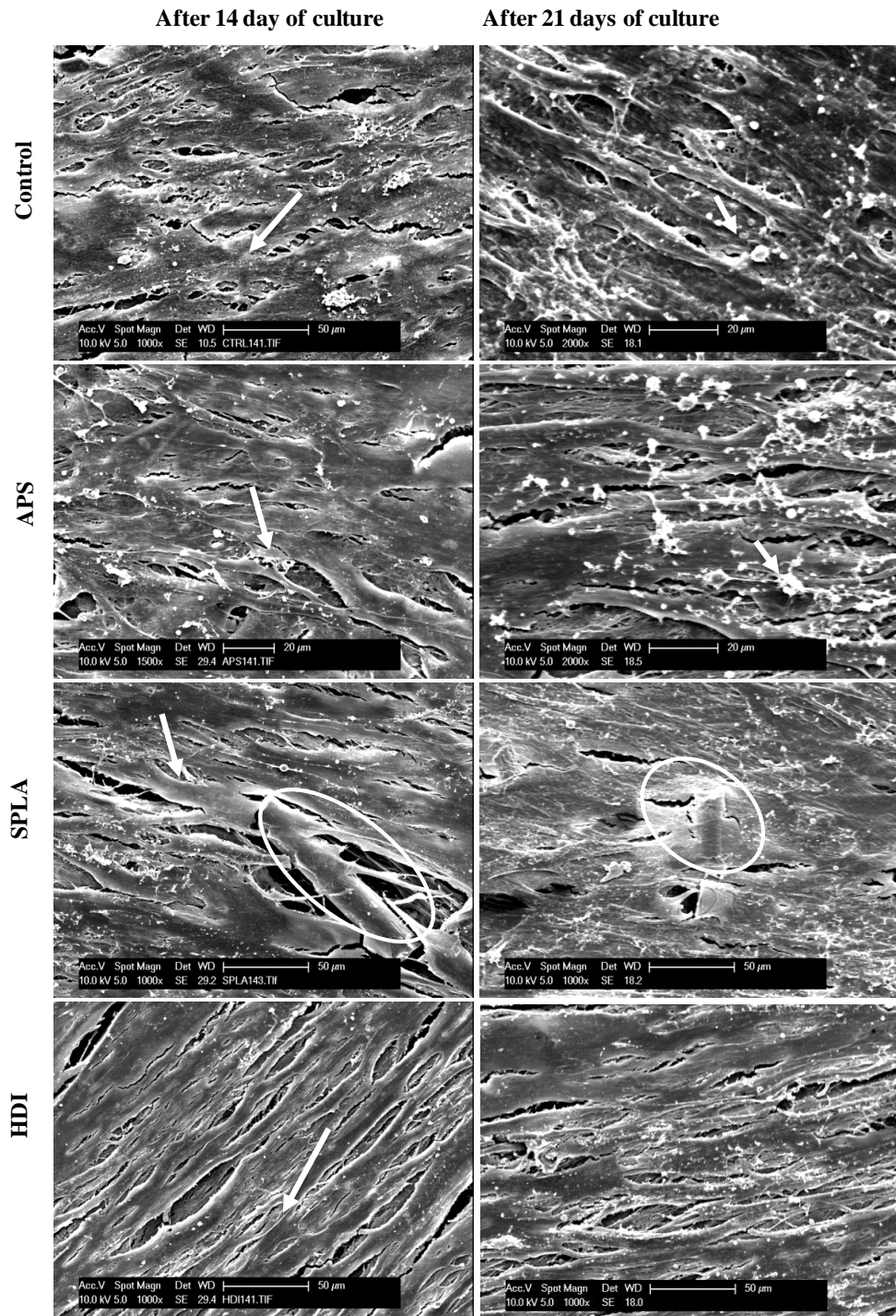


Figure 6-19: SEM images of human osteoblast cultured on (from top to bottom): untreated (control) composite, APS treated, SPLA treated, HDI treated unidirectional PGF reinforced PLA composite, after 14 days (left) and 28 (right) days of culture. Micrometer scale-bar = 50 μm. Arrows indicates at complete coverage of composite surface with cell matrix and circles pointing out glass fibre.

In general, SEM images of primary human osteoblast cells cultured on composites and TCP up to 21 days shows spindle-shaped cell with lamellipodia extending to neighbouring cells and thus making a sheet like structure after 14 days. After 21 days in culture cell became more mature and small nodules were located on all surfaces except SPLA treated samples. Production of collagen fibrils and deposition of mineral was also noticed after 21 days culture.

6.4 Discussion:

High tensile modulus glass fibre reinforcement for polymers is well known to improve the resulting composite's mechanical properties [1, 23, 24, 27, 140, 144, 158-160, 195]. The resultant modulus could be predicted with a simple rule of mixture formula and expected to be different in different directions of force.

- Modulus of Elasticity in longitudinal direction (E_{cl})

$$E_{cl} = E_m * V_m + E_f * V_f$$

- Modulus of Elasticity in transverse direction (E_{ct})

$$1/E_{ct} = V_m/E_m + V_f/E_f$$

Where:

E_m = Modulus of elasticity for matrix

V_m = volume fraction of matrix

E_f = Modulus of elasticity for fibre

V_f = volume fraction of fibre

Reinforcement with these glass fibres enable polymer composite to sustain higher tensile loads and consequently prevent a sudden failure of fibre reinforced composite which in case of bone fracture repairing implant would be catastrophic for patients.

An ideal implant should provide strong support in the early stages of the implantation period and allow a gradual transfer of load to the healing bone during the later stages [4]. This goal could only be achieved with a totally resorbable implant that can provide high initial mechanical strength and then a controlled gradual loss of mechanical properties with time.

A number of composites with self [20], particulate [137, 156, 170, 179] [115,189–190] and fibre [23] reinforcements have been developed with sufficient initial mechanical properties for bone repair applications. However, these composites are reported to either not have enough initial strength to support load-bearing bone fracture repair or lose their strength rapidly within the first few days of degradation.

A few studies have investigated this rapid loss (>50 % mechanical integrity loss within 1 week of exposure to aqueous environment) of mechanical properties and reported that it was due to water ingress in the polymer/matrix interface which led to polymer swelling, plasticisation of interface resulting in an inefficient load transfer between the phases [13, 20, 23, 158, 243].

Chemical agents such as different silanes, poly-HEMA and phosphonic acids are being employed to improve load transfer between two phases of composites with some success [25, 26, 244, 245], resulting in improved initial mechanical properties. For this project eight different chemical surface treatments were selected which were passed through various screening stages; chemical bonding with PBG, IFSS improvement and three-step cytocompatibility assessments.

Four out of eight treatments were selected to be employed within PGF reinforced PLA composites. However, etidronic acid (EA) was found to be corrosive for PGF and thereof excluded from current study.

Two different types, non-woven random PGF/PLA and unidirectional PGF/PLA composites, were produced using film staking followed by hot and cold press. Composites were tested for initial flexural properties as well as retention of flexural properties with degradation in PBS at 37 °C.

After treatment and washing out unbound, chopped fibres (mPGF) were found difficult to separate, this resulted in non-uniform distribution of mPGF within the composite. This might have led to a comparatively low flexural modulus composite with larger error in mechanical properties measurements for treated composite specimen. In spite of this inhomogeneity and low modulus an increase in initial strength for APS and SPLA treated composite specimen was observed. It was observed that the initial flexural strength of non-woven randomly dispersed PGF reinforced composite (~125 MPa) was increased by 20 MPa with surface treatments (Figure 6-2). It was also noted that with air-lay method approximately 10 to 20 weight % fibres were lost and hence the fibre volume fraction was difficult to maintain.

A significant improvement (from ~210 MPa up to 310 MPa) in flexural mechanical properties of UD composite was observed for APS and SPLA modified phosphate glass fibres (mPGF) reinforced PLA composite compared to control (untreated) unidirectional PGF reinforced PLA composite (Figure 6-3); implies that the surface treatment of PGFs improved the interface between PGF and PLA and thus provided an efficient load distribution resulted in enhanced mechanical properties [161, 165]. However, comparatively lower initial flexural properties was observed for HDI (Figure 6-3) treated sample which could be due to the fact that HDI grafting on PGF, which involves soaking fibres in DMF and distilled water, may have reduced the fibre strength which was reflected in comparatively low flexural properties.

A positive effect for silane on glass fibre reinforced composites has been reported by Jiang *et al.* who reported a marked improvement in flexural mechanical properties with APS treatment on Bioglass[®] reinforced poly caprolactone [154]. In that study,

amine silane treated glass fibre composite had a Young's modulus of 16 GPa and 200 MPa in strength compared to 9 GPa and 130 MPa modulus and strength, respectively, when treated with propylsilane. In another study on PCL composites an improvement of 10 MPa in flexural strength was reported by Khan *et al.* when PGF were treated with Poly(2-Hydroxyethyl methacrylate) HEMA [159]. Similarly, Haque reported a 20 MPa flexural strength and 3 GPa flexural modulus improvements in PGF reinforced PLA composite after SPLA treatment [167]. These reports attributed the improvements to a better shear bond strength, compatibilisation and/or concealing of micro-cracks between the phases.

UD composites samples were analysed for water uptake, mass loss and retention of mechanical properties with degradation. A quick loss of mechanical properties was observed for all composites. A rapid loss of mechanical properties of fibre reinforced composite is well reported. For example; Khan *et al.* (PGF/PCL) [28, 159, 160], Ahmed *et al.* (PGF/PLA) [158], Haque (PGF/PLA) [167] Felfel *et al.* (PGF/PLA) [23, 24] all have reported a rapid drop in mechanical properties within first week of degradation.

Degradation of totally resorbable fibre reinforced polymer composite is a combination of physical degradation (e.g. polymer swelling), degradation of polymer matrix in case of totally resorbable composite; break down of interfaces between the fibre and matrix and loss of fibre strength due to corrosion. Interface degradation can set off wicking (a form of capillary action between the loose fibre and matrix interface). Water filled capillaries can decrease the mechanical strength of fibre reinforced composites. It is also known that there is a direct relation between fibre volume fraction and water uptake which suggests that low volume fraction of fibres

can be impregnated into polymer matrix better than high volume fraction. It was reported by Felfel *et al.* that water ingress for UD composite was higher than random fibre composite which was attributed toward better impregnation of random fibres into polymer matrix as compared to UD fibres [23]. The results presented in current study agree with the conclusion made by Felfel *et al.*

SPLA treated samples were found to take up water (Figure 6-9) that resulted in a swollen composite. Similar response from SPLA-mPGF/PLA composite was reported by Haque *et al.*, they reported a 1.2% water uptake after 7 days of immersion in PBS at 37 °C. It was also reported that SPLA treated composite lost ~50 MPa (from 160 MPa) of their strength with 7 days of immersion [167]. This behaviour of SPLA treated samples can be attributed to the hydrophilicity of SPLA which led to degradation of SPLA oligomer and hence autocatalytic degradation of PLA matrix. One possible explanation for comparatively high water uptake could be the fact that after dip coating the UD mats with S-PLA oligomer, no soxhlet extraction was carried out and thus there were more hydrophilic SPLA oligomers to absorb water compared to random fibre reinforced composite.

APS treated specimen although took up higher amount of water than control samples yet maintained superior mechanical properties which can be attributed to PGF-APS-PLA bridge formed by covalent bonding and/or to the hydrophobicity at the interface.

No significant difference in water uptake (Figure 6-9) and degradation (Figure 6-10) was found between HDI treated samples and controls. However, HDI treated samples were the strongest at the end of study (Figure 6-11 and 6-12). This retention

of mechanical integrity suggests a strong covalent bond between reinforcement and matrix and hydrophobicity at interface within the composite.

Mechanical properties of a polymer are (up to a certain molar mass) directly proportional to the chain length. Therefore mechanical property retention of polyester (such as PLA, PGA or PCL) based composites can also depend on the degradation of the polymer via hydrolysis of the ester group in the polymer backbone. Hydrolysis of polyesters is catalysed by protons (i.e. in an acidic environment). PLA has been known to hydrolyse more readily than other aliphatic polyesters. The acid dissociation constant (pKa) of oligomeric PLA is 3.1. Therefore, the dissociation of the acid end-group is expected to result in an acidic environment and contribute significantly toward acid-catalysed hydrolysis. As the reaction proceeds, the carboxylic acid concentration and the rate of hydrolysis increase, and the reaction is said to be autocatalytic [246], which can result in loss of mechanical properties of the polymer. This also highlights that the approach to reduce hydration (by improving the fibre/PLA interface) is therefore likely to improve mechanical performance not only by prevention of swelling and cracking, but by also delaying polymer hydrolysis. The effect of autocatalysis of the polyester matrix was reported to significantly affect the mechanical properties of PGF reinforced composite [243]

Scanning electron microscopy (Figure 6-7 and 6-8) of non-degraded and degraded composite sample cross section correlates with the results observed for water uptake. Hence supports that the composite lost their strength gradually as the water uptake due to capillary action increased with time. Total loss of interface for S-PLA oligomer treated sample can be seen from the SEM images of degraded samples. Conversely, with APS and HDI treatment interfacial integrity of the composite was

intact. The degree of this interfacial integrity retention was greater for HDI treated samples compared to APS treated and control composite which was reflected in the flexural strength and modulus observed for the samples.

Although, biocompatibility of PLA is well established in the literature and cytocompatibility for phosphate glass and chemicals selected for surface treatments in this study was investigated and reported separately in chapter 3 and 5 respectively. Human osteoblast interaction, cultured directly onto a composite surface, was investigated bearing in mind that the surface properties, synergistic effect of degradation products and their concentration for the composite would be different to those for the polymer, glass and surface treatments alone.

A small number of studies have reported cytocompatibility of PLA based composites with various reinforcements like HA, Bioglass or PBG comparable to tissue culture polystyrene [1, 140, 157, 158, 247]. However, the cell culture duration for the studies (~7 days) was not long enough to observe the effect of degradation products as well as changes in surface structure due to degradation. For example, Ahmed *et al.* cultured a human osteosarcoma cell line (MG63) on annealed and non-annealed phosphate glass fibre (~14% by volume) reinforced PLA composite and imaged live/dead stained cells attached to the surfaces of the composite specimens up to 7 days in culture through confocal laser scanning microscope. It was reported that both PLA (alone) and the heat-treated fibre reinforced composites maintained higher cell viability as compared to the non-annealed fibre composites. This was attributed to the slower degradation of the annealed fibre reinforced composites [158]. Andriano *et al.* prepared poly(ortho ester) reinforced composite with randomly oriented, crystalline microfibers of calcium-sodium-metaphosphate with or without silane

treatment. Only cytotoxicity was investigated using tissue culture agar overlay up to 24 hours by direct cell contact method and L929 mouse fibroblast cells. It was reported that the component materials showed no acute cytotoxicity [1].

Cells can be exposed to all components of a composite by culturing them on cross-section of composite and hence a short term study would be sufficient. Brauer *et al* produced a methacrylate-modified oligolactide matrix reinforced with slow degrading phosphate invert glass fibres of the glass system P_2O_5 -CaO-MgO- Na_2O - TiO_2 . MC3T3-E1 murine pre-osteoblast cell were seeded on cross-section of the prepared samples and cultured up to 8 days. Short-term biocompatibility was tested in an FDA/EtBr viability assay and a cytocompatibility of the composite materials was reported on the basis of live-cell density attached to the surfaces [140].

For this study, primary human osteoblast was selected because the intended application of these composite is load-bearing fracture fixation. Cells were cultured up to 21 days on composite surfaces to encompass all cell function from initial cell attachment to proliferation and differentiation with degradation products coming out from both PLA and mPGFs.

DNA concentration was measured as an indicator of proliferation which was found $\sim 0.2\mu\text{g/ml}$ after 14 days of culture for all the samples (Figure 6-13). A positive proliferation trend was observed on all samples. DNA concentration was found $\sim 0.3\mu\text{g/ml}$ after 21 days on all samples. There was no significant difference found when 2 way ANOVA was carried out.

Typical down regulation in ALP activity from day 14 to 21 was observed (Figure 6-14) which correlates well with the results observed for osteoblast cultured on

mPBG. Although statistically not significant, highest ALP activity was observed for control composite sample where the cell proliferation was the slowest.

Collagen concentration was found to not change with time when normalised with DNA concentration (Figure 6-15). Same trend was observed by Kim *et al.* when osteoblasts were cultured on bioactive glass nano-fibre filled PLA composite up to 15 days [247].

A down regulation of osteocalcin concentration was observed when normalised with DNA content (Figure 6-17). The trend was consistent when compared with the results reported in chapter 5 for osteocalcin production by primary human osteoblasts cultured on mPBG.

Scanning electron microscope images (Figure 6-19) of primary human osteoblast cultured on control and treated PGF composite showed typical cell adhesion, proliferation, collagen production and mineral deposition with no discrepancies between samples. Osteoblast were found fully confluent after 14 days on all surfaces showing spindle-shaped cells arranged like a shoal of a fish and cells cultured on composite surfaces showed presence of collagen and mineral deposition. After 21 days as the top PLA layer was degraded some fibres were exposed with cells attached to them. At 21 days cell clusters were found on control and APS treated samples which were absent on S-PLA and HDI treated samples this behaviour correlates with values obtained differentiation markers.

6.5 Conclusions

Selected surface treatments (APS, SPLA) for PGFs improved the initial flexural properties of composite and some (APS, HDI) also slowed down loss of flexural strength and modulus with degradation. This improvement in initial flexural properties can be associated with the improved shear bond strength at the interface due to covalent bridge between glass fibres and polymer matrix provided by surface treatment. Delay in mechanical property loss (with APS and HDI treatment) with degradation also confirmed the hypothesis that hydrophobicity at the interface would retard the interfacial integrity loss and consequently loss of mechanical integrity of composite. All modified and control composite demonstrated cytocompatibility comparable to control, supporting their use for implantable devices.

CHAPTER 7. GENERAL DISCUSSION, CONCLUSIONS & RECOMMENDATIONS

7.1 General Discussion

Throughout history bone fractures have been treated with immobilization, traction, amputation, and internal fixation. Over the past 40 years, advancements in biological, mechanical and material sciences have led to contemporary fixation techniques [248]. Excellent reviews on the subject of biomaterials development for bone fracture fixation and describing state-of-the-art technology have been published [56, 57, 238-242]. Historically, metal has been the most popular material for fracture fixation and, whilst it has excellent results, it is not without its problems like stress shielding, corrosion, pain and growth restriction [248].

An ideal implant for bone fracture fixation should support the fracture during the initial phase of healing and then gradually lose its strength with the same rate of strength gain by the healing bone [15]. Over the last two decades the use of biodegradable materials has expanded to include fixation applications. Degradable polymers available as implantable material include polyesters (polylactic acid, polyglycolic acid), polylactones, polyanhydrides and poly(ortho esters). However, for orthopaedic applications a degradable polymer should possess mechanical properties close to cortical bone (bending strength 100–200 MPa, $E = 10\text{--}30$ GPa). It is also required to degrade at a steady pace comparable to bone healing. Furthermore, the degradation products should also be biocompatible and resorbable through

metabolic pathways. Currently available polymers do not satisfy this combination of requirements. The most common biodegradable polymers previously used in orthopaedics were created from L-lactide, D-lactide and glycolide [249, 250]. The rapid degradation of pure polyglycolic acid and the slow degradation of pure poly-L-lactic acid or polycaprolactone implants eventually led to the utilization of copolymers. However, implants made out of polymeric materials alone are usually mechanically weaker than conventional metallic fixation devices or cortical bone.

The difference between the strength/modulus of cortical bone and commonly used polymers led researchers to reinforce the polymers with high modulus degradable fibres like bioactive glass or phosphate glass [27, 154, 158]. Although, initial mechanical properties of such composites were reported to match or even exceed the requirements, a rapid loss of mechanical integrity was reported [27, 140, 154, 158, 251]. This rapid drop in mechanical properties of composites was associated with a loss of interfacial integrity between the polymer matrix and fibre reinforcement and is the motivation behind the current project.

The aim of this project was to develop a totally degradable composite for bone fracture fixation applications with emphasis on improving the fibre/matrix interface. The composite was intended to be used as a load bearing bone-plate/screw fixation system. Therefore, initial flexural properties matching cortical bone (Flexural strength 100–200 MPa, Modulus = 10–30 GPa) was desirable [17-19, 29].

Healing occurs in three distinct but overlapping stages: the early inflammatory stage; 2) the repair stage (soft callus formation around the repair site; and 3) the late remodelling stage. The soft callus formed around the repair site is very weak in the

first 4 to 6 weeks of the healing process and requires adequate protection in the form of bracing or internal fixation [252]. Therefore, the intended resorbable implant required to maintain its strength for at least during the repair stage (4-6 weeks). As stated above, rapid mechanical integrity loss was identified as the major problem with such devices [27, 140, 154, 158, 251]. This rapid loss was attributed to hydrolytic interfacial break down and aimed to be addressed by introducing hydrophobicity and covalent bond between glass fibre and polymer matrix. The starting material (polymer matrix, fibre and coupling agent/surface treatment chemicals) for a degradable composite was carefully selected based on the criteria of their degradability, biocompatibility and mechanical properties. For matrix material, several degradable polymers such as polylactic acid, polyglycolic acid, polycaprolactone, poly (ortho ester), were considered. However, polylactic acid was the obvious choice because of relatively high strength, suitable degradation rate and biocompatibility. The major biodegradable fibres, includes bast fibres/plant-originated fibres (e.g. flax, hemp, jute, ramie, kenaf, abaca), alginate fibres, and polymer fibres (e.g. poly (lactic acid) and poly (hydroxyalkanoate)). However, to improve the strength and stiffness (Young's modulus) a degradable glass fibre with strength closer to E-glass fibre (tensile strength ~2000 MPa; tensile modulus ~ 80 GPa) was required. Silica glass fibres (e.g. bioglass) are generally considered as non-degradable. However, Kursawe *et al.* synthesised nano scale (4 to 5 nm) degradable silica fibres for medical use through sol-gel route. Tensile strengths of the silica fibres up to 300 MPa and tensile modulus up to 20 GPa was reported [253]. Similarly, all the degradable fibres reported above exhibit inferior mechanical properties (strength ~ 300 MPa) compared to E-glass fibre. Phosphate glass fibres are easy to fabricate and exhibit high tensile strength (up to 550 MPa), high tensile modulus (up

to 80 GPa) and controllable degradation rate. The phosphate glass system (P–Ca–Na–Mg–Fe) was investigated with an aim to take advantage of the effect of network modifiers like Ca, Mg and Fe on degradation rate and cytocompatibility of the glasses in conjunction with increasing chain length, attributable to increasing phosphate content, the latter results in an ease of fibre–drawing and stronger fibres [86, 109, 167, 168, 196]. The ratio of bridging to non–bridging oxygen within phosphate glass network was calculated from binding energy peaks of O1s from XPS data and used as an indicator of chain length (Table 3-4). It was found that phosphate glasses containing higher phosphate content demonstrated longer chain lengths. As hypothesised glasses with longer chain lengths were easier to draw into fibres and were found to be stronger when tested with single fibre tensile test which was in agreement with published work [191]. Cytocompatibility examination of phosphate glasses were carried out and it was concluded that all glass formulations demonstrated cytocompatibility in terms of typical cell adhesion, metabolic activity, proliferation, differentiation and normal cell morphology (Figure 3-7 to 3-9). Degradation rates had no effect on cell functions such as adhesion, proliferation and alkaline phosphatase activity; however, degradation products affected alkaline phosphatase activity of cells. Due to time limitations for this project, no identification of degradation products was carried out. However, it is reported in the literature that different glass formulations release different ionic species which were dependent on time scale as well as the size of ionic species. For example, Ahmed *et al.* investigated different ion release (Ca^{++} and Na^+) [85] and different species of phosphate oligomers [87]. It was suggested that phosphate glass with different degradation rate and formulation may release different ionic products in variable amounts, chain length of phosphate oligomer released in the media were proportional

to the amount of phosphate in the glass formulation. Similarly, another study [94] suggested that ionic species and their amounts were dependent on glass formulation and degradation rates. However, no correlation was made between the degradation products and cytocompatibility. A correlation of the results for cytocompatibility acquired in current study and cumulative release of different anionic species from similar glass reported elsewhere was attempted. The species found were represented as orthophosphate, cyclic trimetaphosphate, pyrophosphate and linear polyphosphate. The comparison suggest that with higher phosphate content and faster degradation rate longer chained phosphate oligomers were released which were detrimental for MG63 cells [94]. Results, for the loss of alkaline phosphatase activity with higher phosphate containing glasses in current study are in agreement with the conclusion drawn above.

It is well reported that the rapid loss (>50% within 1st week of immersion in degradation medium) of interfacial integrity due to water ingress may result in premature fracture of composite [1, 158, 254, 255]. The most frequently used methods for surface modifications involve chemical surface treatment of polymer matrix or reinforcement but also to some extent roughening or plasma treatment. Chemical surface treatment is usually done to increase the low surface free energy of glass or ceramic. This is achieved by the creation of polar functional groups such as hydroxyl, carboxyl and amine that make the surface more hydrophilic [256]. Although hydrophilic surfaces provide better adhesion to the polymer, the interface is susceptible to hydrolytic degradation due to water uptake. Hydrolytic degradation of interface could result in catastrophic failure of the composite.

It was hypothesised that strengthening the interface with more hydrophobic chemicals should result in stronger composite with slower loss of mechanical integrity with degradation. Eight different glass-surface treatment agents: glycerol 2-phosphate disodium salt (GP); 3-phosphonopropionic acid (PPA); 3-aminopropyltriethoxy silane (APS); etidronic acid (EA); hexamethylene diisocyanate (HDI); sorbitol/sodium ended PLA-oligomers (S/Na-PLA) and amino phosphonic acid (APA), were selected on the bases of their potential to bind to a phosphate glass surface and/or their reported biocompatibility. Ideally a functional layer on glass surface should provide a strong bridge between glass fibre and polymer matrix through covalent bonding. It is also required that the layer should not hydrolyse easily. Evidence for covalent bonds between the phosphate glass and 3-aminopropyltriethoxy silane, etidronic acid and hexamethylene diisocyanate were found through IR-spectroscopy and XPS, but not the other chemicals tested (Figure 4-4 and 4-5). It was supposed that glycerol 2-phosphate disodium salt, 3-phosphonopropionic acid, sorbitol/sodium ended PLA-oligomers and amino phosphonic acid were linked through hydrogen bond with phosphate glass (Figure 4-10).

It was suggested that the surface treatment agents with greater number of -OH ions (e.g. sorbitol ended PLA-oligomer) improves the interfacial shear strength better than with lower number of -OH ions (e.g. glycerol 2-phosphate disodium salt). Significant improvement (from ~7 MPa to ~22 MPa) in interfacial shear strength was observed with 3-aminopropyltriethoxy silane, etidronic acid, hexamethylene diisocyanate and PLA-oligomers. However, the effect of other surface treatments was comparatively small (2-5 MPa) and disappeared with the exposure to an aqueous

environment, supporting the suggestion that these were linked through hydrogen bond rather than covalent link. The effect of PLA–oligomers on interfacial shear strength and mechanical properties of composite was also disappeared within first three days which was attributed to their hydrophilicity and hydrolysis of hydrogen bonding with phosphate glass. Hydrophobicity was induced with 3–aminopropyltriethoxy silane and hexamethylene diisocyanate treatment and no change in hydrophilicity was observed for etidronic acid treatment. Conversely, glycerol 2–phosphate disodium salt, 3–phosphonopropionic acid and PLA–oligomers treatments resulted in hydrophilic surfaces (Figure 4-9).

The interactions leading to adhesion between two bodies arise from either mechanical retention, interatomic forces acting across the interface due to the formation of covalent and/or ionic bonds and complex formation across the interface [257]. Two major areas of investigation in the field of fibre–matrix adhesion in composite materials are: the fundamental role that fibre–matrix adhesion plays on composite mechanical properties and the method used to measure fibre–matrix adhesion in composite materials. To gauge the interfacial shear strength between glass fibre and polymer matrix, despite the extensive comparative studies [165, 200-207], no standard test has been agreed upon. Therefore, for the purpose of this project, a modified push out test to estimate interfacial shear strength between glass and polymer matrix and the effect of surface chemical treatments on interfacial shear strength was devised. A glass rod pushed out of encircling polymer disc was used as a model to estimate the interfacial shear strength. Although, this model was found reliable and repeatable, it cannot be extrapolated for exact quantity of glass fibre/polymer adhesion strength.

A simple rule of mixtures expression can be used to predict composite properties when the applied load is coincident with the fibre direction. Drazel and Madhukar [255] suggested that fibre–matrix adhesion affects composite properties in different ways depending on the state of stress created at the fibre–matrix interphase. At 0° to the fibre alignment, tensile and compressive strength increases with increasing interfacial shear strength, however no effect on flexural strength can be observed. At 90° the tensile and flexural strengths of the composite increases with increasing interfacial shear strength. A short beam shear test and three point bend test were considered to measure flexural properties of composite and the extent of effect of interface on it. Short beam shear test can determine interlaminar shear strength of parallel fibres with minimal information about flexural strength. However, 3–point bend test was selected for current study because, when applied at 90° to the fibre orientation, 3–point bend test provides the flexural mechanical properties as well as information about contribution of Interfacial shear strength on flexural properties.

Surface treated glasses were screened through a three stage cytocompatibility assessment. Although, some dose dependent toxicity in terms of lower neutral red uptake (Figure 5-1) was observed for PLA–oligomers and hexamethylene diisocyanate, all the surface treatments fell in the category of non–cytotoxic according to definition given in ISO 10993–5. Surface treated phosphate glass did not affect the cellular functions like initial attachment, proliferation, markers of differentiation indicating alkaline phosphatase activity, collagen production and osteocalcin production were not greatly different than untreated phosphate glass or tissue culture polystyrene. Normal osteoblastic morphology was also maintained on all tested surfaces, as observed by SEM (Figure 5-9 to 5-15).

Collective analysis of the results obtained for interfacial shear strength, surface wettability and cytocompatibility helped to decide on four to be employed in composites; 3-aminopropyltriethoxy silane, etidronic acid, sorbitol ended PLA-oligomer and hexamethylene diisocyanate. P45Fe4 glass fibres treated with optimised concentrations of surface treatments before being sandwiched between PLA layers and pressed. Phosphate glass fibres treated were found severely corroded when treated with etidronic acid (Figure 6-4 and 6-5), therefore, excluded from the study. Fibre reinforced composites can be prepared with different fibre arrangements (short/random fibre, long unidirectional, woven fibre). Each arrangement has its own advantages and disadvantages. For the purpose of this project, two different types of phosphate glass fibre reinforced PLA composites (short/random non-woven and unidirectional) were produced. The effect of fibre length, strength, orientation and volume fraction are well known to affect the properties of a composite [258-260]. Felfel *et al.* [23] reported ~10-15 higher flexural properties for unidirectional phosphate glass fibre compared to random short phosphate glass fibre reinforced PLA composites. It was also reported that the unidirectional reinforced composite absorbed greater amount (0.2 % more than random) of water due to insufficient wetting of phosphate glass fibre with PLA [261]. It is also known that fibre volume fraction is directly proportional to water uptake and composite strength [262]. Therefore, relatively lower flexural properties were found for random/non-woven fibre reinforced PLA composite (Figure 6-2) compared to unidirectional phosphate glass fibre reinforced composites (Figure 6-3). Initial mechanical properties of 3-aminopropyltriethoxy silane and sorbitol ended PLA-oligomer treated unidirectional phosphate glass fibre composite were significantly higher (~20 MPa) than control composite, reflecting the effect of stronger interface due to the glass

fibre surface treatment. Conversely, samples treated with hexamethylene diisocyanate, the most effective in terms of interfacial shear strength, showed relatively lower (~5 MPa) flexural strength and modulus (~1 GPa) which was believed to be due to the chemical attack of the phosphate glass fibre during the hexamethylene diisocyanate grafting process, which involved 15 minutes exposure to distilled water. 3-aminopropyltriethoxy silane and hexamethylene diisocyanate treated composites did slow down the loss of mechanical integrity of the composites (Figure 6-11 and 6-12). Sorbitol ended PLA-oligomer treated samples lost the mechanical integrity after 14 days in PBS at 37 °C. SEM images (Figure 6-7 and 6-8) of samples treated with 3-aminopropyltriethoxy silane and hexamethylene diisocyanate revealed relatively unbroken interface while sorbitol ended PLA-oligomer treated sample and control lost the interfacial integrity. Degradation rate of hexamethylene diisocyanate, 3-aminopropyltriethoxy silane and sorbitol ended PLA-oligomer treated phosphate glass (Figure 4-8) correlates with the rate of water uptake for the composite prepared with the same surface treatments (Figure 6-9). Water uptake plays a major role in interfacial integrity loss which results in loss of mechanical integrity of a composite [23, 24, 140].

Human osteoblasts cultured on composite samples revealed no significant difference between composite samples and control in terms of cell functions (attachment, proliferation and differentiation) and morphology (Figure 6-13 to 6-19). However, it should be considered here that cells were exposed to three completely different degradation products of phosphate glass fibre, surface chemical agents and polylactic acid. A synergy was expected that acidic degradation products from polylactic acid may increase the degradation rate of glass fibre and/or react with the layer.

Potentially hexamethylene diamine could be leached as a result of hexamethylene diisocyanate reaction with lactic acid. Results from cytocompatibility study suggested that all three phases and their degradation products were compatible with cells even after long term exposure.

The targets set before starting this project have been achieved to a degree. A comparison of results obtained for flexural mechanical properties and its retention in this study to the similar reports [1, 23, 24, 27, 140, 158-160, 254] clearly indicates that a stronger composite with greater ability to retain its mechanical integrity has been produced. Despite all the variations of fibre volume fraction, polymer matrix choice, and fibre type; the maximum initial flexural strength values of ~80 MPa to ~200 MPa and flexural/tensile modulus values of ~5 GPa to 30 GPa has been reported by various authors [1, 23, 24, 27, 140, 158-160]. These values were decreased to 40 MPa to 50 MPa and 1.2 GPa to 15 GPa strength and modulus respectively after approximately 4 weeks of degradation *in vitro*. The composite produced in this study were found to have initial flexural strengths and moduli in the range of 200 MPa to 300 MPa and 22 GPa to 25 GPa respectively. After four weeks of degradation at 37 °C in phosphate buffered saline the best composite (hexamethylene diisocyanate–modified unidirectional phosphate glass fibre reinforced PLA) was found to have 105 MPa strength and 16 GPa modulus in bending. The initial improvement was attributed to superior fibre strengths, compared to the one reported in literature [86, 109, 167, 168, 196], as well as improved interfacial shear strength. The retention of mechanical integrity was attributed to better interfacial shear strength as well as hydrophobicity of the interface. With all the improvements achieved, mechanical properties of composite

are still closer to the lower limits of the targeted mechanical properties. Therefore, further improvement in terms of fibre tensile properties, polymer choice (more hydrophobic and strong), fibre volume fraction, treatment and composite design are required.

7.2 Conclusions

The following conclusions can be made from the work carried out for this thesis:

Phosphate based glasses containing higher content (~45 to 50 molar percent) P_2O_5 possess long chain lengths and therefore can be drawn into continuous fibres. However, phosphate glass containing higher amounts of P_2O_5 can be disadvantageous for cellular functions as the inorganic phosphate known to be detrimental for cell functions. By adding 4–5% Fe_2O_3 into the quinary glass system the degradation rate of the glass can be reduced without significantly affecting the structure (chain length) of phosphate glass. After certain level of durability is achieved degradation products do not play a major role on cell functions. There is a requirement of correlation between a range of glass desolution rates and cell activities to define a threshold of degradation rate effective on cell functions.

A chemical agent (e.g. 3-aminopropyltriethoxy silane, hexamethylene diisocyanate, and etidronic acid) able to bind with phosphate glass covalently and also has the other functional group to make covalent bond with polymer, can improve the interfacial shear strength significantly. Of the surface treatments tested, covalently linked chemicals with phosphate glass can also improve the hydrophobicity of the glass surface. If a chemical reagent attaches with phosphate glass through hydrogen bonding (e.g. phosphonopropionic acid, glycerol phosphate, and sorbitol ended-PLA oligomer), the effectiveness of on interfacial shear strength will be proportional to the number $-OH$ ions present on glass surface. However, this effect is susceptible to aqueous environment. Also, because of their hygroscopic nature phosphonopropionic

acid, glycerol phosphate and sorbitol ended-PLA oligomer made the glass surface more hydrophilic.

All the surface treatments used in this study were found to be cytocompatible i.e. did not affect the cellular functions negatively. Improvement in interfacial shear strength due to surface treatments (3-aminopropyltriethoxy silane, hexamethylene diisocyanate, and sorbitol ended-PLA oligomer) can improve initial flexural mechanical properties and hydrophobicity at the interface (3-aminopropyltriethoxy silane and hexamethylene diisocyanate) can slow down the mechanical integrity loss

Therefore, finally it can be concluded that; phosphate based glass fibre reinforced polymer composite can be prepared with a strength and modulus comparable to the cortical bone and that a sufficient mechanical integrity can be maintained for an extended period of time if a surface chemical layer (coupling agent, compatibiliser or surface graft), providing covalent bonding and hydrophobicity, is used to improve and maintain the interfacial shear strength between phosphate glass fibre and polymer matrix.

7.3 Recommendations for Future Work

The work carried out over past three years and current knowledge of totally resorbable glass fibre reinforced polymer composite for bone fracture fixation applications can be progressed on following recommendations:

By changing the chemistry of phosphate glass, more durable, continuous fibres can be drawn and woven phosphate glass fibre reinforced composite can be prepared. Effect for addition of trivalent cation (iron content) on degradation rate of phosphate glass was investigated as a part of this project. More interesting trivalent cations such as Ti^{3+} , B^{3+} and Sr^{3+} should be investigated for their effect on degradation and cytocompatibility along with structural changes of phosphate glass. It is expected that these modifiers would help in terms of cytocompatibility/bioactivity (Ti^{3+} and Sr^{3+}) [95, 96, 263] and/or degradation, density (B^{3+}) and fibre drawing (B^{3+}).

The push-out test devised to estimate interfacial shear strength between glass and polymer, in its current state, cannot be applied directly to glass fibre and polymer matrix interfacial shear strength. Further modifications such as using thicker fibres (~100 μ m), embedding in thinner polymer disc would be more applicable. Glass fibre can be pushed out by a micro-indenter style setup with continuous compressive force.

Due to susceptibility of surface treatment layer to water, interfacial shear strength of modified push out samples should also be investigated with degradation *in vitro*.

Biochemical agents such as 3-aminopropyltriethoxy silane, etidronic acid and hexamethylene diisocyanate should be used to ensure a covalent bridge between polymer matrix and reinforcing fibres. However, surface treatments such as sorbitol

ended PLA–oligomer or glycerol phosphate can be employed if the composite is made out of hydrophobic polymer such as poly–caprolactone.

The results showed that cytocompatible bisphosphonates are effective on improving interfacial shear strength and hydrophobicity. However, due to corrosive behaviour of etidronic acid and time restriction etidronic acid treated composite could not be prepared successfully. It is suggested here that reaction conditions (concentration, exposure time, curing temperature etc) for etidronic acid and other bisphosphonates such as alendronate, and pamidronate should be optimised and investigated further. Bisphosphonates and other water susceptible compounds can also be used within partially degradable composites (e.g. PLA or PCL reinforced with bioglass or hydroxyl apatite fibres).

On the basis of our results and current knowledge about the mechanism of mechanical integrity loss which suggests that in addition to loss of interfacial integrity, polymer swelling also plays a major role which can be avoided by using a strong but hydrophobic degradable polymer as the matrix material. A blend or copolymer of polylactic acid, PGA and PCL could possibly achieve this. Encapsulating the glass fibre reinforced polylactic acid composite within a hydrophobic/slow degrading polymer could also slow down the water uptake and hence slow down the loss of the interfacial integrity. Finally, to ensure tissue–compatibility of treated composites an in–vivo study is recommended.

References

- [1] Andriano, K. P., Daniels, A. U., and Heller, J. (1992). "Biocompatibility and mechanical properties of a totally absorbable composite material for orthopaedic fixation devices", *Journal of Applied Biomaterials*, Vol. 3(3), p. 197-206.
- [2] Ratner, B. D., Hoffman, Allan S., Schoen, Frederick J., Lemons, Jack E. , (2004), *Biomaterials Science : An Introduction to Materials in Medicine* Biomaterials Science : An Introduction to Materials in Medicine, Elsevier Academic Press, San Diego, Calif. ; London
- [3] David F, W. (2008). "On the mechanisms of biocompatibility", *Biomaterials*, Vol. 29(20), p. 2941-2953.
- [4] Pietrzak, W. S., Sarver, D., and Verstynen, M. (1996). "Bioresorbable implants -- practical considerations", *Bone*, Vol. 19(1, Supplement 1), p. S109-S119.
- [5] Giori, N. J., Ryd, L., and Carter, D. R. (1995). "Mechanical influences on tissue differentiation at bone—cement interfaces", *The Journal of Arthroplasty*, Vol. 10(4), p. 514-522.
- [6] Ramsay, S. D., Pilliar, R. M., and Santerre, J. P. (2010). "Fabrication of a biodegradable calcium polyphosphate/polyvinyl-urethane carbonate composite for high load bearing osteosynthesis applications", *Journal of Biomedical Materials Research Part B: Applied Biomaterials*, Vol. 94B(1), p. 178-186.
- [7] Ramsay, S., Pilliar, R., Yang, L., and Santerre, J. (2005). "Calcium Polyphosphate/Polyvinyl acid-carbonate Copolymer Based Composites for use in Biodegradable Load-bearing Composites for Orthopaedic Implant Fabrication", *Key Engineering Materials*, Vol. 284-286 ((2005)), p. 787-790.
- [8] Bleach, N. C., Tanner, K. E., Kellomäki, M., and Törmälä, P. (2001). "Effect of filler type on the mechanical properties of self-reinforced polylactide–calcium phosphate composites", *Journal of Materials Science: Materials in Medicine*, Vol. 12(10), p. 911-915.

- [9] Viljanen, J., Pihlajamäki, H., Kinnunen, J., Bondestam, S., and Rokkanen, P. (2001). "Comparison of absorbable poly-L-lactide and metallic intramedullary rods in the fixation of femoral shaft osteotomies: an experimental study in rabbits.", *Journal of Orthopaedic Science*, Vol. 6(2), p. 160-166.
- [10] Törmälä, P., Pohjonen, T., and Rokkanen, P. (1998). "Bioabsorbable polymers: Materials technology and surgical applications", *Proceedings of the Institution of Mechanical Engineers, Part H: Journal of Engineering in Medicine*, Vol. 212(2), p. 101-111.
- [11] Rokkanen, P., Bostman, O., Vainionpää, Makela, E. A., Hirvensalo, E., Partio, E. K., Vihtonen, K., Patiala, H., and Tormala, P. (1996). "Absorbable Devices in the Fixation of Fractures", *The Journal of Trauma*, Vol. 40(3S), p. 123S-127S.
- [12] Christel, P., Chabot, F., Leray, J., Morin, C., and Vert, M., (1980), *Advances in Biomaterials*, Biomaterials, John Wiley and Sons, New York, Biodegradable composites for internal fixation.
- [13] Törmälä, P. (1992). "Biodegradable self-reinforced composite materials; Manufacturing structure and mechanical properties", *Clinical Materials*, Vol. 10(1-2), p. 29-34.
- [14] Pihlajamäki, H., Bostman, O., Hirvensalo, E., Tormala, P., and Rokkanen, P. (1992). "Absorbable pins of self-reinforced poly-L-lactic acid for fixation of fractures and osteotomies", *J Bone Joint Surg Br*, Vol. 74-B(6), p. 853-857.
- [15] Rähkä, J. E., Axelson, P., Skutnabb, K., Rokkanen, P., and Törmälä, P. (1993). "Fixation of cancellous bone and physal fractures with biodegradable rods of self-reinforced polylactic acid", *Journal of Small Animal Practice*, Vol. 34(3), p. 131-138.
- [16] Navarro, M., Michiardi, A., Castaño, O., and Planell, J. A. (2008). "Biomaterials in orthopaedics", *Journal of The Royal Society Interface*, Vol. 5(27), p. 1137-1158.
- [17] Reilly, D. T., and Burstein, A. H. (1974). "The Mechanical Properties of Cortical Bone", *The Journal of Bone and Joint Surgery*, Vol. 56, p. 22.

- [18] Reilly, D. T., Burstein, A. H., and Frankel, V. H. (1974). "The elastic modulus for bone", *Journal of Biomechanics*, Vol. 7(3), p. 271-275.
- [19] Rho, J.-Y., Kuhn-Spearing, L., and Zioupos, P. (1998). "Mechanical properties and the hierarchical structure of bone", *Medical Engineering & Physics*, Vol. 20(2), p. 92-102.
- [20] Törmälä, P., Vasenius, J., Vainionpää, S., Laiho, J., Pohjonen, T., and Rokkanen, P. (1991). "Ultra-high-strength absorbable self-reinforced polyglycolide (SR-PGA) composite rods for internal fixation of bone fractures: In vitro and in vivo study", *Journal of Biomedical Materials Research*, Vol. 25(1), p. 1-22.
- [21] Enislidis, G., Lagogiannis, G., Wittwer, G., Glaser, C., and Ewers, R. (2005). "Fixation of zygomatic fractures with a biodegradable copolymer osteosynthesis system: short- and long-term results", *International Journal of Oral and Maxillofacial Surgery*, Vol. 34(1), p. 19-26.
- [22] Lin, T. C. (1986). "Totally absorbable fiber reinforced composite for internal fracture fixation devices", *Trans soc biomaterials*, Vol. 9.
- [23] Felfel, R. M., Ahmed, I., Parsons, A. J., Haque, P., Walker, G. S., and Rudd, C. D. (2010). "Investigation of Crystallinity, Molecular Weight Change, and Mechanical Properties of PLA/PBG Bioresorbable Composites as Bone Fracture Fixation Plates", *Journal of Biomaterials Applications*.
- [24] Felfel, R. M., Ahmed, I., Parsons, A. J., Walker, G. S., and Rudd, C. D. (2011). "In vitro degradation, flexural, compressive and shear properties of fully bioresorbable composite rods", *Journal of the Mechanical Behavior of Biomedical Materials*, Vol. 4(7), p. 1462-1472.
- [25] Haque, P., Barker, I. A., Parsons, A., Thurecht, K. J., Ahmed, I., Walker, G. S., Rudd, C. D., and Irvine, D. J. (2010). "Influence of compatibilizing agent molecular structure on the mechanical properties of phosphate glass fiber-reinforced PLA composites", *Journal of Polymer Science Part A: Polymer Chemistry*, Vol. 48(14), p. 3082-3094.

- [26] Haque, P., Parsons, A. J., Barker, I. A., Ahmed, I., Irvine, D. J., Walker, G. S., and Rudd, C. D. (2010). "Interfacial properties of phosphate glass fibres/PLA composites: Effect of the end functionalities of oligomeric PLA coupling agents", *Composites Science and Technology*, Vol. 70(13), p. 1854-1860.
- [27] Khan, R. A., Khan, M. A., Sultana, S., Nuruzzaman Khan, M., Shubhra, Q. T. H., and Noor, F. G. (2010). "Mechanical, Degradation, and Interfacial Properties of Synthetic Degradable Fiber Reinforced Polypropylene Composites", *Journal of Reinforced Plastics and Composites*, Vol. 29(3), p. 466-476.
- [28] Khan, R. A., Parsons, A. J., Jones, I. A., Walker, G. S., and Rudd, C. D. (2011). "Interfacial Properties of Phosphate Glass Fiber/Poly(caprolactone) System Measured Using the Single Fiber Fragmentation Test", *Composite Interfaces*, Vol. 18(1), p. 77-90.
- [29] Rho, J. Y., Ashman, R. B., and Turner, C. H. (1993). "Young's modulus of trabecular and cortical bone material: Ultrasonic and microtensile measurements", *Journal of Biomechanics*, Vol. 26(2), p. 111-119.
- [30] Marks Sandy C. , a. H., Donna C. , (1996), *Principles of Bone Biology* Academic Press, Toronto, The structure and development of bone.
- [31] Hancox, N. M., (1972), *Biology of Bone*, Cambridge University Press, New York., Section 1. Historical and Descriptive.
- [32] Noor, Z., Sutiman B Sumitro, Mohammad Hidayat, Agus Hadian Rahim, and Ahmad Taufiq (2011). "Assessment of microarchitecture and crystal structure of hydroxyapatite in osteoporosis", *Universa Medicina*, Vol. 30(1), p. 7.
- [33] Einhorn, A. T., (1996), *Principles of Bone Biology* Academic Press, Toronto, Biomechanics of Bone.
- [34] SEER (2011). "Compact bone & spongy bone", U.S. National Cancer Institute's Surveillance, Epidemiology and End Results (SEER) Program p. Compact bone & spongy bone schematic.

- [35] Ross, F. P., and Asbmr, (2009), Primer on the Metabolic Bone Diseases and Disorders of Mineral Metabolism, John Wiley & Sons, Inc., Chapter 3. Osteoclast Biology and Bone Resorption.
- [36] Baron, R., (2009), Primer on the Metabolic Bone Diseases and Disorders of Mineral Metabolism, John Wiley & Sons, Inc., Washington, DC, General Principles of Bone Biology.
- [37] Thorsten. Schinkle, and Gerad. Karsent, (1996), Principles of Bone Biology Academic Press, Toronto, Transcriptional Control of Osteoblast Differentiation and Function.
- [38] Lian, J. B., Stein, G. S., and Aubin, J. E., (2009), Primer on the Metabolic Bone Diseases and Disorders of Mineral Metabolism, John Wiley & Sons, Inc., Washington, DC, Bone formation: maturation and functional activities of osteoblast lineage cells.
- [39] Burger, E. H., and Klein-Nulend, J. (1999). "Responses of Bone Cells to Biomechanical Forces in Vitro", Advances in Dental Research, Vol. 13(1), p. 93-98.
- [40] Lanyon, L. E. (1993). "Osteocytes, strain detection, bone modeling and remodeling", Calcified Tissue International, Vol. 53(0), p. S102-S107.
- [41] IOF (2011). "Cells concerned with the production, maintenance and modelling of the osteoid", The International Osteoporosis Foundation (IOF) programme.
- [42] Denizard, O. R., (2005), "Biocompatibility Studies of Human Fetal Osteoblast Cells Cultured on Gamma Titanium Aluminide", MSc Thesis, univerisity of Puerto Rico Mayagüez campus,
- [43] Mitton, D., Rumelhart, C., Hans, D., and Meunier, P. J. (1997). "The effects of density and test conditions on measured compression and shear strength of cancellous bone from the lumbar vertebrae of ewes", Medical Engineering & Physics, Vol. 19(5), p. 464-474.

- [44] Kuhn, J. L., Goldstein, S. A., Choi, R., London, M., Feldkamp, L. A., and Matthews, L. S. (1989). "Comparison of the trabecular and cortical tissue moduli from human iliac crests", *Journal of Orthopaedic Research*, Vol. 7(6), p. 876-884.
- [45] Brear, K., Currey, J. D., Raines, S., and Smith, K. J., (1988), *Density and temperature effects on some mechanical properties of cancellous bone*, Institution of Mechanical Engineers, London, ROYAUME-UNI.
- [46] Ko, R., 1953, "The tension test upon the compact substance of the long bones of human extremities", Technical Report No. Kyoto Prefectural University of Medicine, Kyoto.
- [47] Dempster, W. T., and Liddicoat, R. T. (1952). "Compact bone as a non-isotropic material", *American Journal of Anatomy*, Vol. 91(3), p. 331-362.
- [48] Yokoo, S., 1952, "The Compression Test Upon the Diaphysis and the Compact Substance of the Long Bones of Human Extremities", Technical Report No. Kyoto Prefectural University of Medicine, Koyoto.
- [49] Chalmers, J., and Weaver, J. K. (1966). "Cancellous Bone: Its Strength and Changes with Aging and an Evaluation of Some Methods for Measuring Its Mineral Content II. AN EVALUATION OF SOME METHODS FOR MEASURING OSTEOPOROSIS", *The Journal of Bone & Joint Surgery*, Vol. 48(2), p. 299-308.
- [50] FDA (1996). "Guidance Document for Testing Biodegradable Polymer Implant Devices ", Vol. April, p. 7.
- [51] Smith, G., (1985), *Text Book of Small Animal Orthopaedics*, J.B. Lippincott, Orthopaedic Biomaterials.
- [52] Boyan, B. D., Hummert, T. W., Dean, D. D., and Schwartz, Z. (1996). "Role of material surfaces in regulating bone and cartilage cell response", *Biomaterials*, Vol. 17(2), p. 137-146.

- [53] Joshua J. Jacobs, Jeremy L. Gilbert, and Robert M. Urban (1998). "Current concepts review : Corrosion of metal orthopaedic implants", *The Journal of Bone & Joint Surgery.*, Vol. 80(2), p. 268-282.
- [54] Hansen, D. C. (2008). "Metal Corrosion in the Human Body: The Ultimate Bio-Corrosion Scenario", *The Electrochemical Society Interface*, Vol. 17, p. 5.
- [55] Black, J. (1988). "Does corrosion matter?", *J Bone Joint Surg Br*, Vol. 70-B(4), p. 517-520.
- [56] Brettle, J. (1970). "A survey of the literature on metallic surgical implants", *Injury*, Vol. 2(1), p. 26-39.
- [57] Peltier, L. F. (1980). "Materials and Orthopaedic Surgery", *JAMA: The Journal of the American Medical Association*, Vol. 243(15), p. 1574-1575.
- [58] Heimke, G., and Griss, P. (1980). "Ceramic implant materials", *Medical and Biological Engineering and Computing*, Vol. 18(4), p. 503-510.
- [59] Thamaraiselvi, T. V., and Rajeswari, S. (2004). "Biological Evaluation of Bioceramic Materials - A Review", *Trends Biomater. Artif. Organs*, , Vol. 18(1), p. 9.
- [60] Furlong, R., and Osborn, J. (1991). "Fixation of hip prostheses by hydroxyapatite ceramic coatings", *J Bone Joint Surg Br*, Vol. 73-B(5), p. 741-745.
- [61] (IARC), I. A. f. R. o. C. (1999). "Evaluation of cancer risks to humans: Surgical implants and other foreign bodies. ", *IARC Monographs*, Vol. 74.
- [62] Langer, R., and Tirrell, D. A. (2004). "Designing materials for biology and medicine", *Nature*, Vol. 428(6982), p. 487-492.
- [63] Ignatius, A. A., and Claes, L. E. (1996). "In vitro biocompatibility of bioresorbable polymers: poly(L, DL-lactide) and poly(L-lactide-co-glycolide)", *Biomaterials*, Vol. 17(8), p. 831-839.

- [64] Claes, L. E., Ignatius, A. A., Rehm, K. E., and Scholz, C. (1996). "New bioresorbable pin for the reduction of small bony fragments: design, mechanical properties and in vitro degradation", *Biomaterials*, Vol. 17(16), p. 1621-1626.
- [65] Shelby, J. E., (2005), *Introduction to Glass Science and Technology* Royal Society of Chemistry, Cambridge, Introduction.
- [66] Hench, L. (2006). "The story of Bioglass[®]", *Journal of Materials Science: Materials in Medicine*, Vol. 17(11), p. 967-978.
- [67] Cao, W., and Hench, L. L. (1996). "Bioactive materials", *Ceramics International*, Vol. 22(6), p. 493-507.
- [68] Hench, L. L., and Paschall, H. A. (1973). "Direct chemical bond of bioactive glass-ceramic materials to bone and muscle", *Journal of Biomedical Materials Research*, Vol. 7(3), p. 25-42.
- [69] Wazer, J. R. V. (1950). "Structure and Properties of the Condensed Phosphates. III. Solubility Fractionation and Other Solubility Studies", *Journal of the American Chemical Society*, Vol. 72(2), p. 647-655.
- [70] Van Wazer, J. R., and Callis, C. F. (1958). "Metal Complexing By Phosphates", *Chemical Reviews*, Vol. 58(6), p. 1011-1046.
- [71] Van Wazer, J. R., Griffith, E. J., and McCullough, J. F. (1955). "Structure and Properties of the Condensed Phosphates. VII. Hydrolytic Degradation of Pyro- and Tripolyphosphate", *Journal of the American Chemical Society*, Vol. 77(2), p. 287-291.
- [72] Wazer, J. R. V. (2002). "Structure and Properties of the Condensed Phosphates. II. A Theory of the Molecular Structure of Sodium Phosphate Glasses¹", *Journal of the American Chemical Society*, Vol. 72(2), p. 644-647.
- [73] Wazer, J. R. V., and Campanella, D. A. (1950). "Structure and Properties of the Condensed Phosphates. IV. Complex Ion Formation in Polyphosphate Solutions", *Journal of the American Chemical Society*, Vol. 72(2), p. 655-663.

- [74] Brow, R. K. (2000). "Review: the structure of simple phosphate glasses", *Journal of Non-Crystalline Solids*, Vol. 263-264, p. 1-28.
- [75] Brow, R. K., Click, C. A., and Alam, T. M. (2000). "Modifier coordination and phosphate glass networks", *Journal of Non-Crystalline Solids*, Vol. 274(1-3), p. 9-16.
- [76] Brow, R. K., Kirkpatrick, R. J., and Turner, G. L. (1990). "The short range structure of sodium phosphate glasses I. MAS NMR studies", *Journal of Non-Crystalline Solids*, Vol. 116(1), p. 39-45.
- [77] Rashchi, F., and Finch, J. A. (2000). "Polyphosphates: A review their chemistry and application with particular reference to mineral processing", *Minerals Engineering*, Vol. 13(10-11), p. 1019-1035.
- [78] Hoppe, U. (1996). "A structural model for phosphate glasses", *Journal of Non-Crystalline Solids*, Vol. 195(1-2), p. 138-147.
- [79] Kirkpatrick, R. J., and Brow, R. K. (1995). "Nuclear magnetic resonance investigation of the structures of phosphate and phosphate-containing glasses: a review", *Solid State Nuclear Magnetic Resonance*, Vol. 5(1), p. 9-21.
- [80] Martin, S. W. (1991). "Ionic Conduction in Phosphate Glasses", *Journal of the American Ceramic Society*, Vol. 74(8), p. 1767-1784.
- [81] Gresch, R., Müller-Warmuth, W., and Dutz, H. (1979). "X-ray photoelectron spectroscopy of sodium phosphate glasses", *Journal of Non-Crystalline Solids*, Vol. 34(1), p. 127-136.
- [82] Franks, K., Abrahams, I., Georgiou, G., and Knowles, J. C. (2001). "Investigation of thermal parameters and crystallisation in a ternary CaO–Na₂O–P₂O₅-based glass system", *Biomaterials*, Vol. 22(5), p. 497-501.
- [83] Franks, K., Abrahams, I., and Knowles, J. C. (2000). "Development of soluble glasses for biomedical use Part I: In vitro solubility measurement", *Journal of Materials Science: Materials in Medicine*, Vol. 11(10), p. 609-614.

- [84] Salih, V., Franks, K., James, M., Hastings, G. W., Knowles, J. C., and Olsen, I. (2000). "Development of soluble glasses for biomedical use Part II: The biological response of human osteoblast cell lines to phosphate-based soluble glasses", *Journal of Materials Science: Materials in Medicine*, Vol. 11(10), p. 615-620.
- [85] Ahmed, I., Lewis, M., Olsen, I., and Knowles, J. C. (2004). "Phosphate glasses for tissue engineering: Part 1. Processing and characterisation of a ternary-based P₂O₅-CaO-Na₂O glass system", *Biomaterials*, Vol. 25(3), p. 491-499.
- [86] Ahmed, I., Lewis, M., Olsen, I., and Knowles, J. C. (2004). "Phosphate glasses for tissue engineering: Part 2. Processing and characterisation of a ternary-based P₂O₅-CaO-Na₂O glass fibre system", *Biomaterials*, Vol. 25(3), p. 501-507.
- [87] Ahmed, I., Lewis, M. P., Nazhat, S. N., and Knowles, J. C. (2005). "Quantification of Anion and Cation Release from a Range of Ternary Phosphate-based Glasses with Fixed 45 mol% P₂O₅", *Journal of Biomaterials Applications*, Vol. 20(1), p. 65-80.
- [88] Knowles, J. C., Franks, K., and Abrahams, I. (2001). "Investigation of the solubility and ion release in the glass system K₂O-Na₂O-CaO-P₂O₅", *Biomaterials*, Vol. 22(23), p. 3091-3096.
- [89] Franks, K., Salih, V., Knowles, J. C., and Olsen, I. (2002). "The effect of MgO on the solubility behavior and cell proliferation in a quaternary soluble phosphate based glass system", *Journal of Materials Science: Materials in Medicine*, Vol. 13(6), p. 549-556.
- [90] Abou Neel, E., and Knowles, J. (2008). "Physical and biocompatibility studies of novel titanium dioxide doped phosphate-based glasses for bone tissue engineering applications", *Journal of Materials Science: Materials in Medicine*, Vol. 19(1), p. 377-386.
- [91] Abou Neel, E., O'Dell, L., Smith, M., and Knowles, J. (2008). "Processing, characterisation, and biocompatibility of zinc modified metaphosphate based glasses for biomedical applications", *Journal of Materials Science: Materials in Medicine*, Vol. 19(4), p. 1669-1679.

- [92] Abou Neel, E. A., Ahmed, I., Blaker, J. J., Bismarck, A., Boccaccini, A. R., Lewis, M. P., Nazhat, S. N., and Knowles, J. C. (2005). "Effect of iron on the surface, degradation and ion release properties of phosphate-based glass fibres", *Acta Biomaterialia*, Vol. 1(5), p. 553-563.
- [93] Abou Neel, E. A., Ahmed, I., Pratten, J., Nazhat, S. N., and Knowles, J. C. (2005). "Characterisation of antibacterial copper releasing degradable phosphate glass fibres", *Biomaterials*, Vol. 26(15), p. 2247-2254.
- [94] Abou Neel, E. A., Chrzanowski, W., and Knowles, J. C. (2008). "Effect of increasing titanium dioxide content on bulk and surface properties of phosphate-based glasses", *Acta Biomaterialia*, Vol. 4(3), p. 523-534.
- [95] Abou Neel, E. A., Mizoguchi, T., Ito, M., Bitar, M., Salih, V., and Knowles, J. C. (2007). "In vitro bioactivity and gene expression by cells cultured on titanium dioxide doped phosphate-based glasses", *Biomaterials*, Vol. 28(19), p. 2967-2977.
- [96] Abou Neel, E. A., Chrzanowski, W., Pickup, D. M., O'Dell, L. A., Mordan, N. J., Newport, R. J., Smith, M. E., and Knowles, J. C. (2009). "Structure and properties of strontium-doped phosphate-based glasses", *Journal of The Royal Society Interface*, Vol. 6(34), p. 435-446.
- [97] Sales, B. C., and Boatner, L. A. (1984). "Lead phosphate glass as a stable medium for the immobilization and disposal of high-level nuclear waste", *Materials Letters*, Vol. 2(4, Part B), p. 301-304.
- [98] Jager, H.-J. D., and Heyns, A. M. (1998). "Study of the Hydrolysis of Sodium Polyphosphate in Water Using Raman Spectroscopy", *Appl. Spectrosc.*, Vol. 52(6), p. 808-814.
- [99] Bunker, B. C., Arnold, G. W., and Wilder, J. A. (1984). "Phosphate glass dissolution in aqueous solutions", *Journal of Non-Crystalline Solids*, Vol. 64(3), p. 291-316.

- [100] Rinehart, J. D., Taylor, T. D., Tian, Y., and Latour, R. A. (1999). "Real-time dissolution measurement of sized and unsized calcium phosphate glass fibers", *Journal of Biomedical Materials Research*, Vol. 48(6), p. 833-840.
- [101] Brauer, D. S., Rüssel, C., Li, W., and Habelitz, S. (2006). "Effect of degradation rates of resorbable phosphate invert glasses on in vitro osteoblast proliferation", *Journal of Biomedical Materials Research Part A*, Vol. 77A(2), p. 213-219.
- [102] Cozien-Cazuc, S., Parsons, A. J., Walker, G. S., Jones, I. A., and Rudd, C. D. (2009). "Real-time dissolution of P₄₀Na₂₀Ca₁₆Mg₂₄ phosphate glass fibers", *Journal of Non-Crystalline Solids*, Vol. 355(50-51), p. 2514-2521.
- [103] Parsons, A. J., Burling, L. D., Scotchford, C. A., Walker, G. S., and Rudd, C. D. (2006). "Properties of sodium-based ternary phosphate glasses produced from readily available phosphate salts", *Journal of Non-Crystalline Solids*, Vol. 352(50-51), p. 5309-5317.
- [104] Strohner, P., Sarrach, D., Reich, J. G., Day, D. E., Yu, X., Long, G. J., and Brow, R. K. (1997). "Properties and structure of sodium-iron phosphate glasses", *Journal of Non-Crystalline Solids*, Vol. 215(1), p. 21-31.
- [105] Fang, X., Ray, C. S., Marasinghe, G. K., and Day, D. E. (2000). "Properties of mixed Na₂O and K₂O iron phosphate glasses", *Journal of Non-Crystalline Solids*, Vol. 263-264(0), p. 293-298.
- [106] Ahmed, I., Parsons, A., Jones, A., Walker, G., Scotchford, C., and Rudd, C. (2010). "Cytocompatibility and Effect of Increasing MgO Content in a Range of Quaternary Invert Phosphate-based Glasses", *Journal of Biomaterials Applications*, Vol. 24(6), p. 555-575.
- [107] Suzuya, K., Price, D. L., Loong, C. K., and Kohara, S. "The structure of magnesium phosphate glasses", *Journal of Physics and Chemistry of Solids*, Vol. 60(8-9), p. 1457-1460.

- [108] Walter, G., Vogel, J., Hoppe, U., and Hartmann, P. (2001). "The structure of CaO–Na₂O–MgO–P₂O₅ invert glass", *Journal of Non-Crystalline Solids*, Vol. 296(3), p. 212-223.
- [109] Ahmed, I., Collins, C. A., Lewis, M. P., Olsen, I., and Knowles, J. C. (2004). "Processing, characterisation and biocompatibility of iron-phosphate glass fibres for tissue engineering", *Biomaterials*, Vol. 25(16), p. 3223-3232.
- [110] Bitar, M., Salih, V., Mudera, V., Knowles, J. C., and Lewis, M. P. (2004). "Soluble phosphate glasses: in vitro studies using human cells of hard and soft tissue origin", *Biomaterials*, Vol. 25(12), p. 2283-2292.
- [111] Gough, J. E., Christian, P., Scotchford, C. A., and Jones, I. A. (2003). "Long-term craniofacial osteoblast culture on a sodium phosphate and a calcium/sodium phosphate glass", *Journal of Biomedical Materials Research Part A*, Vol. 66A(2), p. 233-240.
- [112] Gough, J. E., Christian, P., Scotchford, C. A., Rudd, C. D., and Jones, I. A. (2002). "Synthesis, degradation, and in vitro cell responses of sodium phosphate glasses for craniofacial bone repair", *Journal of Biomedical Materials Research*, Vol. 59(3), p. 481-489.
- [113] Melba, N., Maria-Pau, G., and Josep, A. P. (2003). "Cellular response to calcium phosphate glasses with controlled solubility", *Journal of Biomedical Materials Research Part A*, Vol. 67A(3), p. 1009-1015.
- [114] Parsons, A. J., Evans, M., Rudd, C. D., and Scotchford, C. A. (2004). "Synthesis and degradation of sodium iron phosphate glasses and their in vitro cell response", *Journal of Biomedical Materials Research Part A*, Vol. 71A(2), p. 283-291.
- [115] Skelton, K. L., Glenn, J. V., Clarke, S. A., Georgiou, G., Valappil, S. P., Knowles, J. C., Nazhat, S. N., and Jordan, G. R. (2007). "Effect of ternary phosphate-based glass compositions on osteoblast and osteoblast-like proliferation, differentiation and death in vitro", *Acta Biomaterialia*, Vol. 3(4), p. 563-572.

- [116] Yong-Keun, L., Jin, S., Sang-Bae, L., Kwang-Mahn, K., Seong-Ho, C., Chong-Kwan, K., Racquel, Z. L., and Kyoung-Nam, K. (2004). "Proliferation, differentiation, and calcification of preosteoblast-like MC3T3-E1 cells cultured onto noncrystalline calcium phosphate glass", *Journal of Biomedical Materials Research Part A*, Vol. 69A(1), p. 188-195.
- [117] de Jager, H.-J., and Heyns, A. M. (1998). "Kinetics of Acid-Catalyzed Hydrolysis of a Polyphosphate in Water", *The Journal of Physical Chemistry A*, Vol. 102(17), p. 2838-2841.
- [118] Navarro, M., Ginebra, M.-P., and Planell, J. A. (2003). "Cellular response to calcium phosphate glasses with controlled solubility", *Journal of Biomedical Materials Research Part A*, Vol. 67A(3), p. 1009-1015.
- [119] Uo, M., Mizuno, M., Kuboki, Y., Makishima, A., and Watari, F. (1998). "Properties and cytotoxicity of water soluble Na₂O–CaO–P₂O₅ glasses", *Biomaterials*, Vol. 19(24), p. 2277-2284.
- [120] Burg, K. J. L., Porter, S., and Kellam, J. F. (2000). "Biomaterial developments for bone tissue engineering", *Biomaterials*, Vol. 21(23), p. 2347-2359.
- [121] Behraves, E., Yasko, A. W., Engel, P. S., and Mikos, A. G. (1999). "Synthetic Biodegradable Polymers for Orthopaedic Applications", *Clinical Orthopaedics and Related Research*, Vol. 367, p. S118-S129.
- [122] Middleton, J. C., and Tipton, A. J. (2000). "Synthetic biodegradable polymers as orthopedic devices", *Biomaterials*, Vol. 21(23), p. 2335-2346.
- [123] Gunatillake, P. A., and Adhikari, R. (2003). "Biodegradable Synthetic Polymers for Tissue Engineering", P A Gunatillake & R Adhikari *European Cells and Materials* Vol. 5, p. 16.
- [124] Garlotta, D. (2001). "A Literature Review of Poly(Lactic Acid)", *Journal of Polymers and the Environment*, Vol. 9(2), p. 63-84.

- [125] Conn, R. E., Kolstad, J. J., Borzelleca, J. F., Dixler, D. S., Filer Jr, L. J., Ladu Jr, B. N., and Pariza, M. W. (1995). "Safety assessment of polylactide (PLA) for use as a food-contact polymer", *Food and Chemical Toxicology*, Vol. 33(4), p. 273-283.
- [126] David, H., Patrick, G., Jim, L., and Jed, R., (2005), *Natural Fibers, Biopolymers, and Biocomposites*, CRC Press, *Polylactic Acid Technology*.
- [127] Drumright, R. E., Gruber, P. R., and Henton, D. E. (2000). "Polylactic Acid Technology", *Advanced Materials*, Vol. 12(23), p. 1841-1846.
- [128] Perego, G., Cella, G. D., and Bastioli, C. (1996). "Effect of molecular weight and crystallinity on poly(lactic acid) mechanical properties", *Journal of Applied Polymer Science*, Vol. 59(1), p. 37-43.
- [129] Rafael Auras, Lim, L.-t., Susan, E. M. S., and Tsuji, H., (2010), *Poly(lactic acid) synthesis, structure, properties, processing, and applications*, *Properties of Poly(lactic acid)*.
- [130] Brandt, R. B., Waters, M. G., Rispler, M. J., and Kline, E. S. (1984). "D- and L-Lactate Catabolism to CO₂ in Rat Tissues", *Proceedings of the Society for Experimental Biology and Medicine*. Society for Experimental Biology and Medicine (New York, N.Y.), Vol. 175(3), p. 328-335.
- [131] Cella, G. P. a. G. D., (2010), *Poly(lactic acid) synthesis, structure, properties, processing, and applications*, *Mechanical properties*.
- [132] Vert, M., Li, S. M., and Garreau, H. (1995). "Attempts to map the structure and degradation characteristics of aliphatic polyesters derived from lactic and glycolic acids", *Journal of Biomaterials Science, Polymer Edition*, Vol. 6, p. 639-649.
- [133] Vert, M., Mauduit, J., and Li, S. (1994). "Biodegradation of PLA/GA polymers: increasing complexity", *Biomaterials*, Vol. 15(15), p. 1209-1213.
- [134] Kontakis, G. M., Pagkalos, J. E., Tosounidis, T. I., Melissas, J., and Katonis, P., (2007), *Bioabsorbable materials in orthopaedics*, *Acta medica belgica*, Bruxelles, BELGIQUE.

- [135] Kulkarni, R. K., Pani, K. C., Neuman, C., and Leonard, F. (1967). "Polylactic acid for surgical implants", *Plastic and Reconstructive Surgery*, Vol. 39(4), p. 430.
- [136] Daniels, A. U., Andriano, K. P., Smutz, W. P., Chang, M. K. O., and Heller, J. (1994). "Evaluation of absorbable poly(ortho esters) for use in surgical implants", *Journal of Applied Biomaterials*, Vol. 5(1), p. 51-64.
- [137] Verheyen, C. C. P. M., de Wijn, J. R., van Blitterswijk, C. A., de Groot, K., and Rozing, P. M. (1993). "Hydroxylapatite/poly(L-lactide) composites: An animal study on push-out strengths and interface histology", *Journal of Biomedical Materials Research*, Vol. 27(4), p. 433-444.
- [138] Taylor, M. S., Daniels, A. U., Andriano, K. P., and Heller, J. (1994). "Six bioabsorbable polymers: In vitro acute toxicity of accumulated degradation products", *Journal of Applied Biomaterials*, Vol. 5(2), p. 151-157.
- [139] Lin, Y. M., Boccaccini, A. R., Polak, J. M., Bishop, A. E., and Maquet, V. (2006). "Biocompatibility of Poly-DL-lactic acid (PDLA) for Lung Tissue Engineering", *Journal of Biomaterials Applications*, Vol. 21(2), p. 109-118.
- [140] Brauer, D., Rüssel, C., Vogt, S., Weisser, J., and Schnabelrauch, M. (2008). "Degradable phosphate glass fiber reinforced polymer matrices: mechanical properties and cell response", *Journal of Materials Science: Materials in Medicine*, Vol. 19(1), p. 121-127.
- [141] Mano, J. F., Sousa, R. A., Boesel, L. F., Neves, N. M., and Reis, R. L. (2004). "Bioinert, biodegradable and injectable polymeric matrix composites for hard tissue replacement: state of the art and recent developments", *Composites Science and Technology*, Vol. 64(6), p. 789-817.
- [142] Ramakrishna, S., Mayer, J., Wintermantel, E., and Leong, K. W. (2001). "Biomedical applications of polymer-composite materials: a review", *Composites Science and Technology*, Vol. 61(9), p. 1189-1224.

- [143] Bradley, J. S., Hastings, G. W., and Johnson-Nurse, C. (1980). "Carbon fibre reinforced epoxy as a high strength, low modulus material for internal fixation plates", *Biomaterials*, Vol. 1(1), p. 38-40.
- [144] Ekstrand, K., Ruyter, I. E., and Wellendorf, H. (1987). "Carbon/graphite fiber reinforced poly(methyl methacrylate): Properties under dry and wet conditions", *Journal of Biomedical Materials Research*, Vol. 21(9), p. 1065-1080.
- [145] Latour, R. A., and Black, J. (1992). "Development of FRP composite structural biomaterials: Ultimate strength of the fiber/matrix interfacial bond in in vivo simulated environments", *Journal of Biomedical Materials Research*, Vol. 26(5), p. 593-606.
- [146] Wenz, L. M., Merritt, K., Brown, S. A., Moet, A., and Steffee, A. D. (1990). "In vitro biocompatibility of polyetheretherketone and polysulfone composites", *Journal of Biomedical Materials Research*, Vol. 24(2), p. 207-215.
- [147] Wan, Y. Z., Wang, Y. L., Li, Q. Y., and Dong, X. H. (2001). "Influence of surface treatment of carbon fibers on interfacial adhesion strength and mechanical properties of PLA-based composites", *Journal of Applied Polymer Science*, Vol. 80(3), p. 367-376.
- [148] Zimmerman Mark, C., Alexander, H., Parsons, J. R., and Bajpai, P. K., (1991), *High-Tech Fibrous Materials*, American Chemical Society, *The Design and Analysis of Laminated Degradable Composite Bone Plates for Fracture Fixation*.
- [149] Pourdeyhimi, B., Robinson, H., Schwartz, P., and Wagner, H. (1986). "Fracture toughness of Kevlar 29/poly(methyl methacrylate) composite materials for surgical implantations", *Annals of Biomedical Engineering*, Vol. 14(3), p. 277-294.
- [150] Pourdeyhimi, B., and Wagner, H. D. (1989). "Elastic and ultimate properties of acrylic bone cement reinforced with ultra-high-molecular-weight polyethylene fibers", *Journal of Biomedical Materials Research*, Vol. 23(1), p. 63-80.

- [151] Reddy, N., Nama, D., and Yang, Y. (2008). "Polylactic acid/polypropylene polyblend fibers for better resistance to degradation", *Polymer Degradation and Stability*, Vol. 93(1), p. 233-241.
- [152] Marcolongo, M., Ducheyne, P., Garino, J., and Schepers, E. (1998). "Bioactive glass fiber/polymeric composites bond to bone tissue", *Journal of Biomedical Materials Research*, Vol. 39(1), p. 161-170.
- [153] Marcolongo, M., Ducheyne, P., and LaCourse, W. C. (1997). "Surface reaction layer formation in vitro on a bioactive glass fiber/polymeric composite", *Journal of Biomedical Materials Research*, Vol. 37(3), p. 440-448.
- [154] Jiang, G., Evans, M. E., Jones, I. A., Rudd, C. D., Scotchford, C. A., and Walker, G. S. (2005). "Preparation of poly(ϵ -caprolactone)/continuous bioglass fibre composite using monomer transfer moulding for bone implant", *Biomaterials*, Vol. 26(15), p. 2281-2288.
- [155] Salernitano E., and C., M. (2003). "Composite materials for biomedical applications: a review", *Journal of Applied Biomaterials & Biomechanics* Vol. 1, p. 16.
- [156] Charles-Harris, M., Koch, M., Navarro, M., Lacroix, D., Engel, E., and Planell, J. (2008). "A PLA/calcium phosphate degradable composite material for bone tissue engineering: an in vitro study", *Journal of Materials Science: Materials in Medicine*, Vol. 19(4), p. 1503-1513.
- [157] Navarro, M., Engel, E., Planell, J. A., Amaral, I., Barbosa, M., and Ginebra, M. P. (2008). "Surface characterization and cell response of a PLA/CaP glass biodegradable composite material", *Journal of Biomedical Materials Research Part A*, Vol. 85A(2), p. 477-486.
- [158] Ahmed, I., Cronin, P. S., Neel, E. A. A., Parsons, A. J., Knowles, J. C., and Rudd, C. D. (2009). "Retention of mechanical properties and cytocompatibility of a phosphate-based glass fiber/polylactic acid composite", *Journal of Biomedical Materials Research Part B: Applied Biomaterials*, Vol. 89B(1), p. 18-27.

- [159] Khan, R. A., Parsons, A. J., Jones, I. A., Walker, G. S., and Rudd, C. D. (2009). "Surface treatment of phosphate glass fibers using 2-hydroxyethyl methacrylate: Fabrication of poly(caprolactone)-based composites", *Journal of Applied Polymer Science*, Vol. 111(1), p. 246-254.
- [160] Khan, R. A., Parsons, A. J., Jones, I. A., Walker, G. S., and Rudd, C. D. (2010). "Preparation and Characterization of Phosphate Glass Fibers and Fabrication of Poly(caprolactone) Matrix Resorbable Composites", *Journal of Reinforced Plastics and Composites*, Vol. 29(12), p. 1838-1850.
- [161] Dibenedetto, A. T., and Lex, P. J. (1989). "Evaluation of surface treatments for glass fibers in composite materials", *Polymer Engineering & Science*, Vol. 29(8), p. 543-555.
- [162] Soo-Jin, P., and Joong-Seong, J. (2003). "Effect of silane coupling agent on mechanical interfacial properties of glass fiber-reinforced unsaturated polyester composites", *Journal of Polymer Science Part B: Polymer Physics*, Vol. 41(1), p. 55-62.
- [163] UCT, (2011),
- [164] Yazdani, H., Morshedian, J., and Khonakdar, H. A. (2006). "Effects of silane coupling agent and maleic anhydride-grafted polypropylene on the morphology and viscoelastic properties of polypropylene–mica composites", *Polymer Composites*, Vol. 27(5), p. 491-496.
- [165] DiBenedetto, A. T. (2001). "Tailoring of interfaces in glass fiber reinforced polymer composites: a review", *Materials Science and Engineering A*, Vol. 302(1), p. 74-82.
- [166] Park, S.-J., and Jin, J.-S. (2003). "Effect of silane coupling agent on mechanical interfacial properties of glass fiber-reinforced unsaturated polyester composites", *Journal of Polymer Science Part B: Polymer Physics*, Vol. 41(1), p. 55-62.

- [167] Haque, P., (2011), "Oligomeric PLA Coupling Agents For Phosphate Glass Fibres/PLA Composites", PhD Thesis, The university of Nottingham, Nottingham.
- [168] Cozien-Cazuc, S., (2006), "Characterisation of Resorbable Phosphate Glass Fibres", PhD Thesis, The University of Nottingham, Nottingham.
- [169] Phillips, M. J., Duncanson, P., Wilson, K., Darr, J. A., Griffiths, D. V., and Rehman, I. (2005). "Surface modification of bioceramics by grafting of tailored allyl phosphonic acid", *Advances in Applied Ceramics*, Vol. 104(5), p. 261-267.
- [170] Greish, Y. E., and Brown, P. W. (2001). "Chemically formed HAp-Ca poly(vinyl phosphonate) composites", *Biomaterials*, Vol. 22(8), p. 807-816.
- [171] Greish, Y. E., and Brown, P. W. (2001). "Preparation and characterization of calcium phosphate-poly(vinyl phosphonic acid) composites", *Journal of Materials Science: Materials in Medicine*, Vol. 12(5), p. 407-411.
- [172] Tanaka, H., Futaoka, M., and Hino, R. (2004). "Surface modification of calcium hydroxyapatite with pyrophosphoric acid", *Journal of Colloid and Interface Science*, Vol. 269(2), p. 358-363.
- [173] Andres, C., Sinani, V., Lee, D., Gun'ko, Y., and Kotov, N. (2006). "Anisotropic calcium phosphate nanoparticles coated with 2-carboxyethylphosphonic acid", *Journal of Materials Chemistry*, Vol. 16(40), p. 3964-3968.
- [174] Nancollas, G. H., Tang, R., Phipps, R. J., Henneman, Z., Gulde, S., Wu, W., Mangood, A., Russell, R. G. G., and Ebetino, F. H. (2006). "Novel insights into actions of bisphosphonates on bone: Differences in interactions with hydroxyapatite", *Bone*, Vol. 38(5), p. 617-627.
- [175] Shinkai, I., and Ohta, Y. (1996). "Alendronate", *Bioorganic & Medicinal Chemistry*, Vol. 4(1), p. 3-4.

- [176] Nowatzki, P. J., and Tirrell, D. A. (2004). "Physical properties of artificial extracellular matrix protein films prepared by isocyanate crosslinking", *Biomaterials*, Vol. 25(7-8), p. 1261-1267.
- [177] Sun, J.-S., Dong, G.-C., Lin, C.-Y., Sheu, S.-Y., Lin, F.-H., Chen, L.-T., Chang, W. H.-S., and Wang, Y.-J. (2003). "The effect of Gu-Sui-Bu (*Drynaria fortunei* J. Sm) immobilized modified calcium hydrogenphosphate on bone cell activities", *Biomaterials*, Vol. 24(5), p. 873-882.
- [178] Dong, G.-C., Sun, J.-S., Yao, C.-H., Jiang, G. J., Huang, C.-W., and Lin, F.-H. (2001). "A study on grafting and characterization of HMDI-modified calcium hydrogenphosphate", *Biomaterials*, Vol. 22(23), p. 3179-3189.
- [179] Liu, A., Hong, Z., Zhuang, X., Chen, X., Cui, Y., Liu, Y., and Jing, X. (2008). "Surface modification of bioactive glass nanoparticles and the mechanical and biological properties of poly(l-lactide) composites", *Acta Biomaterialia*, Vol. 4(4), p. 1005-1015.
- [180] Liu, Q., de Wijn, J. R., and van Blitterswijk, C. A. (1998). "Composite biomaterials with chemical bonding between hydroxyapatite filler particles and PEG/PBT copolymer matrix", *Journal of Biomedical Materials Research*, Vol. 40(3), p. 490-497.
- [181] Ahmed, I., Parsons, A., Arthur, J., Gavin, W., Colin, S., and Chris, R., (2010), *Cytocompatibility and Effect of Increasing MgO Content in a Range of Quaternary Invert Phosphate-based Glasses*, Sage, London, ROYAUME-UNI.
- [182] Knowles, J. C. (2003). "Phosphate based glasses for biomedical applications", *Journal of Materials Chemistry*, Vol. 13(10), p. 2395-2401.
- [183] Yu, X., Day, D. E., Long, G. J., and Brow, R. K. (1997). "Properties and structure of sodium-iron phosphate glasses", *Journal of Non-Crystalline Solids*, Vol. 215(1), p. 21-31.
- [184] Burling, L. D., (2005), "Novel Phosphate Glasses for Bone Regeneration Applications", PhD Thesis, The university of Nottingham, Nottingham.

- [185] Strohner, P., Sarrach, D., Reich, J. G., Day, D. E., Yu, X., Long, G. J., and Brow, R. K. (1997). "Properties and structure of sodium-iron phosphate glasses", *Journal of Non-Crystalline Solids*, Vol. 215, p. 21-31.
- [186] Moon, H.-J., Kim, K.-N., Kim, K.-M., Choi, S.-H., Kim, C.-K., Kim, K.-D., LeGeros, R., and Lee, Y.-K. (2006). "Effect of calcium phosphate glass on bone formation in calvarial defects of Sprague-Dawley rats", *Journal of Materials Science: Materials in Medicine*, Vol. 17(9), p. 807-813.
- [187] Exarhos, G. (1974). "Interionic vibrations and glass transitions in ionic oxide metaphosphate glasses", *J. Chem. Phys.*, Vol. 60(11), p. 4145.
- [188] Arzeian, J. M., and Hogarth, C. A. (1991). "Some structural, electrical and optical properties of copper phosphate glasses containing the rare-earth europium", *Journal of Materials Science*, Vol. 26(19), p. 5353-5366.
- [189] Reis, S. T., Faria, D. L. A., Martinelli, J. R., Pontuschka, W. M., Day, D. E., and Partiti, C. S. M. (2002). "Structural features of lead iron phosphate glasses", *Journal of Non-Crystalline Solids*, Vol. 304(1-3), p. 188-194.
- [190] Shih, P. Y., Yung, S. W., and Chin, T. S. (1999). "FTIR and XPS studies of P2O5-Na2O-CuO glasses", *Journal of Non-Crystalline Solids*, Vol. 244(2), p. 211-222.
- [191] Stockhorst, H., and Brückner, R. (1986). "Structure sensitive measurements on phosphate glass fibers", *Journal of Non-Crystalline Solids*, Vol. 85(1-2), p. 105-126.
- [192] Marino, A. E., Arrasmith, S. R., Gregg, L. L., Jacobs, S. D., Chen, G., and Duc, Y. (2001). "Durable phosphate glasses with lower transition temperatures", *Journal of Non-Crystalline Solids*, Vol. 289(1-3), p. 37-41.
- [193] Ahmed, I., Cronin, P. S., Abou Neel, E. A., Parsons, A. J., Knowles, J. C., and Rudd, C. D. (2009). "Retention of mechanical properties and cytocompatibility of a phosphate-based glass fiber/polylactic acid composite", *Journal of Biomedical Materials Research Part B: Applied Biomaterials*, Vol. 89B(1), p. 18-27.

- [194] Parsons, A. J., Ahmed, I., Han, N., Felfel, R., and Rudd, C. D. (2010). "Mimicking Bone Structure and Function with Structural Composite Materials", *Journal of Bionic Engineering*, Vol. 7(Supplement 1), p. S1-S10.
- [195] Parsons, A. J., Ahmed, I., Haque, P., Fitzpatrick, B., Niazi, M. I. K., Walker, G. S., and Rudd, C. D. (2009). "Phosphate Glass Fibre Composites for Bone Repair", *Journal of Bionic Engineering*, Vol. 6(4), p. 318-323.
- [196] Cozien-Cazuc, S., Parsons, A., Walker, G., Jones, I., and Rudd, C. (2008). "Effects of aqueous aging on the mechanical properties of P40Na20Ca16Mg24 phosphate glass fibres", *Journal of Materials Science*, Vol. 43(14), p. 4834-4839.
- [197] Jiang, G., Evans, M. E., Jones, I. A., Rudd, C. D., Scotchford, C. A., and Walker, G. S. (2005). "Preparation of poly([epsilon]-caprolactone)/continuous bioglass fibre composite using monomer transfer moulding for bone implant", *Biomaterials*, Vol. 26(15), p. 2281-2288.
- [198] Onal, L., Cozien-Cazuc, S., Jones, I. A., and Rudd, C. D. (2008). "Water absorption properties of phosphate glass fiber-reinforced poly- ϵ -caprolactone composites for craniofacial bone repair", *Journal of Applied Polymer Science*, Vol. 107(6), p. 3750-3755.
- [199] Panzavolta, S., Torricelli, P., Bracci, B., Fini, M., and Bigi, A. (2010). "Functionalization of biomimetic calcium phosphate bone cements with alendronate", *J Inorg Biochem*.
- [200] Miller, B., Muri, P., and Rebenfeld, L. (1987). "A microbond method for determination of the shear strength of a fiber/resin interface", *Composites Science and Technology*, Vol. 28(1), p. 17-32.
- [201] Zinck, P., Wagner, H. D., Salmon, L., and Gerard, J. F. (2001). "Are microcomposites realistic models of the fibre/matrix interface ? I. Micromechanical modelling", *Polymer*, Vol. 42(12), p. 5401-5413.

- [202] Zinck, P., Wagner, H. D., Salmon, L., and Gerard, J. F. (2001). "Are microcomposites realistic models of the fibre/matrix interface? II. Physico-chemical approach", *Polymer*, Vol. 42(15), p. 6641-6650.
- [203] Piggott, M. R. (1997). "Why interface testing by single-fibre methods can be misleading", *Composites Science and Technology*, Vol. 57(8), p. 965-974.
- [204] Choi, N.-S., Park, J.-E., and Kang, S.-K. (2009). "Quasi-Disk Type Microbond Pull-Out Test for Evaluating Fiber/Matrix Adhesion in Composites", *Journal of Composite Materials*, Vol. 43(16), p. 1663-1677.
- [205] Piggott, M. R. (1987). "Debonding and friction at fibre-polymer interfaces. I: Criteria for failure and sliding", *Composites Science and Technology*, Vol. 30(4), p. 295-306.
- [206] Pitkethly, M. J., Favre, J. P., Gaur, U., Jakubowski, J., Mudrich, S. F., Caldwell, D. L., Drzal, L. T., Nardin, M., Wagner, H. D., Di Landro, L., Hampe, A., Armistead, J. P., Desaegeer, M., and Verpoest, I. (1993). "A round-robin programme on interfacial test methods", *Composites Science and Technology*, Vol. 48(1-4), p. 205-214.
- [207] DiFrancia, C., Ward, T. C., and Claus, R. O. (1996). "The single-fibre pull-out test. 1: Review and interpretation", *Composites Part A: Applied Science and Manufacturing*, Vol. 27(8), p. 597-612.
- [208] Polacek, P., and Jancar, J. (2008). "Effect of filler content on the adhesion strength between UD fiber reinforced and particulate filled composites", *Composites Science and Technology*, Vol. 68(1), p. 251-259.
- [209] Shafrin, E. G., and Zisman, W. A. (1960). "Constitutive Relations in the Wetting of Low Energy Surfaces and the Theory of the Retraction method of Preparing Monolayers", *The Journal of Physical Chemistry*, Vol. 64(5), p. 519-524.
- [210] Kurth, D. G., and Bein, T. (1993). "Surface reactions on thin layers of silane coupling agents", *Langmuir*, Vol. 9(11), p. 2965-2973.

- [211] Chunli Yang, Wenjian Weng, Piyi Du, Ge Shen, and Gaorong Han (2007). "XPS Studies of Hydroxyapatite Powders by Grafting Octadecyltrichlorosilane", *Key Engineering Materials* Vol. Vols. 330-332 ((2007)), p. 765-768.
- [212] Papapoulos, S. E. (1993). "The role of bisphosphonates in the prevention and treatment of osteoporosis", *The American Journal of Medicine*, Vol. 95(5, Supplement 1), p. S48-S52.
- [213] Gong, C., Shi, S., Dong, P., Kan, B., Gou, M., Wang, X., Li, X., Luo, F., Zhao, X., Wei, Y., and Qian, Z. (2009). "Synthesis and characterization of PEG-PCL-PEG thermosensitive hydrogel", *International Journal of Pharmaceutics*, Vol. 365(1-2), p. 89-99.
- [214] ISO, (2009), 10993 Biological evaluation of medical devices
- [215] Sánchez-Vaquero, V. (2010). "Characterization and cytocompatibility of hybrid aminosilane-agarose hydrogel scaffolds", *Biointerphases*, Vol. 5(2), p. 23.
- [216] Dong, G.-C., Lin, F.-H., Sun, J.-S., Yao, C.-H., Jiang, G., and Huang, C.-W. (2001). "Biodegradability and Cytocompatibility Evaluation of Surface Modified Calcium Hydrogenphosphate", *Journal of Medical and Biological Engineering*, Vol. 21(4), p. 7.
- [217] ISO, (2009), 10993 Biological evaluation of medical devices
- [218] Biocolor, (2011), Sircol soluble Collagen Assay Manual 2011,
- [219] Price, P. A., Otsuka, A. A., Poser, J. W., Kristaponis, J., and Raman, N. (1976). "Characterization of a gamma-carboxyglutamic acid-containing protein from bone", *Proceedings of the National Academy of Sciences*, Vol. 73(5), p. 1447-1451.
- [220] Poser, J. W., Esch, F. S., Ling, N. C., and Price, P. A. (1980). "Isolation and sequence of the vitamin K-dependent protein from human bone. Undercarboxylation of the first glutamic acid residue", *Journal of Biological Chemistry*, Vol. 255(18), p. 8685-91.
- [221] Invitrogen, (2011), Human osteocalcin ELISA kit instructions,

- [222] Beck, G. R., Zerler, B., and Moran, E. (2000). "Phosphate is a specific signal for induction of osteopontin gene expression", *Proceedings of the National Academy of Sciences*, Vol. 97(15), p. 8352-8357.
- [223] ADAMI, #160, S., ZAMBERLAN, and N., (1996), *Adverse effects of bisphosphonates : A comparative review*, Adis, Auckland, NOUVELLE-ZELANDE.
- [224] Spenlehauer, G., Vert, M., Benoit, J. P., and Boddaert, A. (1989). "In vitro and In vivo degradation of poly(D,L lactide/glycolide) type microspheres made by solvent evaporation method", *Biomaterials*, Vol. 10(8), p. 557-563.
- [225] Mei, Y., Kumar, A., Gao, W., Gross, R., Kennedy, S. B., Washburn, N. R., Amis, E. J., and Elliott, J. T. (2004). "Biocompatibility of sorbitol-containing polyesters. Part I: Synthesis, surface analysis and cell response in vitro", *Biomaterials*, Vol. 25(18), p. 4195-4201.
- [226] Owen, T. A., Aronow, M., Shalhoub, V., Barone, L. M., Wilming, L., Tassinari, M. S., Kennedy, M. B., Pockwinse, S., Lian, J. B., and Stein, G. S. (1990). "Progressive development of the rat osteoblast phenotype in vitro: Reciprocal relationships in expression of genes associated with osteoblast proliferation and differentiation during formation of the bone extracellular matrix", *Journal of Cellular Physiology*, Vol. 143(3), p. 420-430.
- [227] Lian, J. B., and Stein, G. S. (1992). "Concepts of Osteoblast Growth and Differentiation: Basis for Modulation of Bone Cell Development and Tissue Formation", *Critical Reviews in Oral Biology & Medicine*, Vol. 3(3), p. 269-305.
- [228] Stein, G. S., and Lian, J. L., (2002), *Principles of Bone Biology* (Second Edition), Academic Press, San Diego, Chapter 5 - mechanisms regulating osteoblast proliferation and differentiation.
- [229] Dias, A. G., Lopes, M. A., Trigo Cabral, A. T., Santos, J. D., and Fernandes, M. H. (2005). "In vitro studies of calcium phosphate glass ceramics with different solubility with the use of human bone marrow cells", *Journal of Biomedical Materials Research Part A*, Vol. 74A(3), p. 347-355.

- [230] Ma, S., Yang, Y., Carnes, D. L., Kim, K., Park, S., Oh, S. H., and Ong, J. L. (2005). "Effects of Dissolved Calcium and Phosphorous on Osteoblast Responses", *Journal of Oral Implantology*, Vol. 31(2), p. 61-67.
- [231] Au, A. Y., Au, R. Y., Demko, J. L., McLaughlin, R. M., Eves, B. E., and Frondoza, C. G. (2010). "Consil® bioactive glass particles enhance osteoblast proliferation and selectively modulate cell signaling pathways in vitro", *Journal of Biomedical Materials Research Part A*, Vol. 94A(2), p. 380-388.
- [232] Bosetti, M., and Cannas, M. (2005). "The effect of bioactive glasses on bone marrow stromal cells differentiation", *Biomaterials*, Vol. 26(18), p. 3873-3879.
- [233] Bosetti, M., Zanardi, L., Hench, L., and Cannas, M. (2003). "Type I collagen production by osteoblast-like cells cultured in contact with different bioactive glasses", *Journal of Biomedical Materials Research Part A*, Vol. 64A(1), p. 189-195.
- [234] Leonardi, E., Ciapetti, G., Baldini, N., Novajra, G., Verné, E., Baino, F., and Vitale-Brovarone, C. (2010). "Response of human bone marrow stromal cells to a resorbable P2O5–SiO2–CaO–MgO–Na2O–K2O phosphate glass ceramic for tissue engineering applications", *Acta Biomaterialia*, Vol. 6(2), p. 598-606.
- [235] Carpenter, T. O., Moltz, K. C., Ellis, B., Andreoli, M., McCarthy, T. L., Centrella, M., Bryan, D., and Gundberg, C. M. (1998). "Osteocalcin Production in Primary Osteoblast Cultures Derived from Normal and Hyp Mice", *Endocrinology*, Vol. 139(1), p. 35-43.
- [236] Varanasi, V. G., Saiz, E., Loomer, P. M., Ancheta, B., Uritani, N., Ho, S. P., Tomsia, A. P., Marshall, S. J., and Marshall, G. W. (2009). "Enhanced osteocalcin expression by osteoblast-like cells (MC3T3-E1) exposed to bioactive coating glass (SiO2–CaO–P2O5–MgO–K2O–Na2O system) ions", *Acta Biomaterialia*, Vol. 5(9), p. 3536-3547.
- [237] Attawia, M. A., Herbert, K. M., Uhrich, K. E., Langer, R., and Laurencin, C. T. (1999). "Proliferation, morphology, and protein expression by osteoblasts cultured on poly(anhydride-co-imides)", *Journal of Biomedical Materials Research*, Vol. 48(3), p. 322-327.

- [238] Rubin, L. R. (1987). "Biomaterials in Reconstructive Surgery", *Plastic and Reconstructive Surgery*, Vol. 80(1), p. 143-144.
- [239] Laros, G. S., and Spiegel, P. G. (1979). "Rigid Internal Fixation of Fractures", *Clinical Orthopaedics and Related Research*, Vol. 138, p. 2-3.
- [240] Cornell, C. N., Levine, D., and Pagnani, M. J. (1994). "Internal Fixation of Proximal Humerus Fractures Using the Screw-Tension Band Technique", *Journal of Orthopaedic Trauma*, Vol. 8(1), p. 23-27.
- [241] Hofmann, G. O. (1995). "Biodegradable implants in traumatology: a review on the state-of-the-art", *Archives of Orthopaedic and Trauma Surgery*, Vol. 114(3), p. 123-132.
- [242] Anglen, J., Kyle, R. F., Marsh, J. L., Virkus, W. W., Watters, W. C., Keith, M. W., Turkelson, C. M., Wies, J. L., and Boyer, K. M. (2009). "Locking Plates for Extremity Fractures", *Journal of the American Academy of Orthopaedic Surgeons*, Vol. 17(7), p. 465-472.
- [243] Kobayashi, H. Y. L. S., Brauer, D. S., and Rüssel, C. (2010). "Mechanical properties of a degradable phosphate glass fibre reinforced polymer composite for internal fracture fixation", *Materials Science and Engineering: C*, Vol. 30(7), p. 1003-1007.
- [244] Dupraz, A. M. P., Wijn, J. R. d., Meer, S. A. T. v. d., and Groot, K. d. (1996). "Characterization of silane-treated hydroxyapatite powders for use as filler in biodegradable composites", *Journal of Biomedical Materials Research*, Vol. 30(2), p. 231-238.
- [245] Andriano, K. P., Daniels, A. U., and Heller, J. (1992). "Effectiveness of silane treatment on absorbable microfibers", *Journal of Applied Biomaterials*, Vol. 3(3), p. 191-195.
- [246] Siparsky, G. L., Voorhees, K. J., and Miao, F. (1998). "Hydrolysis of Poly(lactic Acid (PLA) and Polycaprolactone (PCL) in Aqueous Acetonitrile

Solutions: Autocatalysis", *Journal of Polymers and the Environment*, Vol. 6(1), p. 31-41.

[247] Kim, H.-W., Lee, H.-H., and Chun, G.-S. (2008). "Bioactivity and osteoblast responses of novel biomedical nanocomposites of bioactive glass nanofiber filled poly(lactic acid)", *Journal of Biomedical Materials Research Part A*, Vol. 85A(3), p. 651-663.

[248] Uthoff, H. K., Poitras, P., and Backman, D. S. (2006). "Internal plate fixation of fractures: short history and recent developments", *Journal of Orthopaedic Science*, Vol. 11(2), p. 118-126.

[249] Böstman, O., and Pihlajamäki, H. (2000). "Clinical biocompatibility of biodegradable orthopaedic implants for internal fixation: a review", *Biomaterials*, Vol. 21(24), p. 2615-2621.

[250] Böstman, O. M., and Pihlajamäki, H. K. (2000). "Adverse Tissue Reactions to Bioabsorbable Fixation Devices", *Clinical Orthopaedics and Related Research*, Vol. 371, p. 216-227.

[251] Navarro, M., Ginebra, M. P., Planell, J. A., Barrias, C. C., and Barbosa, M. A. (2005). "In vitro degradation behavior of a novel bioresorbable composite material based on PLA and a soluble CaP glass", *Acta Biomaterialia*, Vol. 1(4), p. 411-419.

[252] Kalfas, I. H. (2001). "Principles of bone healing", *Neurosurg Focus*, Vol. 10(4), p. 4.

[253] Monika Kursawe, W. G. A. A. T. (1998). "Biodegradable Silica Fibers from Sols", *Journal of Sol-Gel Science and Technology* Vol. 13, p. 5.

[254] Daniels, A. U., Chang, M. K. O., Andriano, K. P., and Heller, J. (1990). "Mechanical properties of biodegradable polymers and composites proposed for internal fixation of bone", *Journal of Applied Biomaterials*, Vol. 1(1), p. 57-78.

- [255] Drzal, L. T., and Madhukar, M. (1993). "Fibre-matrix adhesion and its relationship to composite mechanical properties", *Journal of Materials Science*, Vol. 28(3), p. 569-610.
- [256] Zhang, T., Hu, D., Jin, J., Yang, S., Li, G., and Jiang, J. (2009). "Improvement of surface wettability and interfacial adhesion ability of poly(p-phenylene benzobisoxazole) (PBO) fiber by incorporation of 2,5-dihydroxyterephthalic acid (DHTA)", *European Polymer Journal*, Vol. 45(1), p. 302-307.
- [257] Arefi-Khonsari, F., Kurdi, J., Tatoulian, M., and Amouroux, J. (2001). "On plasma processing of polymers and the stability of the surface properties for enhanced adhesion to metals", *Surface and Coatings Technology*, Vol. 142-144(0), p. 437-448.
- [258] Thomason, J. L., and Vlug, M. A. (1996). "Influence of fibre length and concentration on the properties of glass fibre-reinforced polypropylene: 1. Tensile and flexural modulus", *Composites Part A: Applied Science and Manufacturing*, Vol. 27(6), p. 477-484.
- [259] Piggott, M. R. (1995). "The effect of fibre waviness on the mechanical properties of unidirectional fibre composites: A review", *Composites Science and Technology*, Vol. 53(2), p. 201-205.
- [260] Kretsis G (1987). "A review of the tensile, compressive, flexural and shear properties of hybrid fibre-reinforced plastics", *Composites*, Vol. 18(1), p. 13-23.
- [261] Slivka, M. A., and Chu, C. C. (1997). "Fiber-matrix interface studies on bioabsorbable composite materials for internal fixation of bone fractures. II. A new method using laser scanning confocal microscopy", *Journal of Biomedical Materials Research*, Vol. 37(3), p. 353-362.
- [262] Wan, Y. Z., Wang, Y. L., Xu, X. H., and Li, Q. Y. (2001). "In vitro degradation behavior of carbon fiber-reinforced PLA composites and influence of interfacial adhesion strength", *Journal of Applied Polymer Science*, Vol. 82(1), p. 150-158.

[263] Kiani, A., Lakhkar, N. J., Salih, V., Smith, M. E., Hanna, J. V., Newport, R. J., Pickup, D. M., and Knowles, J. C. (2012). "Titanium-containing bioactive phosphate glasses", *Philosophical Transactions of the Royal Society A: Mathematical, Physical and Engineering Sciences*, Vol. 370(1963), p. 1352-1375.